https://ntrs.nasa.gov/search.jsp?R=19850010134 2020-03-20T20:09:24+00:00Z

General Disclaimer

One or more of the Following Statements may affect this Document

- This document has been reproduced from the best copy furnished by the organizational source. It is being released in the interest of making available as much information as possible.

- This document may contain data, which exceeds the sheet parameters. It was furnished in this condition by the organizational source and is the best copy available.

- This document may contain tone-on-tone or color graphs, charts and/or pictures, which have been reproduced in black and white.

- This document is paginated as submitted by the original source.

- Portions of this document are not fully legible due to the historical nature of some of the material. However, it is the best reproduction available from the original submission.

Produced by the NASA Center for Aerospace Information (CASI)

(NASA-TM-86170) DATA REPORT ON VARIATIONS IN THE COMPOSITION OF SEA ICE DURING MIZEX/EAST'83 WITH THE NIMBUS-7 SMMR (NASA) 144 p HC A07/MF A01 CSCL 08L

N85-18443

Unclas G3/43 14134

NASA

Technical Memorandum 86170

DATA REPORT ON VARIATIONS IN THE COMPOSITION OF SEA ICE DURING MIZEX/EAST'83 WITH THE NIMBUS-7 SMMR

Per Gloersen

MAR 1985 RECEIVED NASA STI FACILITY ACCESS DEPT.

DECEMBER 1984

National Aeronautics and Space Administration

Goddard Space Flight Center
Greenbelt, Maryland 20771

DATA REPORT ON VARIATIONS IN THE COMPOSITION OF SEA ICE DURING MIZEX/EAST'83 WITH THE NIMBUS-7 SMMR

Per Gloersen

Goddard Laboratory for Atmospheric Sciences
NSAS Goddard Space Flight Center
Greenbelt, Maryland 20771, USA

ABSTRACT

Data acquired with the Scanning Multichannel Microwave Radiometer (SMMR) on board the Nimbus-7 Satellite for a six-week period including the 1983 MIZEX in Fram Strait have been analyzed with the use of a previously developed procedure for calculating sea ice concentration, multiyear fraction, and ice temperature. These calculations will be compared with independent observations made on the surface and from aircraft in order to check the validity of the calculations based on SMMR data. The calculation of multiyear fraction, which was known earlier to be invalid near the melting point of sea ice, was of particular interest during this period. The indication of multiyear ice was found to disappear a number of times, presumably corresponding to freeze/thaw cycles which occurred in this time period. This report includes both grid-print maps and grey-scale images of total sea ice concentration and multiyear sea ice fraction for the entire period.

Keywords: MIZEX/East'83, Sea Ice Concentration & Age, Nimbus-7 SMMR

PRECEDING PAGE BLANK NOT FILMED

1. INTRODUCTION

In support of the Pilot Marginal Ice Zone Experiment in the Fram Strait region of the East Greenland Sea in June/July 1983 (MIZEX/East'83), the Nimbus Project at the NASA Goddard Space Flight Center provided near real-time images of the sea ice concentrations, calculated from SMMR radiances, to the researchers in the field by means of electronic mail. In addition to providing those in the field with mesoscale information regarding the location and character of the ice edge, and the ice concentration and the ice age within the pack, these data were analyzed with an eye towards understanding known errors in the sea ice properties calculations near the melt point of sea ice. While the surface temperature information was not yet in a form convenient for comparison at this writing, the SMMR data are presented in anticipation of such comparison. MIZEX/East'83 represents the first opportunity for comparing remote observations of sea ice with those on the surface during summer freeze/thaw conditions.

In this report are described the near real-time mode of SMMR data analysis, the processing algorithm, the product transmitted by electronic mail, and some subsequent analysis of the retrieved products. In the Appendices are included a complete set of grid-print maps and grey-scale images for total concentration of the sea ice and fraction of multiyear ice present.

2. DATA ACQUISITION

Nimbus-7 SMMR data are recorded onto on-board spacecraft tape recorders during the course of an orbit for subsequent higher data-rate telemetering to various satellite receiving stations situated in various places on the globe. For various logistical reasons, the station at Gilmore Creek, Alaska was the only one suited for near real-time transmission of the data over land links to Goddard Space Flight Center (GSFC), where the ground station is located (see Figure 1.).) Thus, the data were available at GSFC in as little as one hour after the satellite tape dump to Gilmore Creek, which generally consisted of more than one orbit's worth of information. Because of power constraints on the spacecraft, the SMMR is operated only every other day.

As received at GSFC, the data contain information from several of the instruments on board the Nimbus-7. Furthermore, these data are not earth-located, are in a format designed for efficient and reliable telemetry, and are unsuitable for automatic data processing on standardized computer operating systems. Thus, a data formatting process (Figure 1.) is required before the SMMR data can be analyzed. This consists of first stripping the SMMR data off the sensor data tape onto a user-formatted output (UFO) tape. Next, the UFO tape data and predicted ephemeris data on an image location tape (ILT) are combined, using the time codes on each tape for synchronization, to produce a so-called antenna temperature tape (TAT) on which the raw SMMR data have also been normalized with the internal radiance reference sources to provide automatic gain control (AGC). The TAT so produced is identical in most respects to the TATs which the Nimbus Project provides in the standard data production scheme, albeit several months after acquisition to keep production costs down with non-priority data processing. The one distinctive difference between the near real-time and production TATs is that the latter use ILTs containing definitive emphemeris data based on actual orbit element observations, which again are not available for at least three weeks after a given pass.

The final stage in this process consists of calibrating the SMMR data, remapping the radiances onto a standard polar projection, performing the calculations of the sea ice properties (to be described in the next section), mapping the results on the same projection, and producing an ASCII-character representation of that map suitable for transmission on electronic mail (see "Data Processing", Figure 1.). The ASCII-character maps of sea ice concentration (and age) were produced on the in-house computers at GSFC and stored on disk. The disks were then interrogated by a desk-top microcomputer and stored locally on word processor files on floppy disks. The data were briefly reviewed at the local terminal, edited if necessary, and transmitted via electronic mail to a number of recipients here and in the field. The tremendous advantage of using electronic mail for these purposes is that it combines prompt with convenient access to the data. Direct data links, on the other hand, require the simultaneous presence of both the transmitter and receiver. The average time between acquisition of the data from the last desired SMMR orbit of the day and the transmission via electronic mail was ten hours, with a six-hour minimum actually achieved. In principle, a much shorter time is possible, but not without risk to the main task of assuring reliable data acquisition for the standard production scheme or inordinately high processing costs.

3. CALCULATIONS

The method of calculating sea ice concentration and age, along with an estimate of the accuracies and some of the pitfalls has been described elsewhere in detail (Refs. 1,2). A brief summary follows:

The process begins by forming two dimensionless parameters from selected SMMR radiances in order to reduce the effects of physical temperature of the sea ice on the calculations. SMMR radiances are available at five wavelengths ranging from 0.8 to 4.6 cm and both polarized components. (The incidence angle is at the constant value of 50 degrees.) From these ten channels, we have selected three to produce the polarization (PR) at a wavelength of 1.7 cm and a spectral gradient ratio (GR) with the use of the vertically polarized channels at the 0.8 and 1.7 cm wavelengths:

$$PR = (1.7V - 1.7H)/(1.7V + 1.7H)$$

$$GR = (0.8V - 1.7V)/(0.8V + 1.7V)$$

In the vicinity of sea ice of varying age, these parameters are nearly orthogonal in that PR is approximately zero for all types of sea ice and 0.3 for calm open water in clear weather, and GR is near zero for first-year or younger sea ice whereas it is near -0.15 for old (multiyear) ice. This results from the wavelength-dependent volume scattering of microwave radiation in the freeboard portion of multiyear sea ice, which is not present in first-year and younger ice. The scattering is greater at shorter wavelengths. (Over open water, GR is also positive.) Thus, we calculate total sea ice concentration (C) and multiyear sea ice concentration (F*C, where F is the fraction of ice present that is multiyear) as follows:

$$C=(70.2-267*PR)/(53.2-6.4*F+(200+70.4*F)*PR)$$

$$F*C=(30.7-33.1*C-(368+113*C)*GR)/(27.0-91.0*GR)$$

(The asterisk has been used to denote multiplication.)

These equations are recursive in order to take into account a slight dependence of polarization on the age of the ice and the presence of open water when making the calculation for F*C. The coefficients were calculated by selecting ostensibly pure-sample tiepoints for multiyear ice (a large area northwest of the Queen Elizabeth Islands), first-year ice (a large area in the Chuckchi Sea), and open water with low wind and clouds. The success of retrievals based on this algorithm depends to a large extent on the judicious choice of the tie-points. While those chosen here generally perform well in the Arctic Basin (Ref. 2), retuning of the algorithm may be appropriate in other areas (Refs. 3,4). At any rate, these algorithms were used for this study of summer sea ice in the MIZ.

An example of the total sea ice concentration (C) calculation made during this time period is shown in Figure 2 in the ASCII-character format transmitted to MIZEX observers in the field. Here, C is given in even deciles by numerals, with the odd deciles 1 through 9 represented by '−,=,.,/,−' in order to facilitate viewing the isopleths of C on the grid-print map. (This choice of representing both '1' and '9' by '−' was subsequently regretted and has since been changed.) In Figure 2, the ice edge is best defined as the boundary between the '2 ''s and the '−' 's. Persistent high winds in the area cause most of the open ocean shown here to be covered with '−' 's, since the effect of high winds is to depolarize the microwave radiances emanating from the ocean surface; however, some of the open ocean is shown as blanks, indicating calm seas as used for the ocean tiepoint.

Such grid-print maps of total sea ice concentration for the entire MIZEX/East'83 period are given in Appendix A. In Appendix B, similar maps of the multiyear sea ice fraction are given. Appendices C & D contain grey-scale images of the same data shown in Appendices A & B.

4. DISCUSSION

While the multiyear fraction (F) was produced in near real-time during MIZEX/East'83, this parameter was not transmitted to the field because of known failure of the algorithm near the melting point of the ice, as was realized both from sea ice model considerations (Ref. 2) and earlier observations of summer ice (Refs. 5-7). This failure is due to the presence of moisture in the freeboard portion of the ice at these times which greatly increases the loss tangent in the ice, and thus obscures the volume scattering and hence its distinctly different microwave signature, as has been mentioned earlier. However, such grid-print maps were produced locally and analyzed, with reports of the 'appearance and disappearance' of the multiyear ice reported on other electronic mail dispatches to the experimenters in the field.

The cycling of the retrieval of F is shown in Figure 3. This time-history of the phenomenon was produced by obtaining an average value for F in the vicinity of the MIZEX area (that is, the area was delineated by an overlay shown in Figure 4) for each of the grid maps acquired in near real-time. These average values were plotted every other day for the plot in Figure 4. About eight cycles of varying intensity of the F-retrieval can be seen during the period June 8 - August 5, 1983. Clearly, such rapid oscillations in the amount of multiyear sea ice in the area are geophysically unrealistic and must have other attributes.

5. CONCLUDING REMARKS

These observations were made as a precursor to the main MIZEX summer experiment upon which we are about to embark at this writing. Additional analysis of the 1983 results, particularly combin-

ing the surface observations with the SMMR data, is expected to yield more insight into the freeze/thaw microwave radiance properties of sea ice, especially when combined with the 1984 experiment which is more comprehensive.

6. ACKNOWLEDGMENT

The author wishes to commend W.J. Campbell for his persistent persuasiveness which was instrumental in initiating the effort reported here. This research was supported in part by the Nimbus Project Office and in part by the Office of Naval Research.

7. REFERENCES

1. Gloersen P, Cavalieri D J, Chang A T C, Wilheit T T, Campbell W J, Johannessen O M, Katsaros K B, Kunzi K F, Ross D B, Staelin D, Windsor E P L, Barath F T, Gudmandsen P, Langham E, Ramseier R O, A summary of results from the first Nimbus-7 observations, *J Geophys Res* vol 89, 5335-5344 (1984)

2. Cavalieri D J, Gloersen P, Campbell W J, Determination of sea ice parameters with the Nimbus-7 SMMR, *J Geophys Res* vol 89, 5355-5369 (1984)

3. Cavalieri D J, Gloersen P, Wilheit T T, Calhoun C, Passive microwave characteristics of the Bering Sea ice cover during MIZEX-West, *ESA Report No. SP-215* vol 1, 379-384 (1984)

4. Svendsen E, Kloster K, Farrelly B, Johannessen O M, Johannessen J, Campbell W J, Gloersen P, Cavalieri D, and Maetzler C, Norwegian remote sensing experiment: Evaluation of the Nimbus-7 Scanning Multichannel Microwave Radiometer for sea ice research, *J Geophys Res* vol 88, 2781-2792 (1983)

5. Gloersen P, Zwally H J, Chang A T C, Hall D K, Campbell W J, Ramseier R O, Time-dependence of sea ice concentration and multiyear ice fraction in the Arctic Basin, *Boundary-Layer Meteorology* vol 13, 339-359 (1978)

6. Campbell W J, Wayenberg J, Ramseyer J B, Ramseier R O, Vant M R, Weaver R, Redmond A, Arsenault L, Gloersen P, Zwally H J, Wilheit T T, Chang C, Hall D, Gray L, Meeks D C, Bryan M L, Barath F T, Elachi C, Leberl F, Farr T Microwave remote sensing of sea ice in the AIDJEX Main Experiment, *Boundary-Layer Meteorology* vol 13, 309-337 (1978)

7. Campbell W J, Gloersen P, and Zwally H J, Aspects of Arctic sea ice observable by sequential passive microwave observations from the Nimbus-5 satellite, in *Arctic Technology and Policy, edited by Ira Dyer and Chryssostomos Chryssostomidis*, pp 197-22 (Hemisphere, Washington 1984)

8. FIGURES CAPTIONS

Figure 1. Processing scheme for the SMMR data in near real-time.

Figure 2. Sea ice concentration map calculated from SMMR radiances and displayed as ASCII characters (see text for legend).

Figure 3. Time-history of the average calculated multiyear sea ice fraction in the area defined in Figure 4. during MIZEX/East'83.

Figure 4. Grid map overlay used for determining the area in which data were averaged for Figure 3.

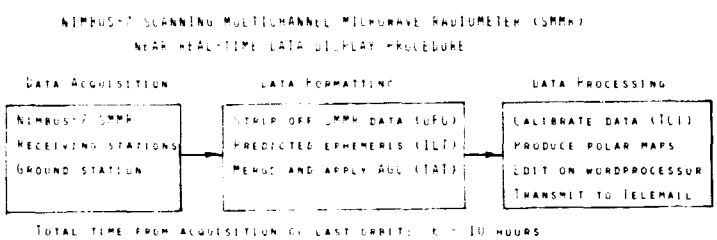

Figure 1. Processing scheme for the SMMR data in near real-time.

OF POOR

ORIGINAL
OF POOR QUALITY

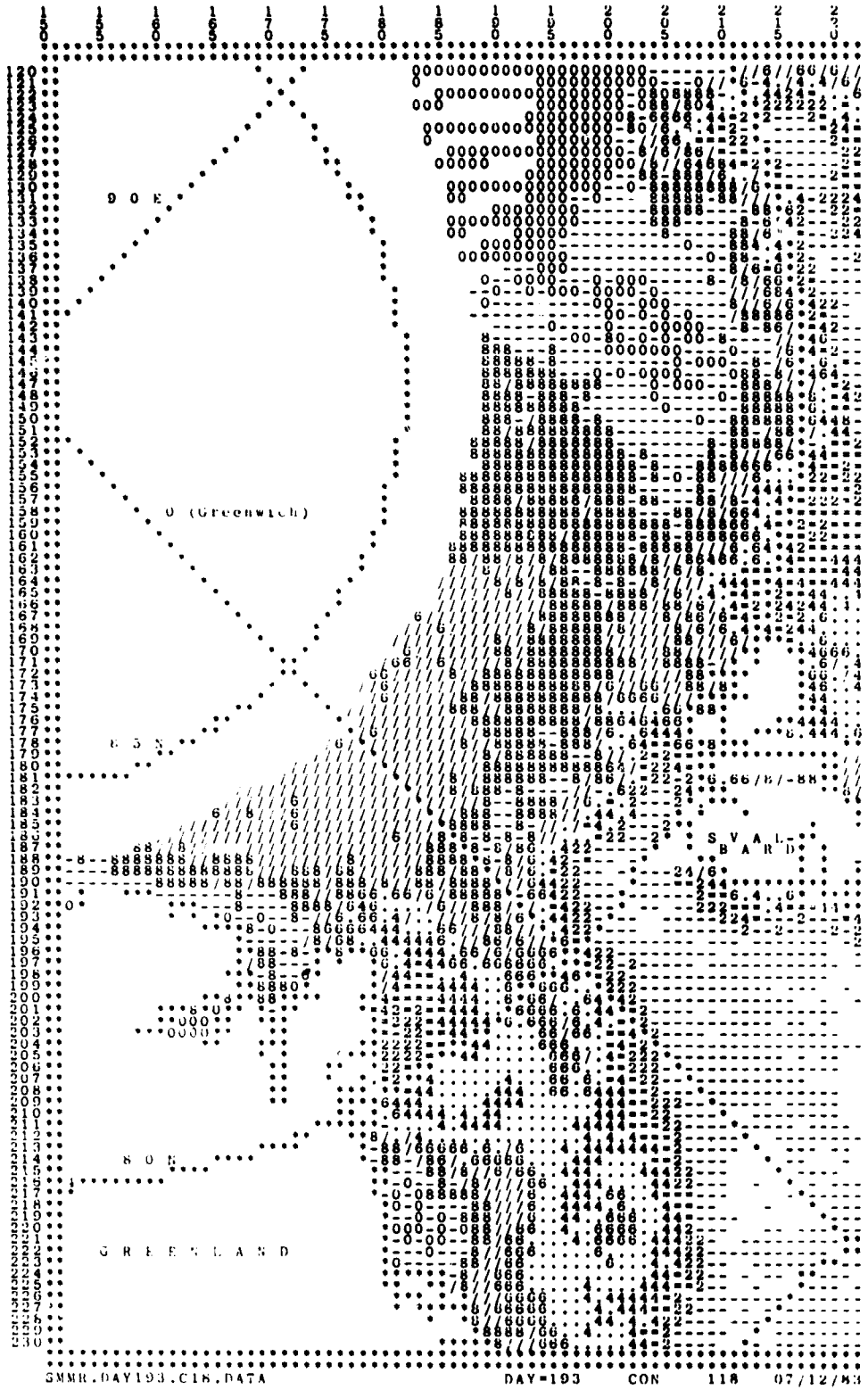

Figure 2. Sea ice concentration map calculated from SMMR radiances and displayed as ASCII characters (see text for legend).

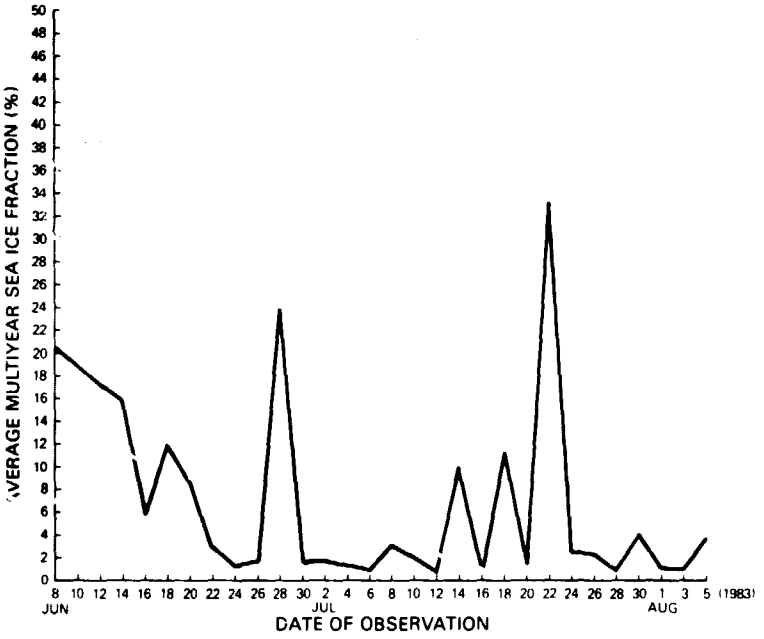

Figure 3. Time-history of the average calculated multiyear sea ice fraction in the area defined in Figure 4. during MIZEX/East'83.

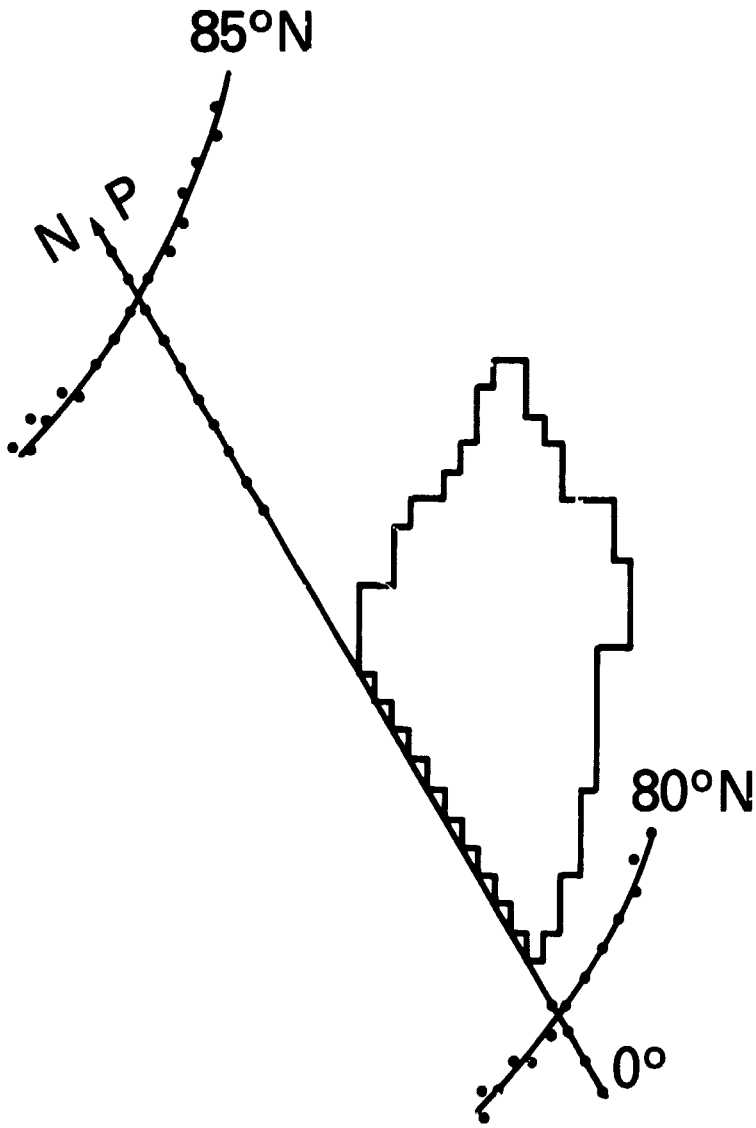

Figure 4. Grid map overlay used for determining the area in which data were averaged for Figure 3.

APPENDIX A

GRID-PRINT MAPS OF TOTAL SEA ICE CONCENTRATION DURING MIZEX/EAST'83

PRECEDING PAGE BLANK NOT FILMED

PAGE 10 INTENTIONALLY BLANK

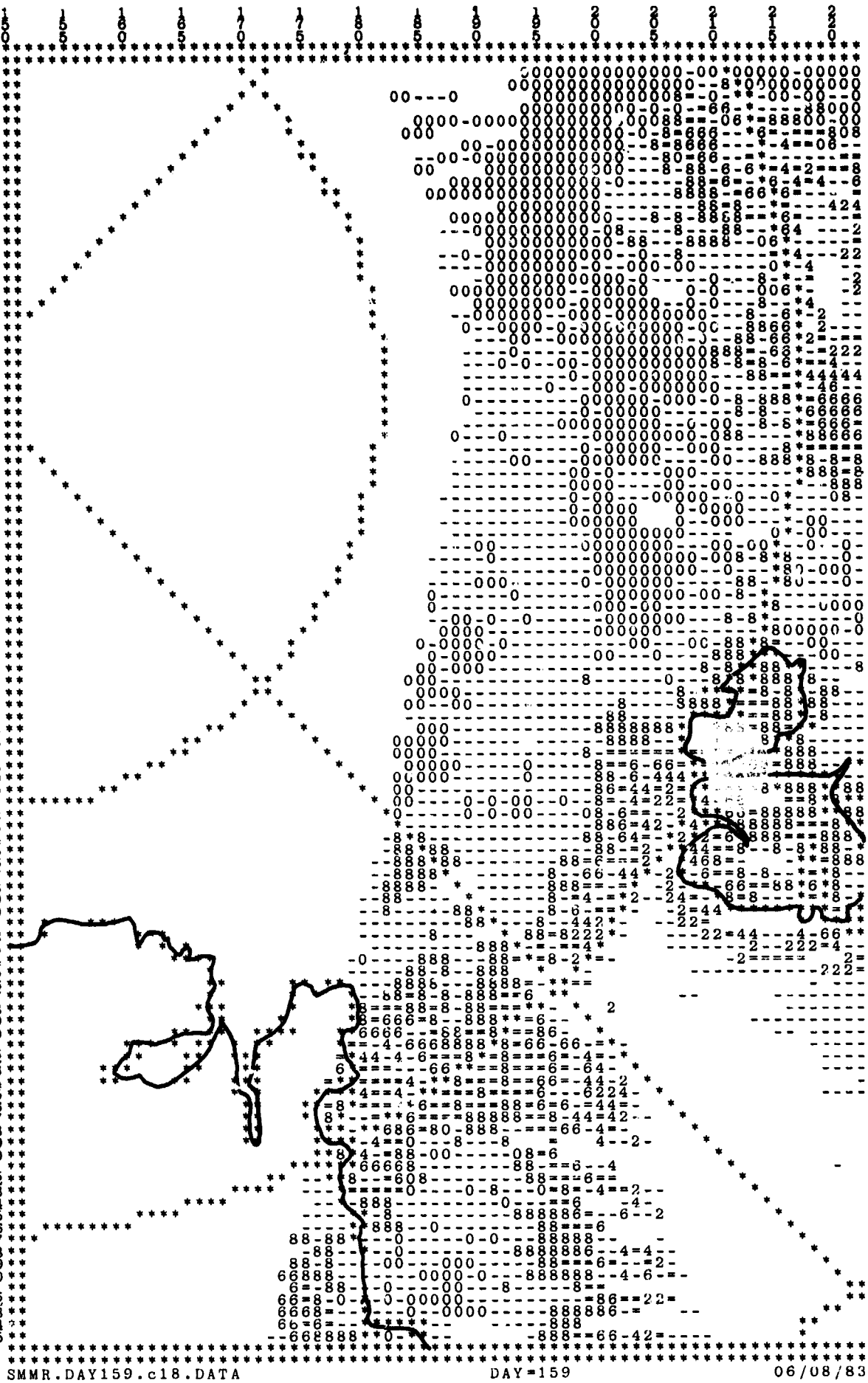

PAGE 12 INTENTIONALLY BLANK

PRECEDING PAGE BLANK NOT FILMED

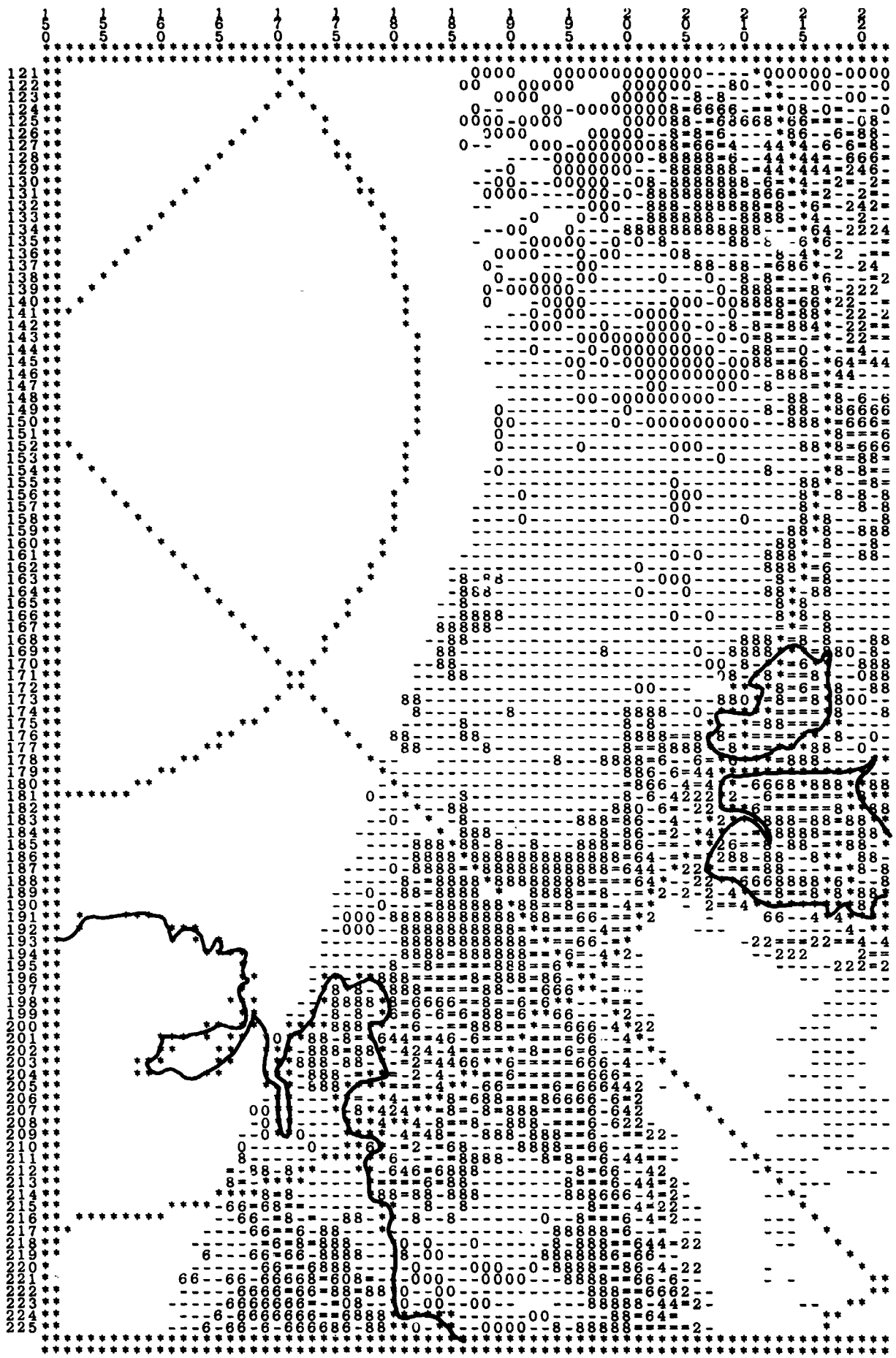
SMMR.DAY161.c18.DATA
DAY=161
06/10/83

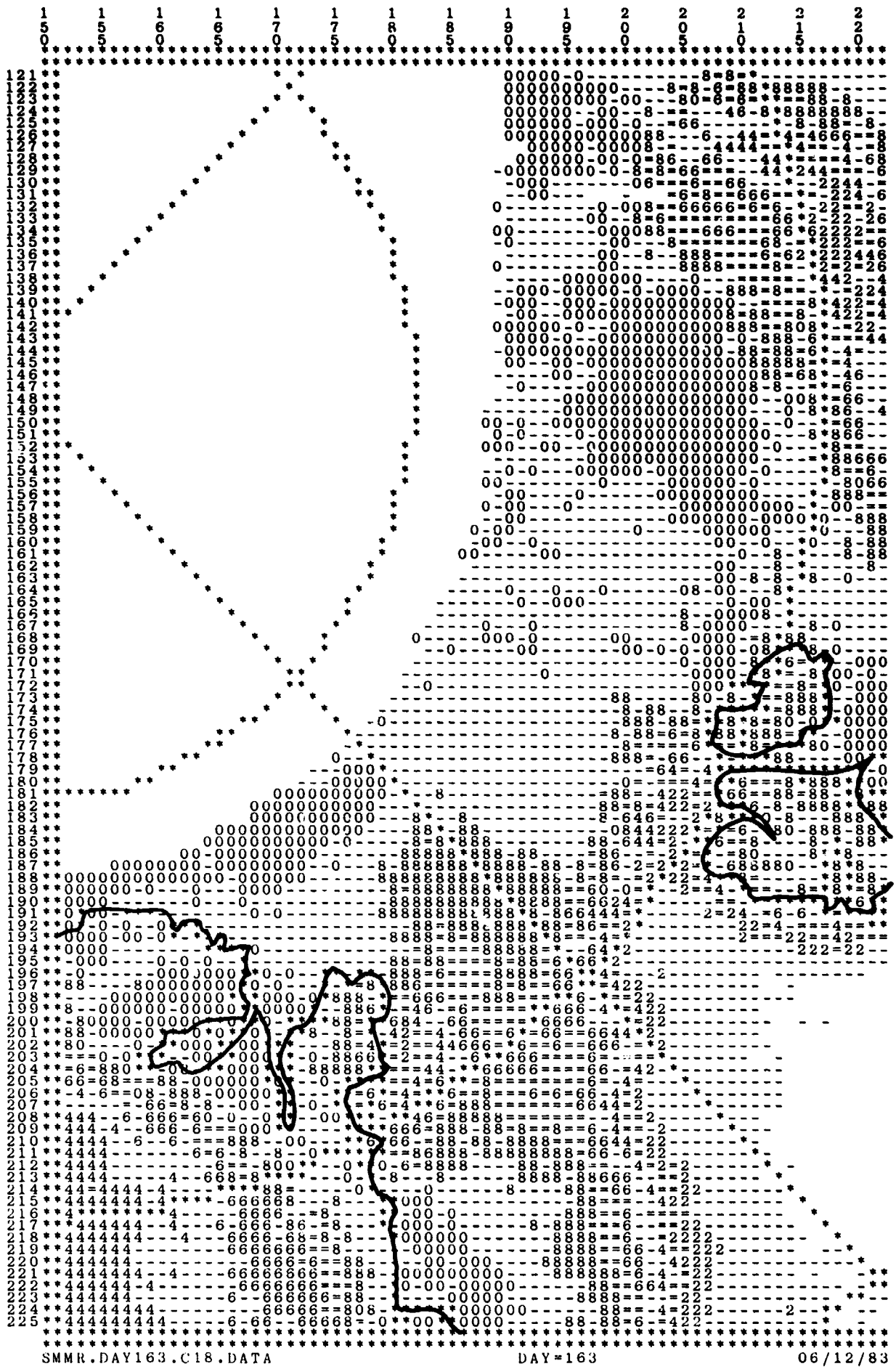
SMMR.DAY163.C18.DATA
DAY=163
06/12/83

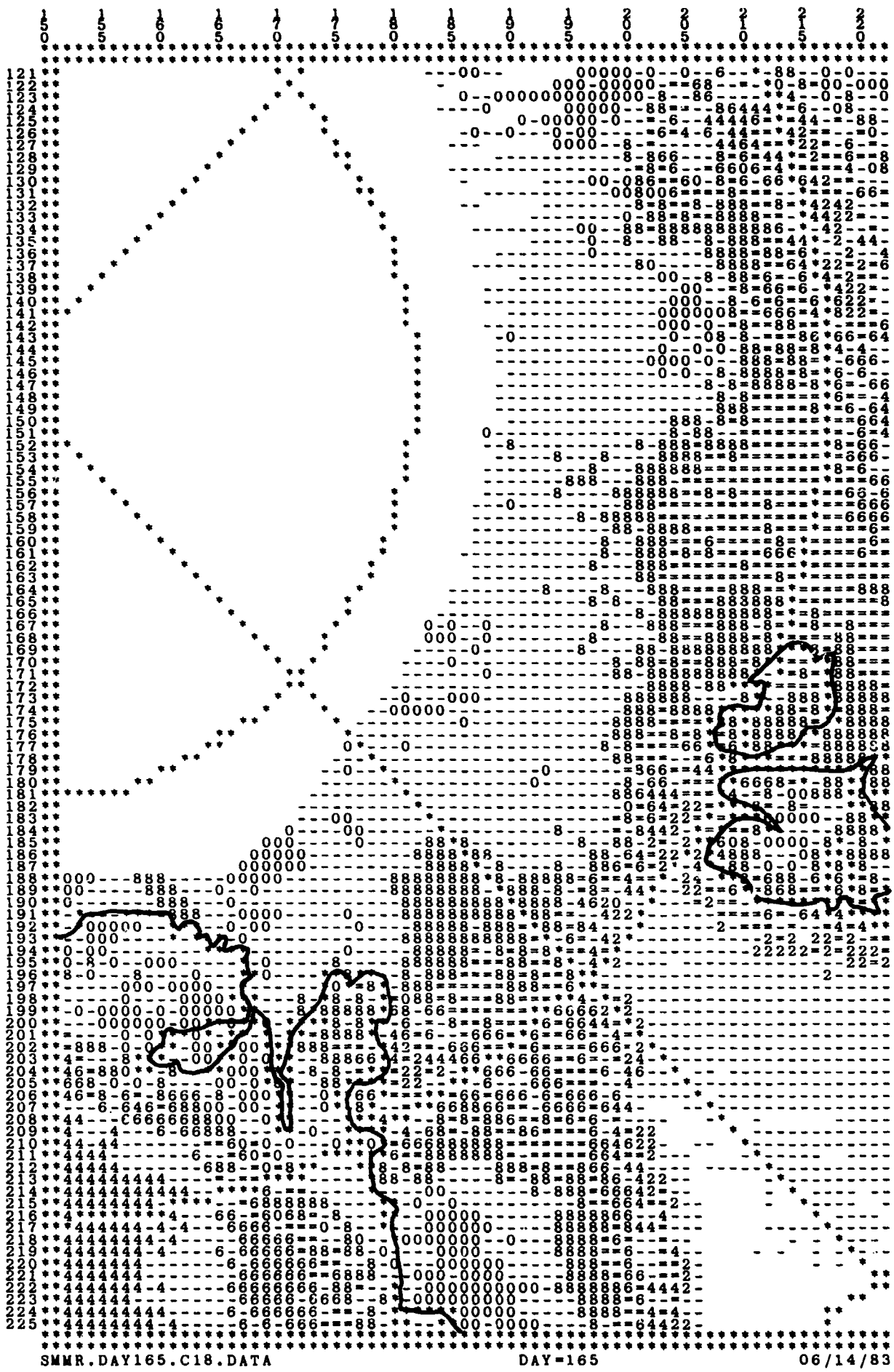
SMMR.DAY165.C18.DATA
DAY=165
06/14/83

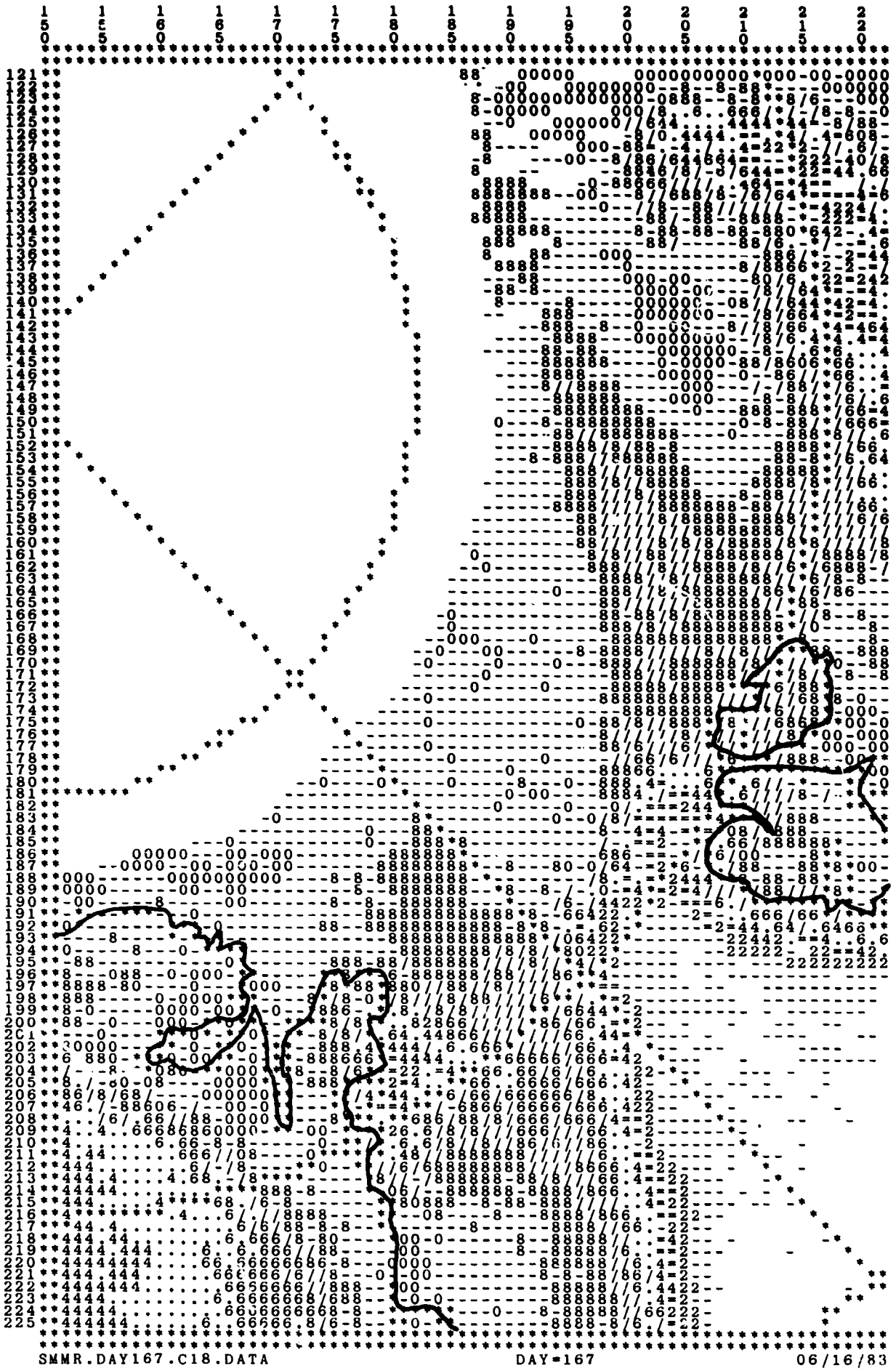
SMMR.DAY167.C18.DATA
DAY=167
06/16/83

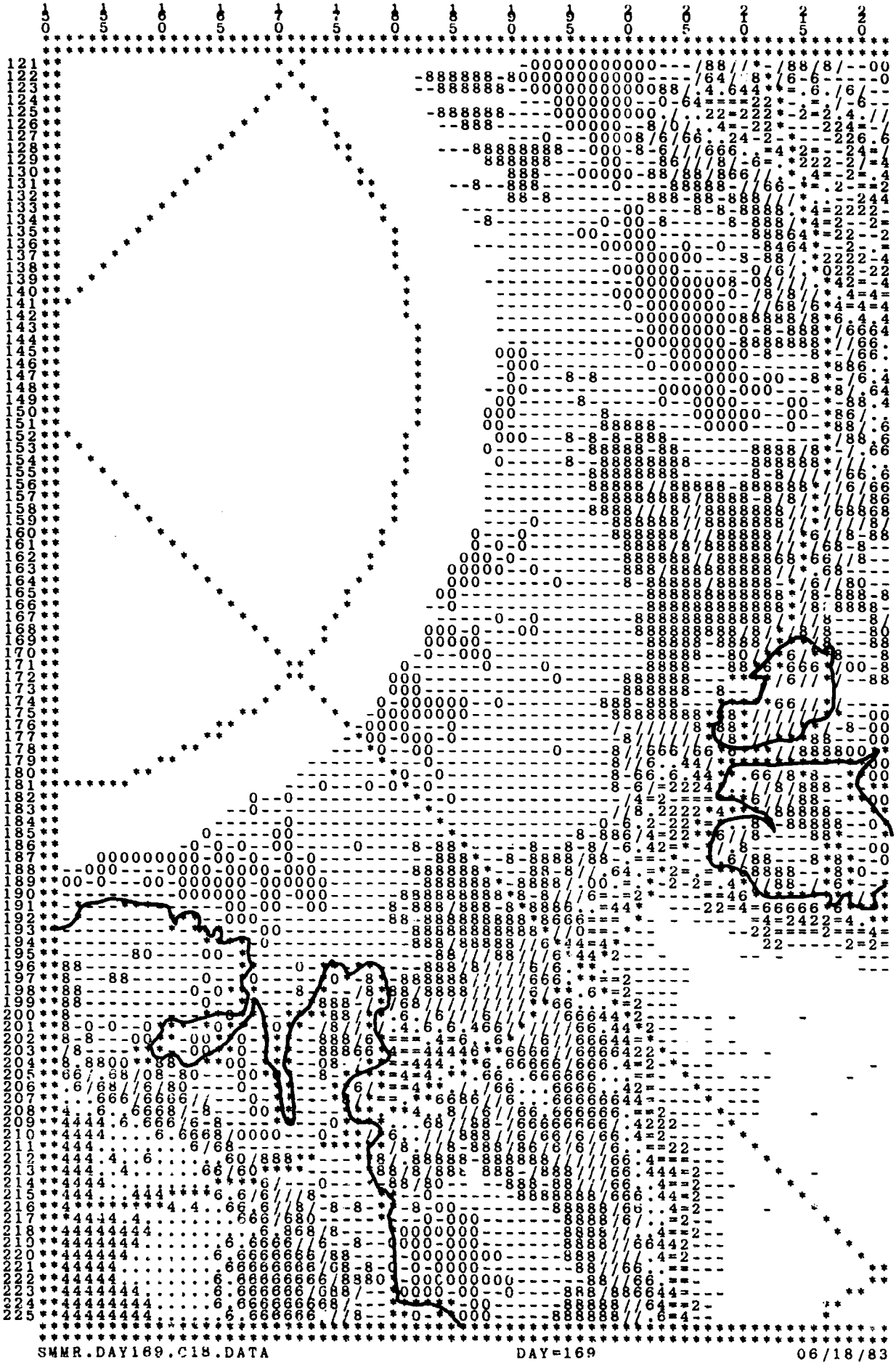
SMMR.DAY169.C18.DATA
DAY=169
06/18/83

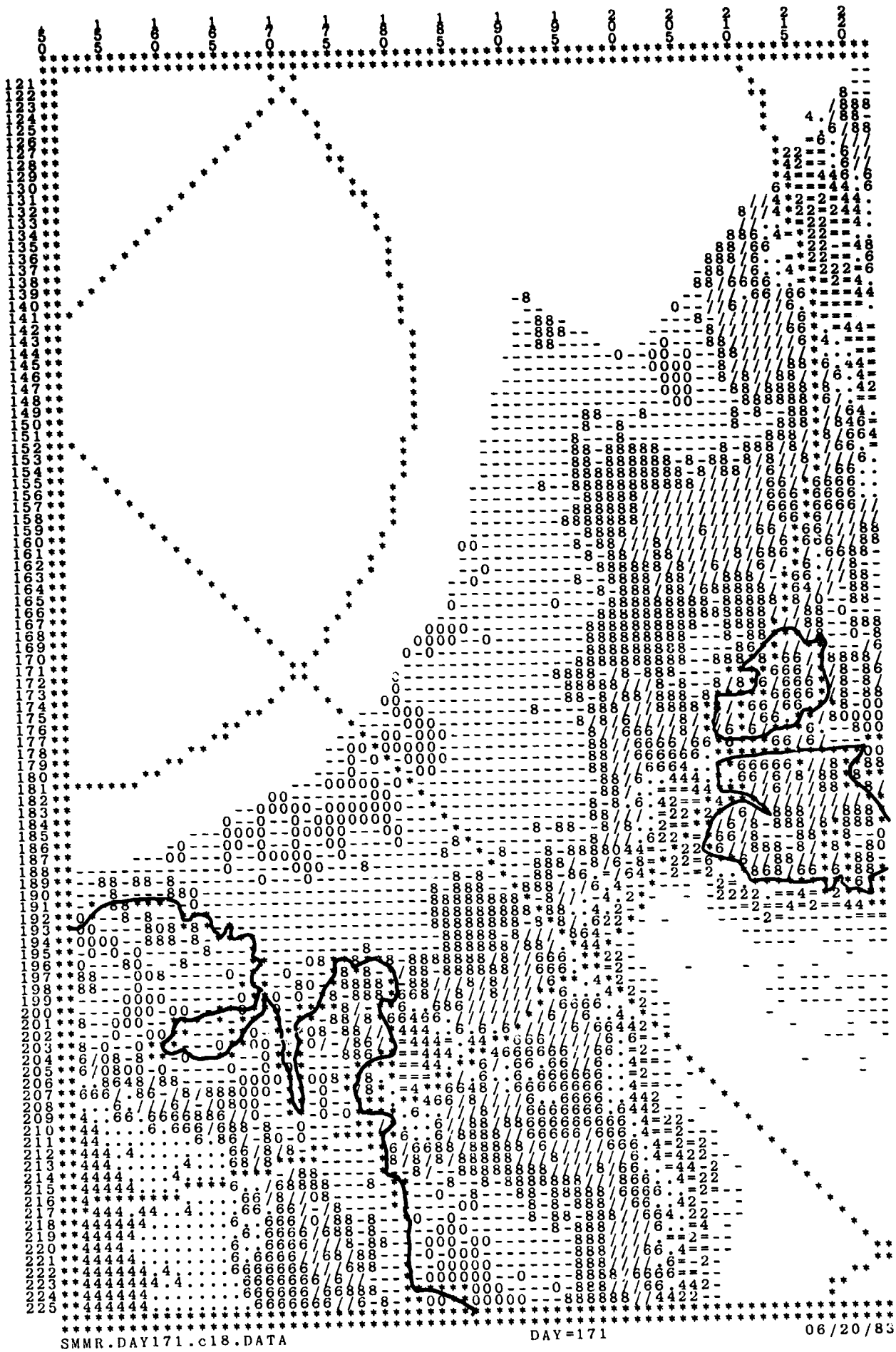
SMMR.DAY171.c18.DATA
DAY=171
06/20/83

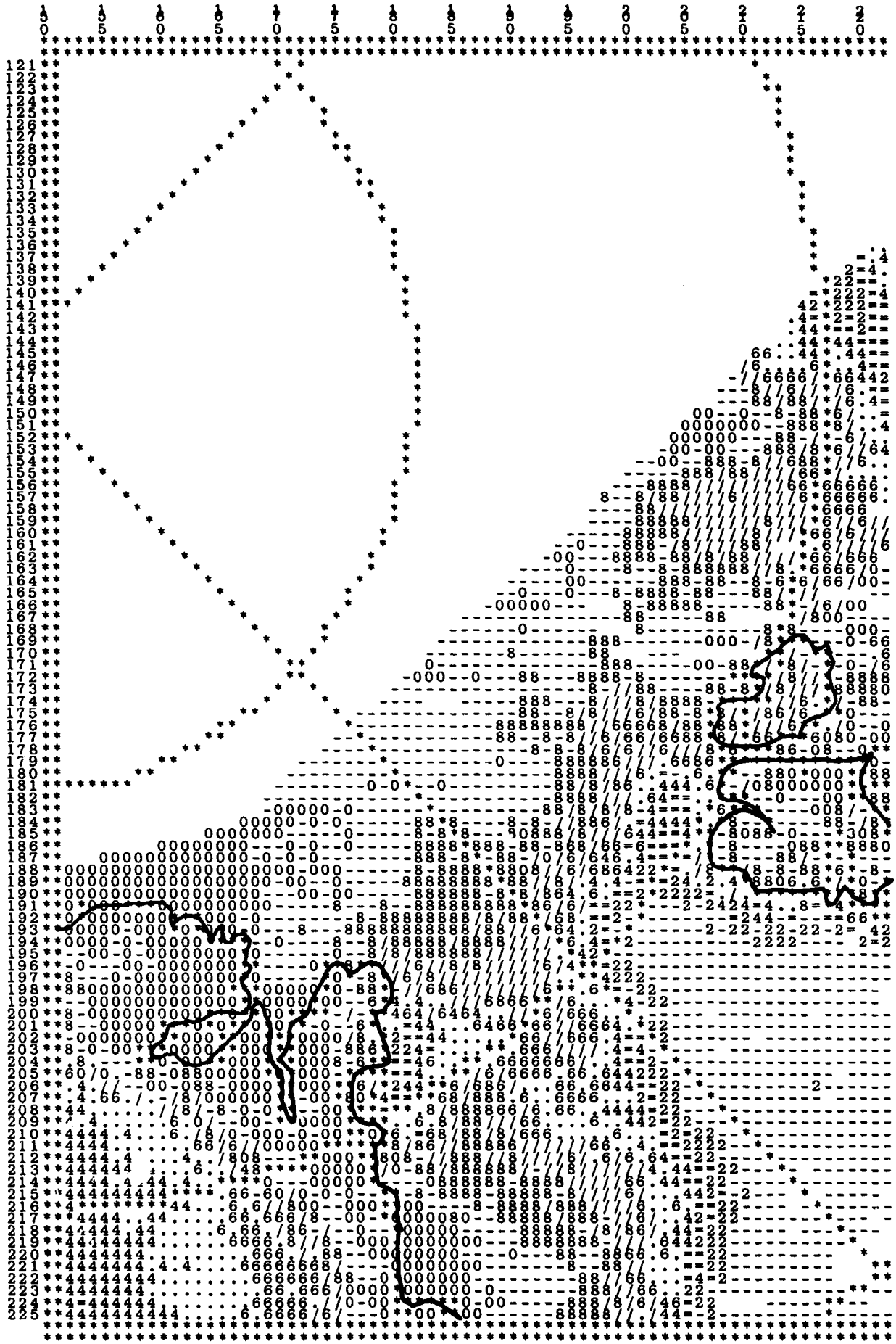
SMMR.DAY173.C18.DATA
DAY=173
06/22/83

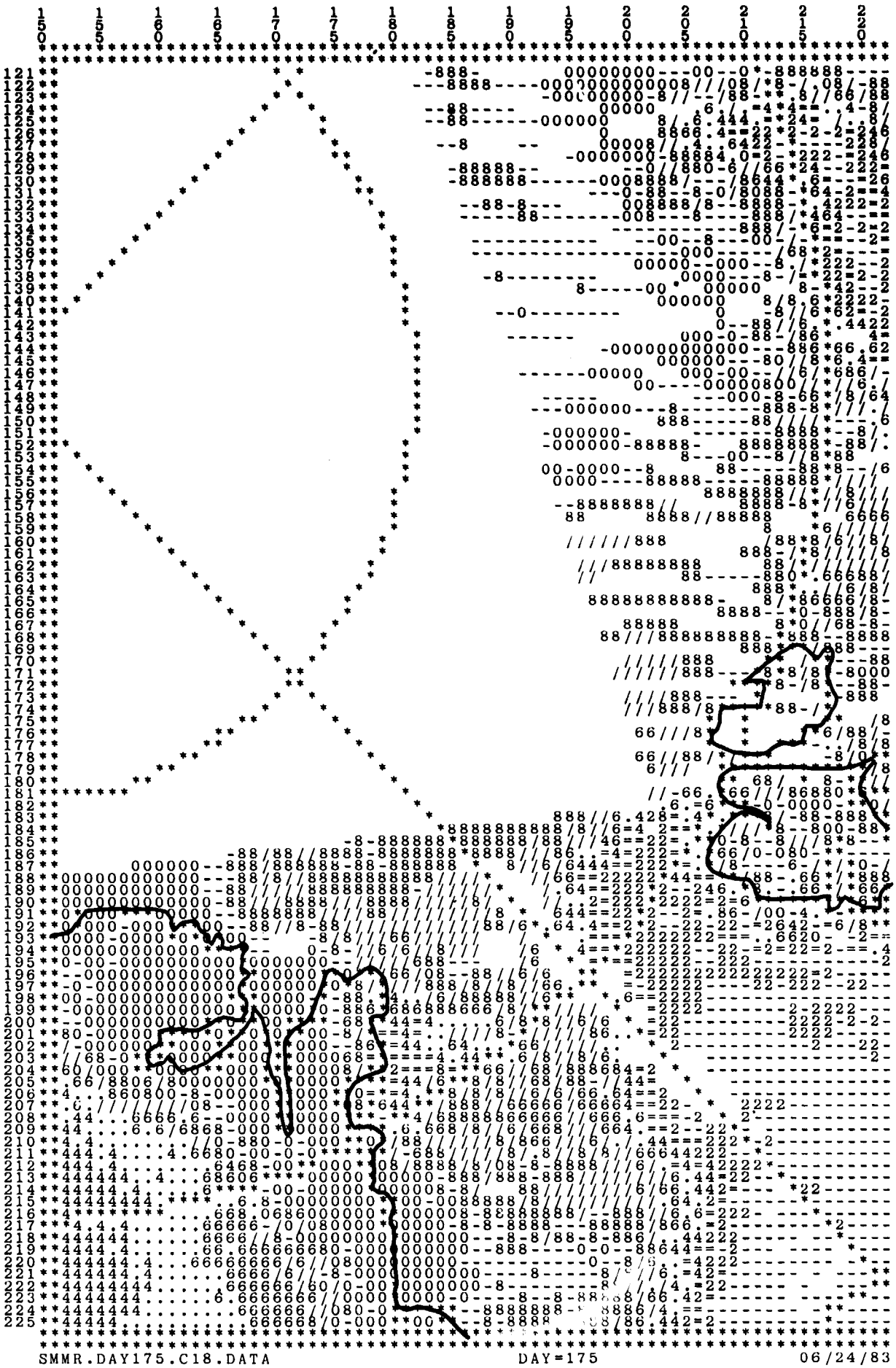
SMMR.DAY175.C18.DATA
DAY=175
06/24/83

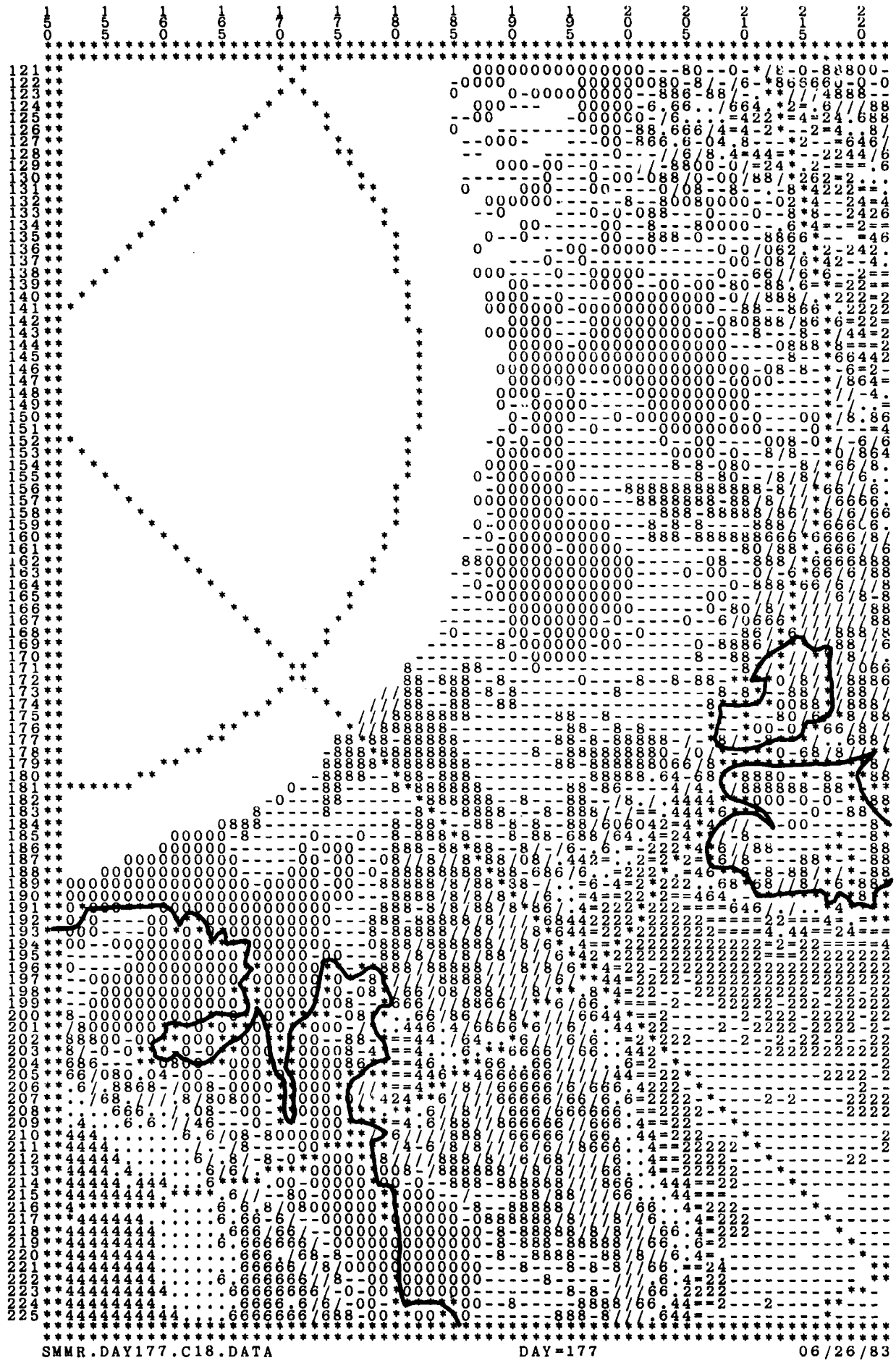
SMMR.DAY177.C18.DATA
DAY=177
06/26/83

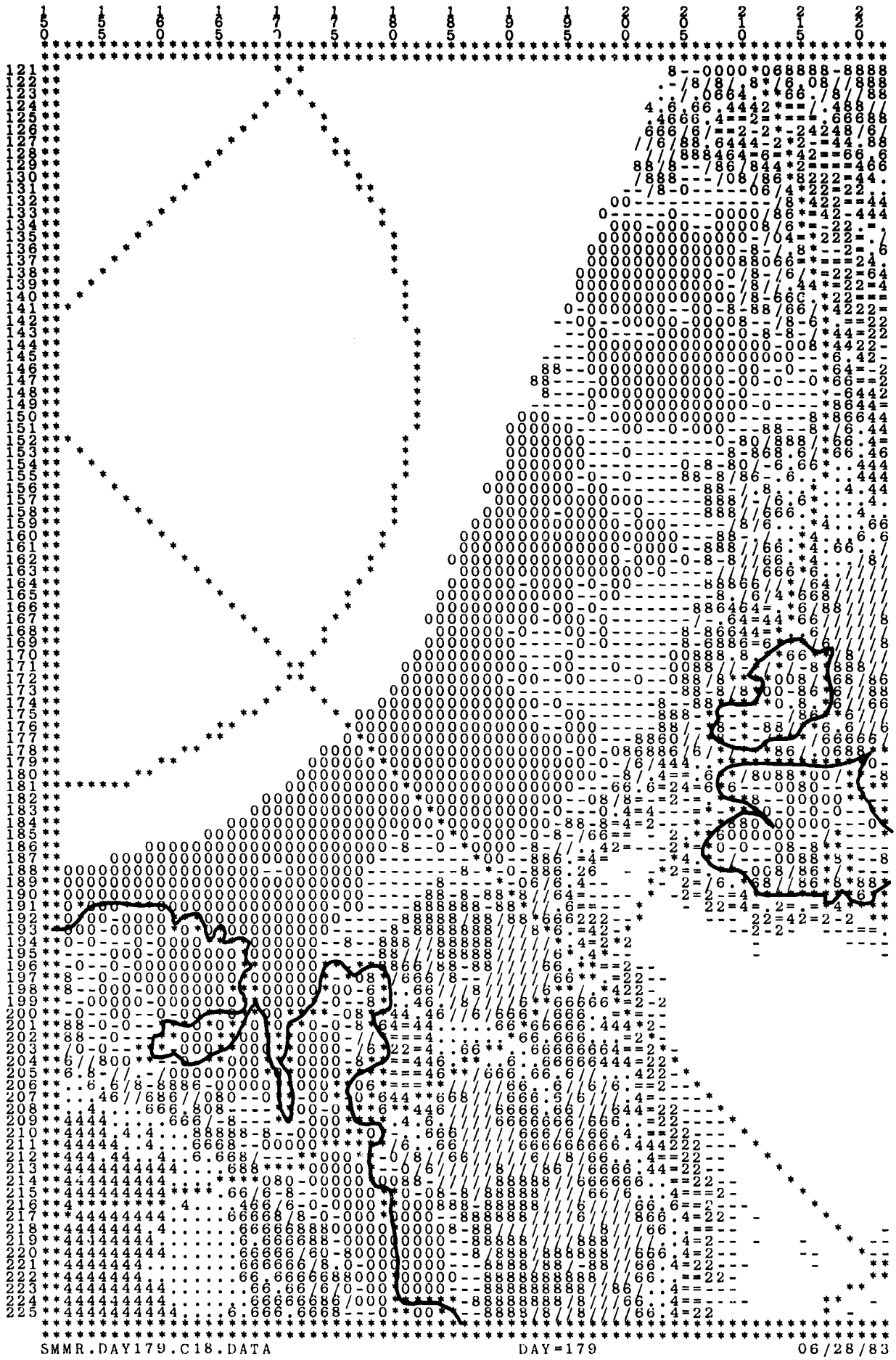
SMMR.DAY179.C18.DATA
DAY=179
06/28/83

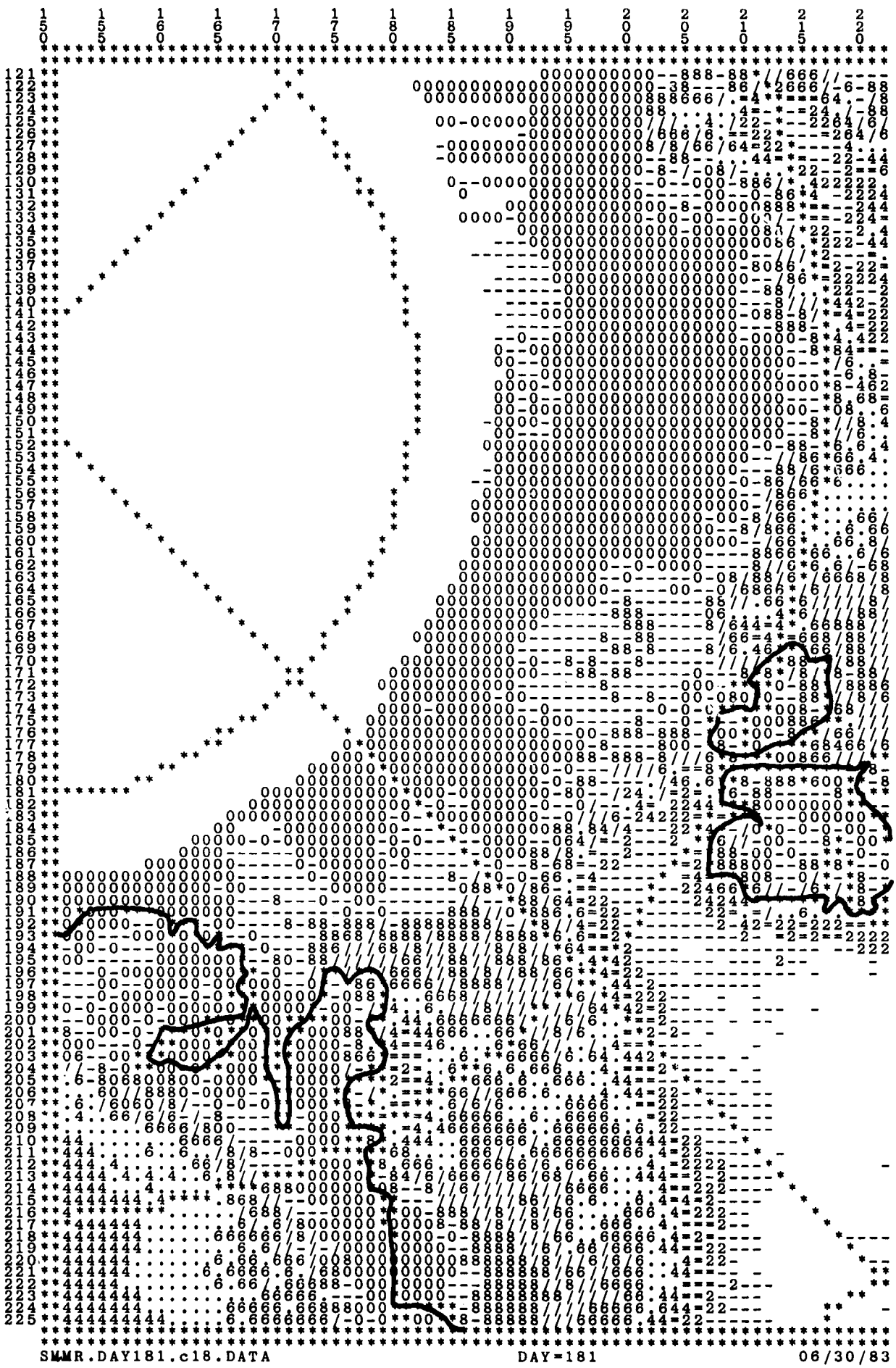
SMMR.DAY181.c18.DATA
DAY=181
06/30/83

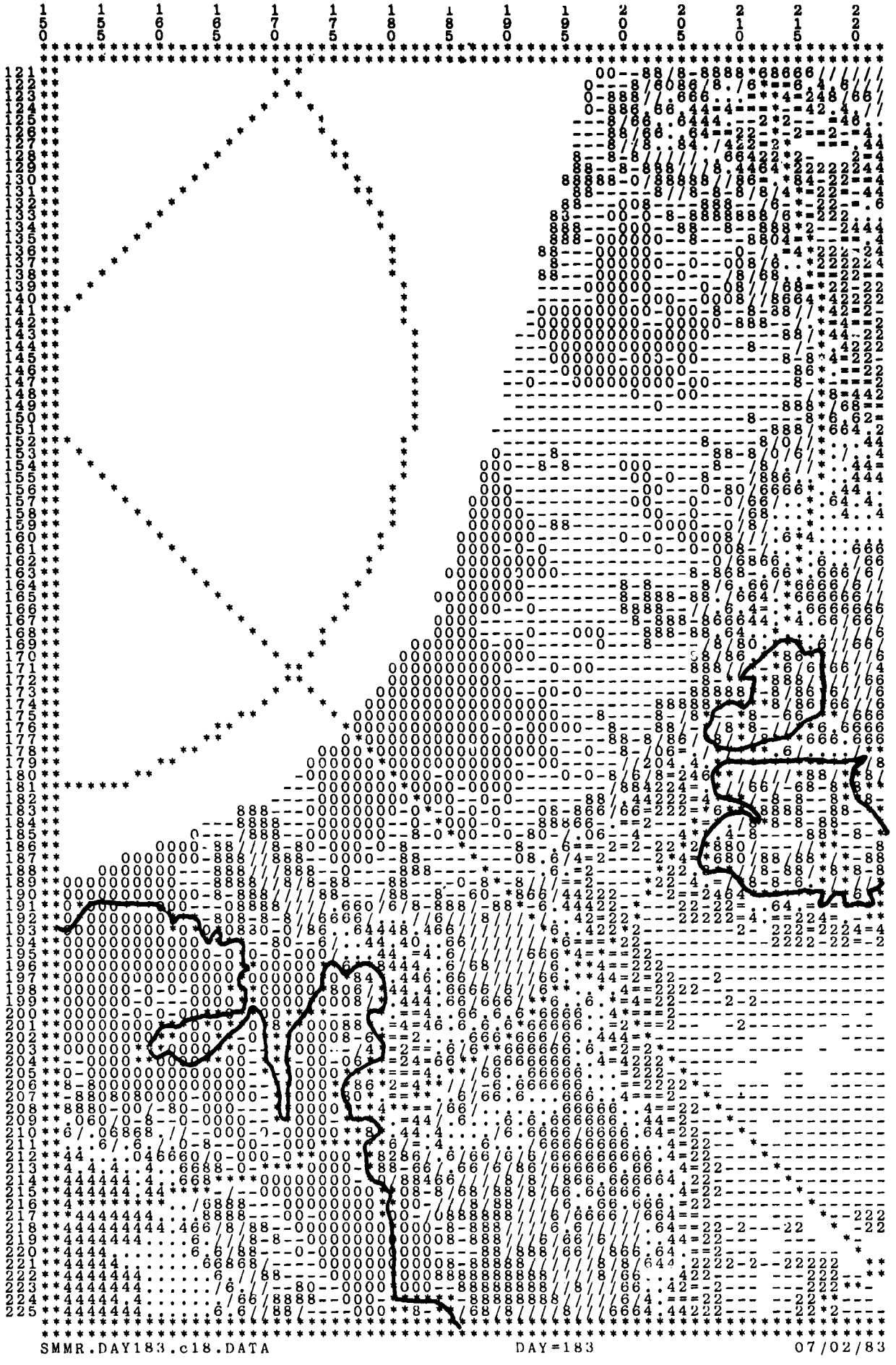
SMMR.DAY183.c18.DATA
DAY=183
07/02/83

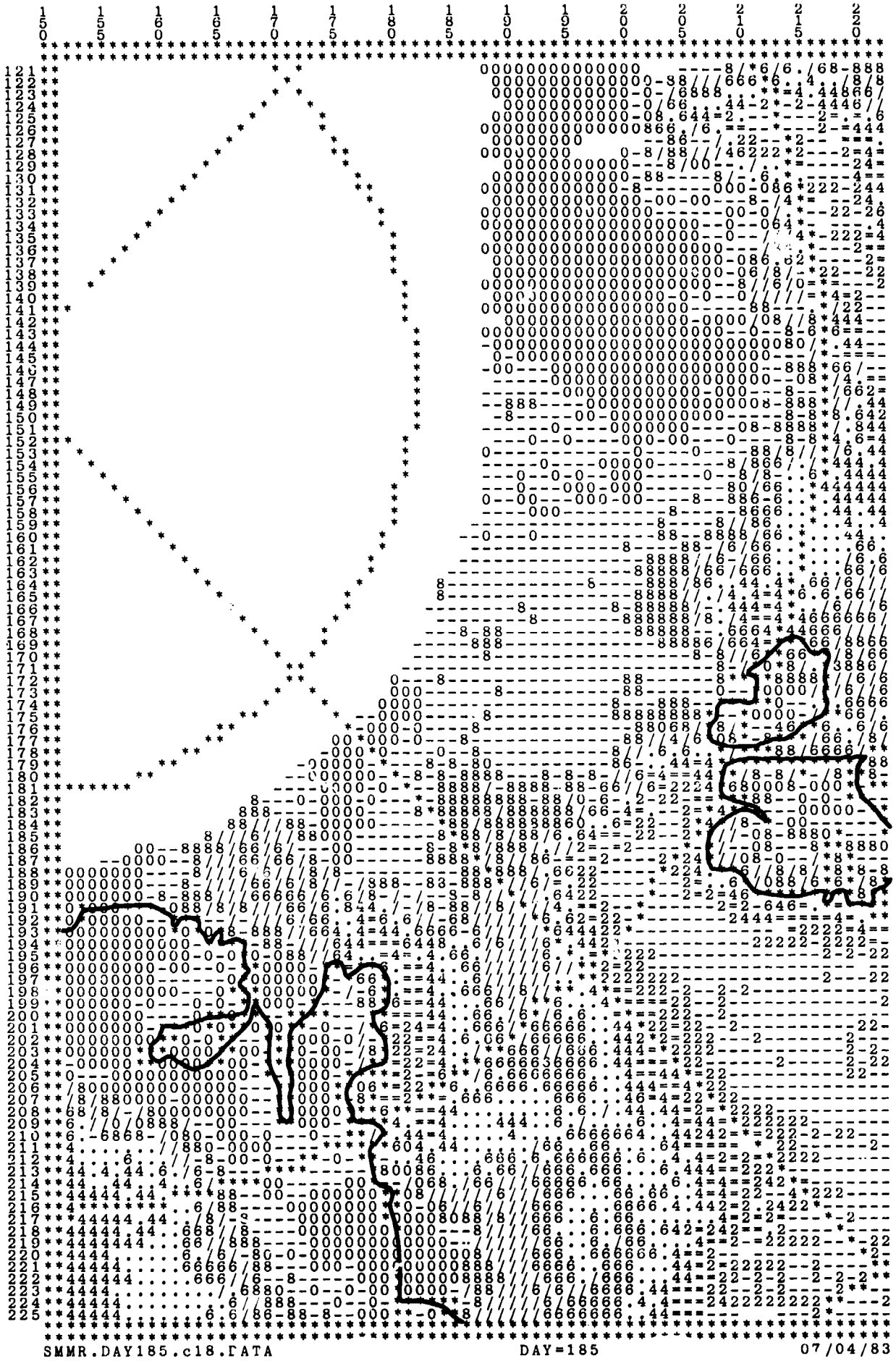
SMMR.DAY185.c18.DATA
DAY=185
07/04/83

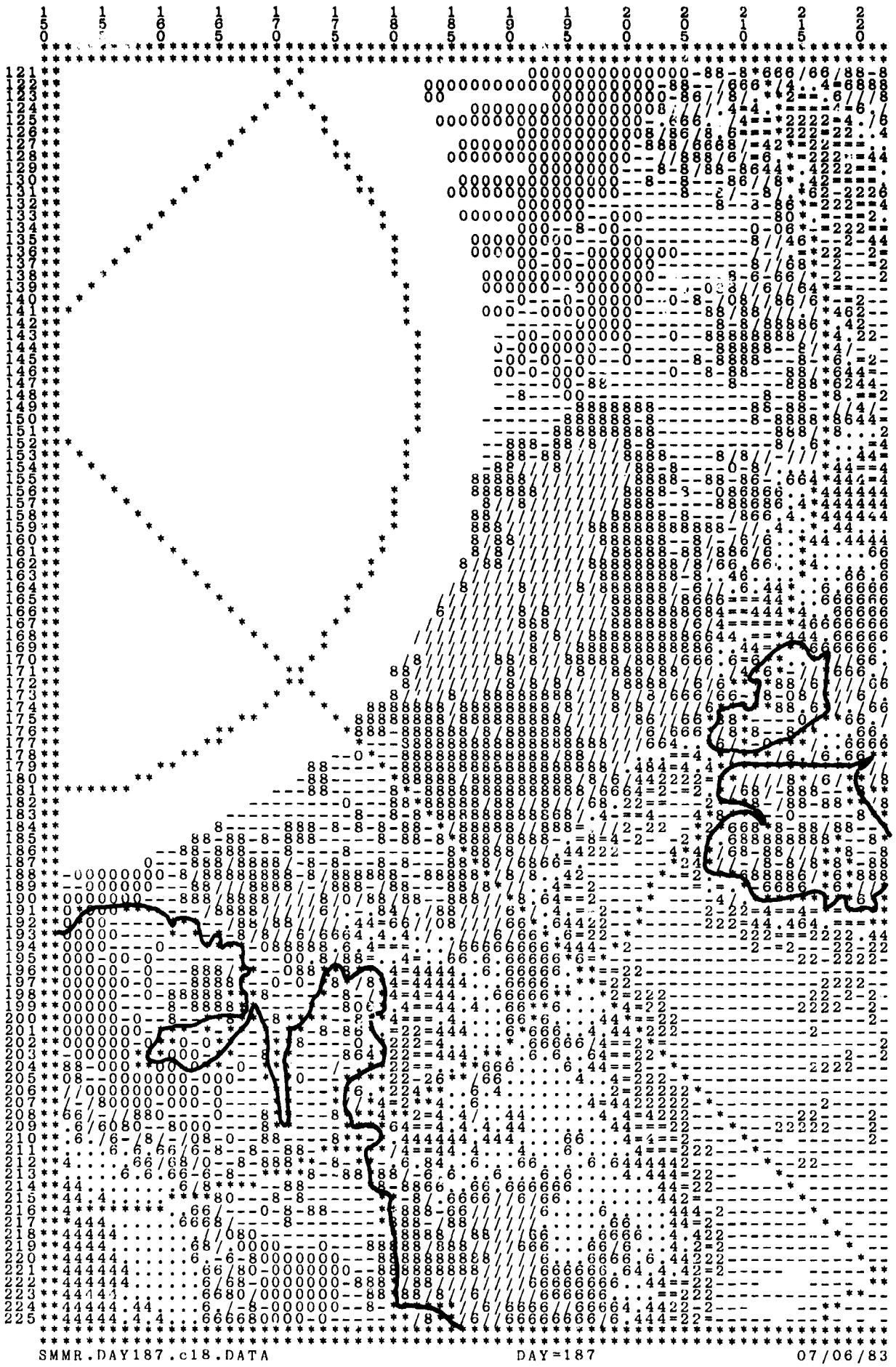
SMMR.DAY187.c18.DATA
DAY=187
07/06/83

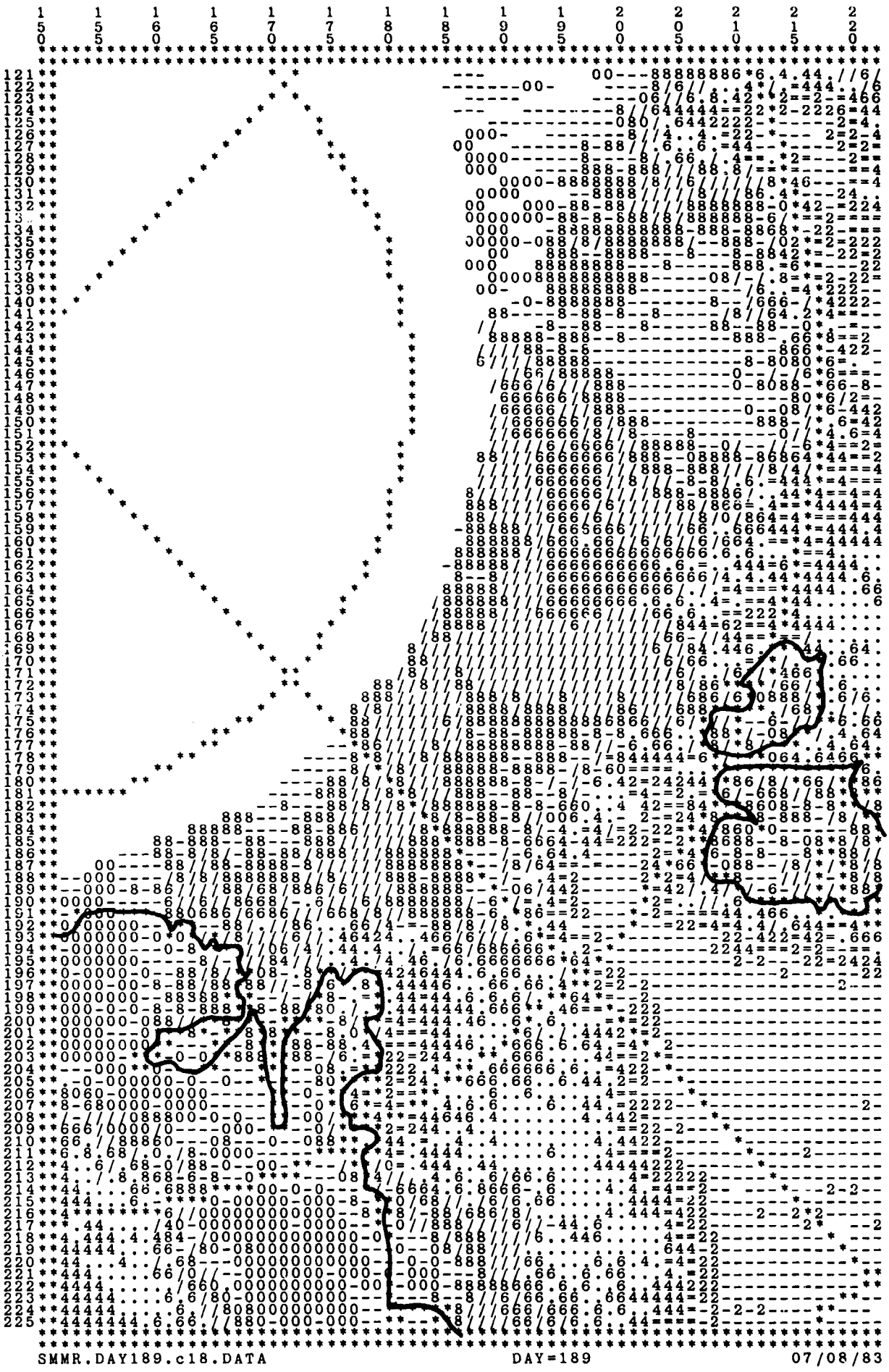
SMMR.DAY189.c18.DATA
DAY=189
07/08/83

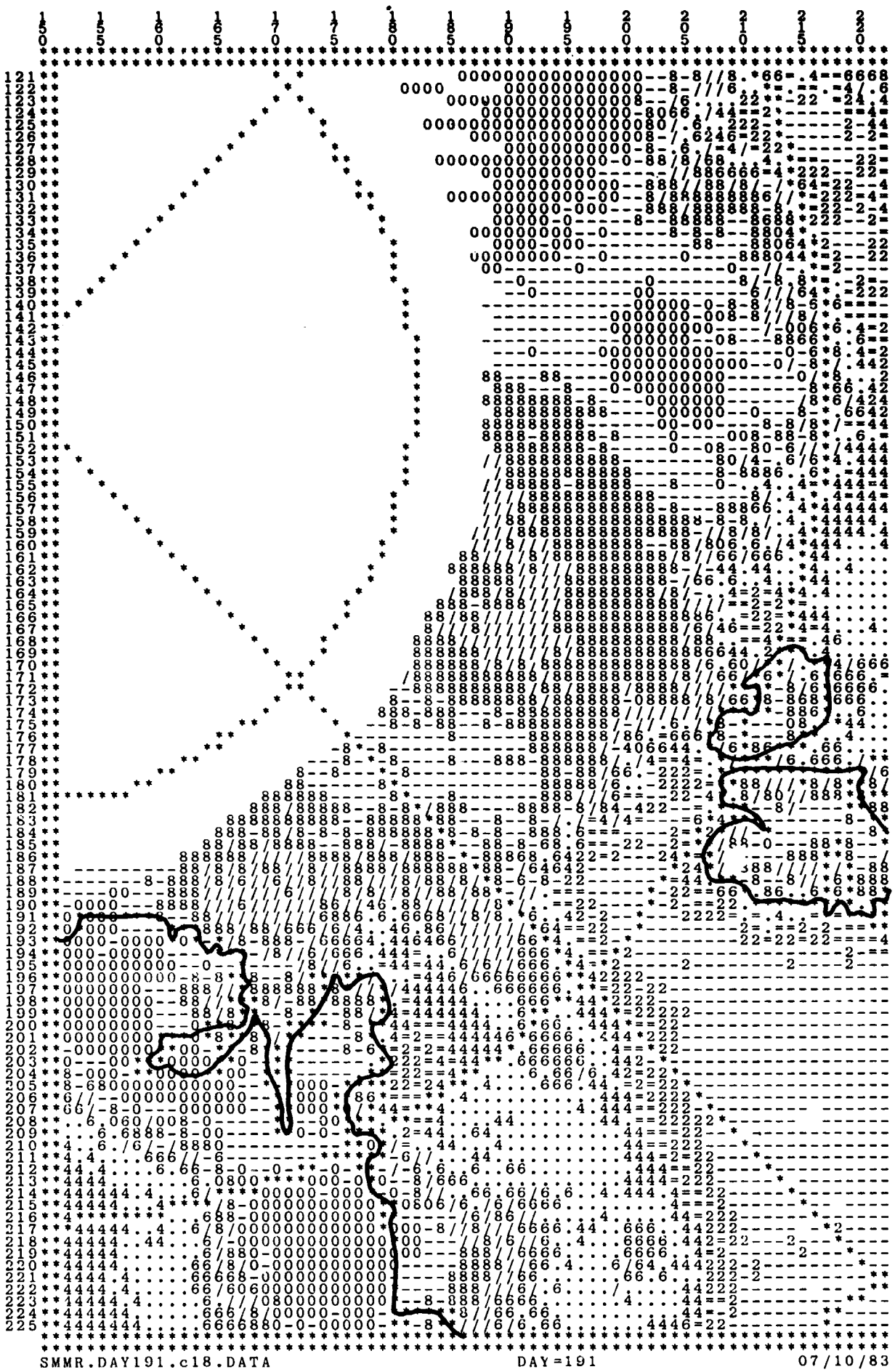
SMMR.DAY191.c18.DATA
DAY=191
07/10/83

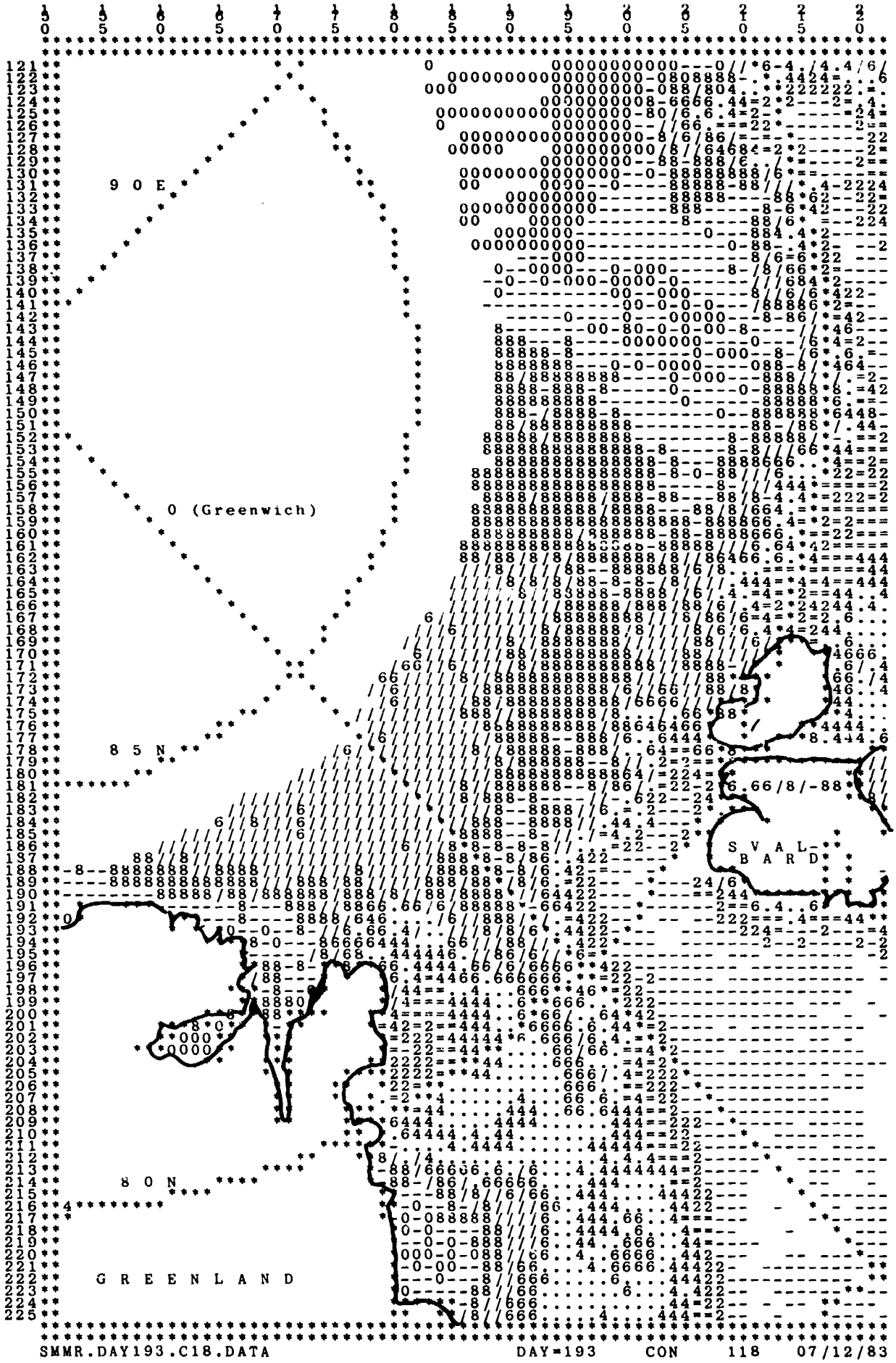
90 E
0 (Greenwich)
85 N
80 N
GREENLAND
SVALBARD
SMMR.DAY193.C18.DATA
DAY=193 CON 118 07/12/83

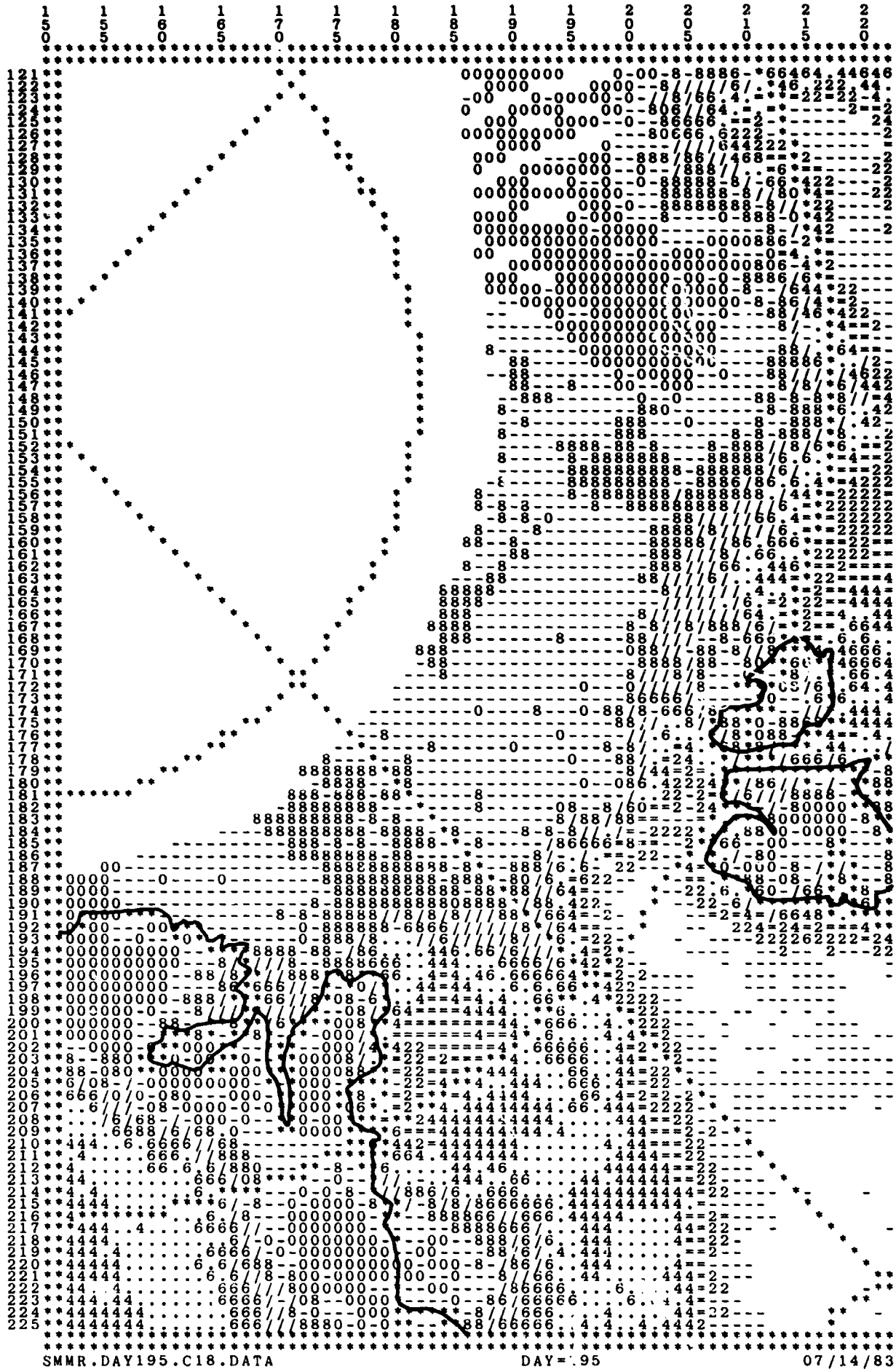
SMMR.DAY195.C18.DATA
DAY=195
07/14/83

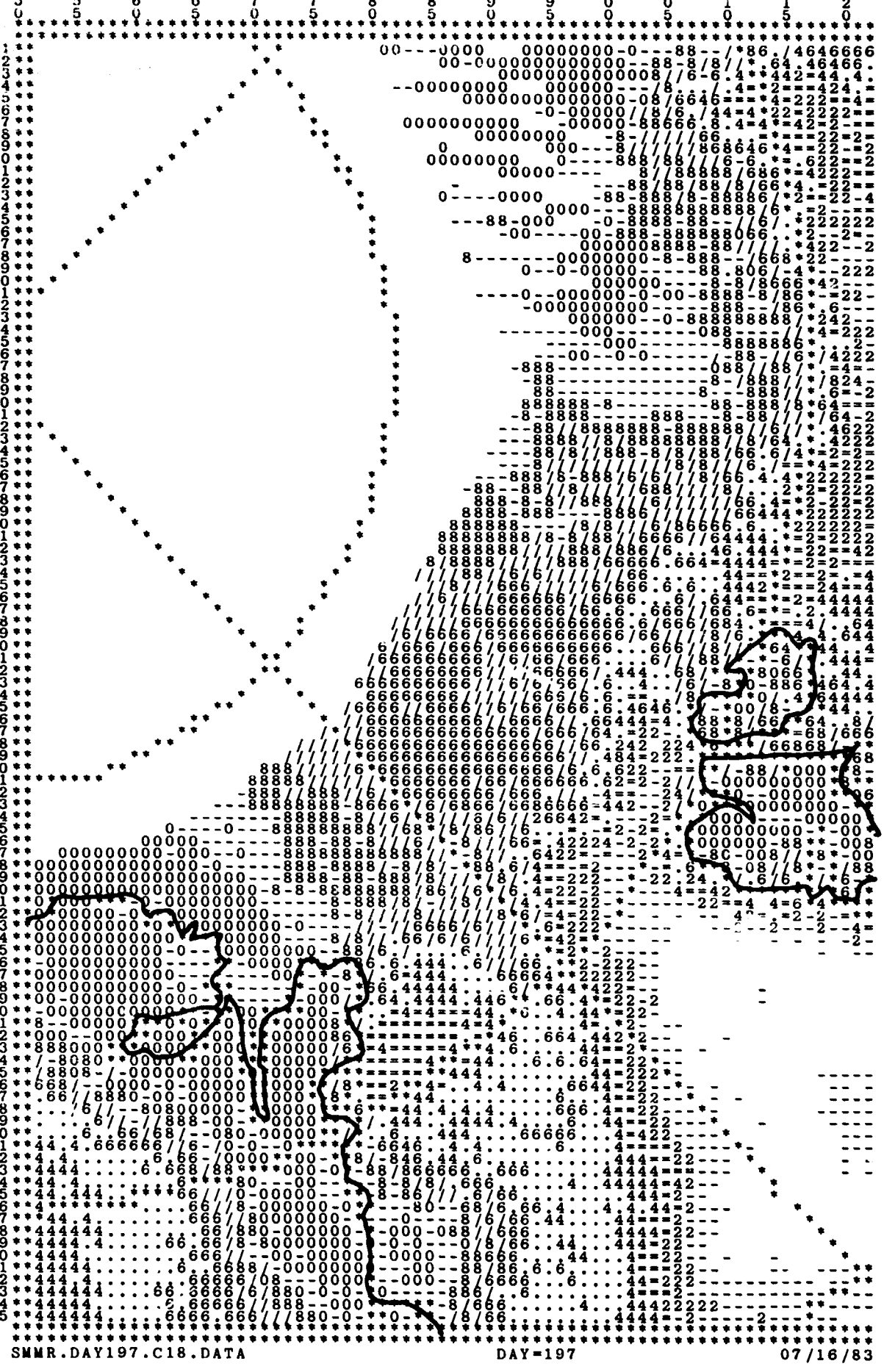
SMMR.DAY197.C18.DATA
DAY=197
07/16/83

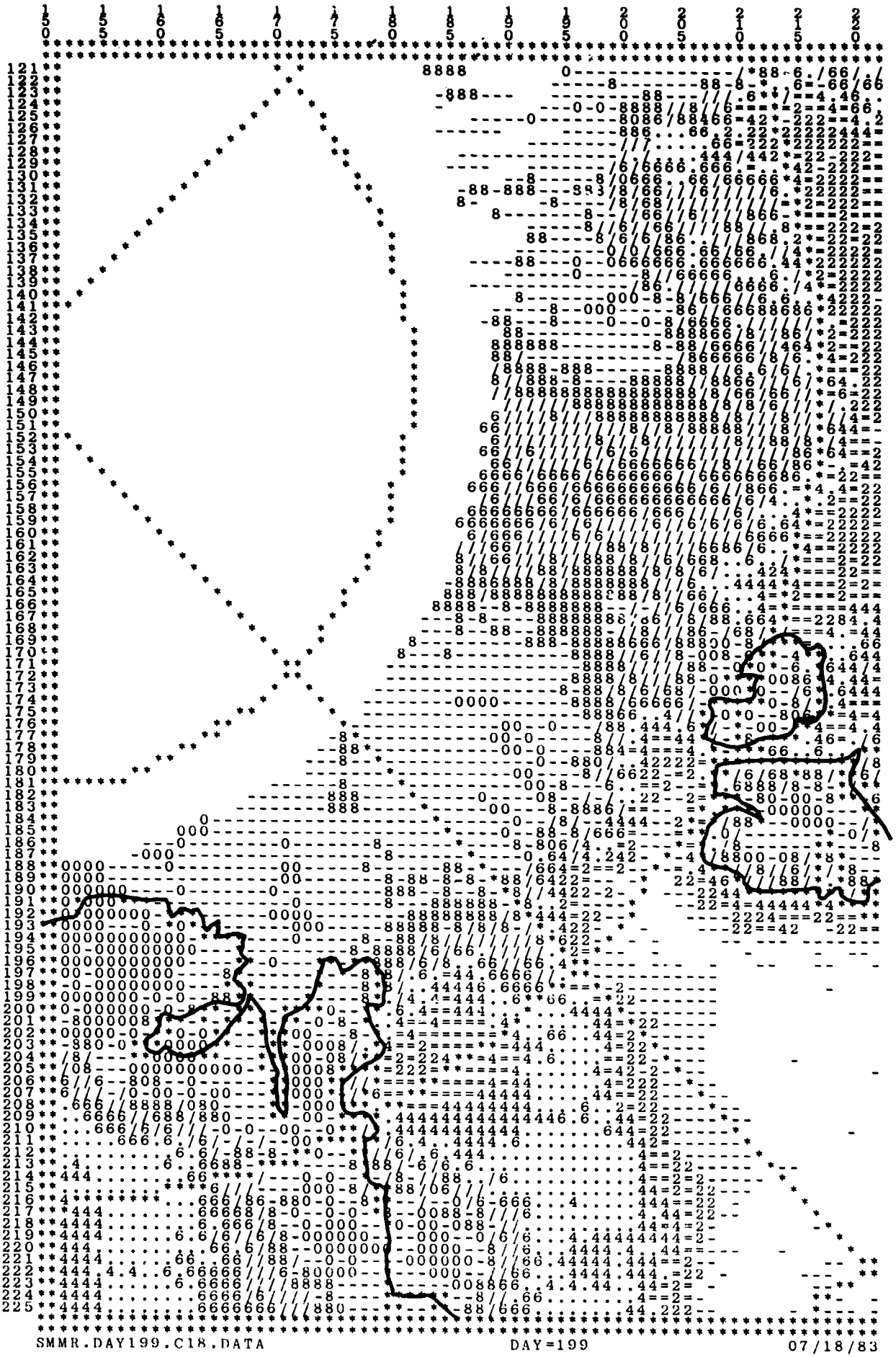
SMMR.DAY199.C18.DATA
DAY=199
07/18/83

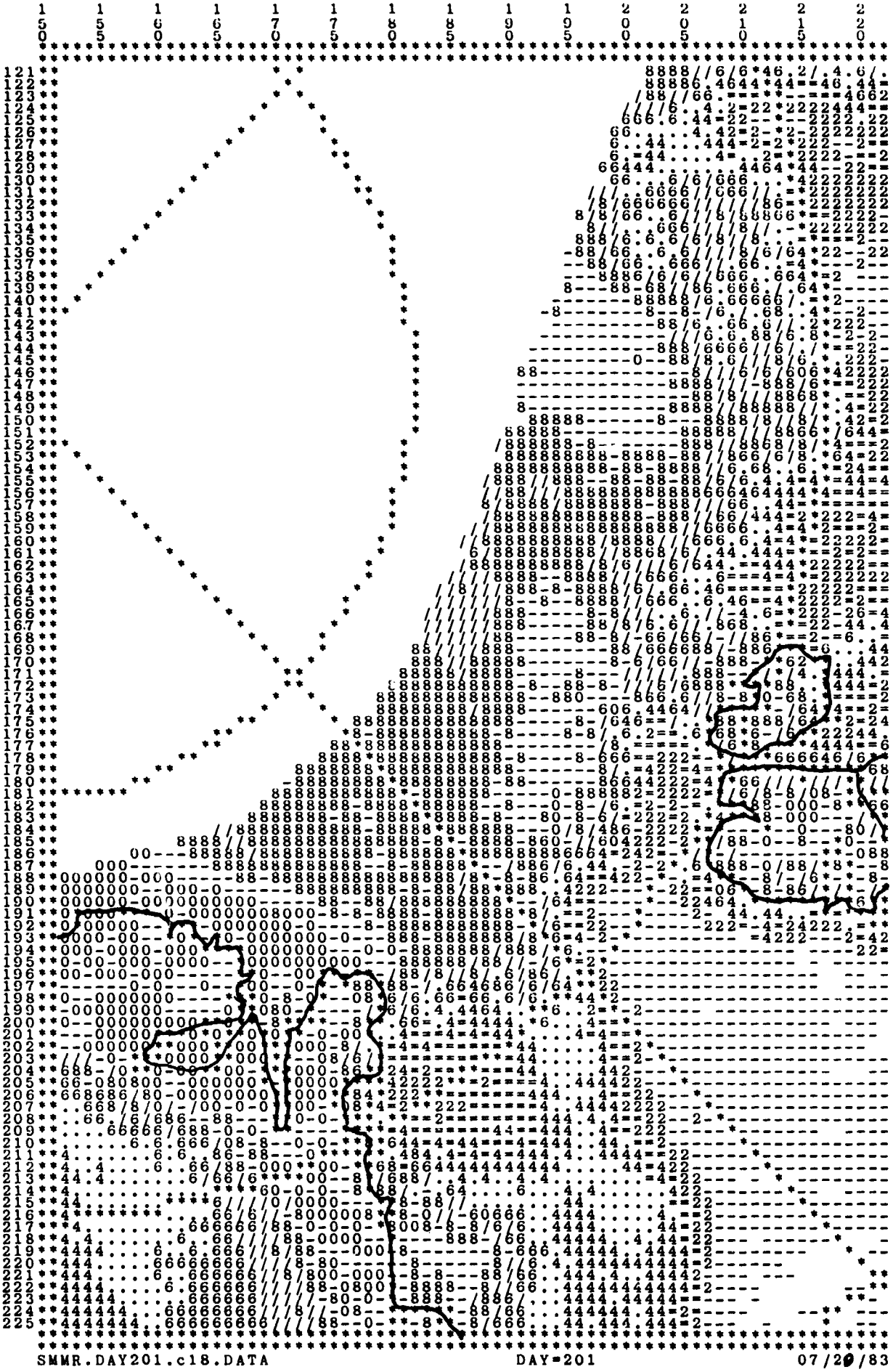
SMMR.DAY201.c18.DATA
DAY=201
07/20/83

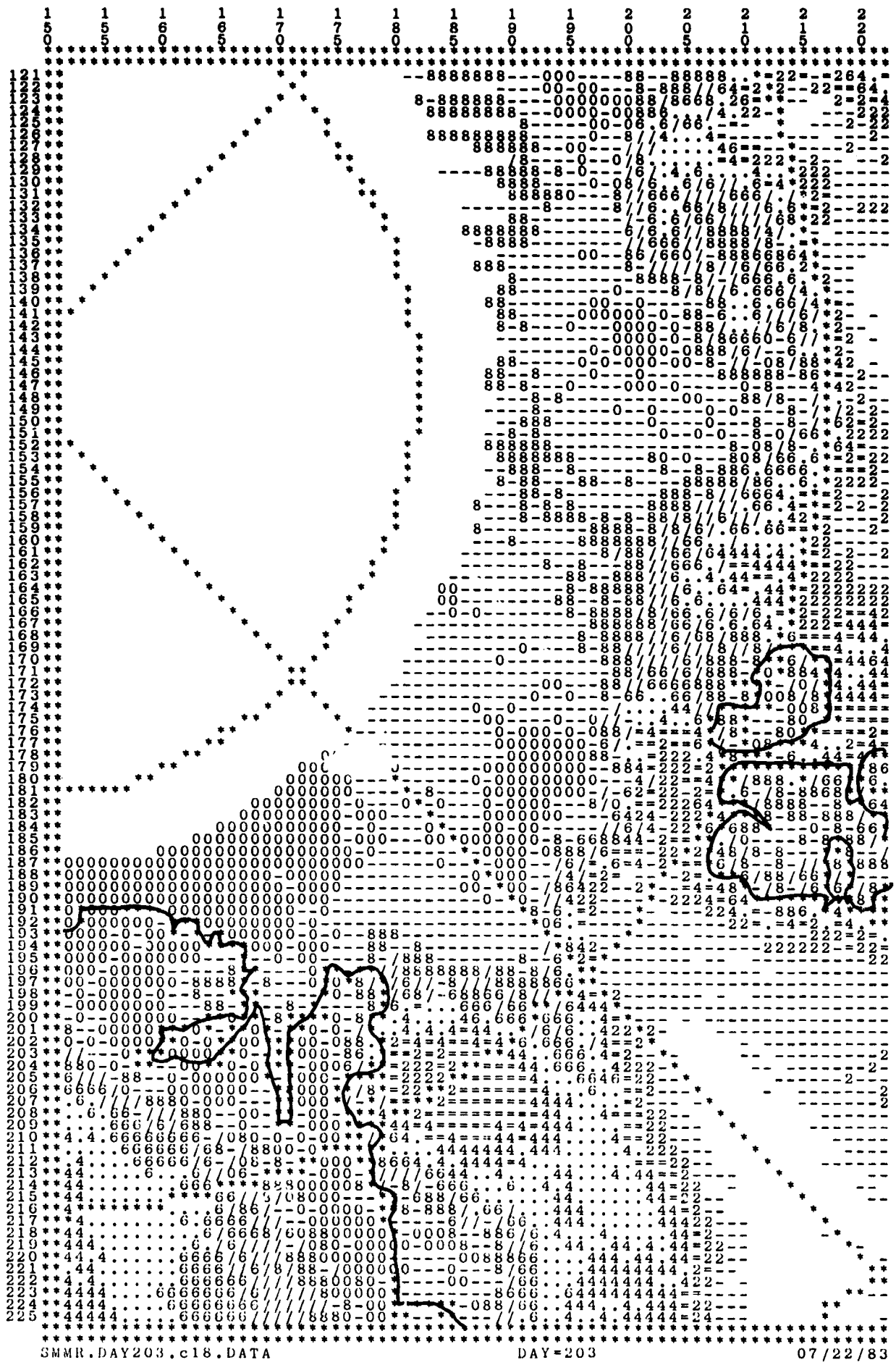
SMMR.DAY203.c18.DATA
DAY=203
07/22/83

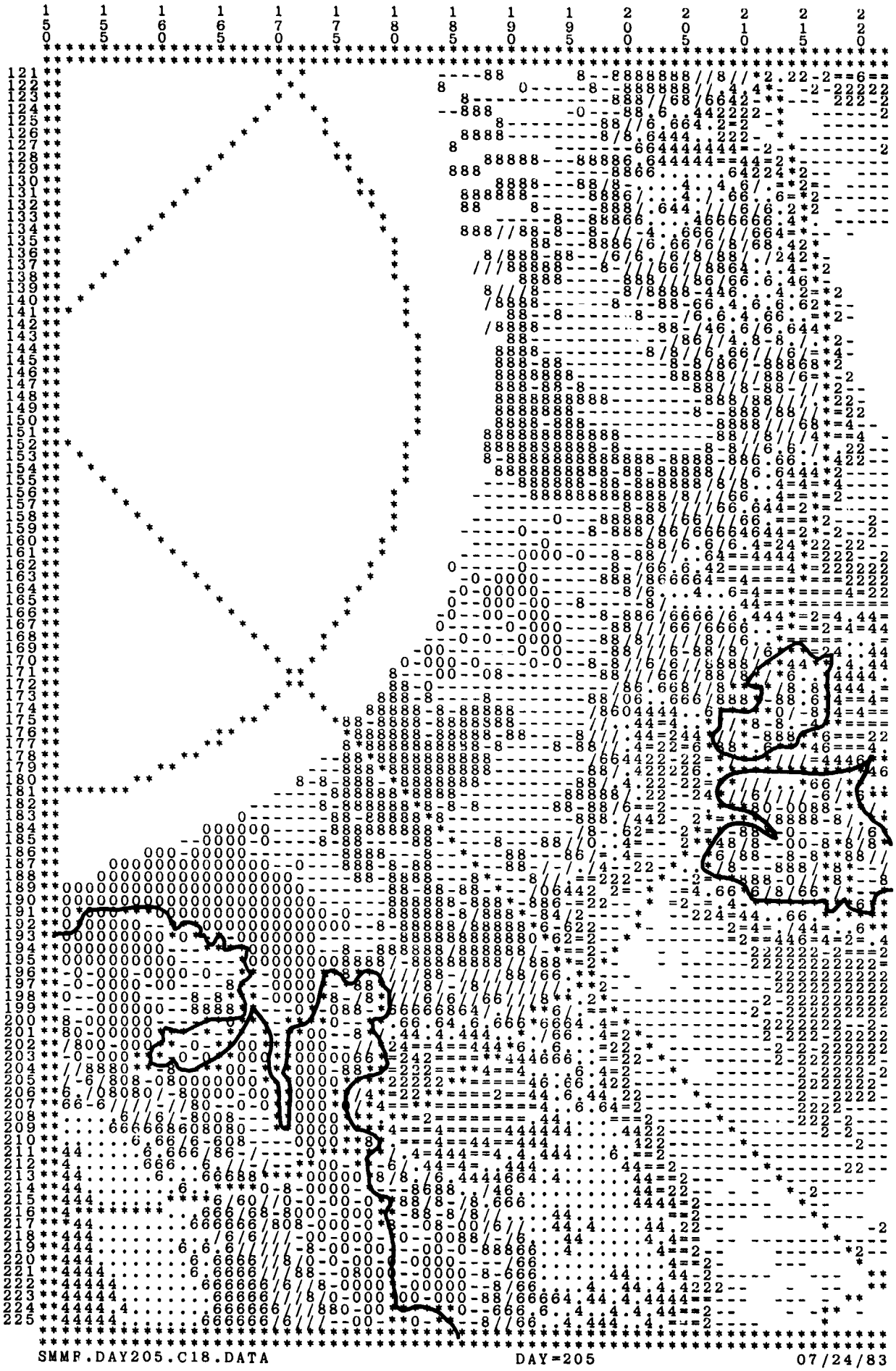
SMMF.DAY205.C18.DATA
DAY=205
07/24/83

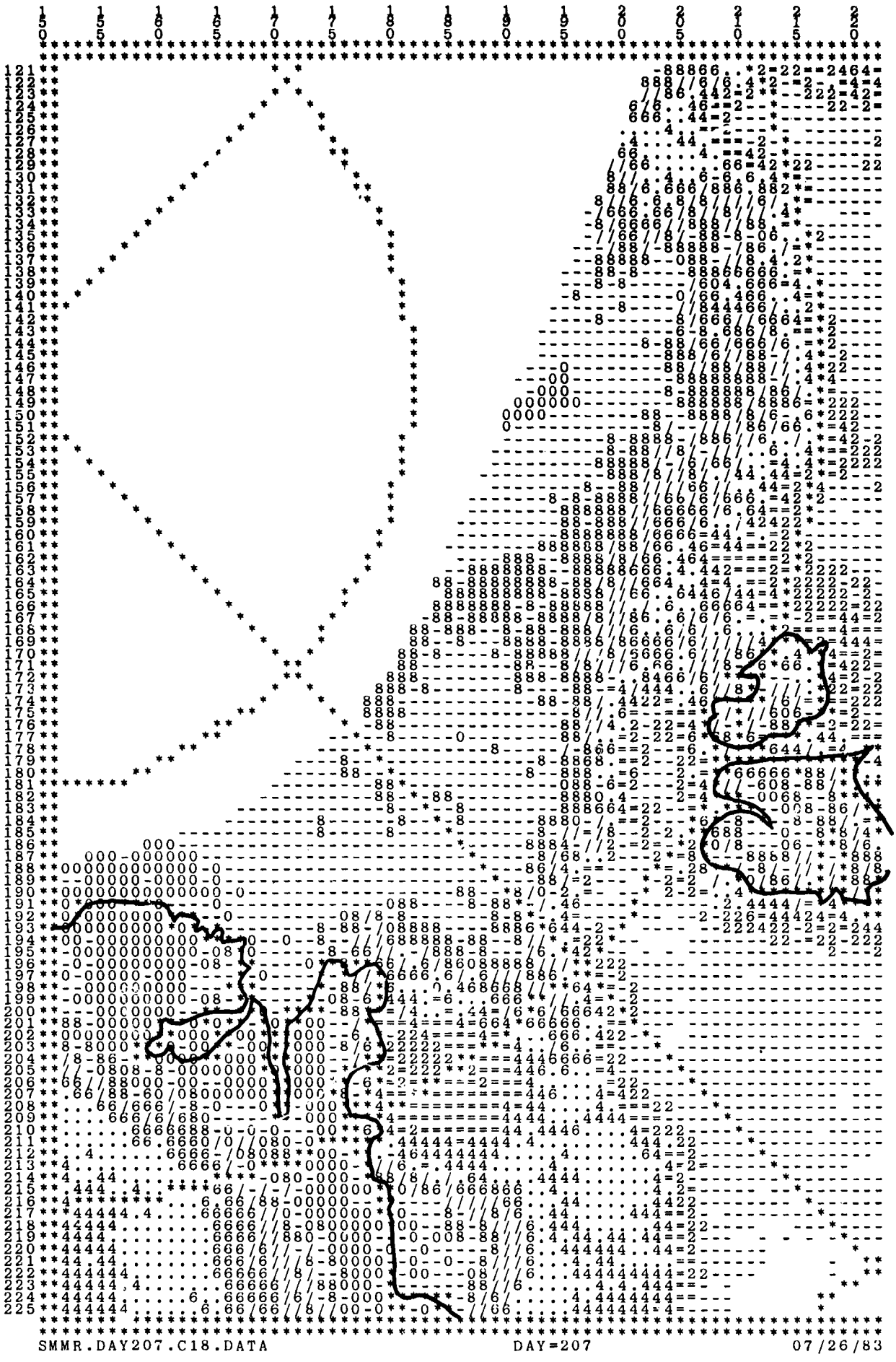
SMMR.DAY207.C18.DATA
DAY=207
07/26/83

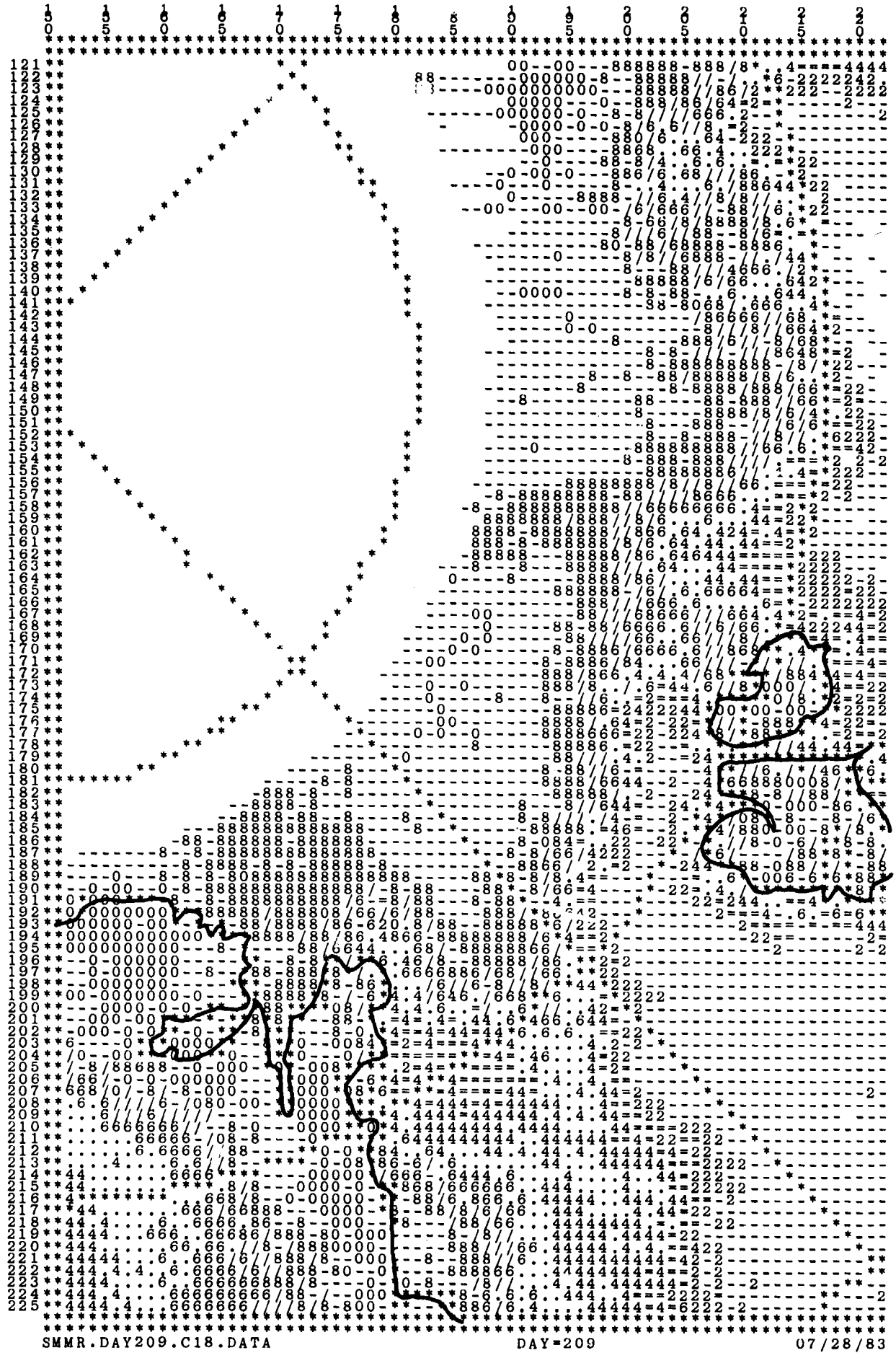
SMMR.DAY209.C18.DATA
DAY=209
07/28/83

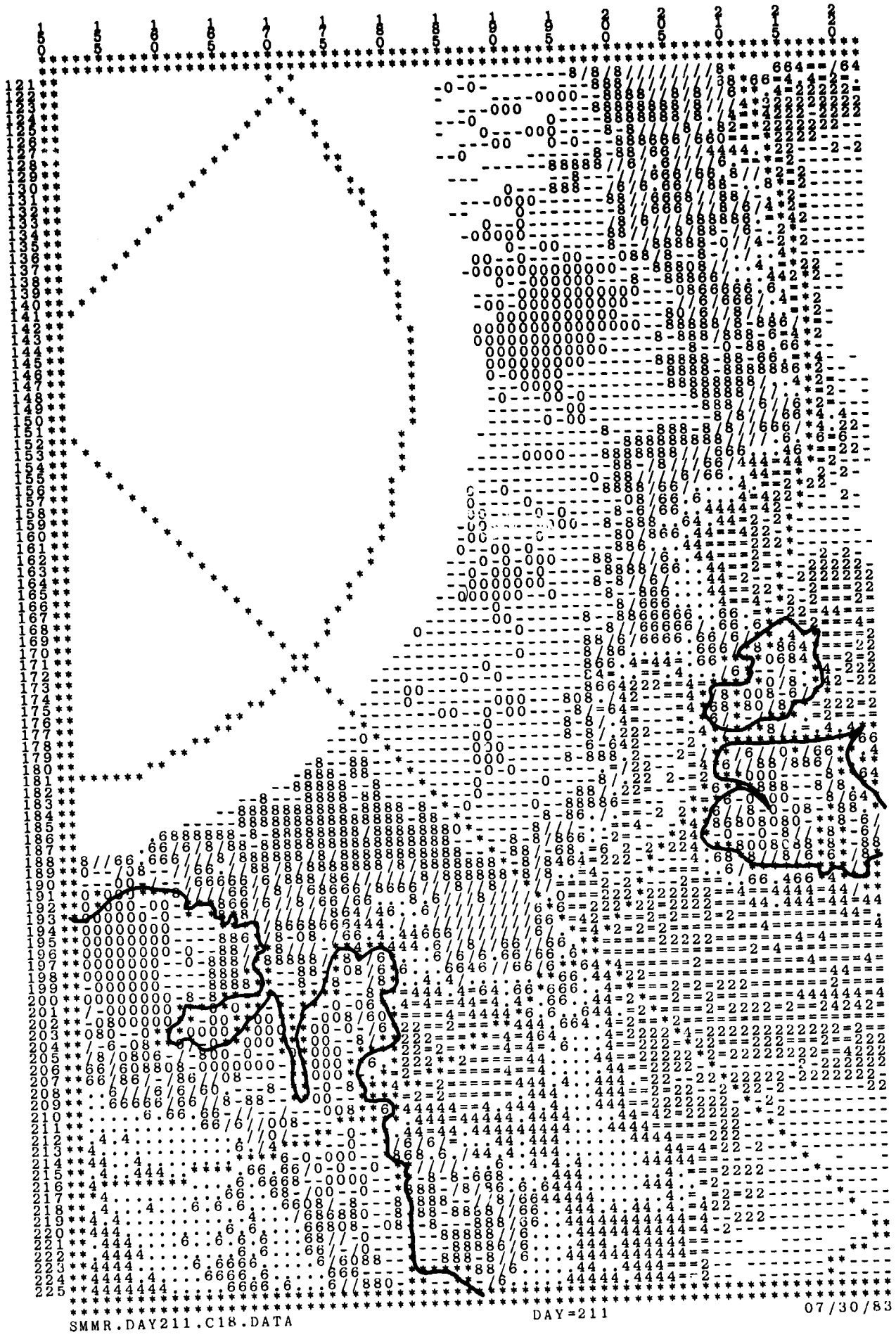
SMMR.DAY211.C18.DATA
DAY=211
07/30/83

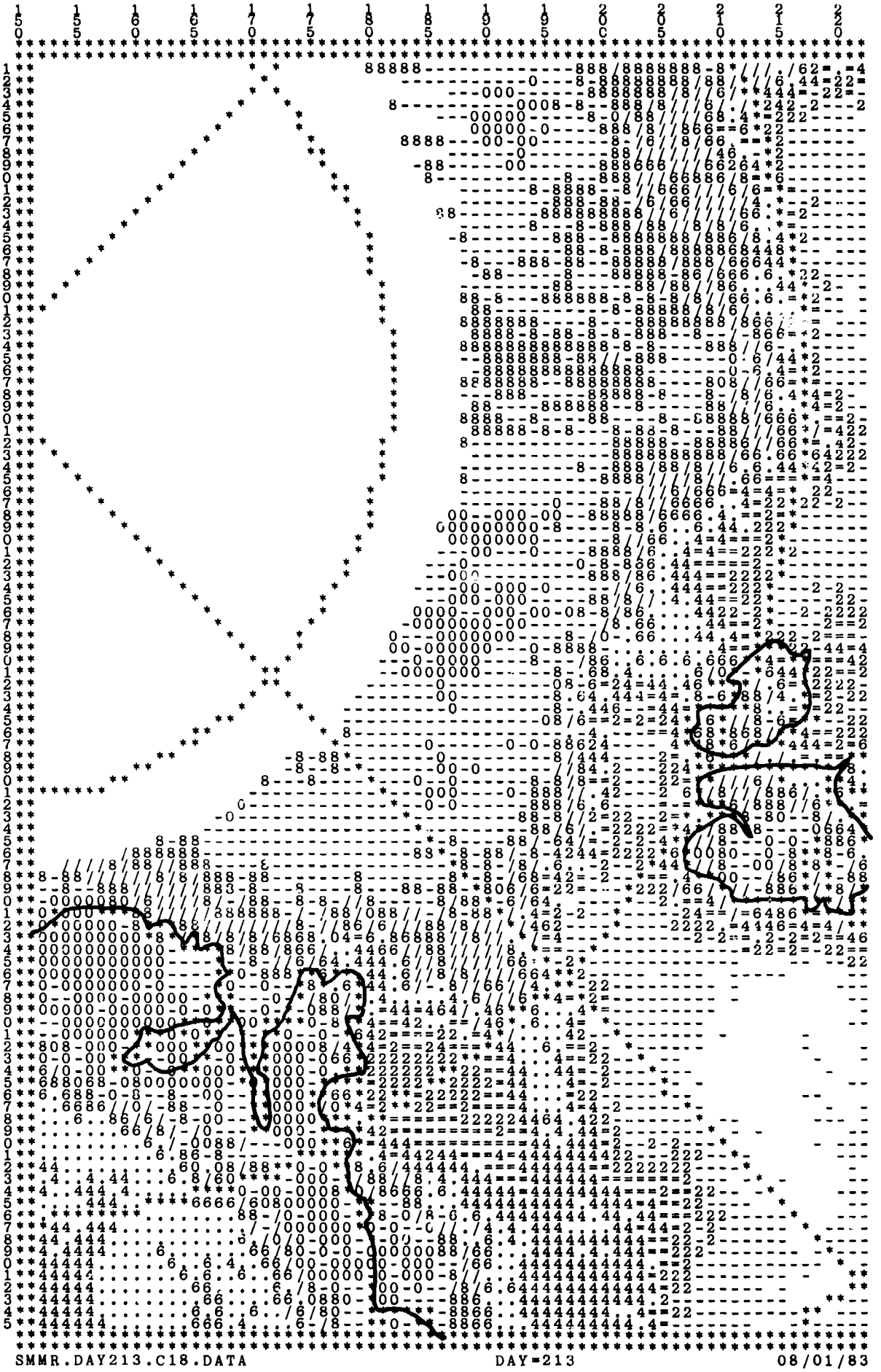
SMMR.DAY213.C18.DATA
DAY=213
08/01/83

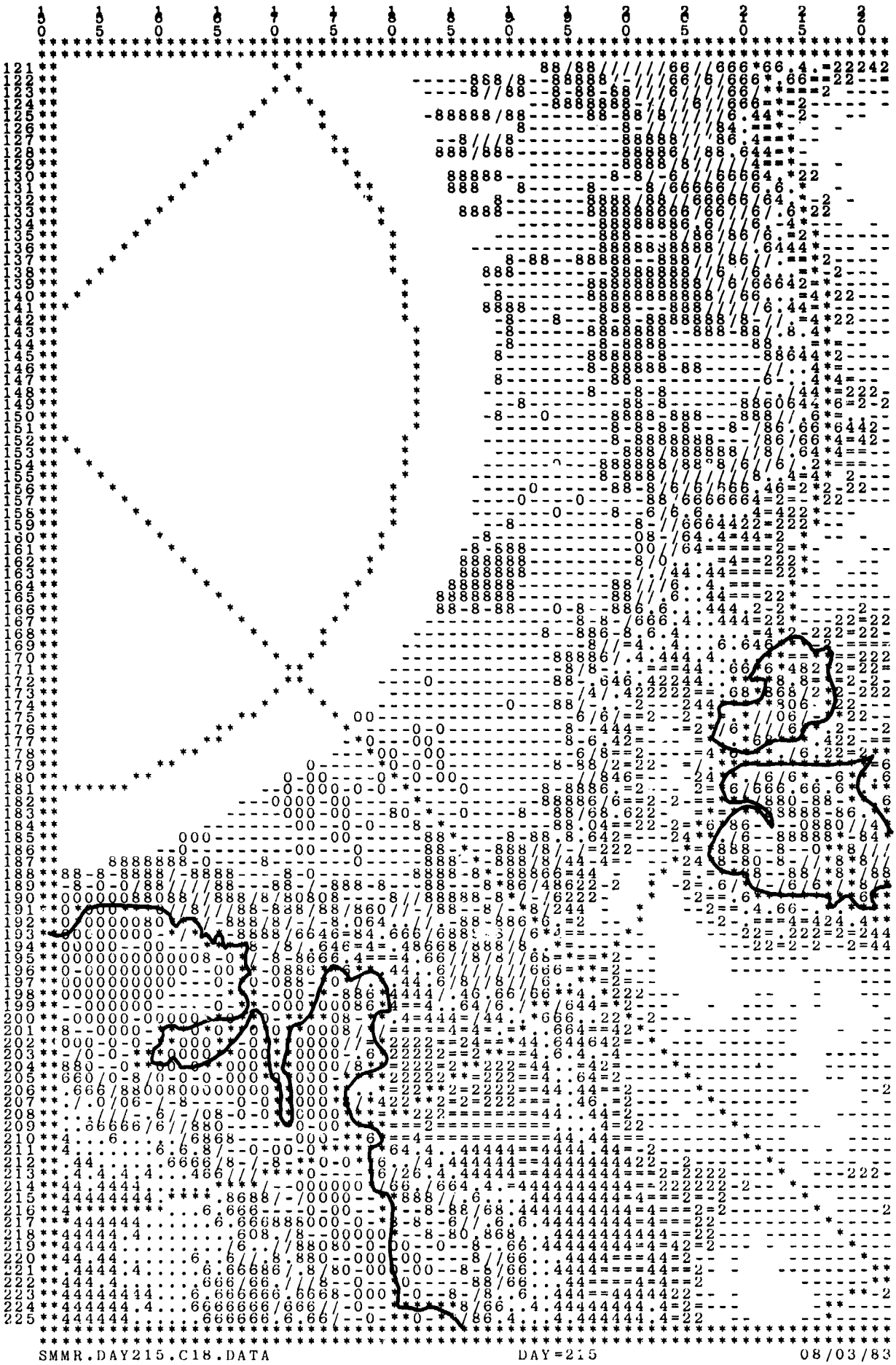
SMMR.DAY215.C18.DATA
DAY=215
08/03/83

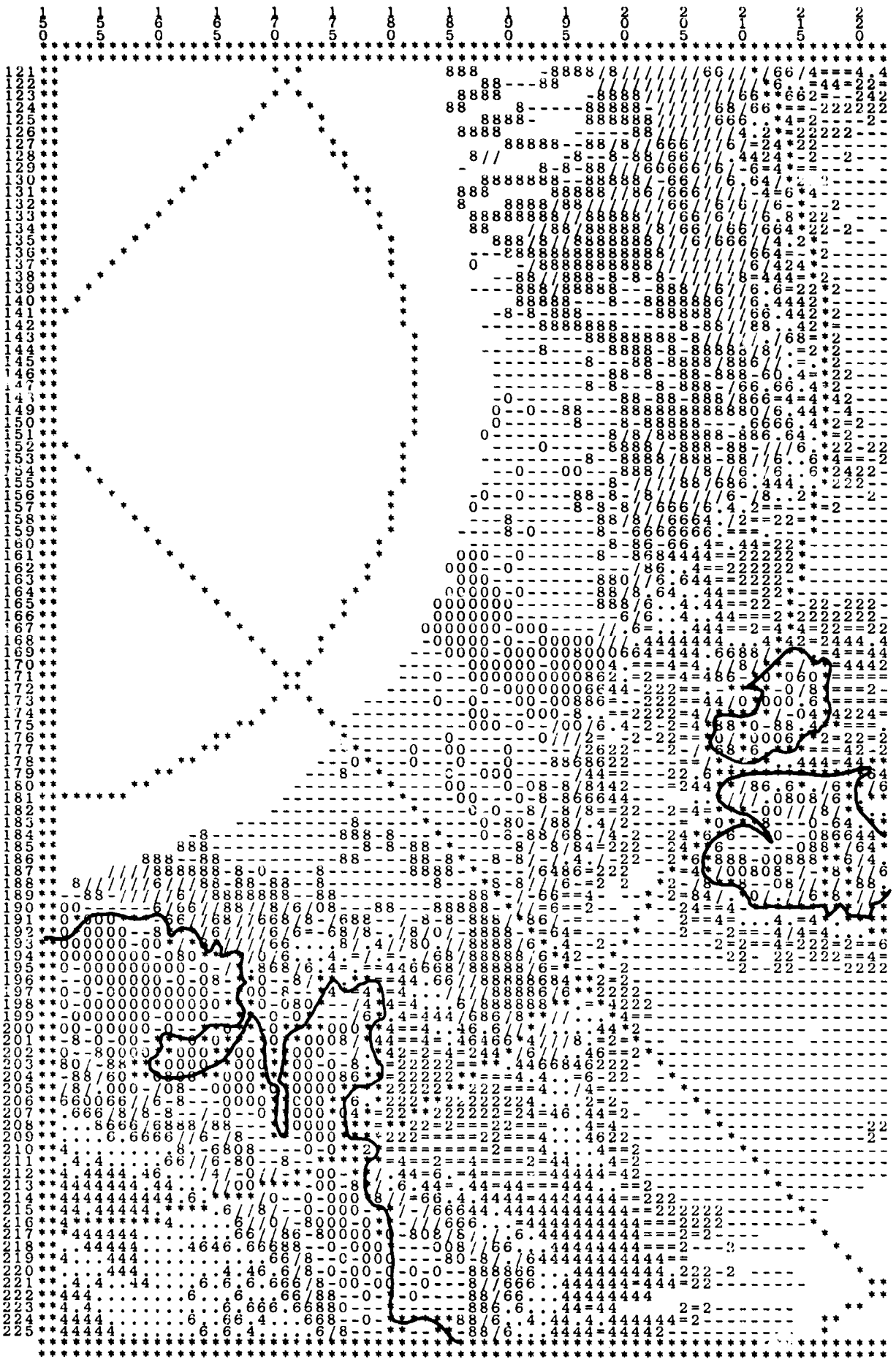
SMMR.DAY217.C18.DATA
DAY=217
08/05/85

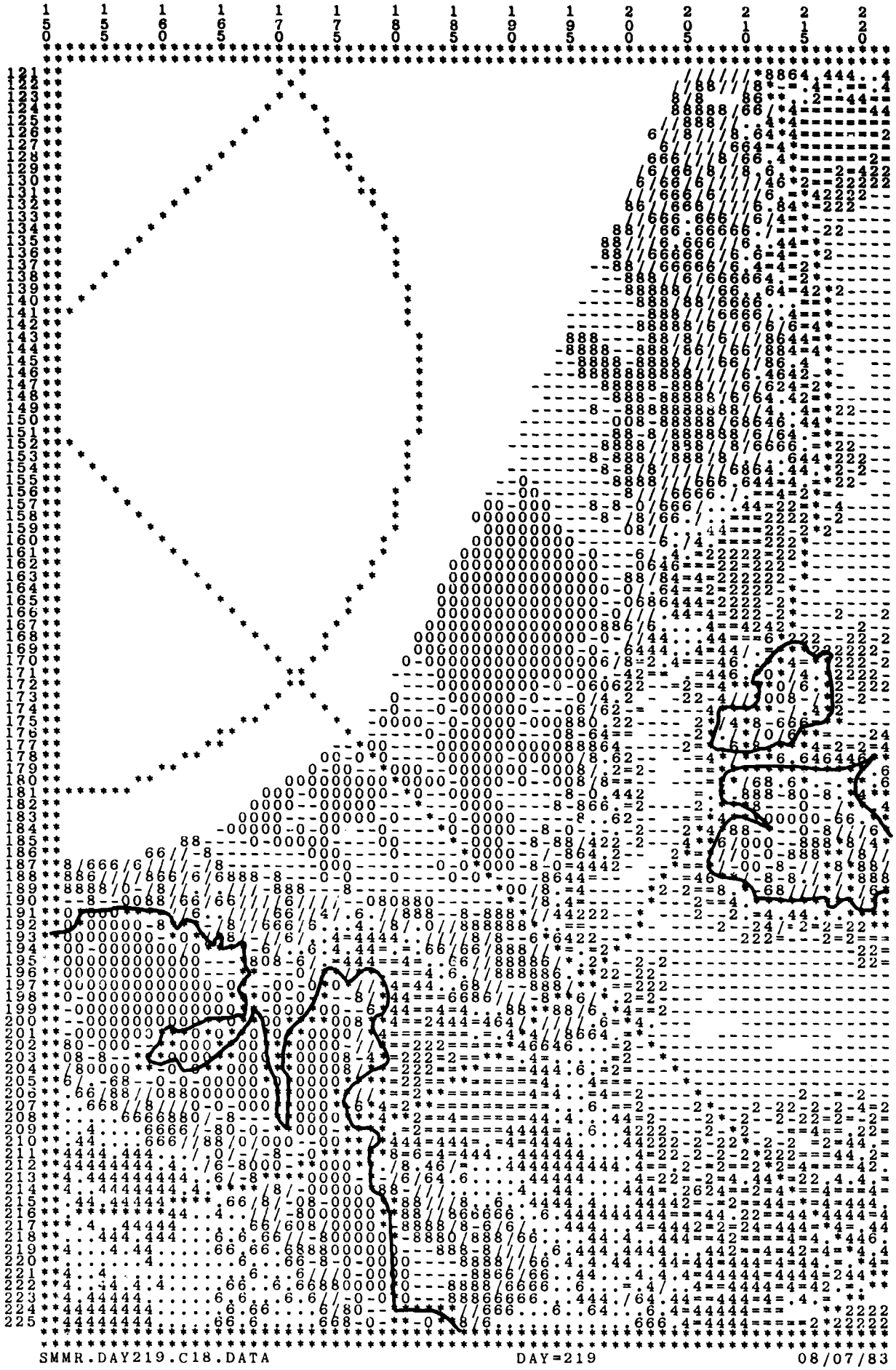
SMMR.DAY219.C18.DATA
DAY=219
08/07/83

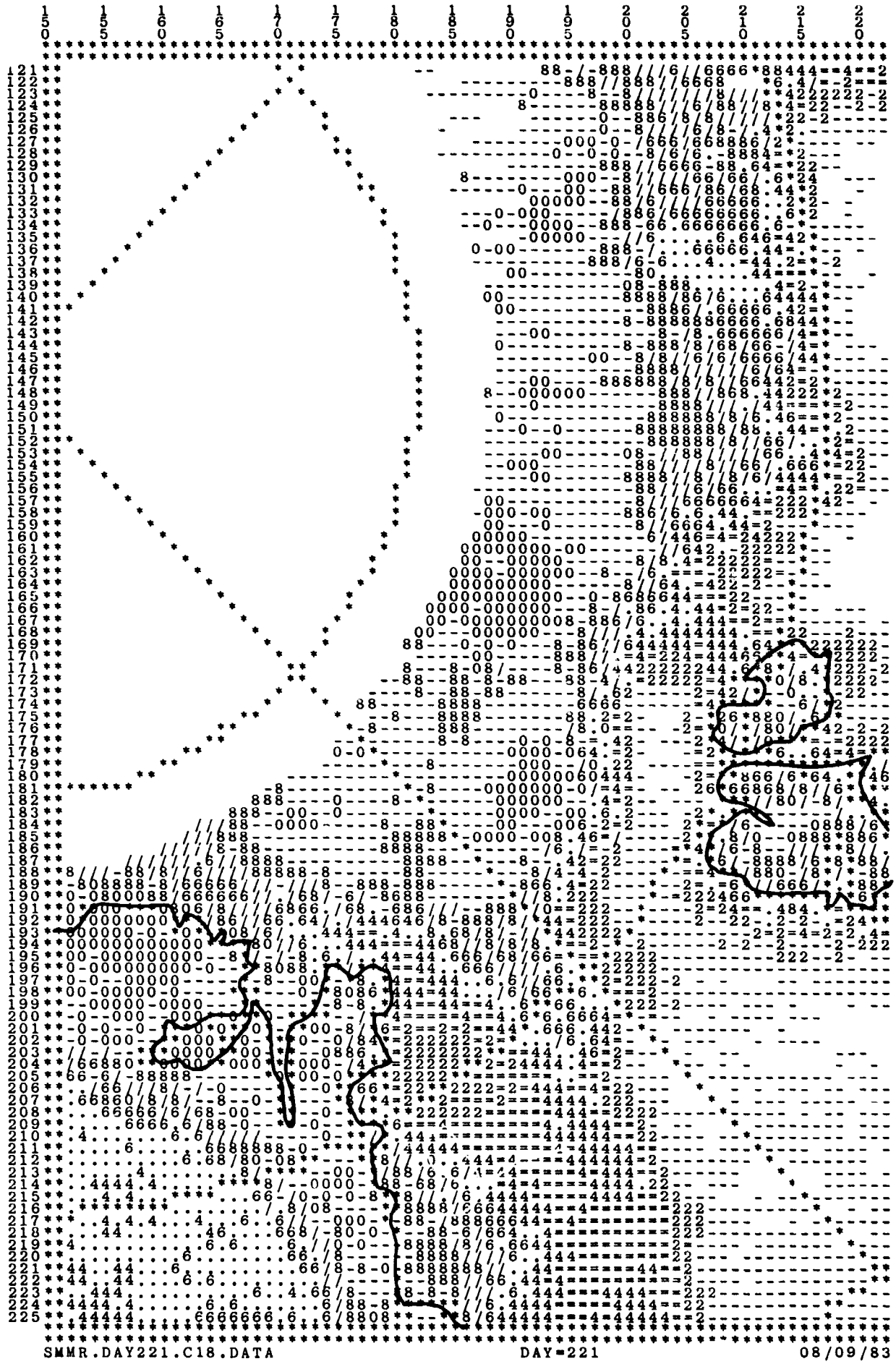
SMMR.DAY221.C18.DATA
DAY=221
08/09/83

APPENDIX B

GRID-PRINT MAPS OF MULTIYEAR SEA ICE FRACTION DURING MIZEX/EAST'83

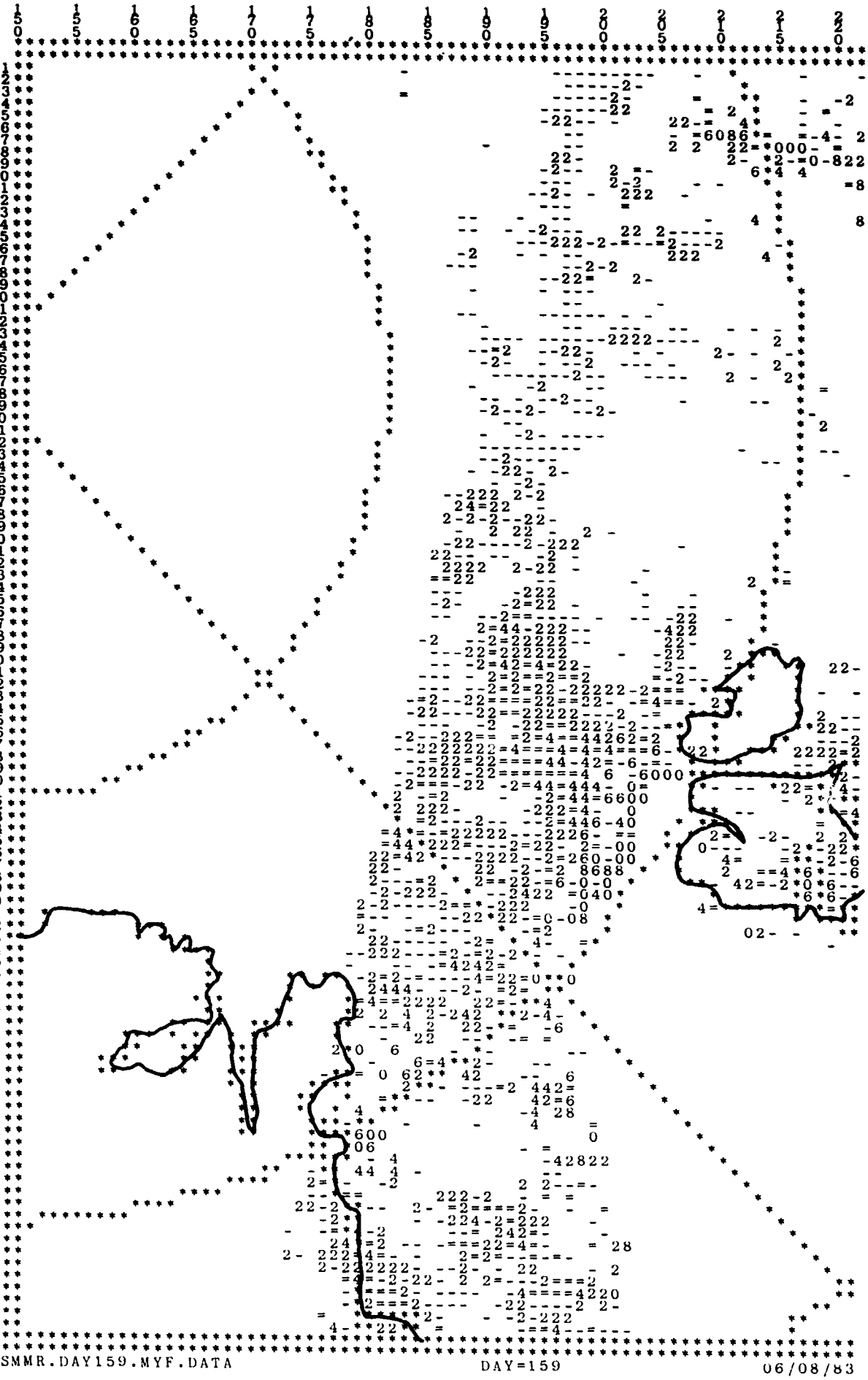
SMMR.DAY159.MYF.DATA
DAY=159
06/08/83

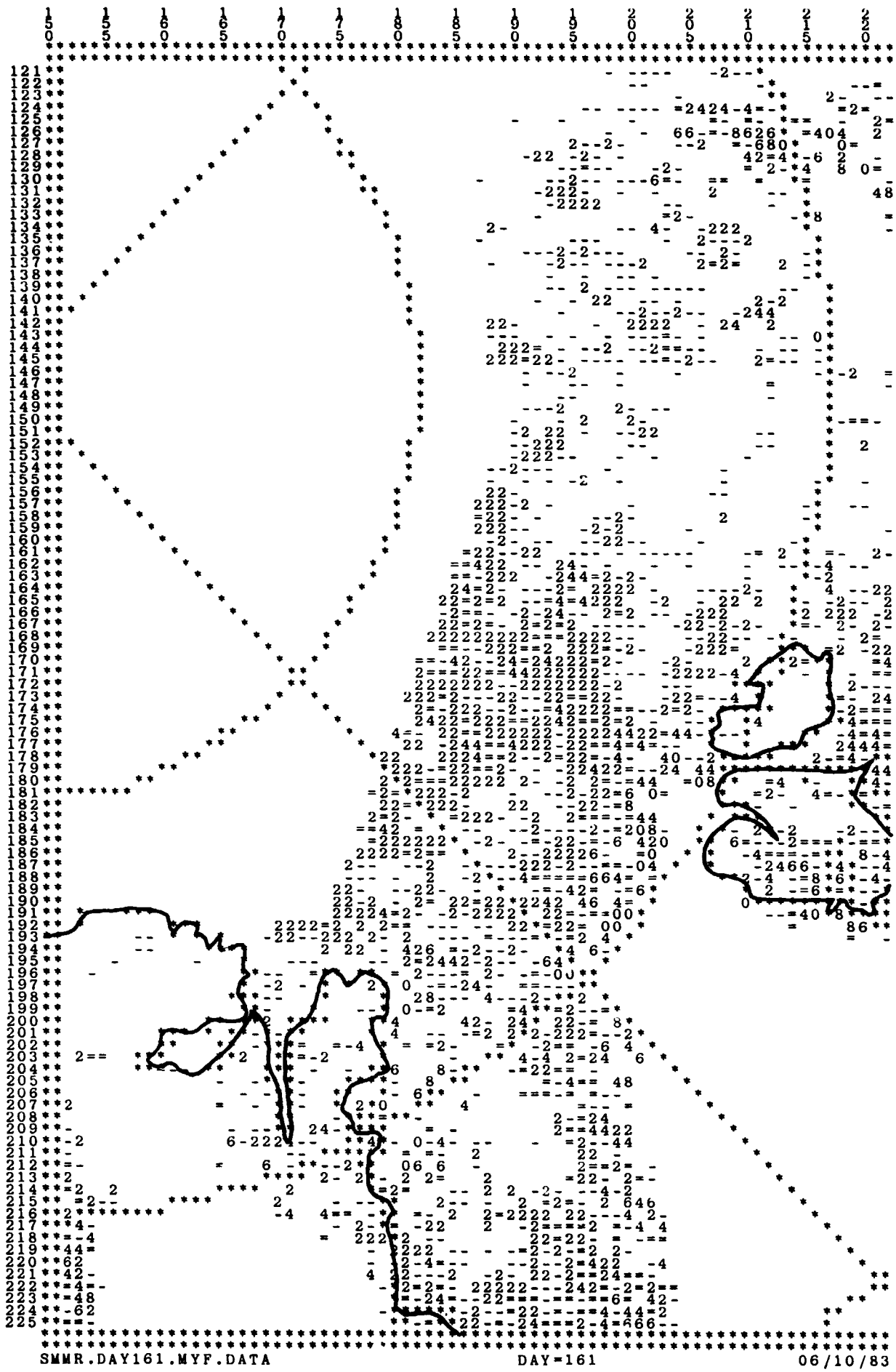
SMMR.DAY161.MYF.DATA
DAY=161
06/10/83

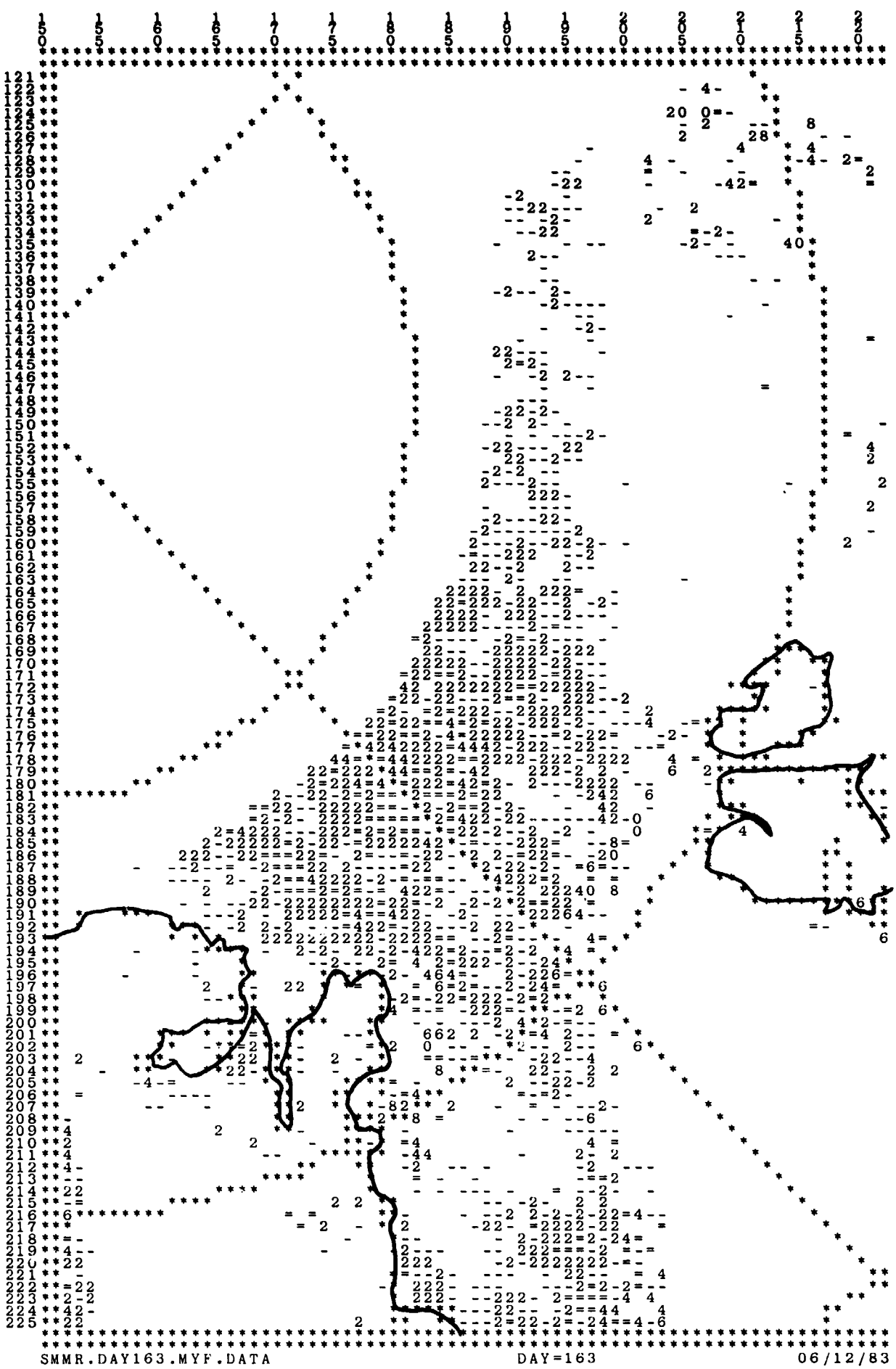
SMMR.DAY163.MYF.DATA
DAY=163
06/12/83

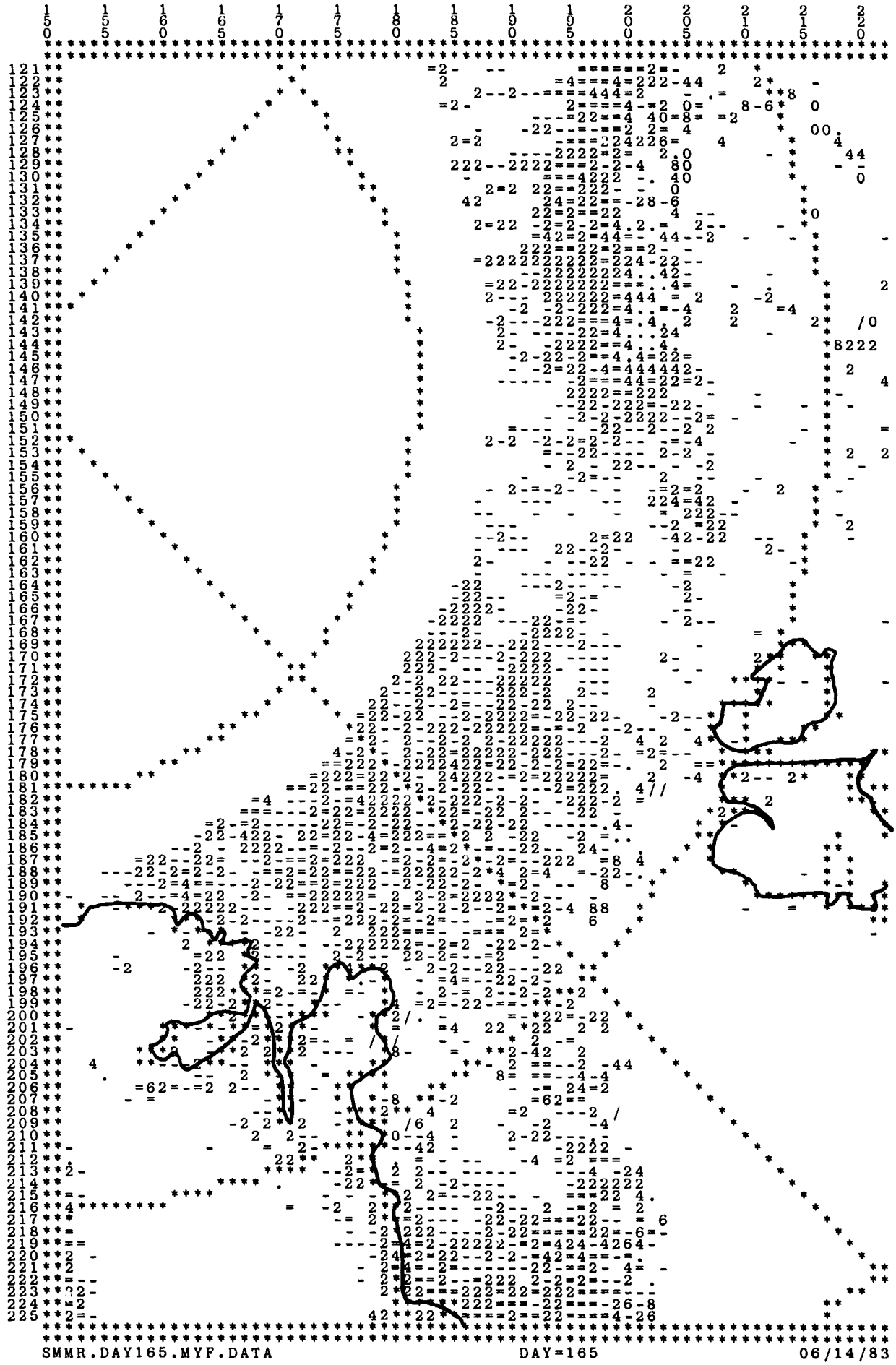
SMMR.DAY165.MYF.DATA
DAY=165
06/14/83

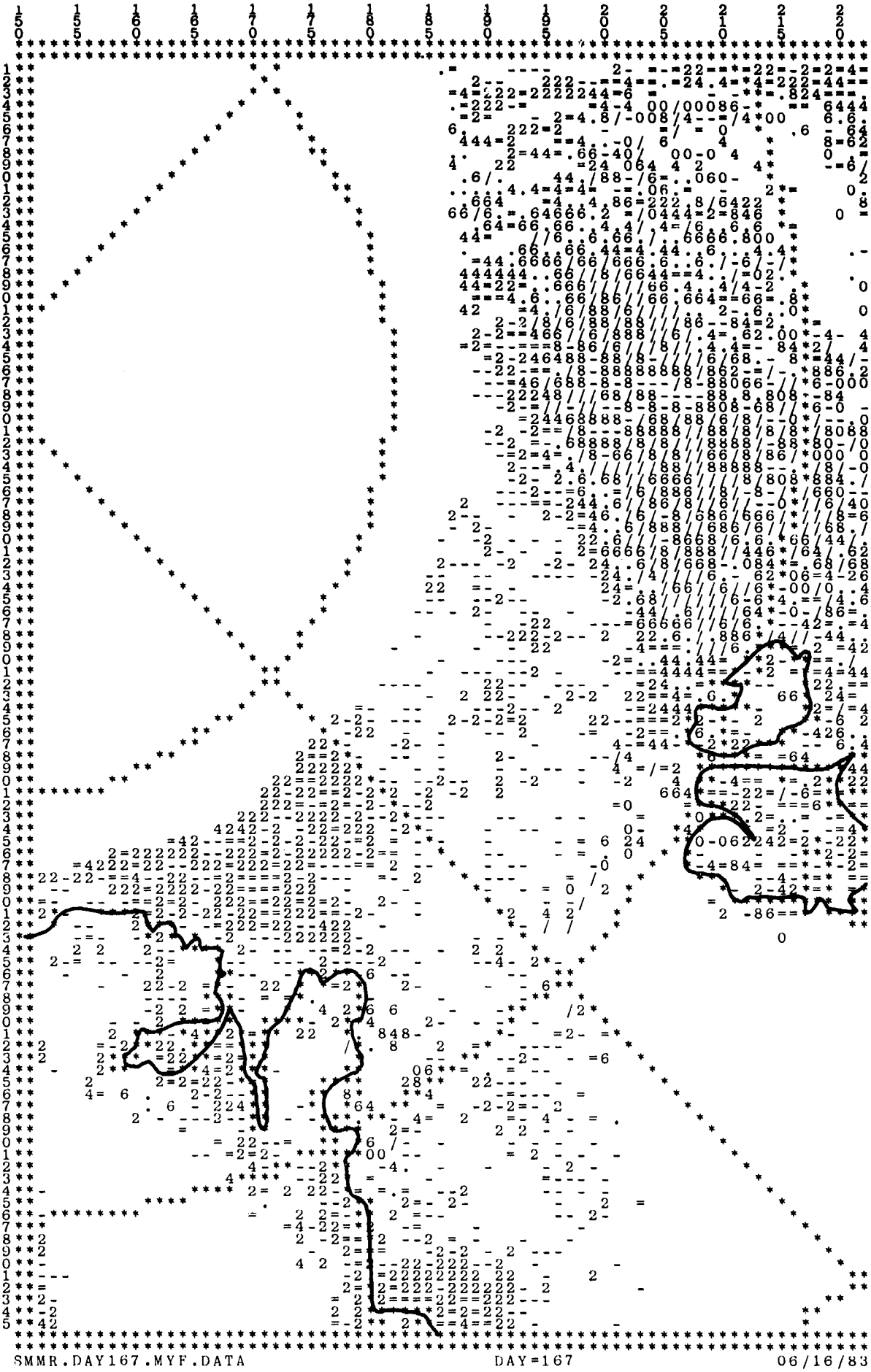
SMMR.DAY167.MYF.DATA
DAY=167
06/16/83

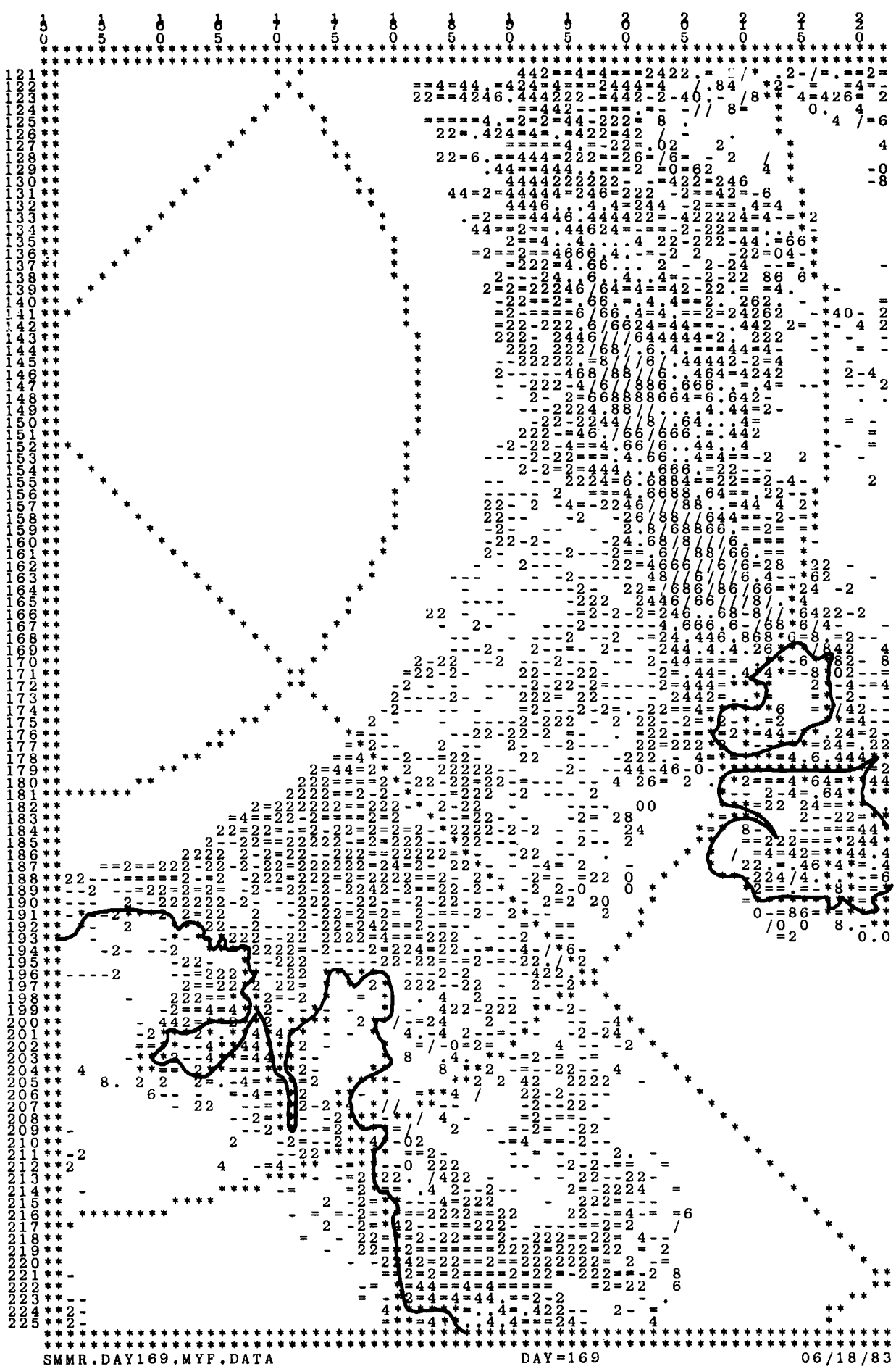
SMMR.DAY169.MYF.DATA
DAY=169
06/18/83

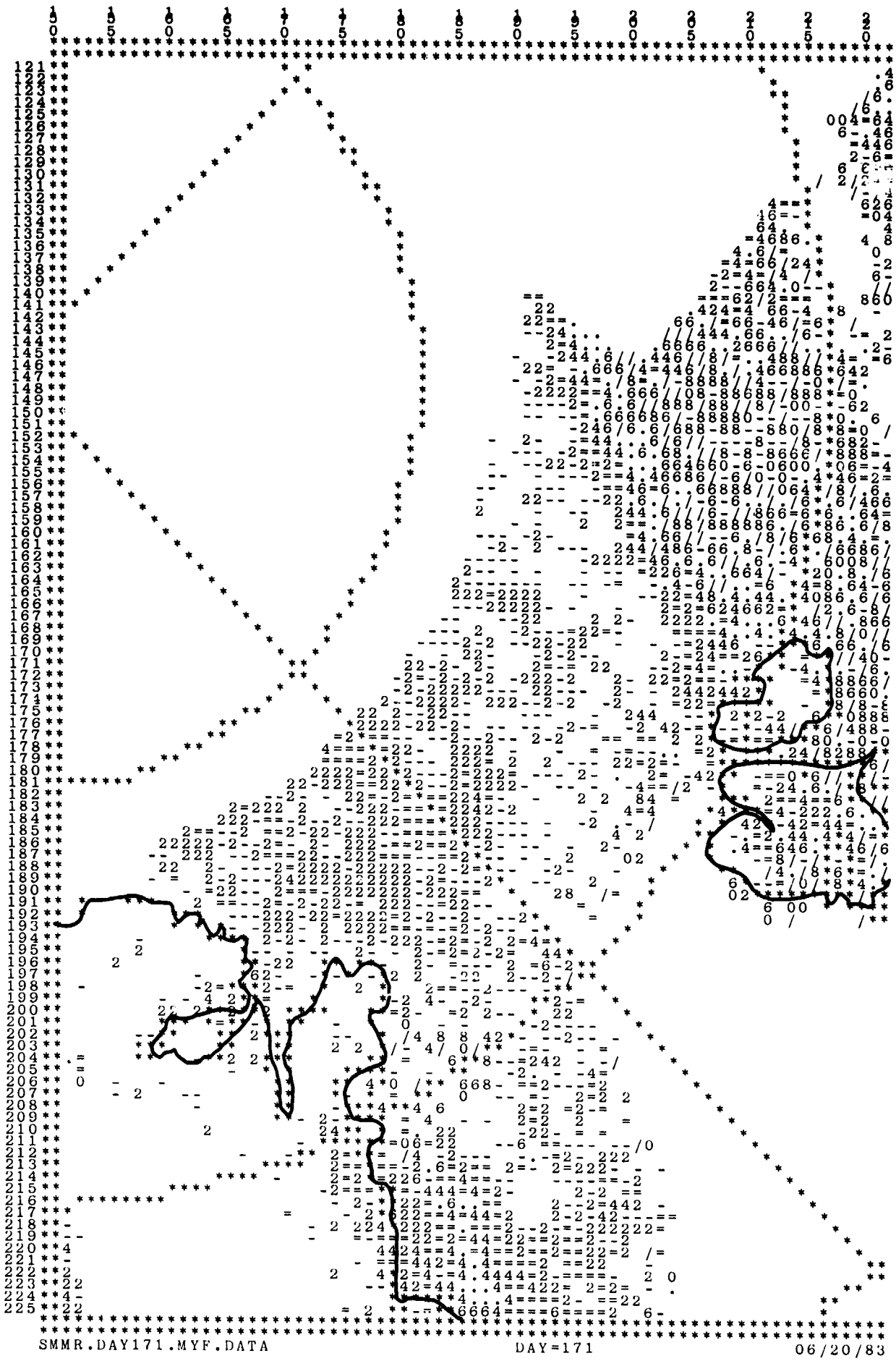
SMMR.DAY171.MYF.DATA
DAY=171
06/20/83

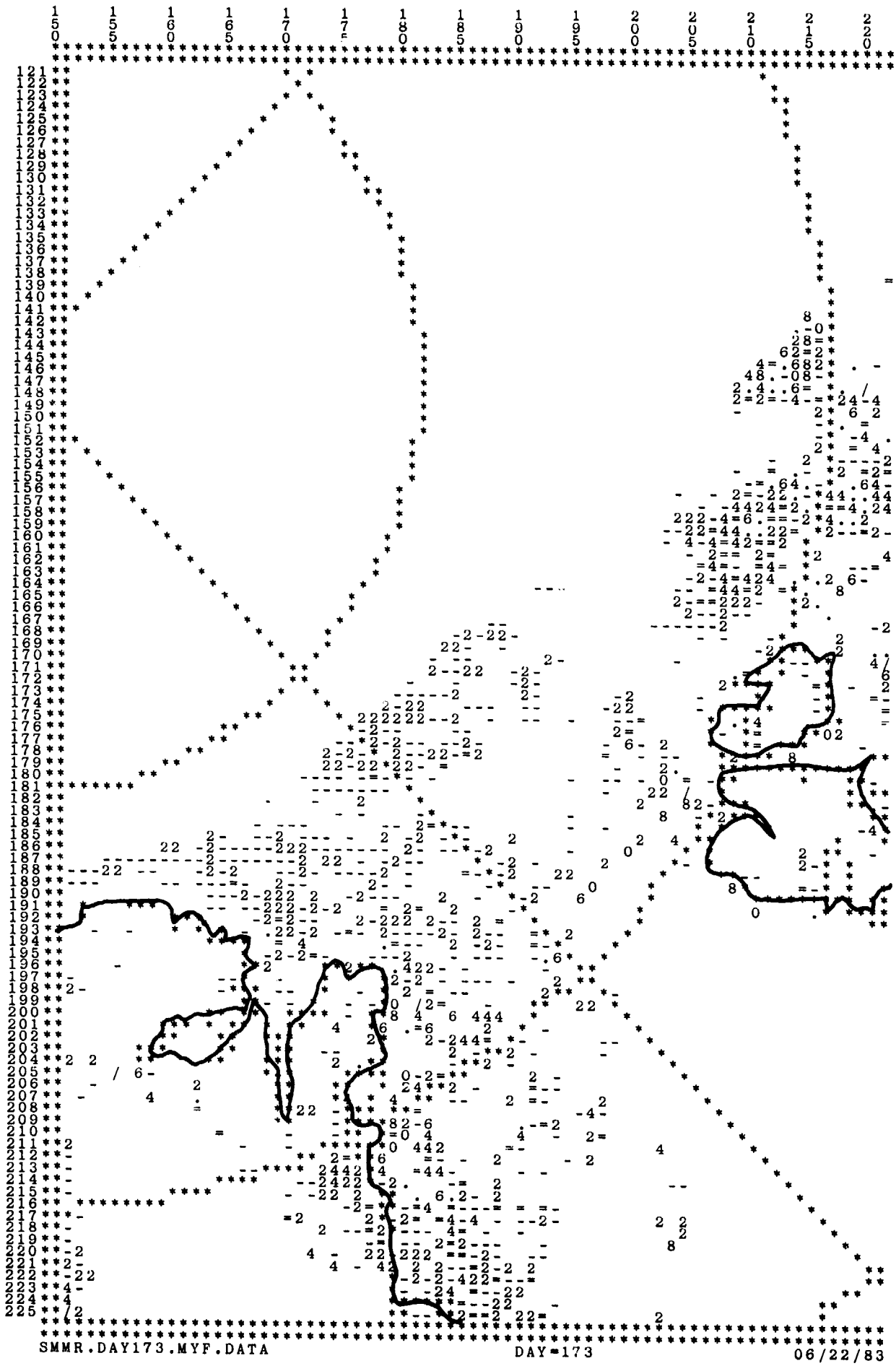
SMMR.DAY173.MYF.DATA
DAY=173
06/22/83

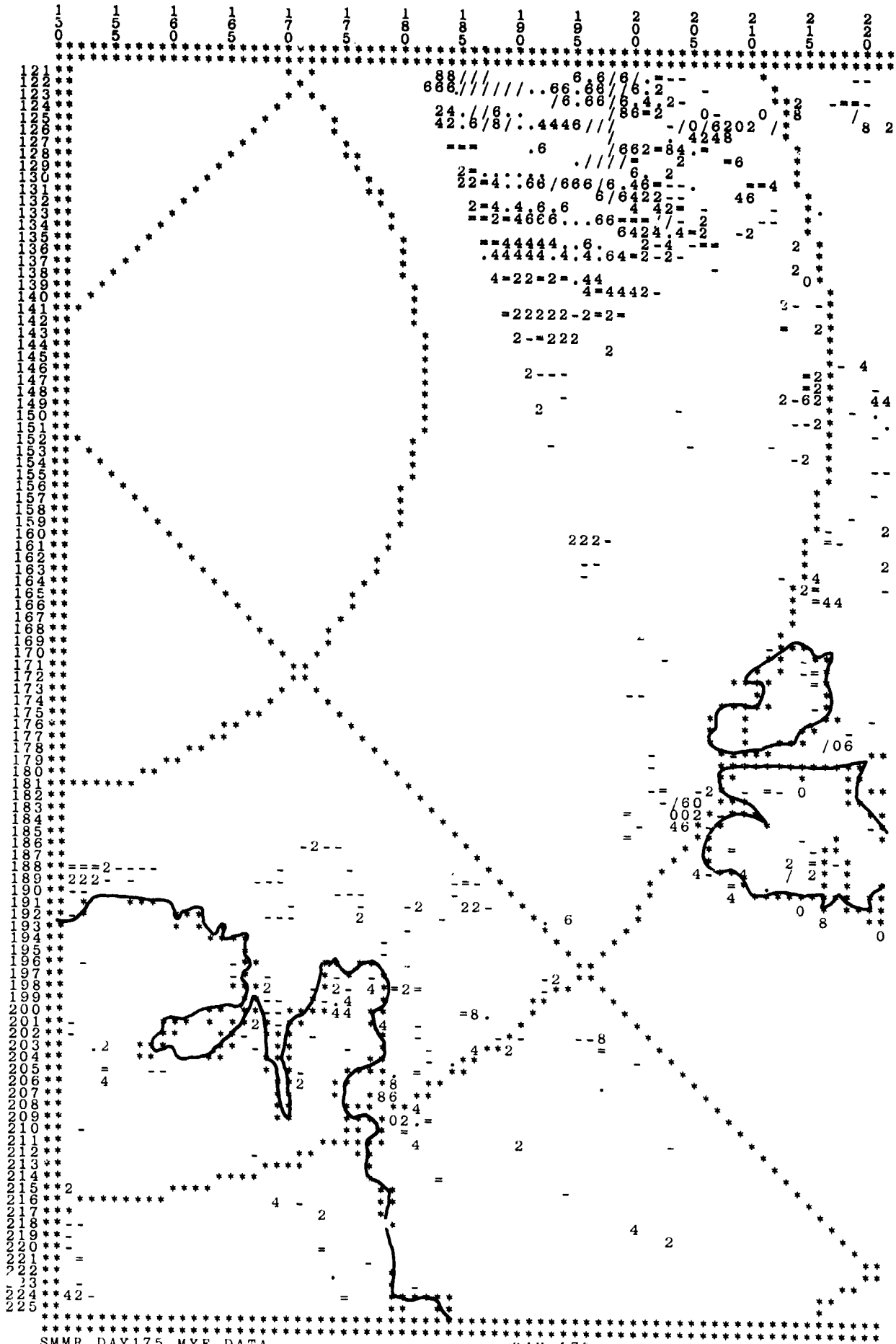
SMMR.DAY175.MYF.DATA
DAY=175
06/24/83

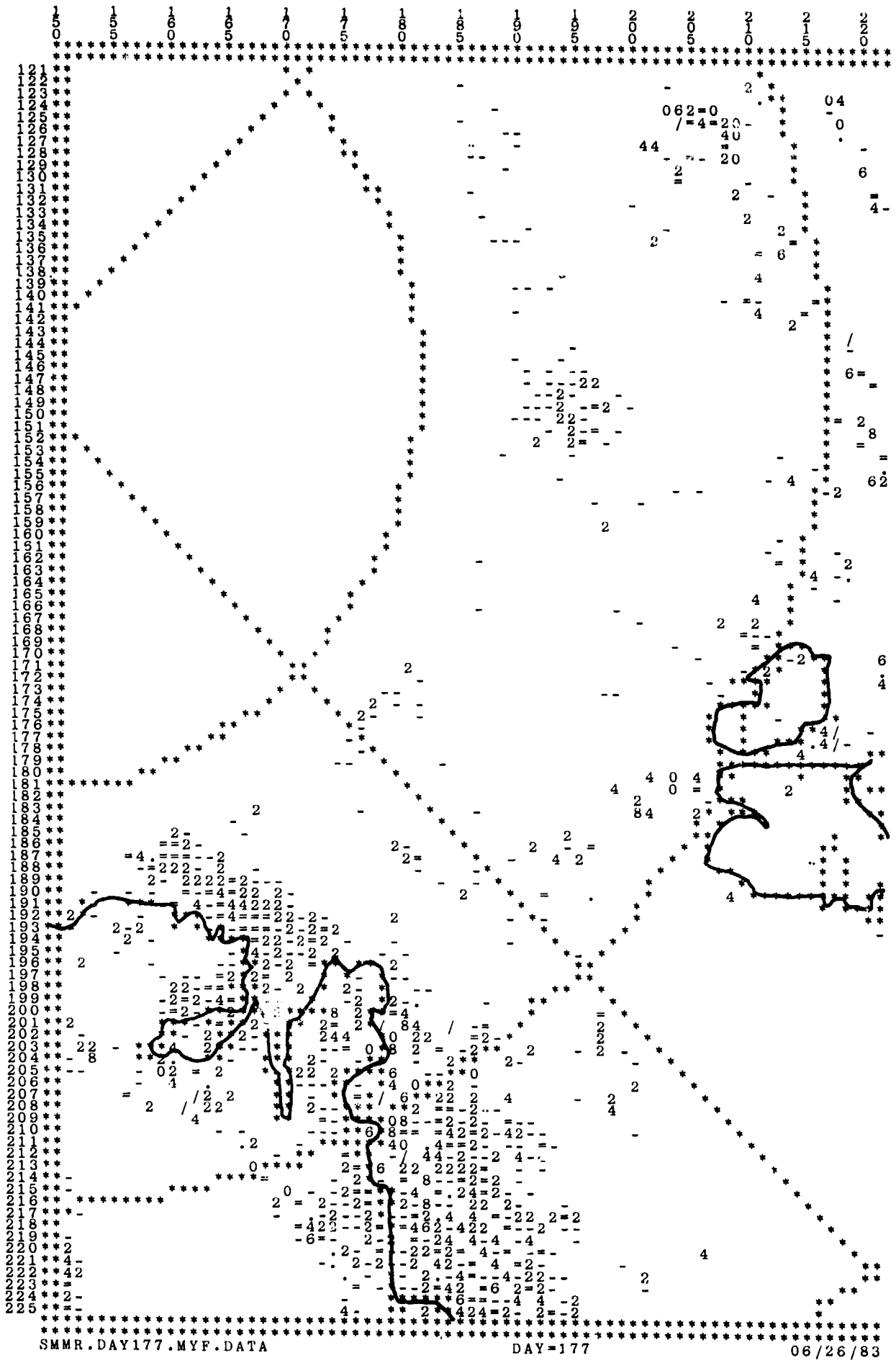
SMMR.DAY177.MYF.DATA
DAY=177
06/26/83

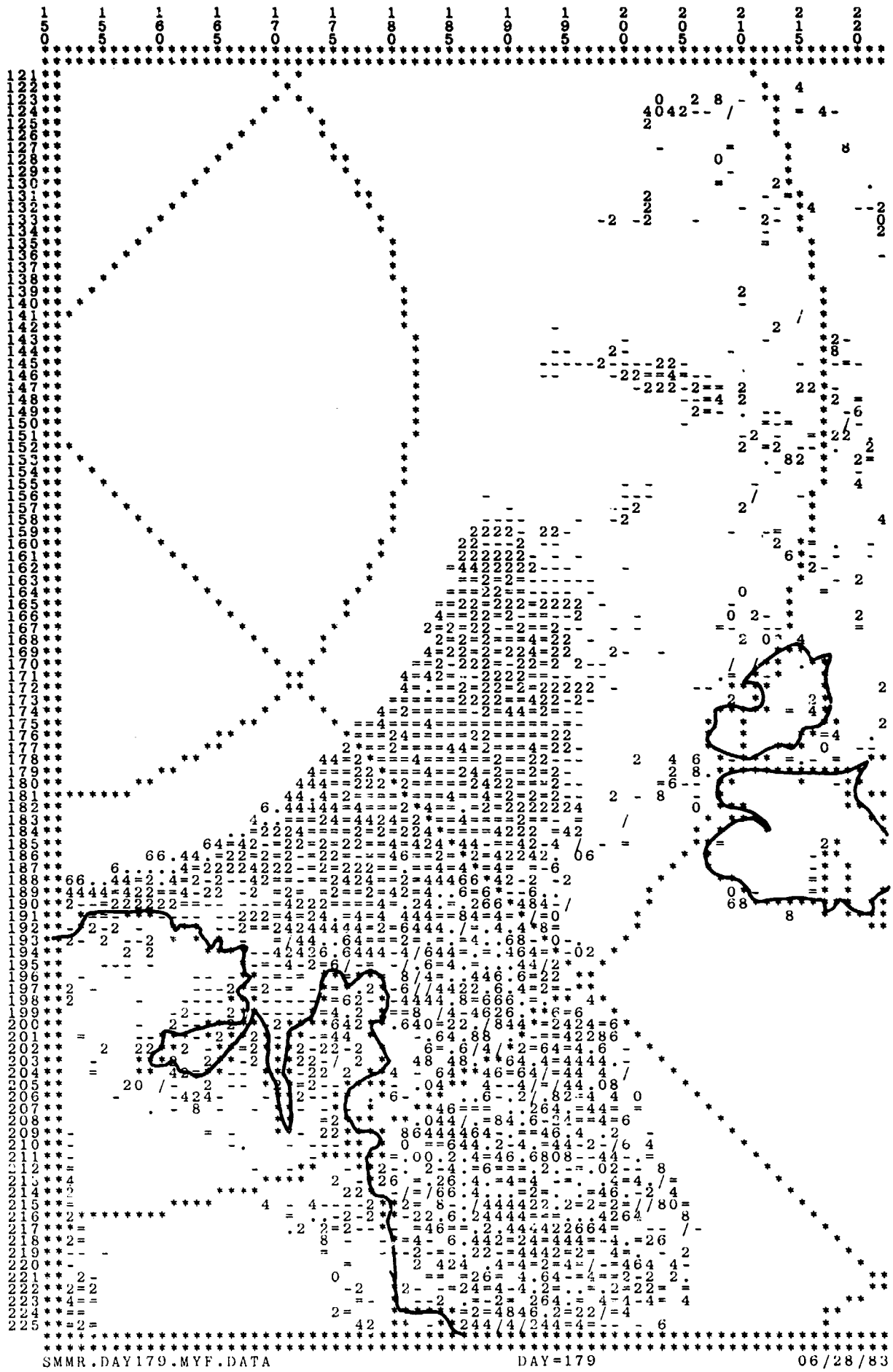
SMMR.DAY179.MYF.DATA
DAY=179
06/28/83

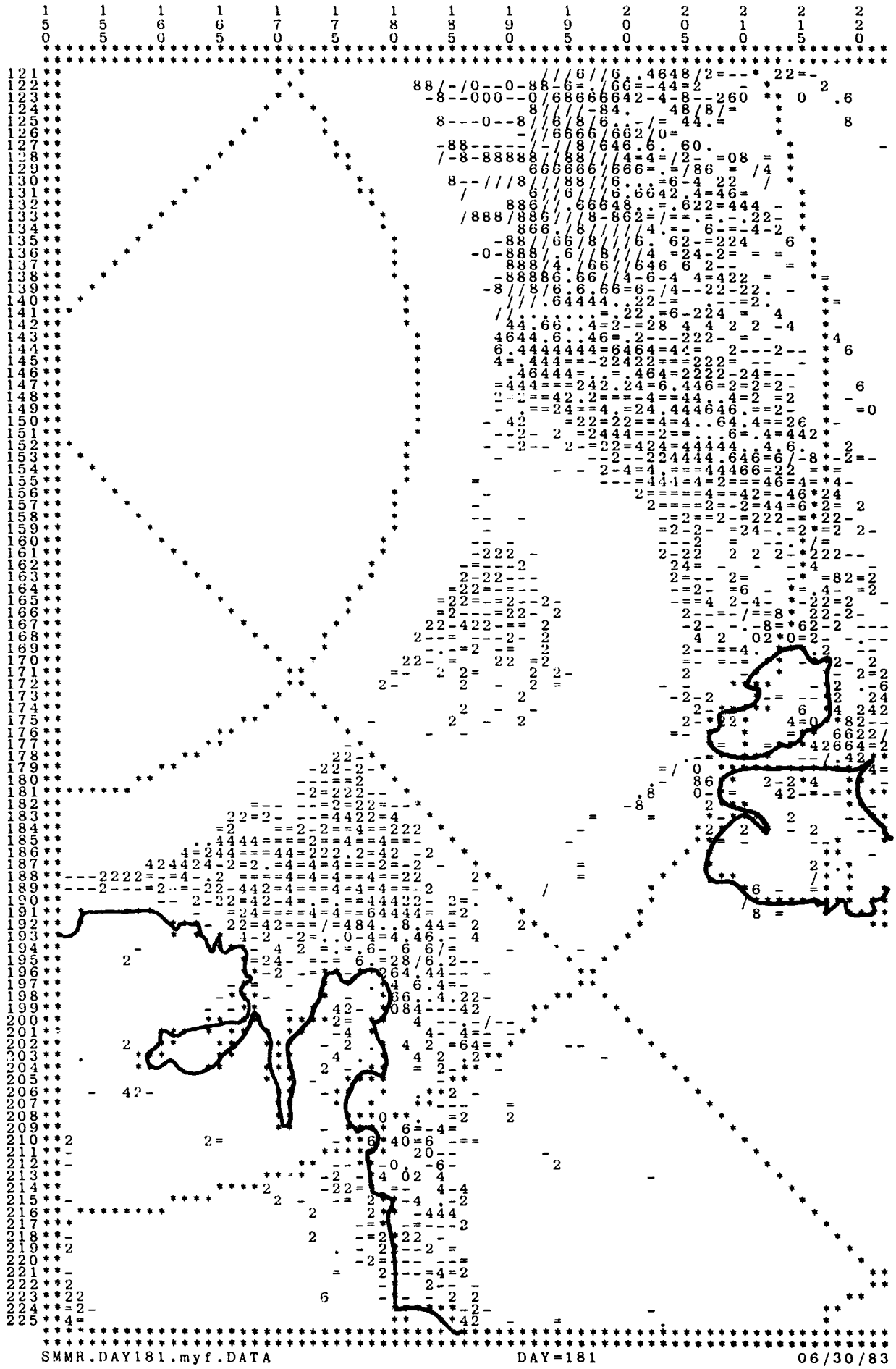
SMMR.DAY181.myf.DATA
DAY=181
06/30/83

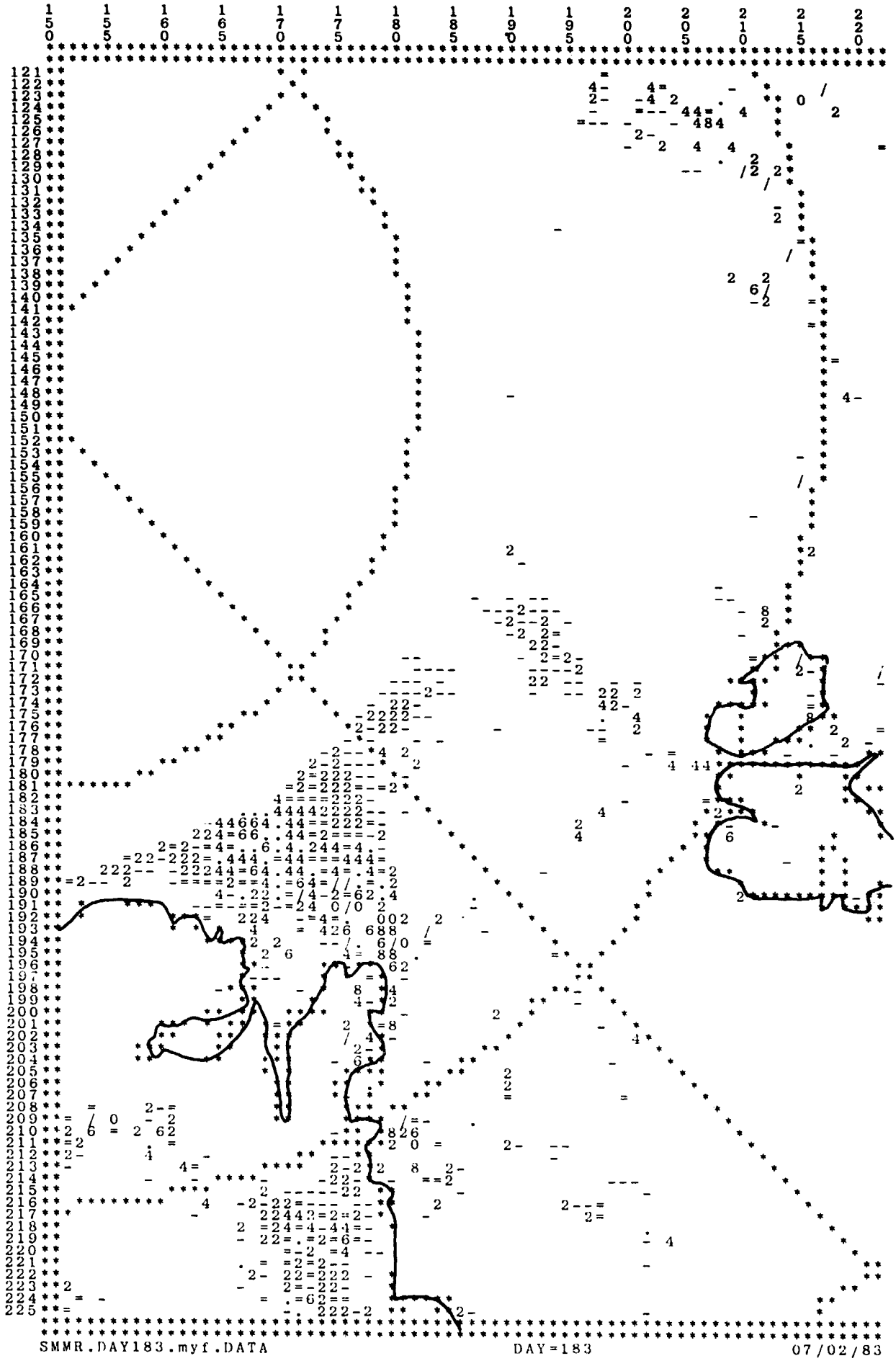
SMMR.DAY183.myf.DATA
DAY=183
07/02/83

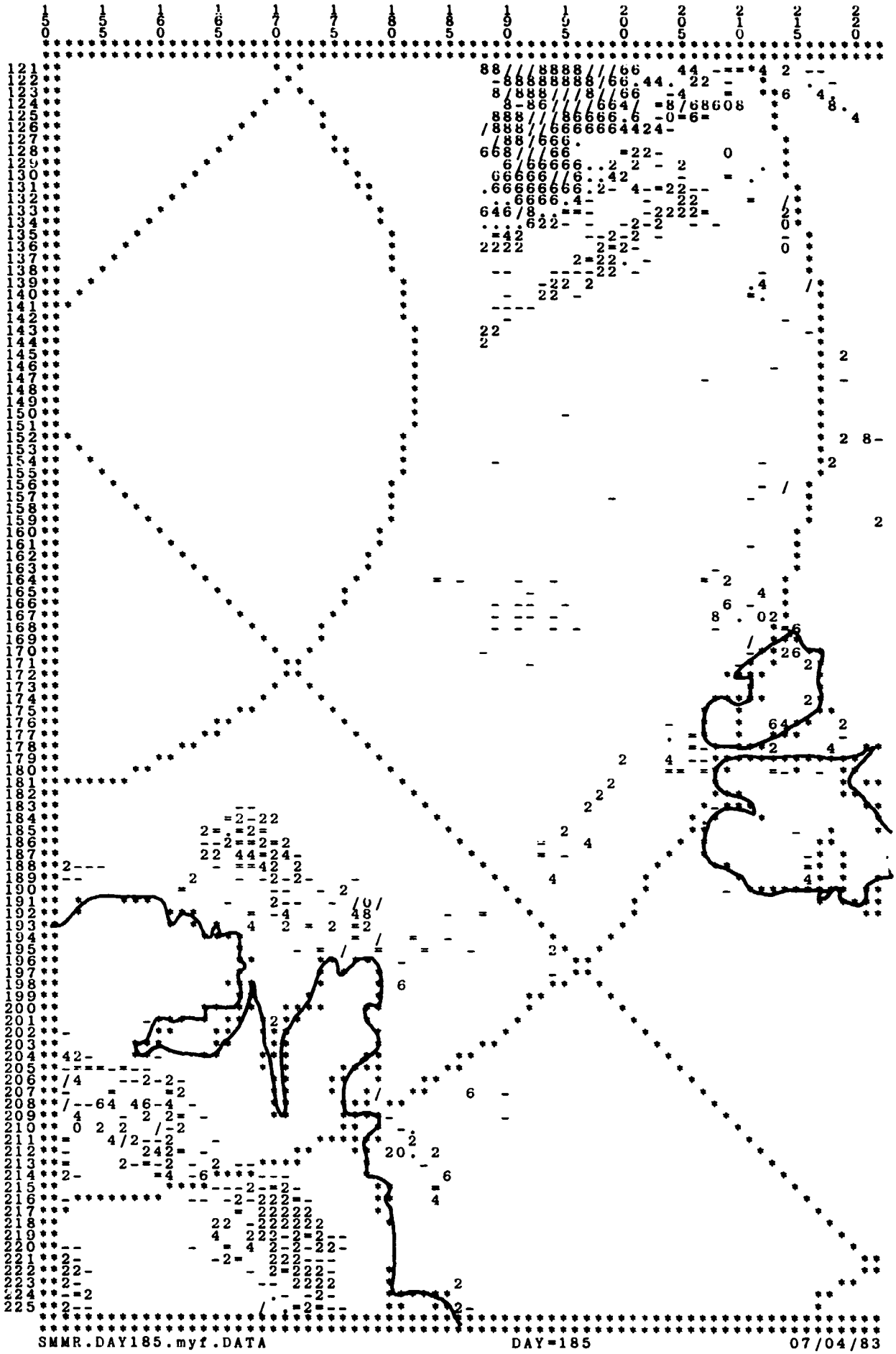
SMMR.DAY185.myf.DATA
DAY=185
07/04/83

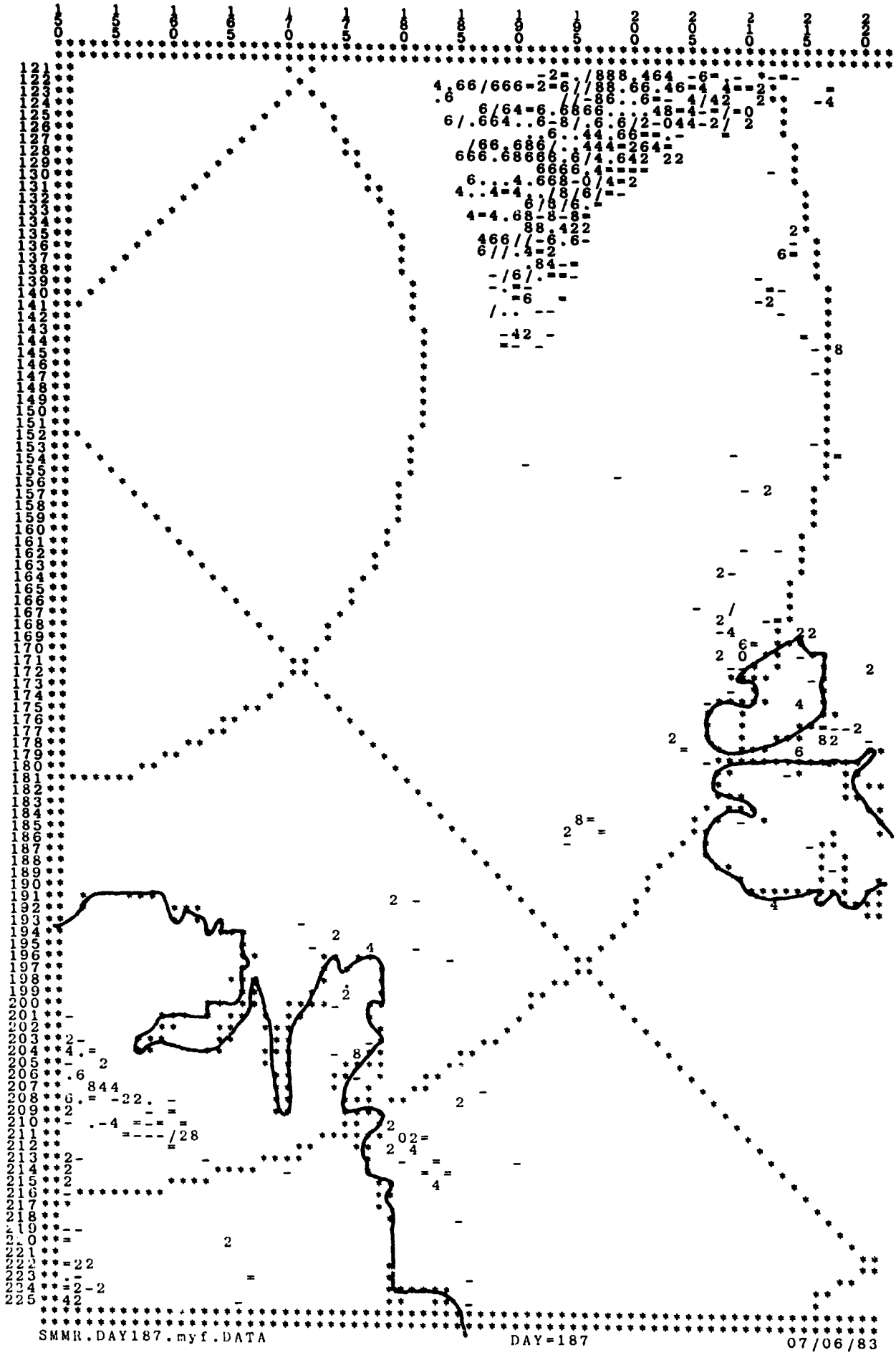
SMMR.DAY187.myf.DATA
DAY=187
07/06/83

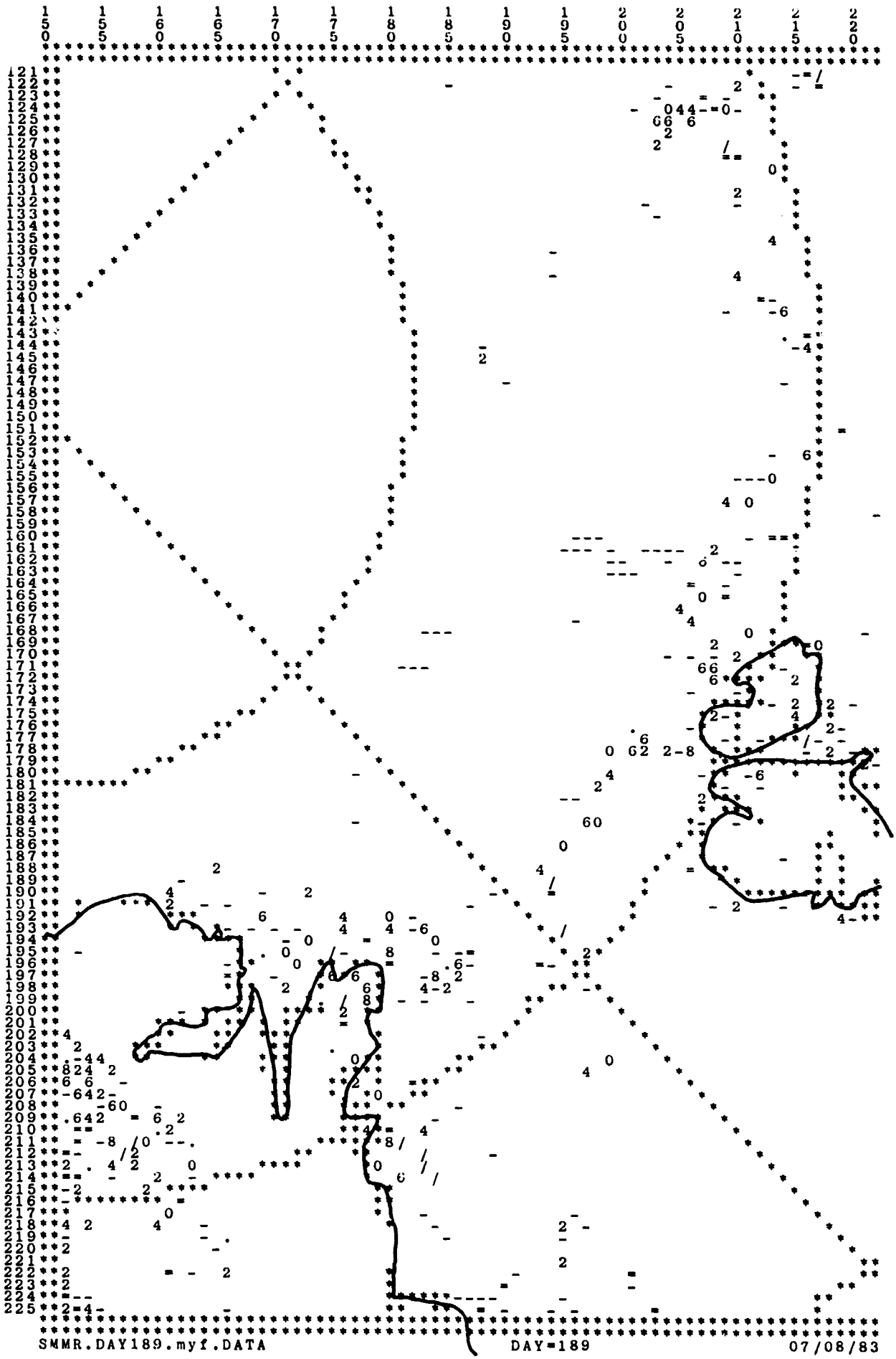
SMMR.DAY189.myf.DATA
DAY=189
07/08/83

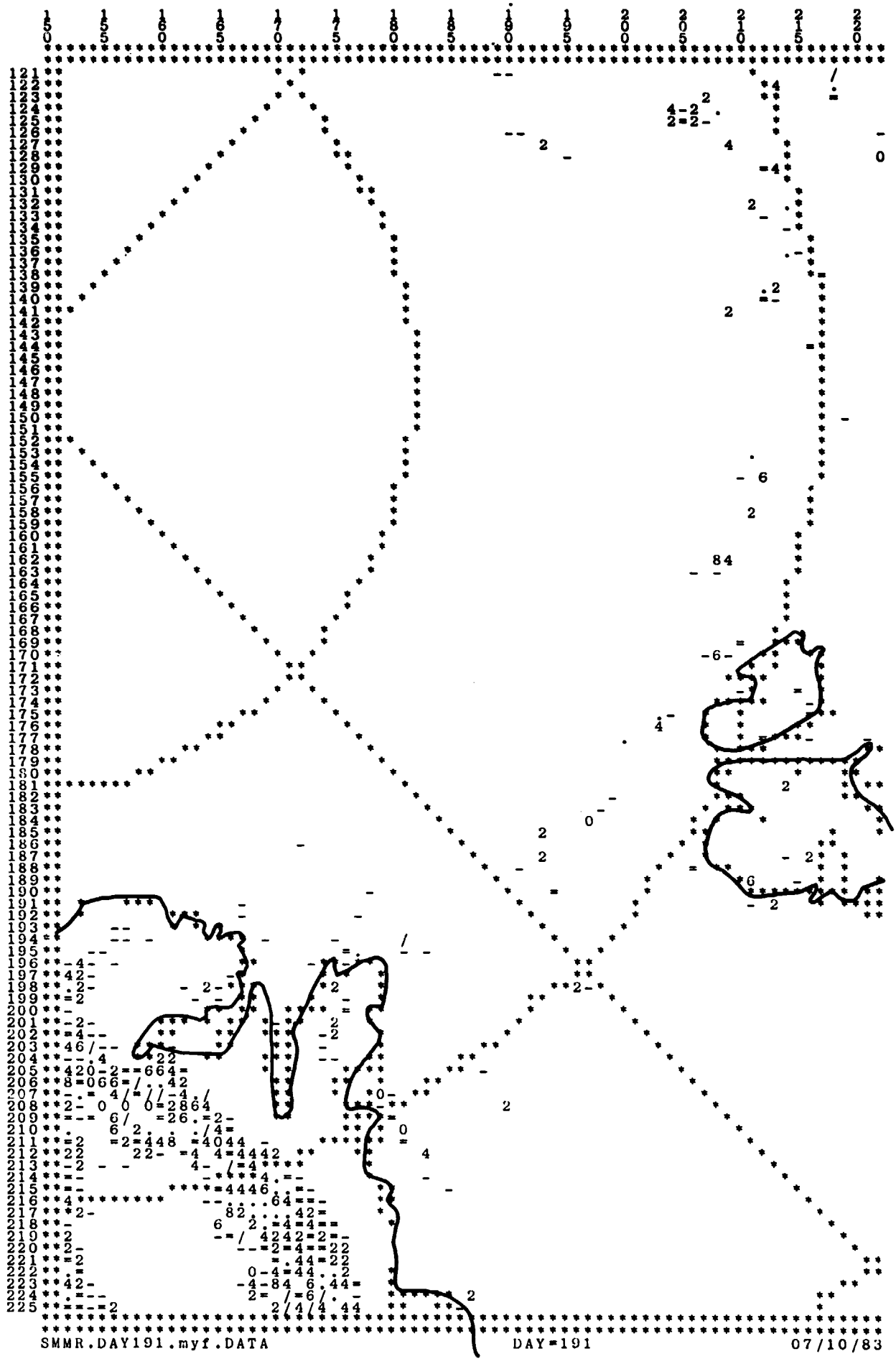
SMMR.DAY191.myf.DATA
DAY=191
07/10/83

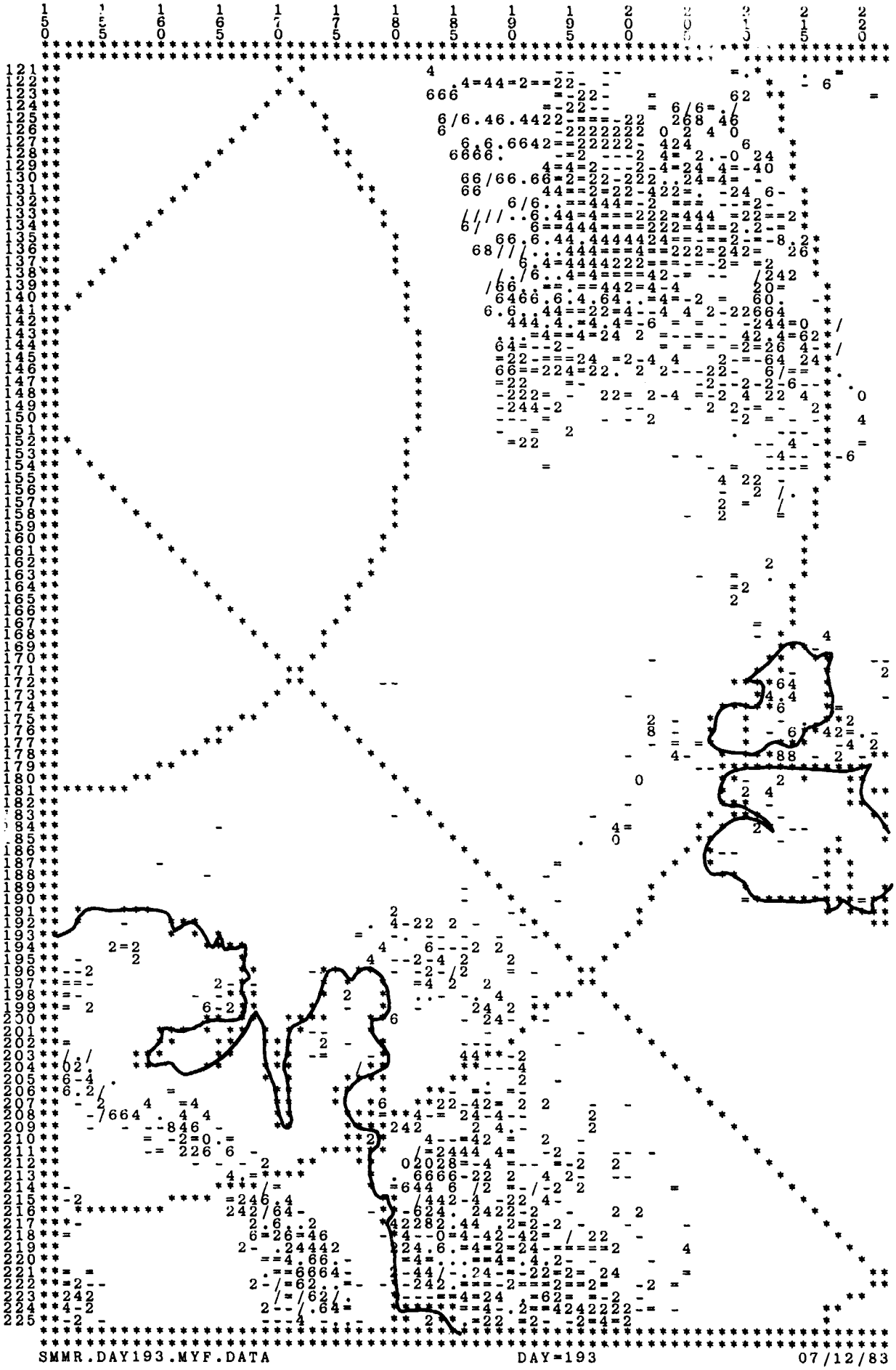
SMMR.DAY193.MYF.DATA
DAY=193
07/12/83

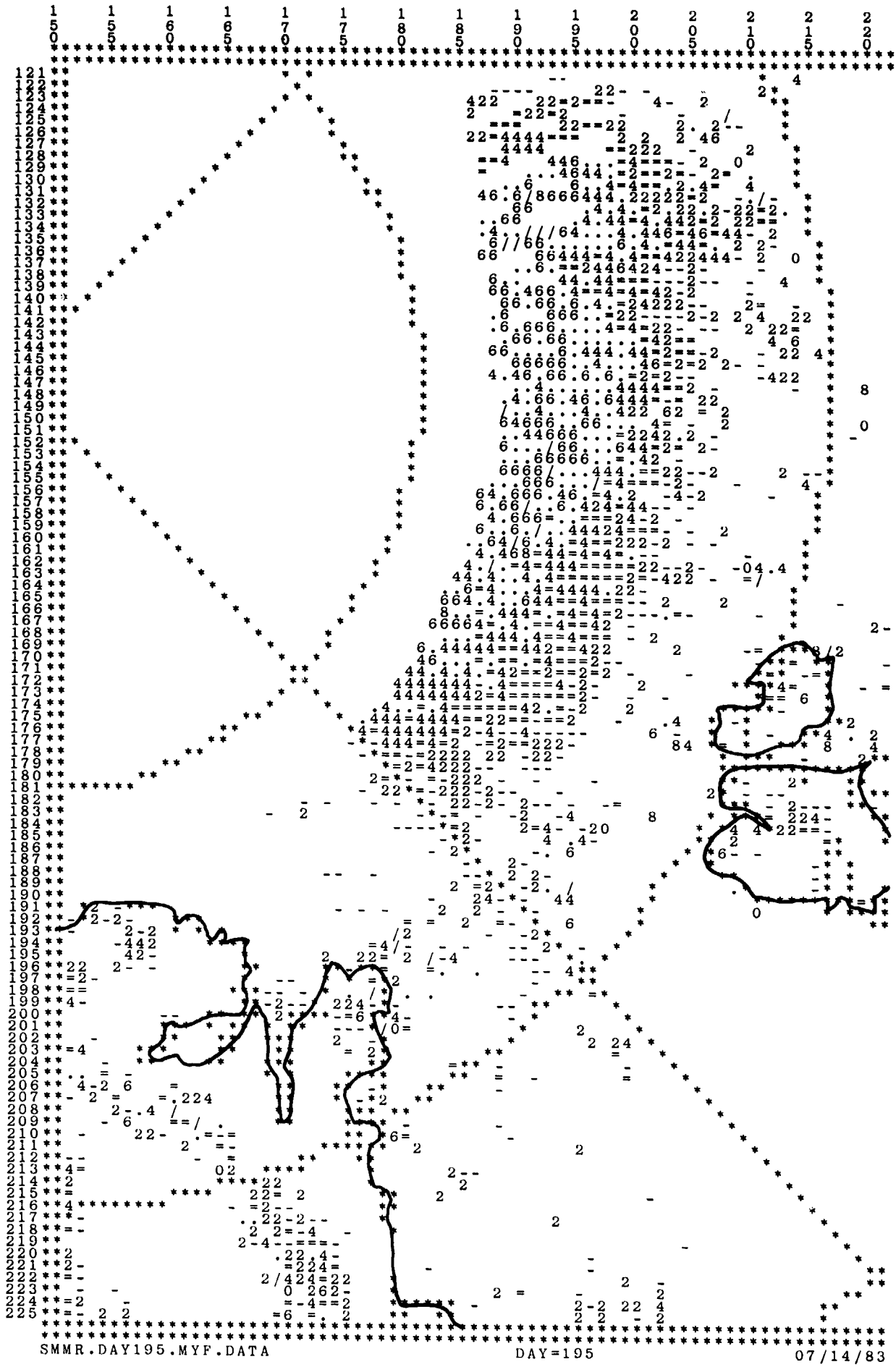
SMMR.DAY195.MYF.DATA
DAY=195
07/14/83

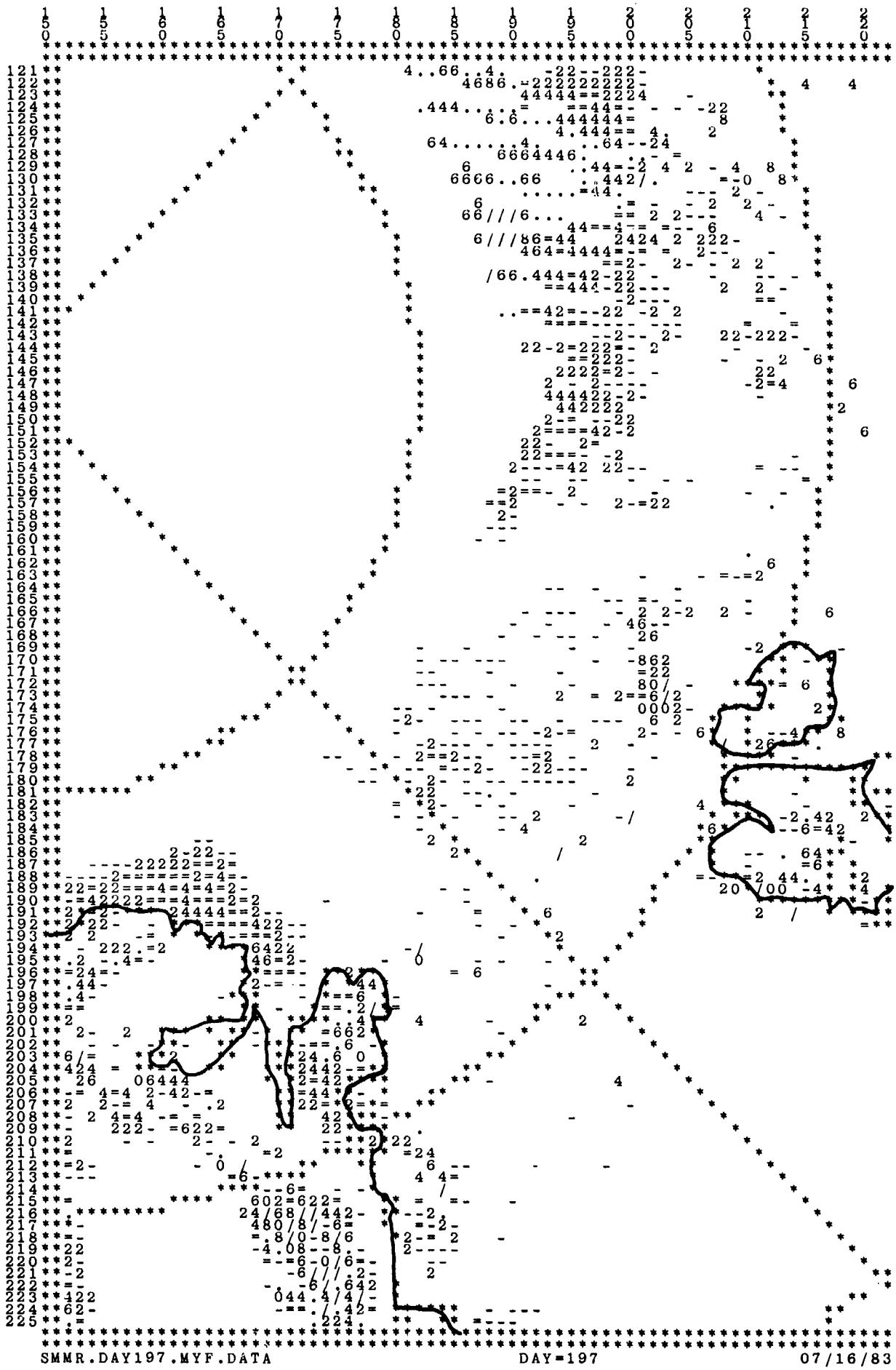
SMMR.DAY197.MYF.DATA
DAY=197
07/16/83

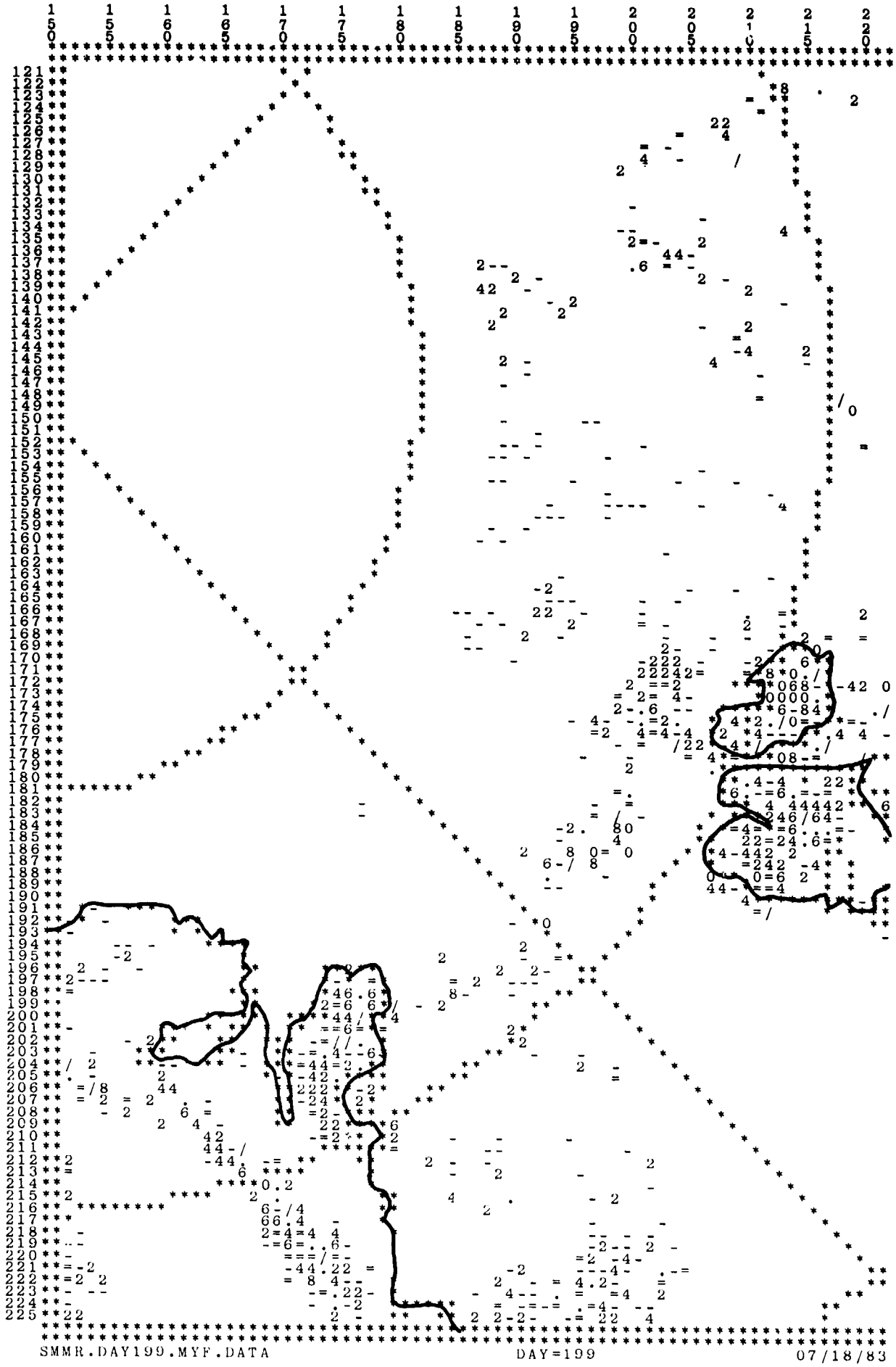
SMMR.DAY199.MYF.DATA
DAY=199
07/18/83

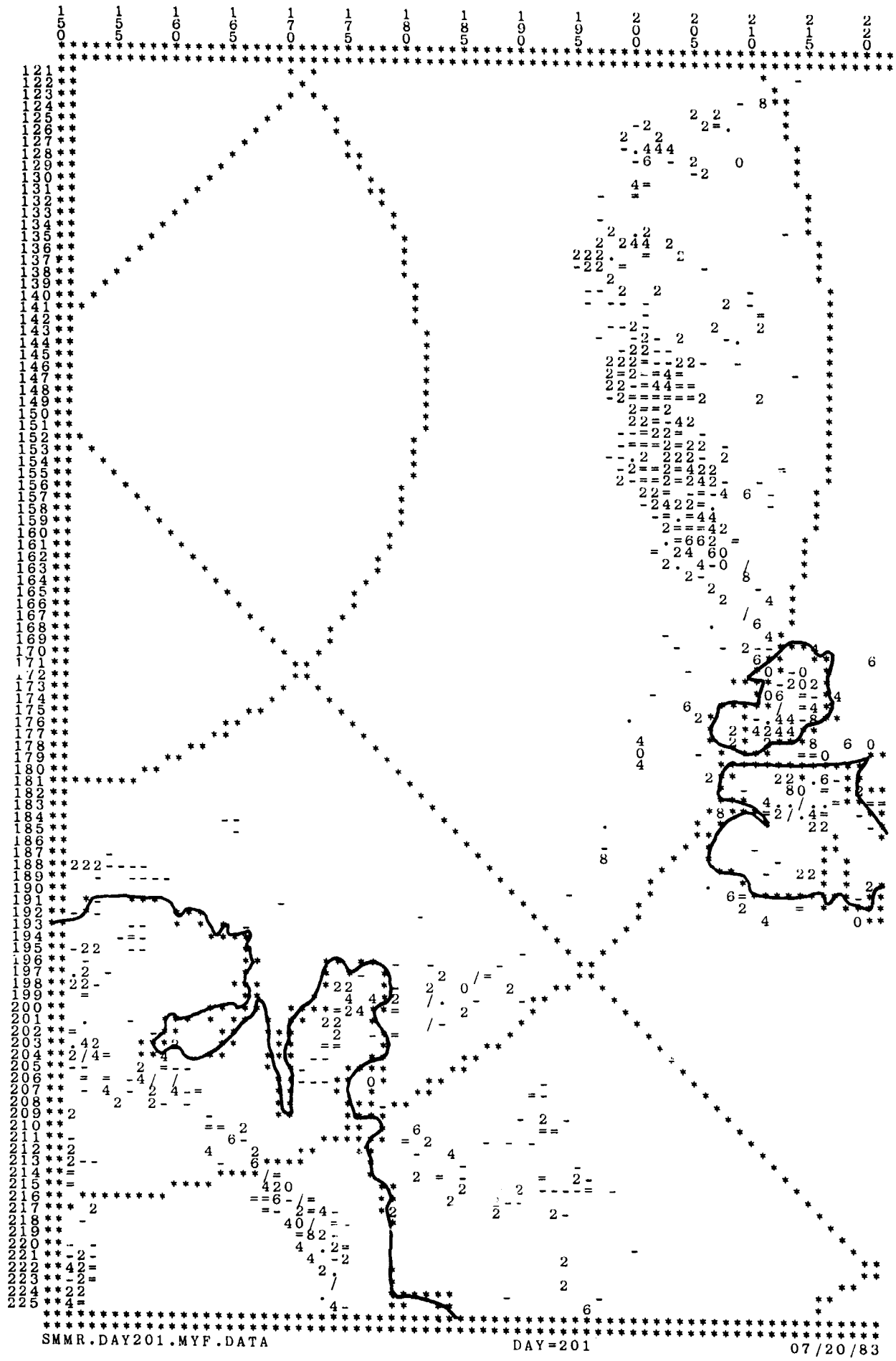
SMMR.DAY201.MYF.DATA
DAY=201
07/20/83

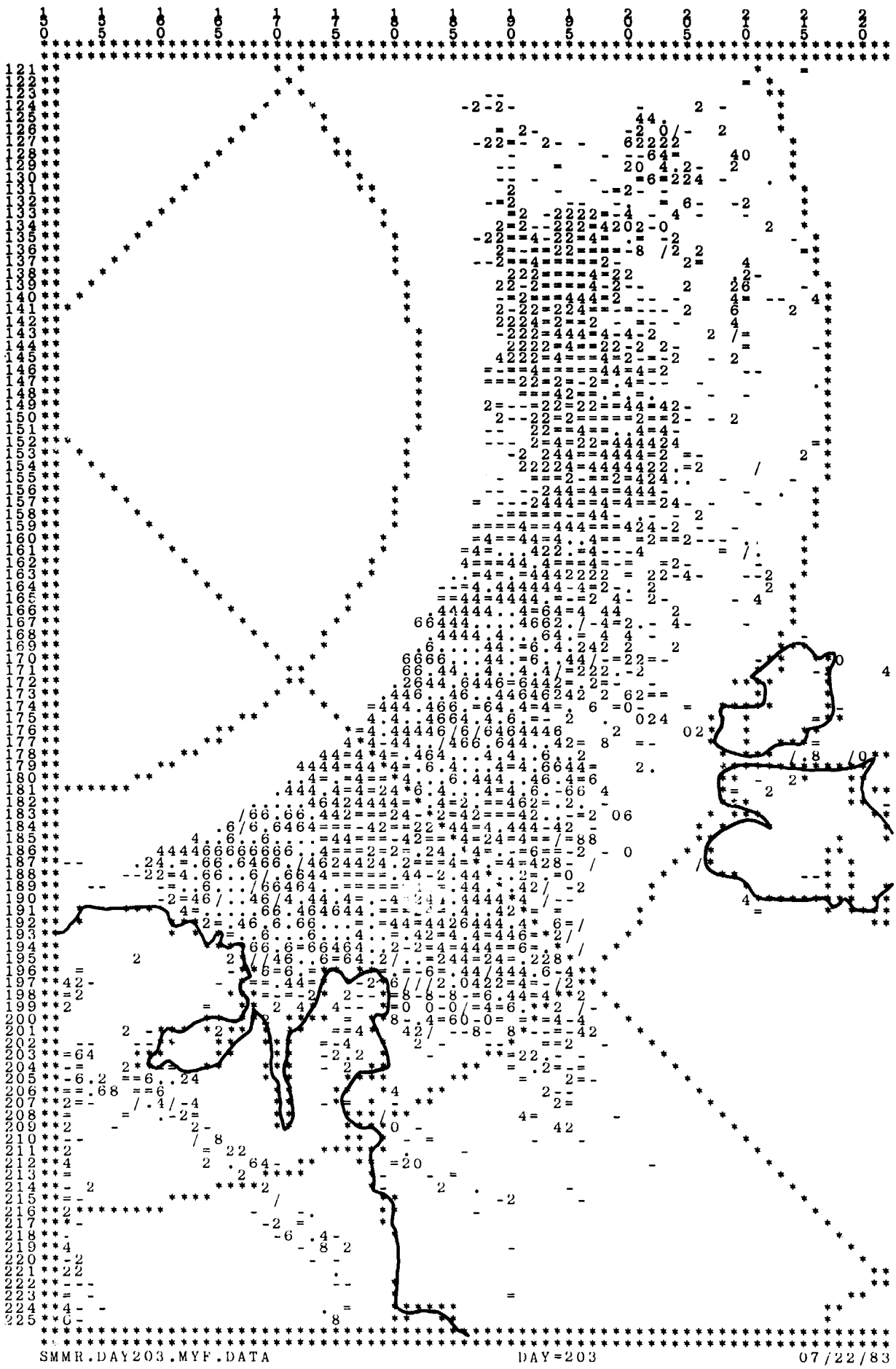
SMMR.DAY203.MYF.DATA
DAY=203
07/22/83

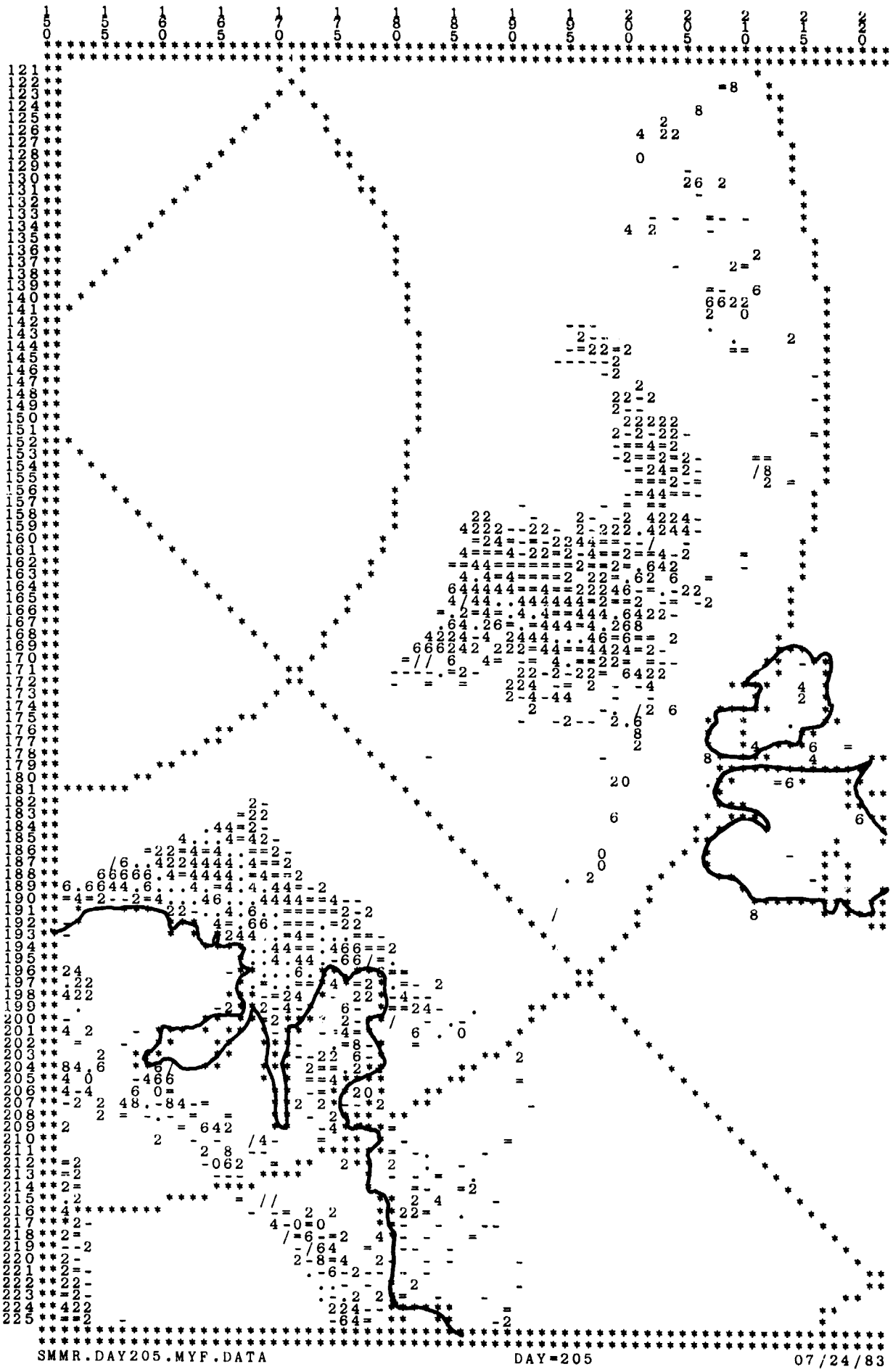
SMMR.DAY205.MYF.DATA
DAY=205
07/24/83

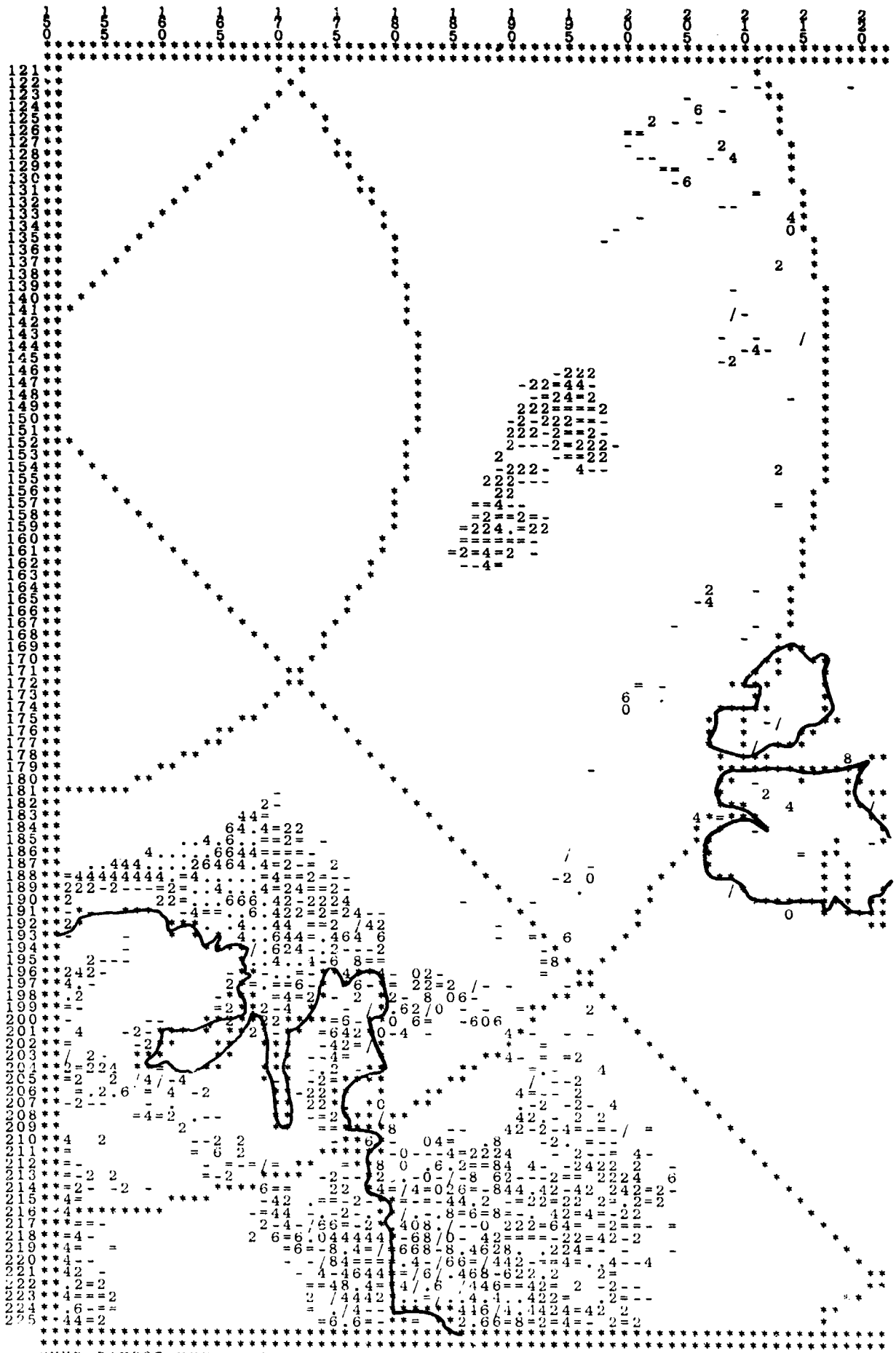
SMMR.DAY207.MYF.DATA
DAY=207
07/26/83

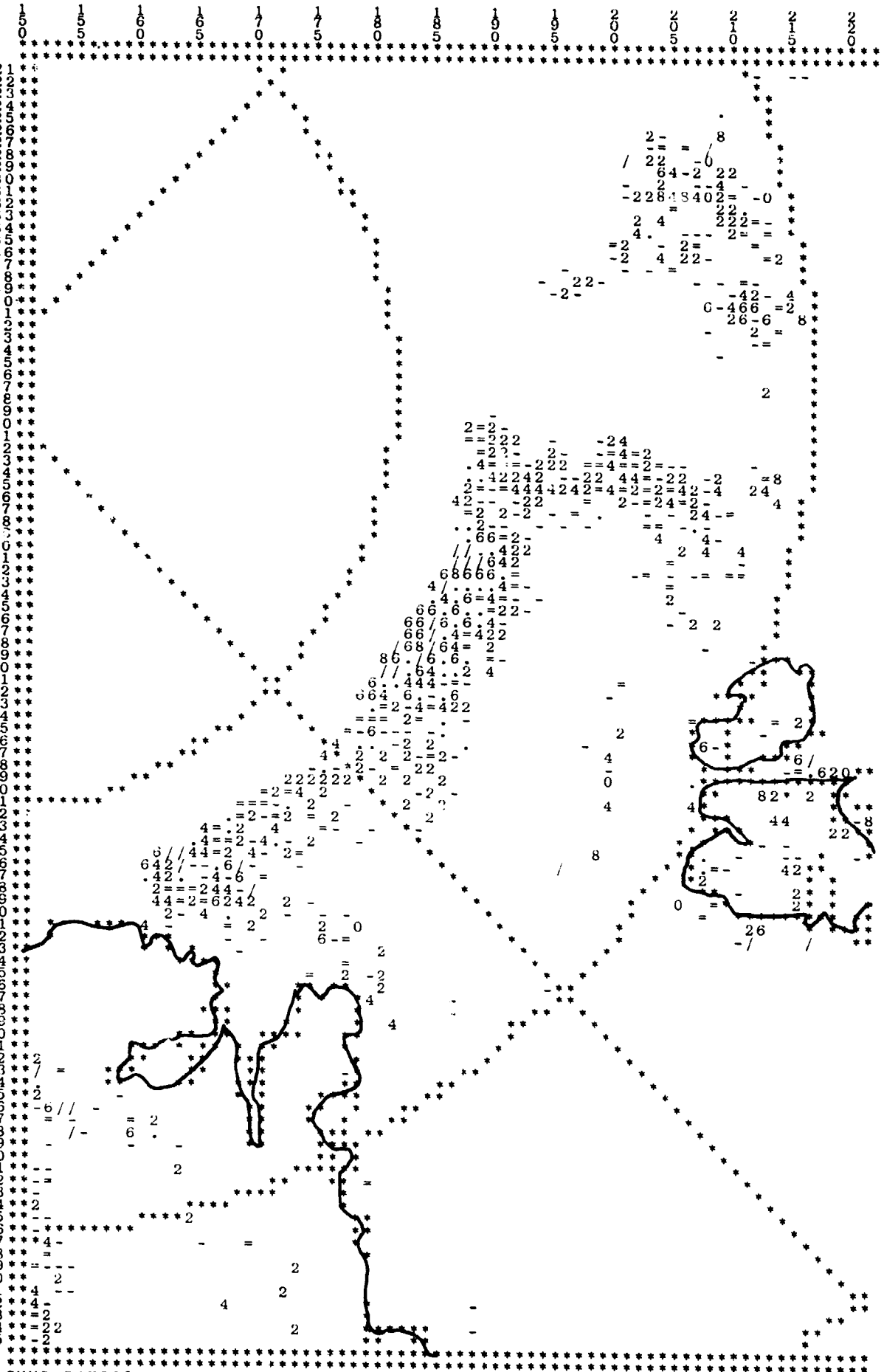
SMMR.DAY209.MYF.DATA
DAY=209
07/28/83

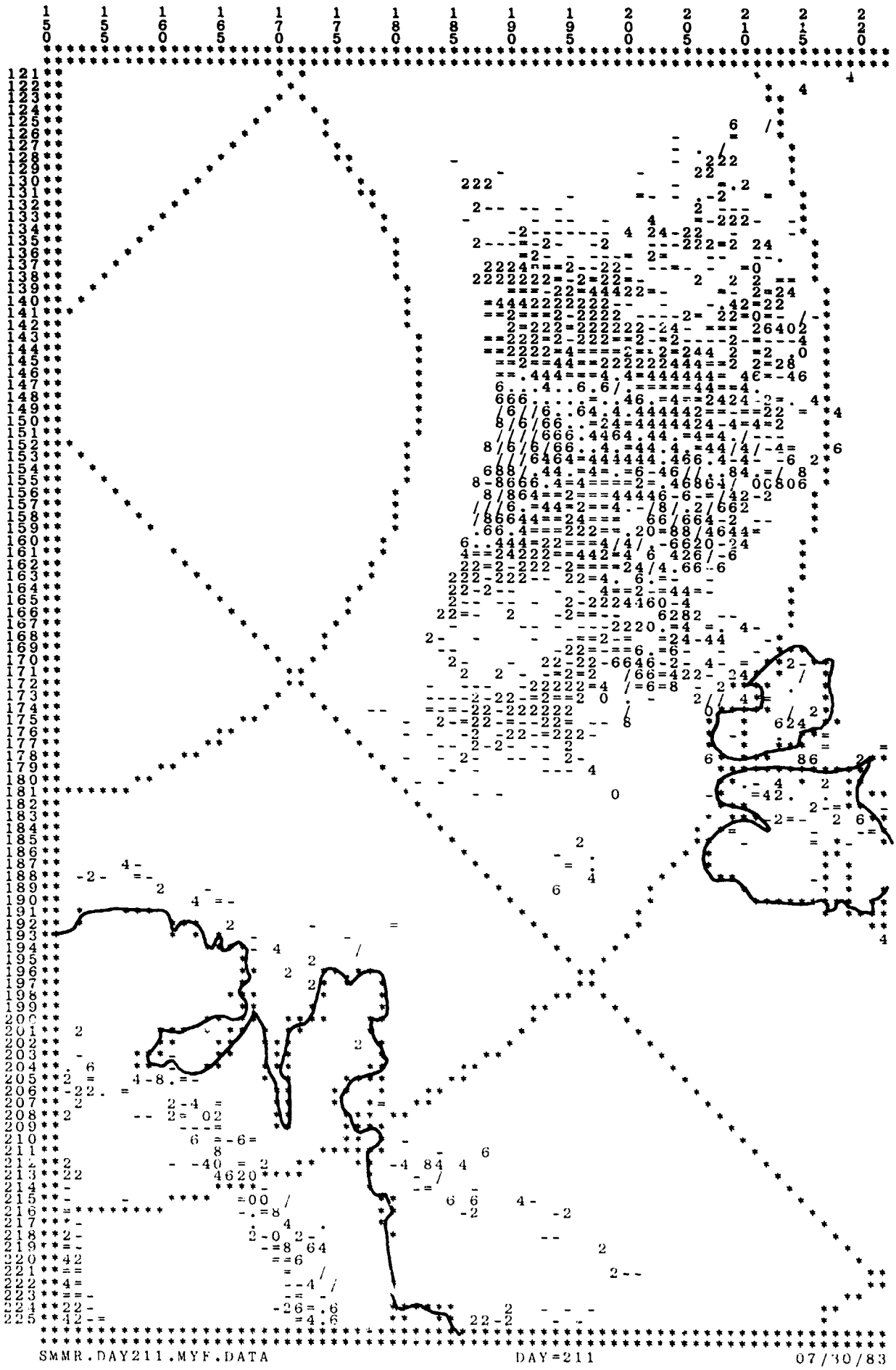
SMMR.DAY211.MYF.DATA
DAY=211
07/30/83

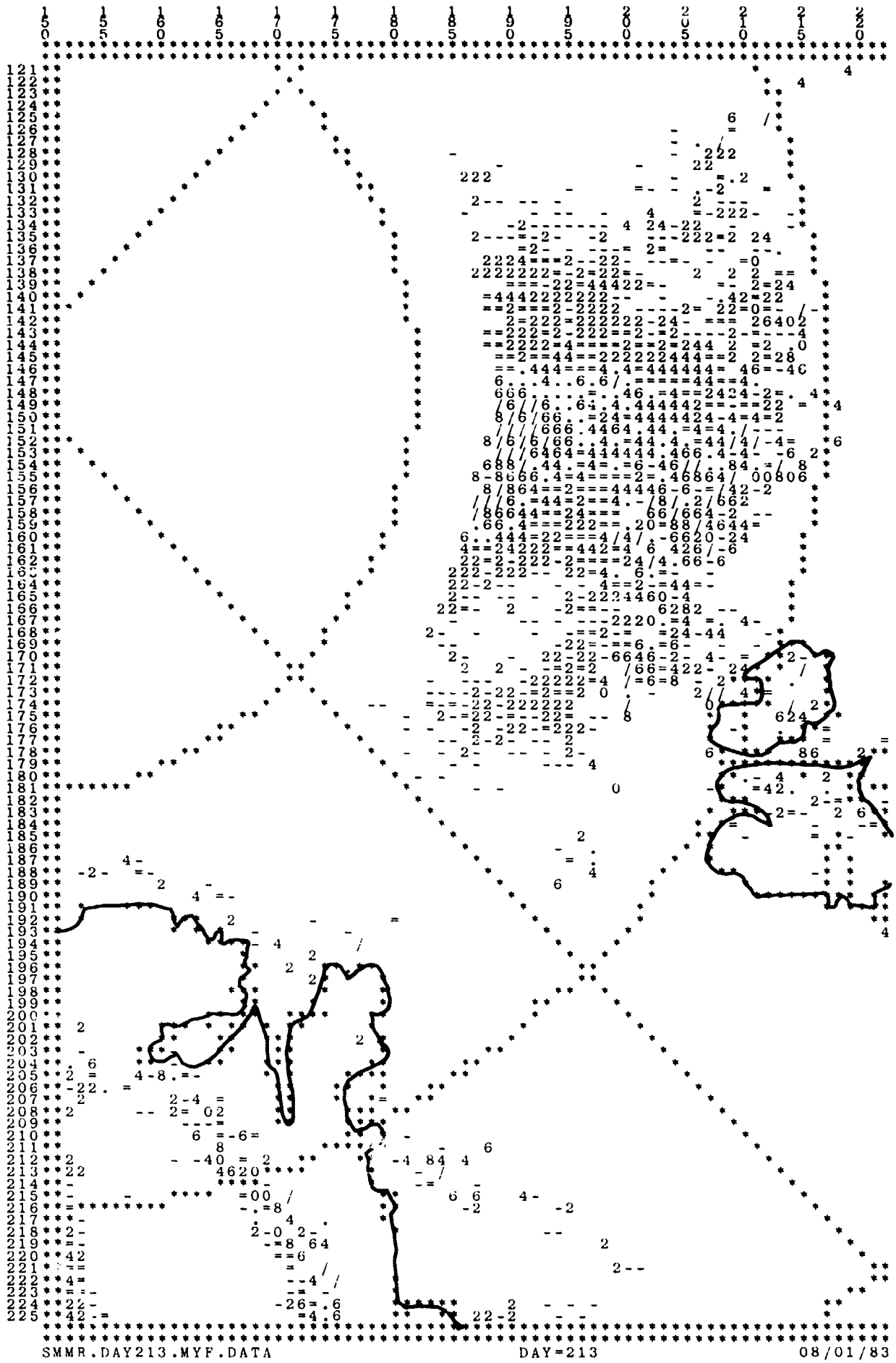
SMMR.DAY213.MYF.DATA
DAY=213
08/01/83

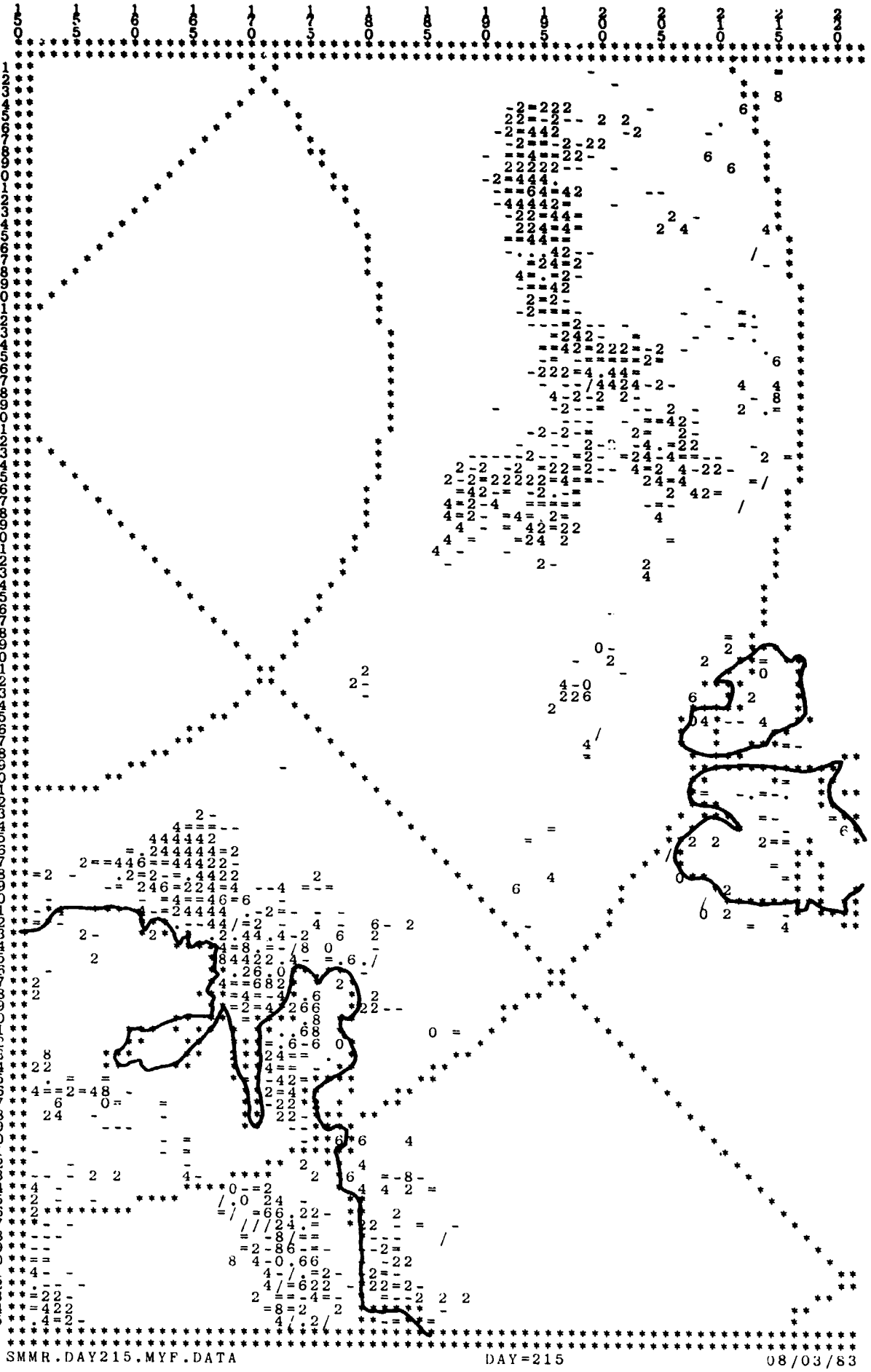
SMMR.DAY215.MYF.DATA
DAY=215
08/03/83

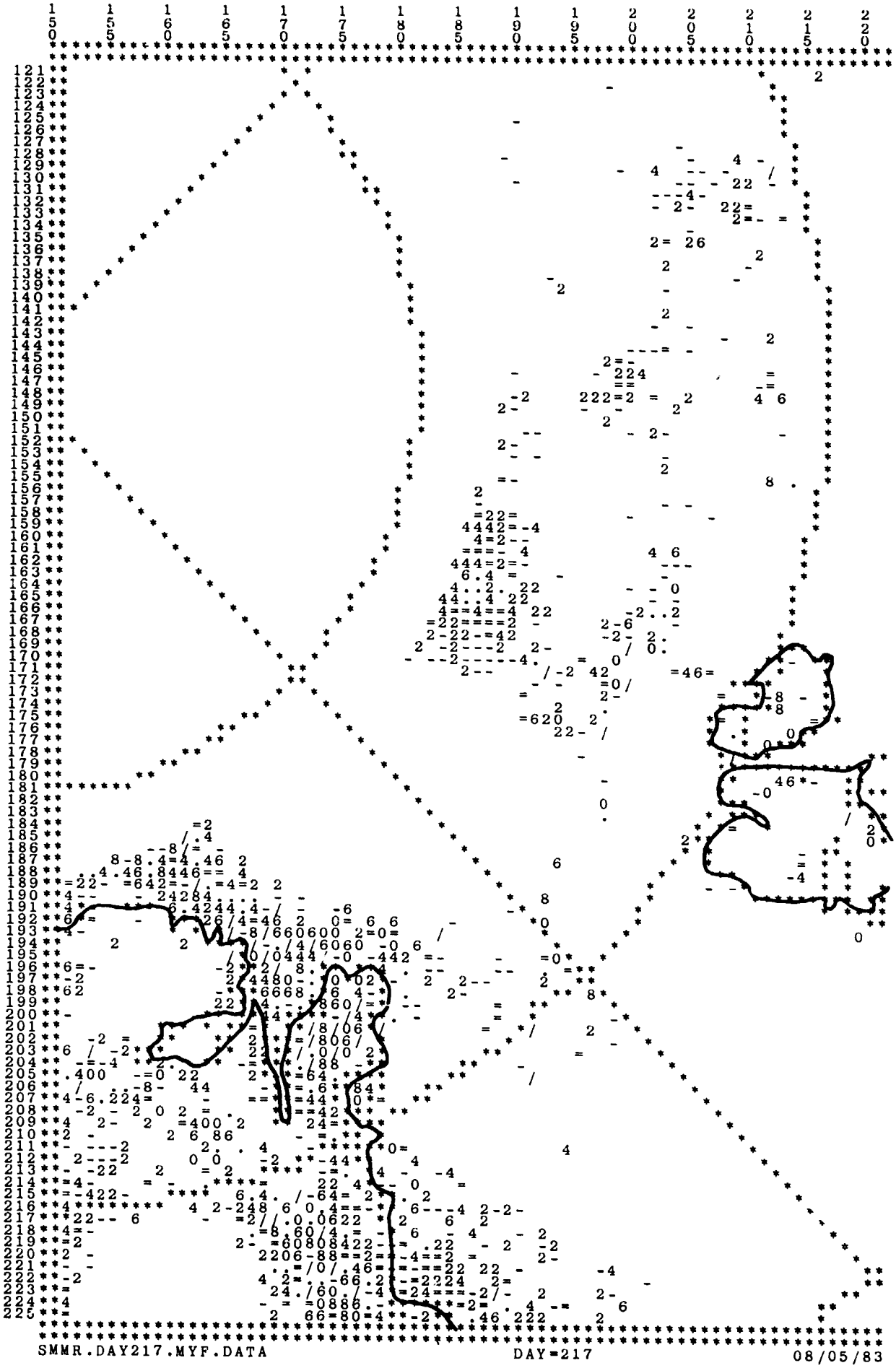
SMMR.DAY217.MYF.DATA
DAY=217
08/05/83

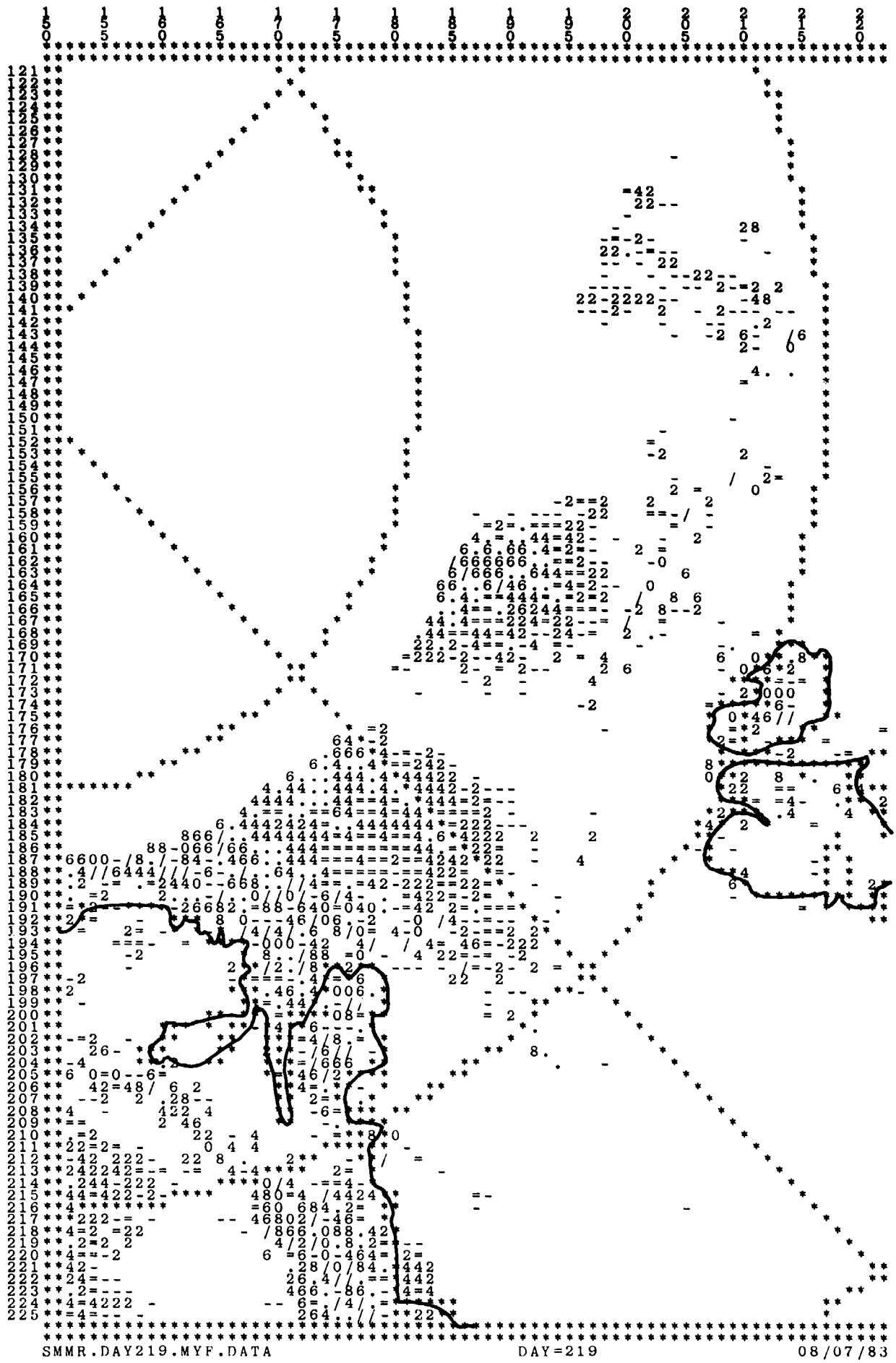
SMMR.DAY219.MYF.DATA
DAY=219
08/07/83

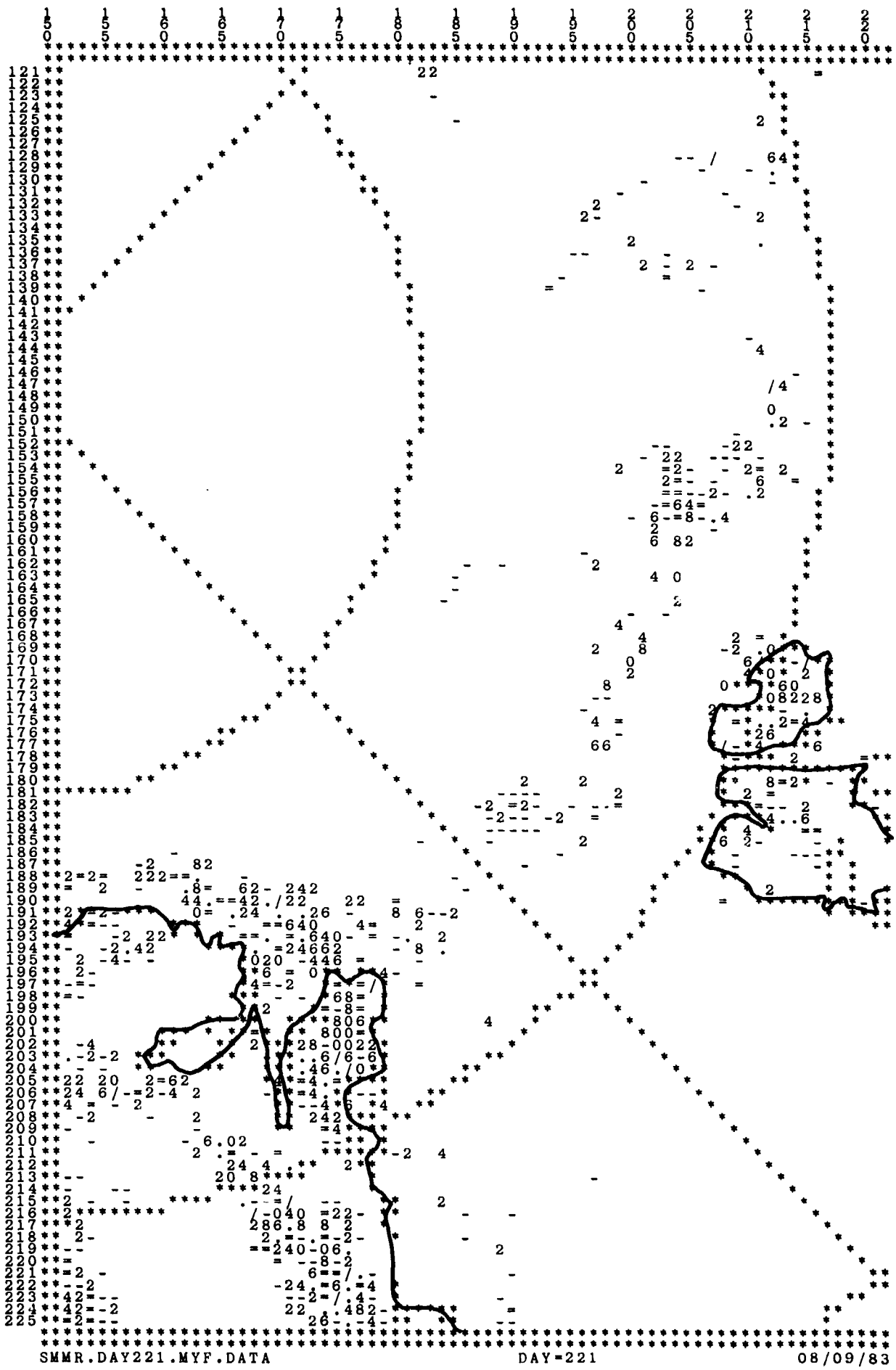
SMMR.DAY221.MYF.DATA
DAY=221
08/09/83

APPENDIX C

GREY-SCALE IMAGES OF TOTAL SEA ICE CONCENTRATION DURING MIZEX/EAST'83

ORIGINAL PAGE IS
OF POOR QUALITY

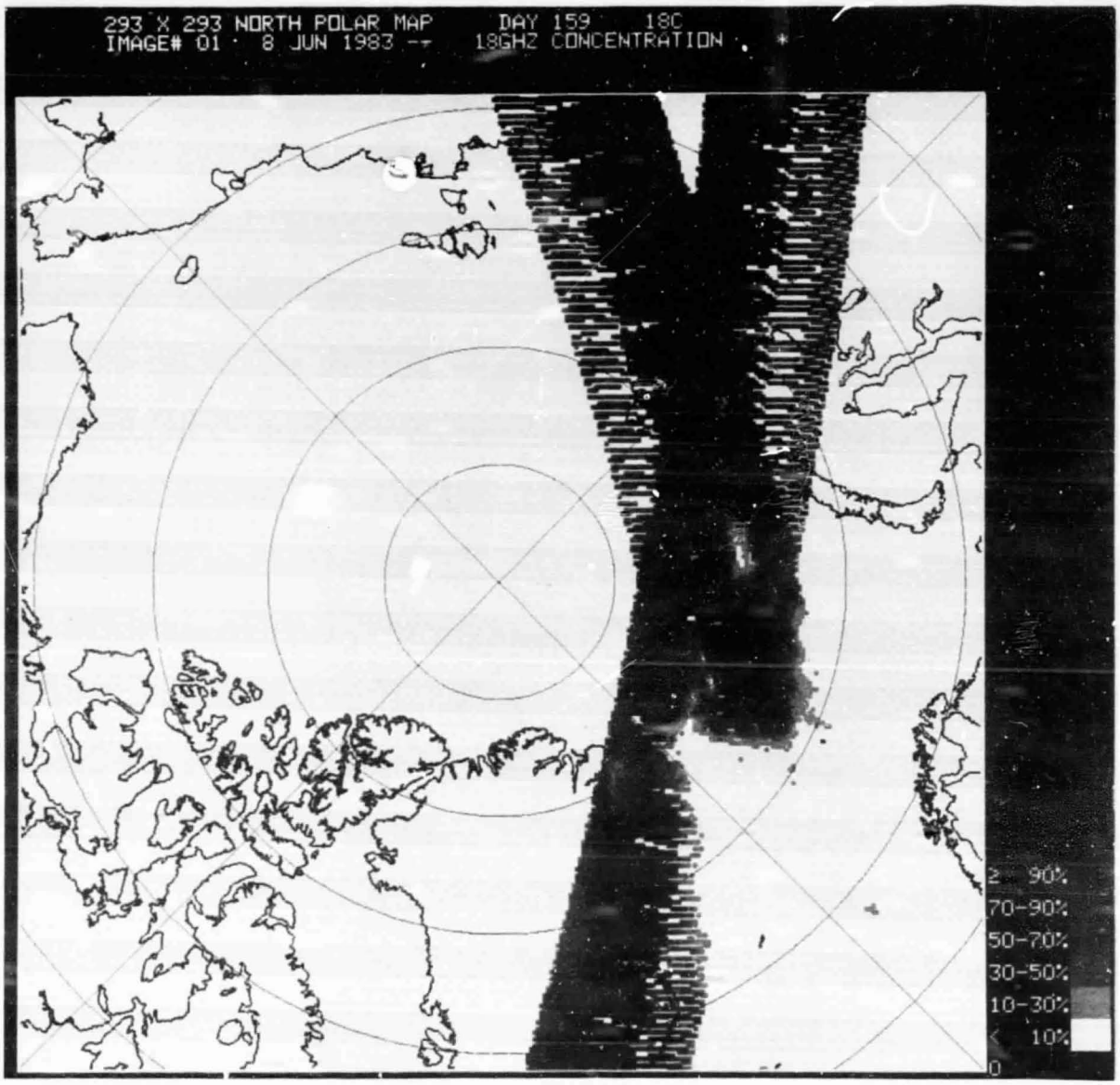

PRECEDING PAGE BLANK NOT FILMED

PAGE 80 INTENTIONALLY BLANK

ORIGINAL
OF POOR QUALITY

ORIGINAL PAGE IS
OF POOR QUALITY

ORIGINAL PAGE IS
OF POOR QUALITY

ORIGINAL PAGE IS
OF POOR QUALITY

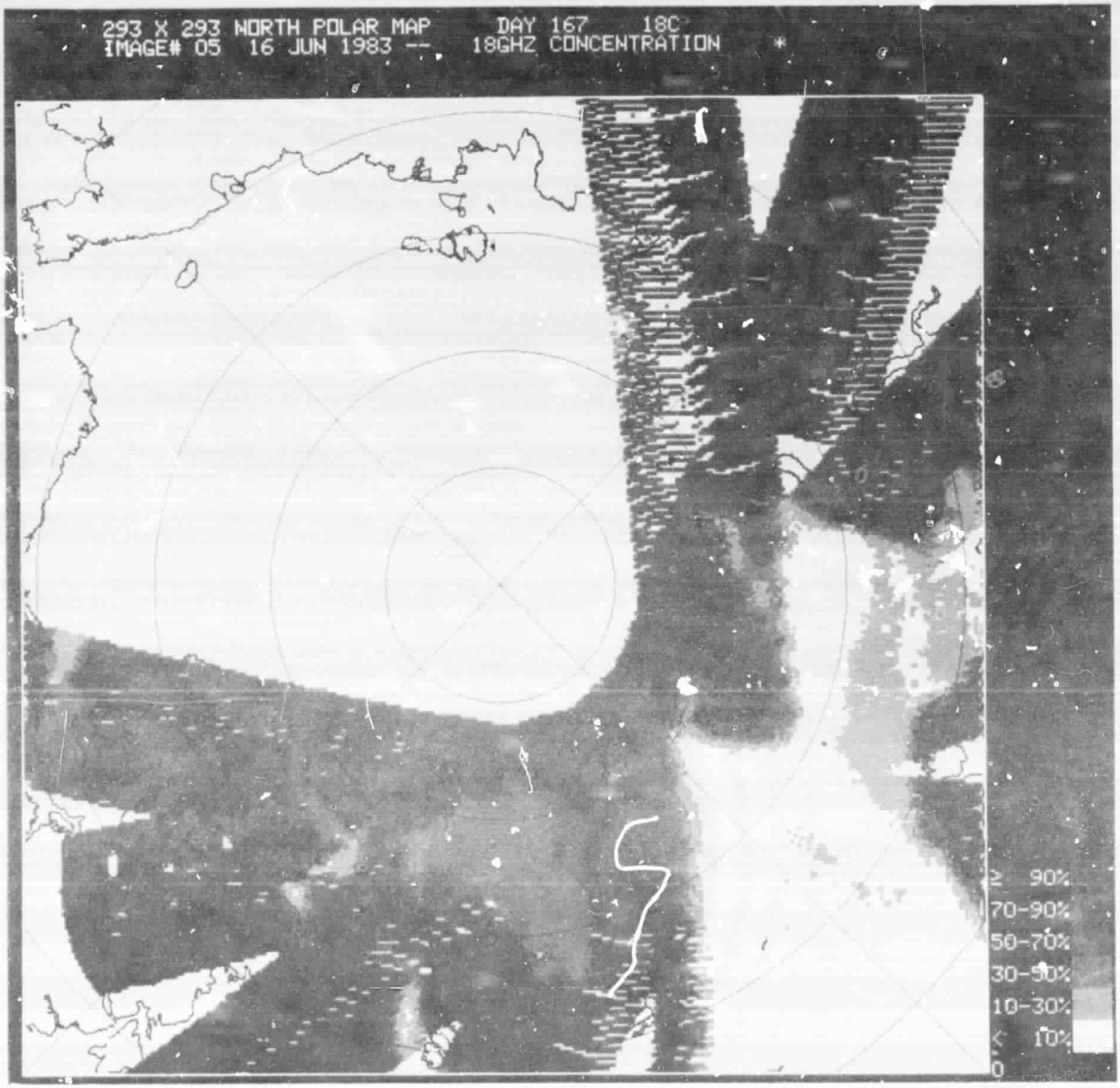

ORIGINAL PAGE IS
OF POOR QUALITY

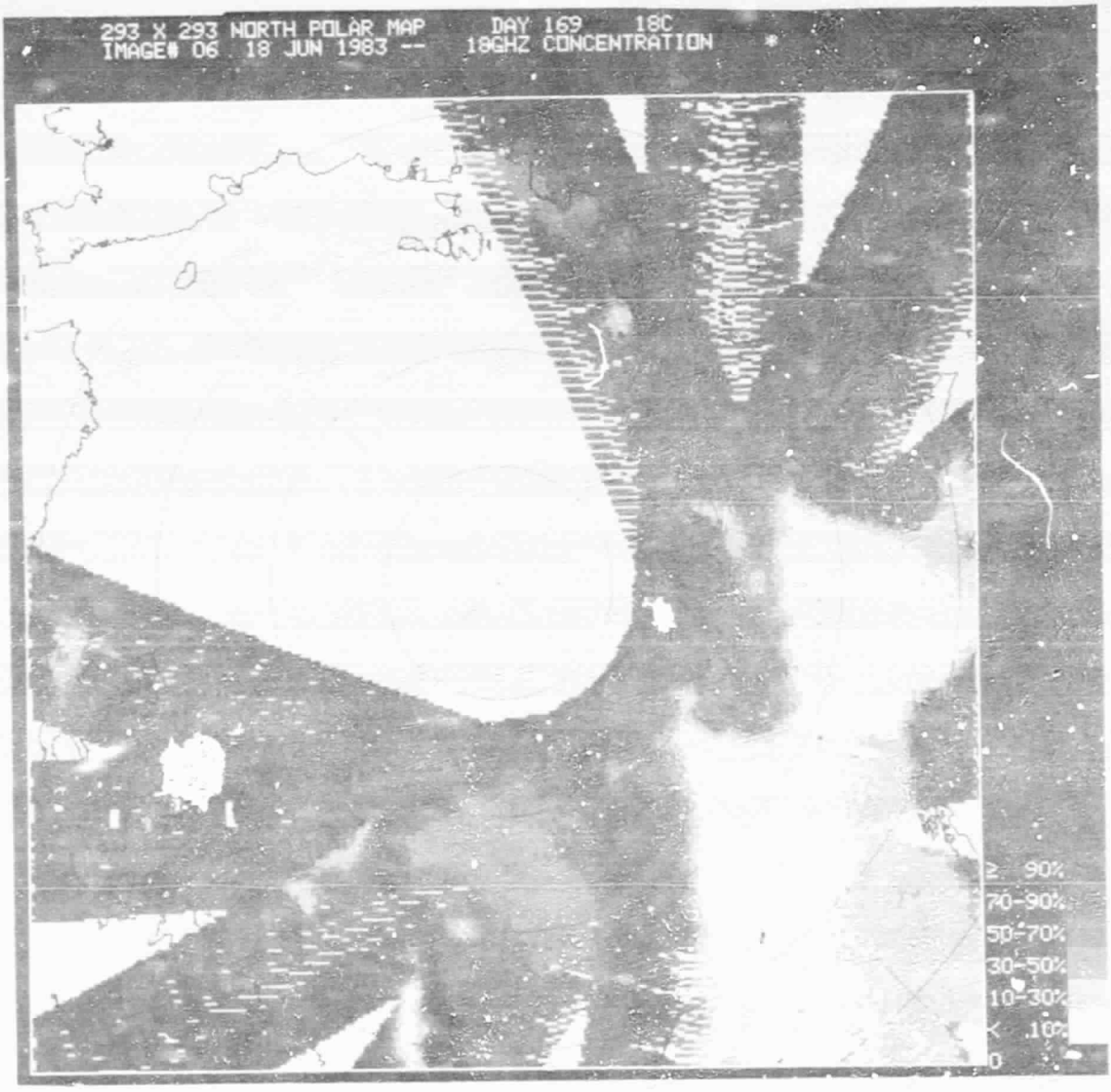

ORIGINAL PAGE IS
OF POOR QUALITY

ORIGINAL PAGE IS
OF POOR QUALITY

ORIGINAL PAGE IS
OF POOR QUALITY

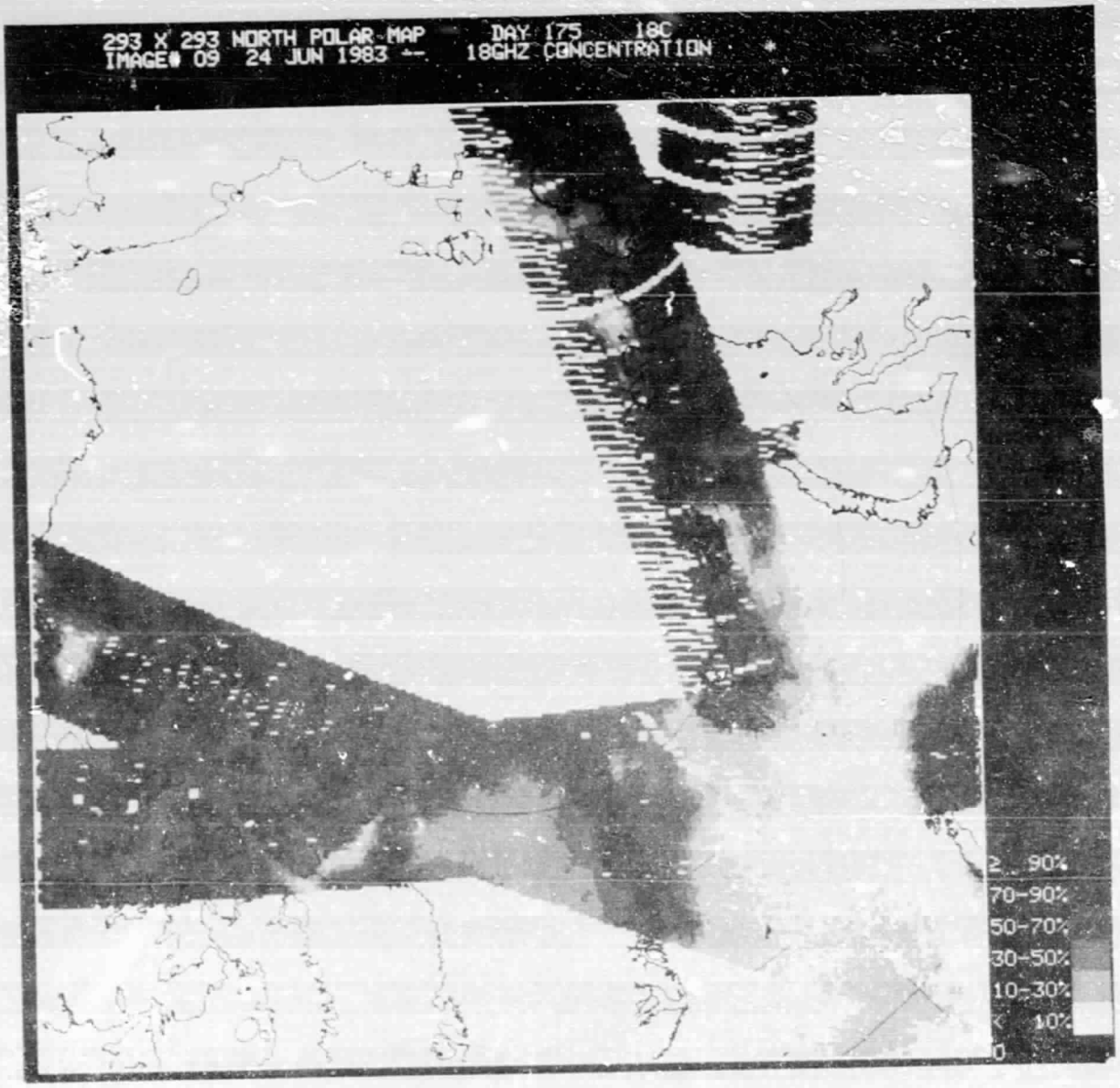

ORIGINAL PAGE IS
OF POOR QUALITY

ORIGINAL PAGE IS
OF POOR QUALITY

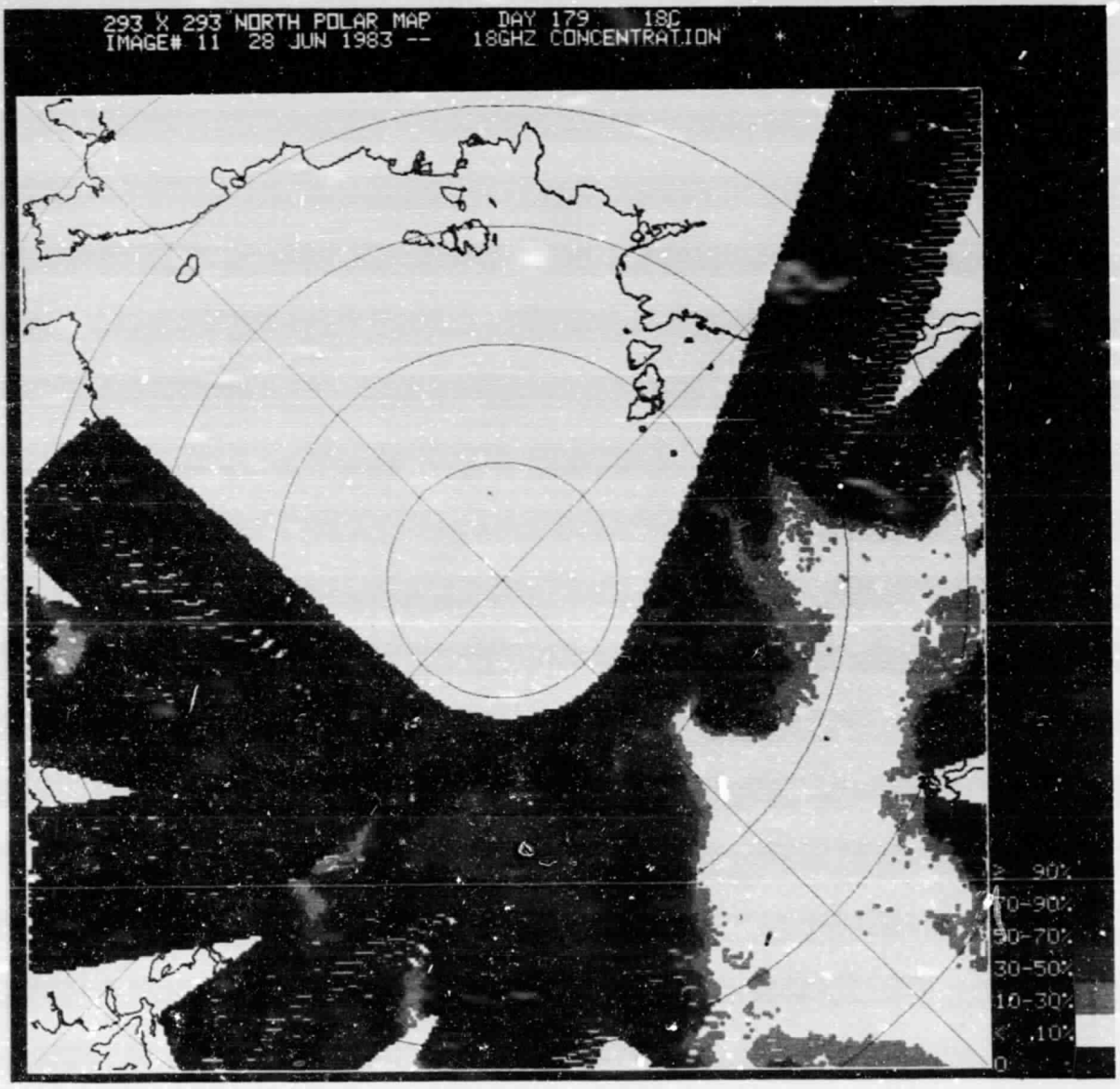

ORIGINAL PAGE IS
OF POOR QUALITY

ORIGINAL PAGE IS
OF POOR QUALITY

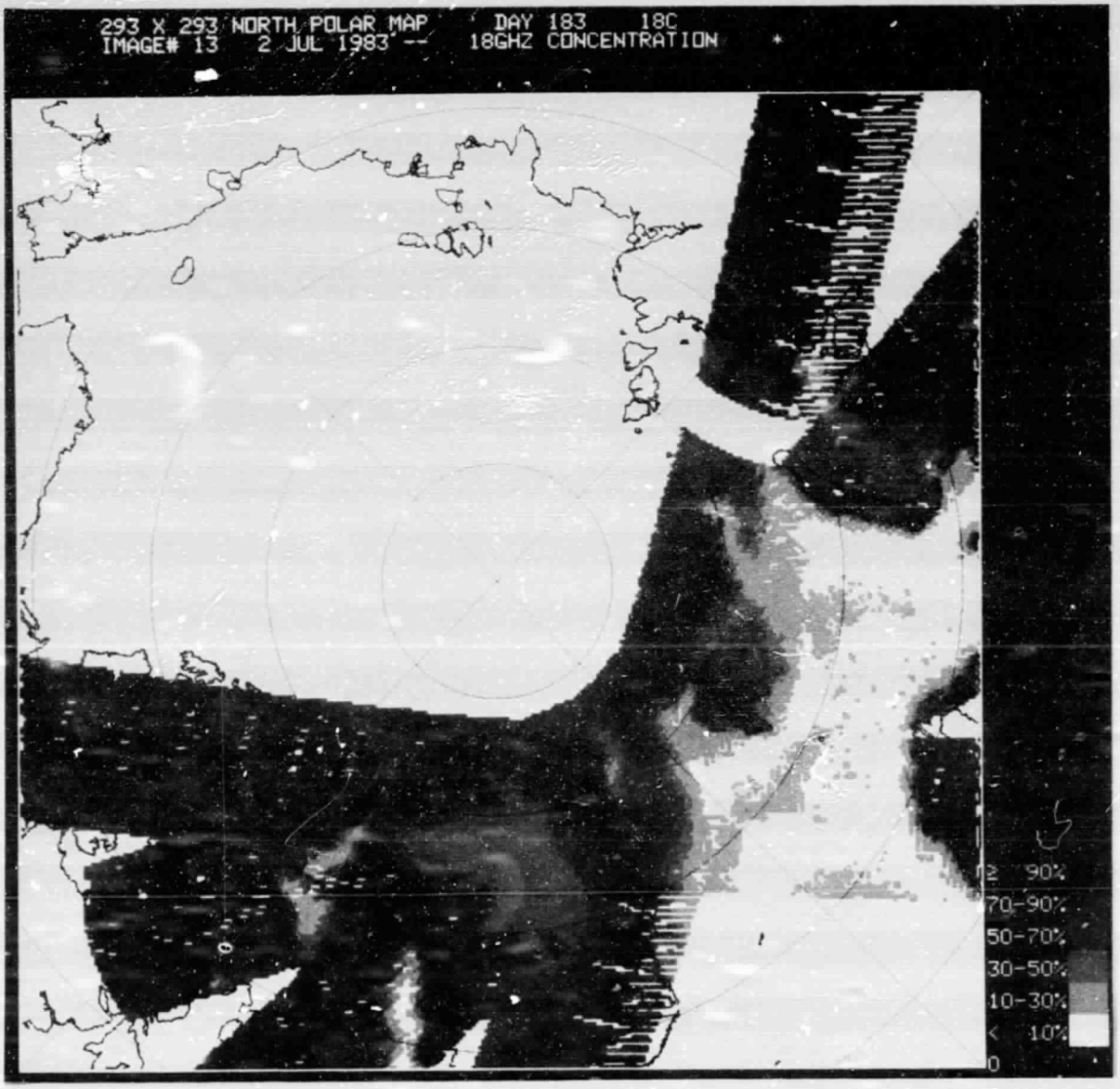

ORIGINAL PAGE IS
OF POOR QUALITY

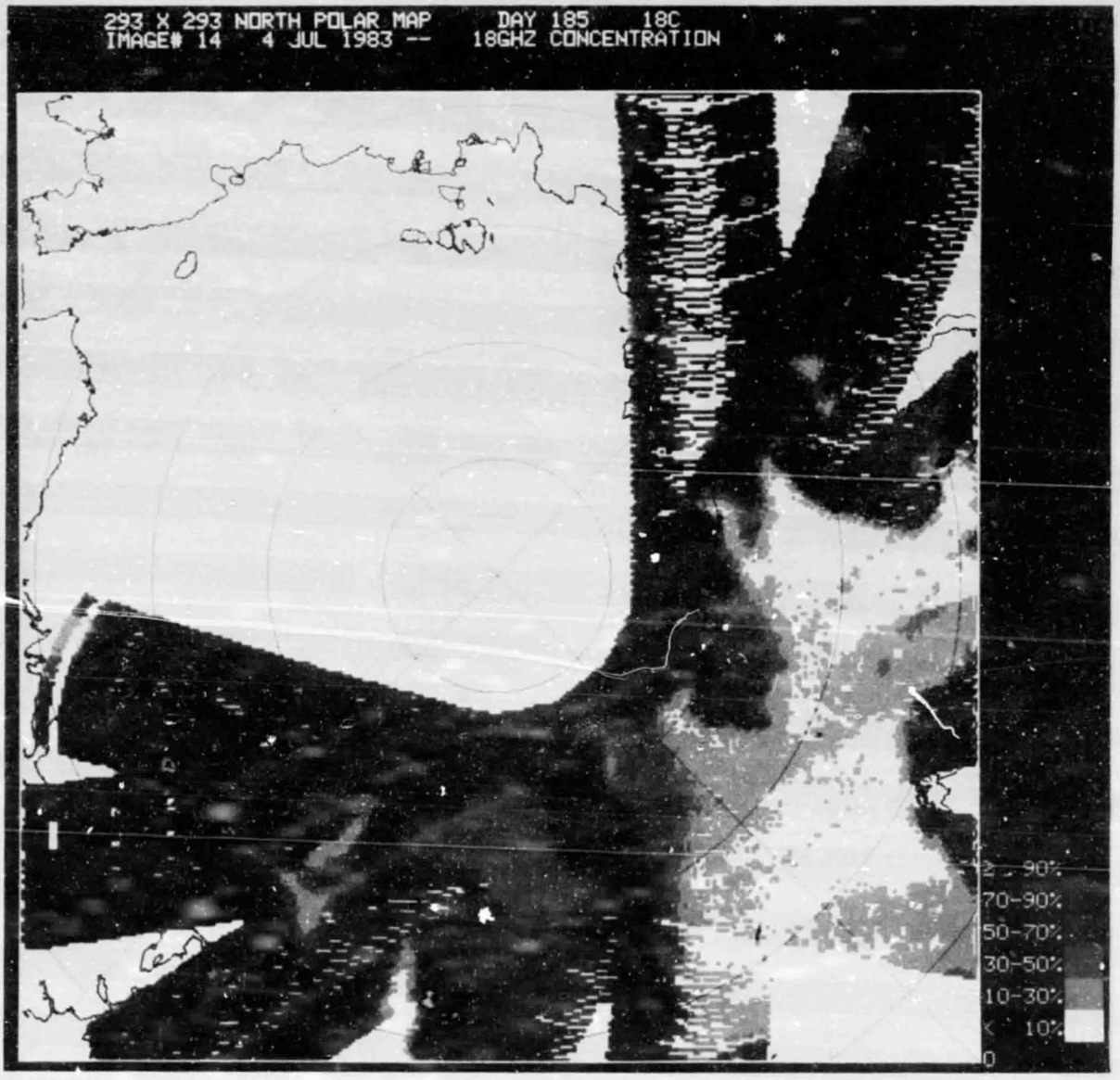

ORIGINAL PAGE IS
OF POOR QUALITY

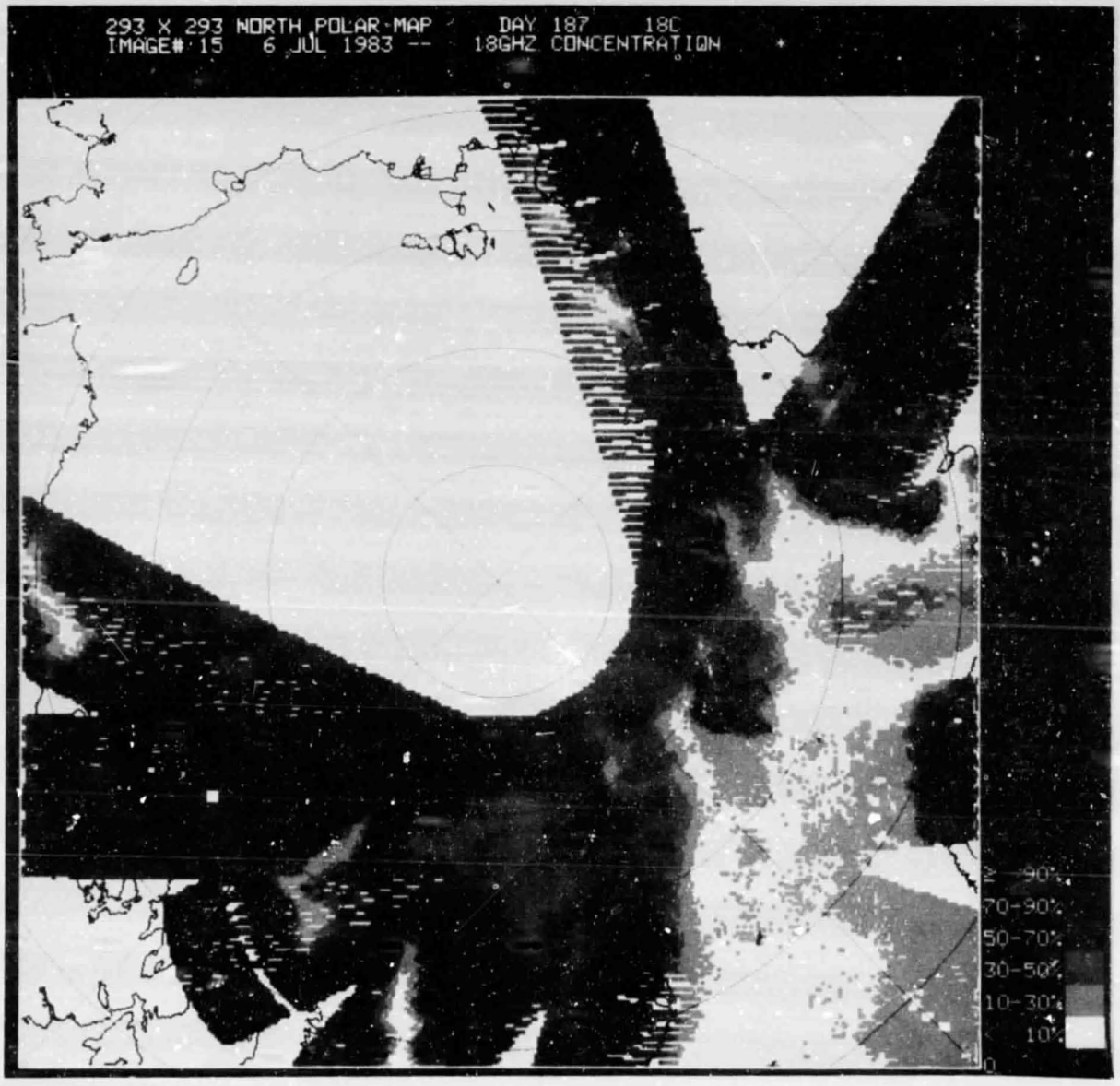

ORIGINAL PAGE IS
OF POOR QUALITY

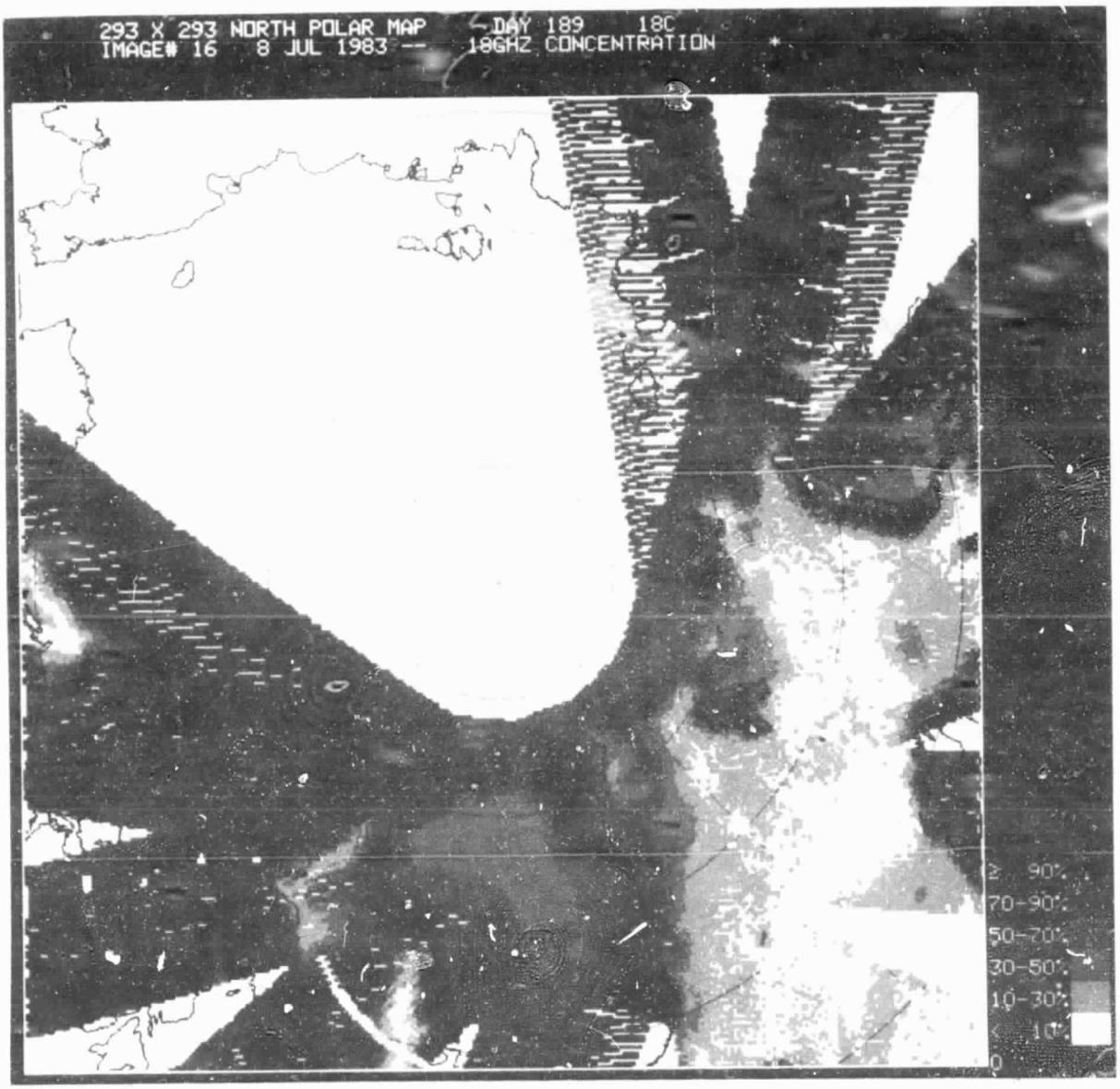

ORIGINAL
OF POOR QUALITY

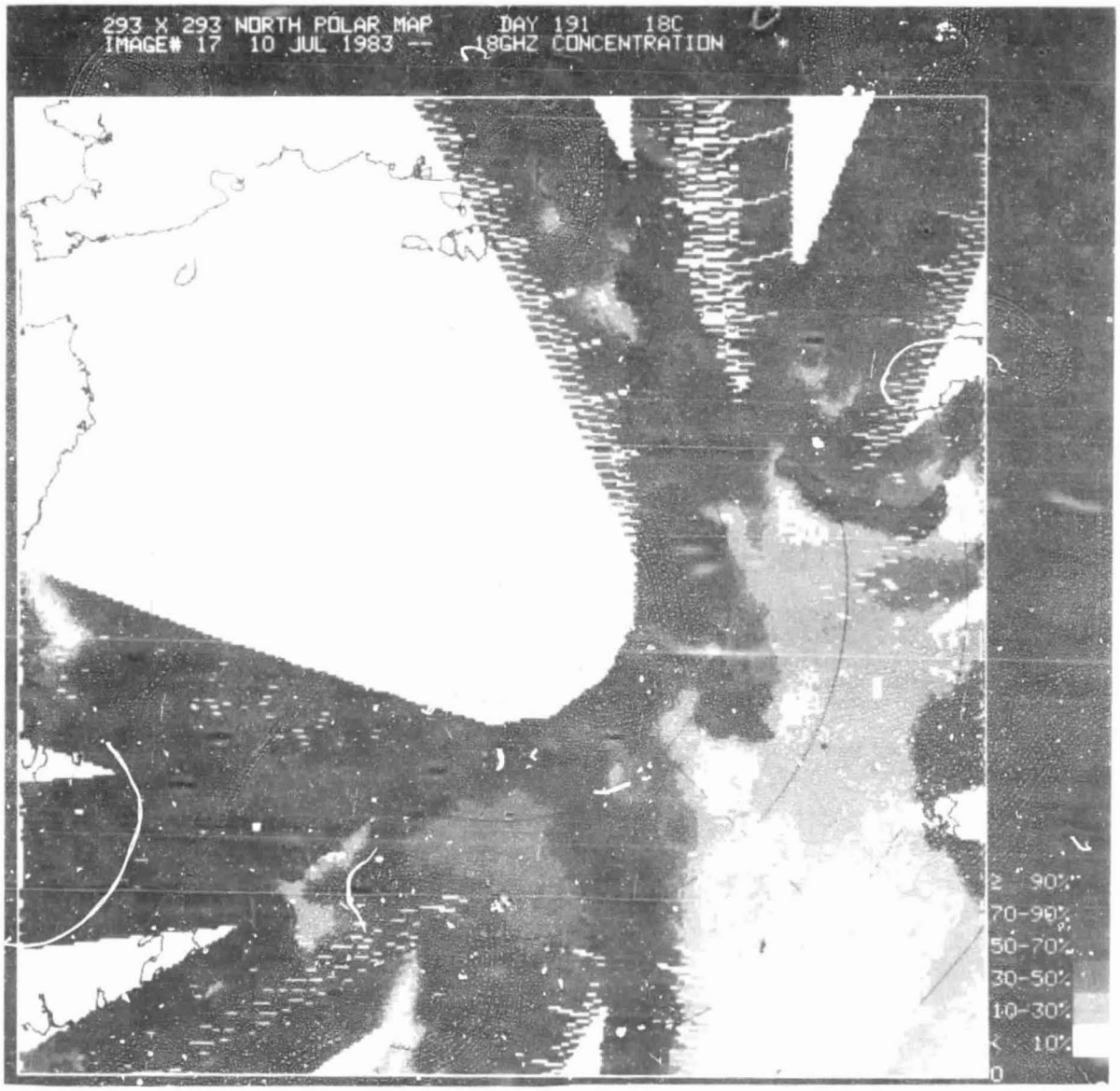

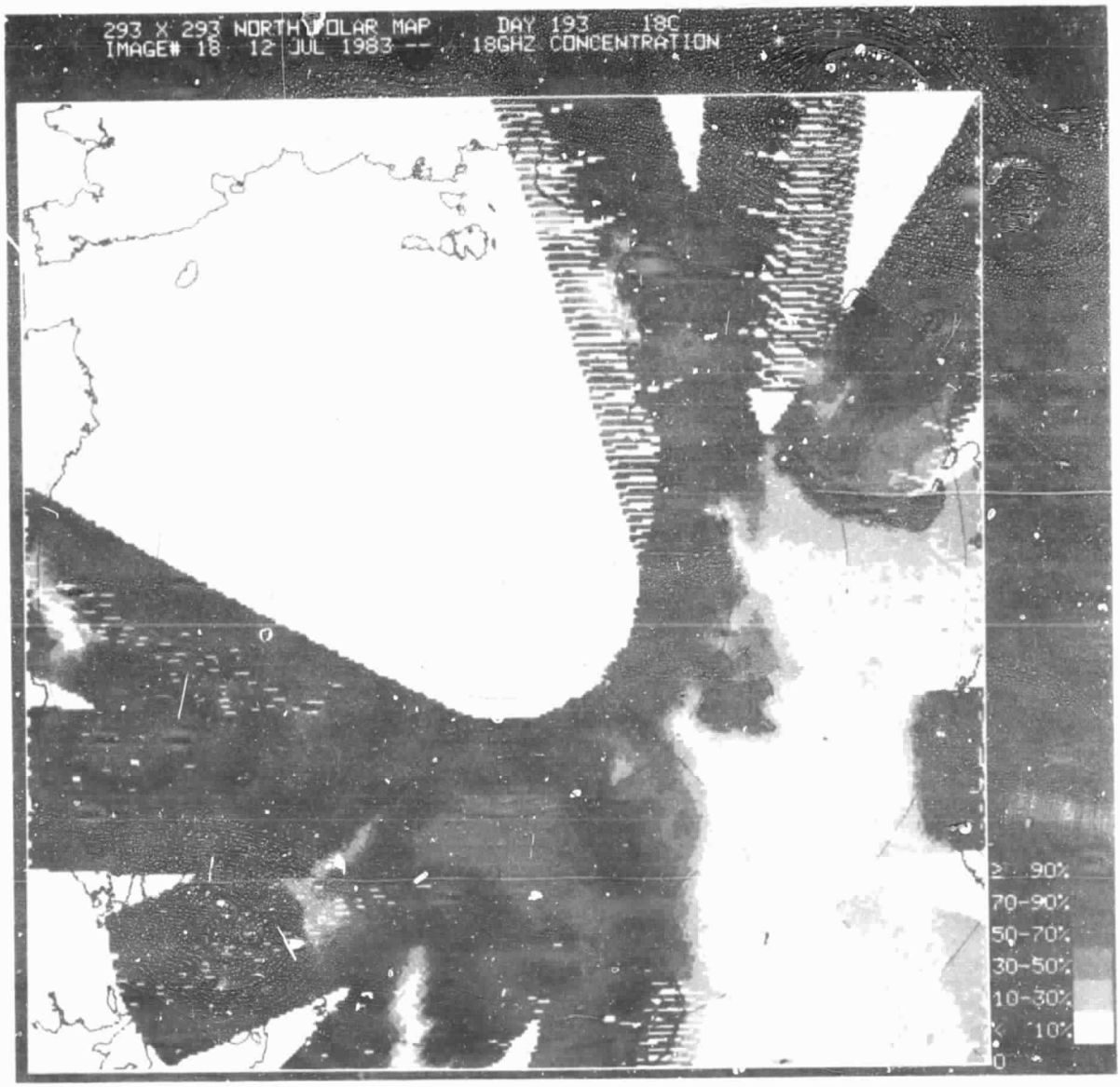
293 X 293 NORTH POLAR MAP DAY 193 18C
IMAGE# 18 12 JUL 1983 -- 18GHZ CONCENTRATION
≥ 90%
70-90%
50-70%
30-50%
10-30%
< 10%
0

ORIGINAL
OF POOR QUALITY


293 X 293 NORTH POLAR MAP DAY 197 18C
IMAGE# 20 16 JUL 1983 -- 18GHZ CONCENTRATION
≥ 90%
70-90%
50-70%
30-50%
10-30%
< 10%
0

OF POOR


293 X 293 NORTH POLAR MAP
IMAGE# 21 18 JUL 1983 --
DAY 199 18C
18GHZ CONCENTRATION
≥ 90%
70-90%
50-70%
30-50%
10-30%
< 10%
0

ORIGINAL PAGE IS
OF POOR QUALITY


293 X 293 NORTH POLAR MAP DAY 203 C18
IMAGE# 23 22 JUL 1983 -- 18 GHZ CONCENTRATION *
≥ 90%
70-90%
50-70%
30-50%
10-30%
< 10%
0

OF POOR

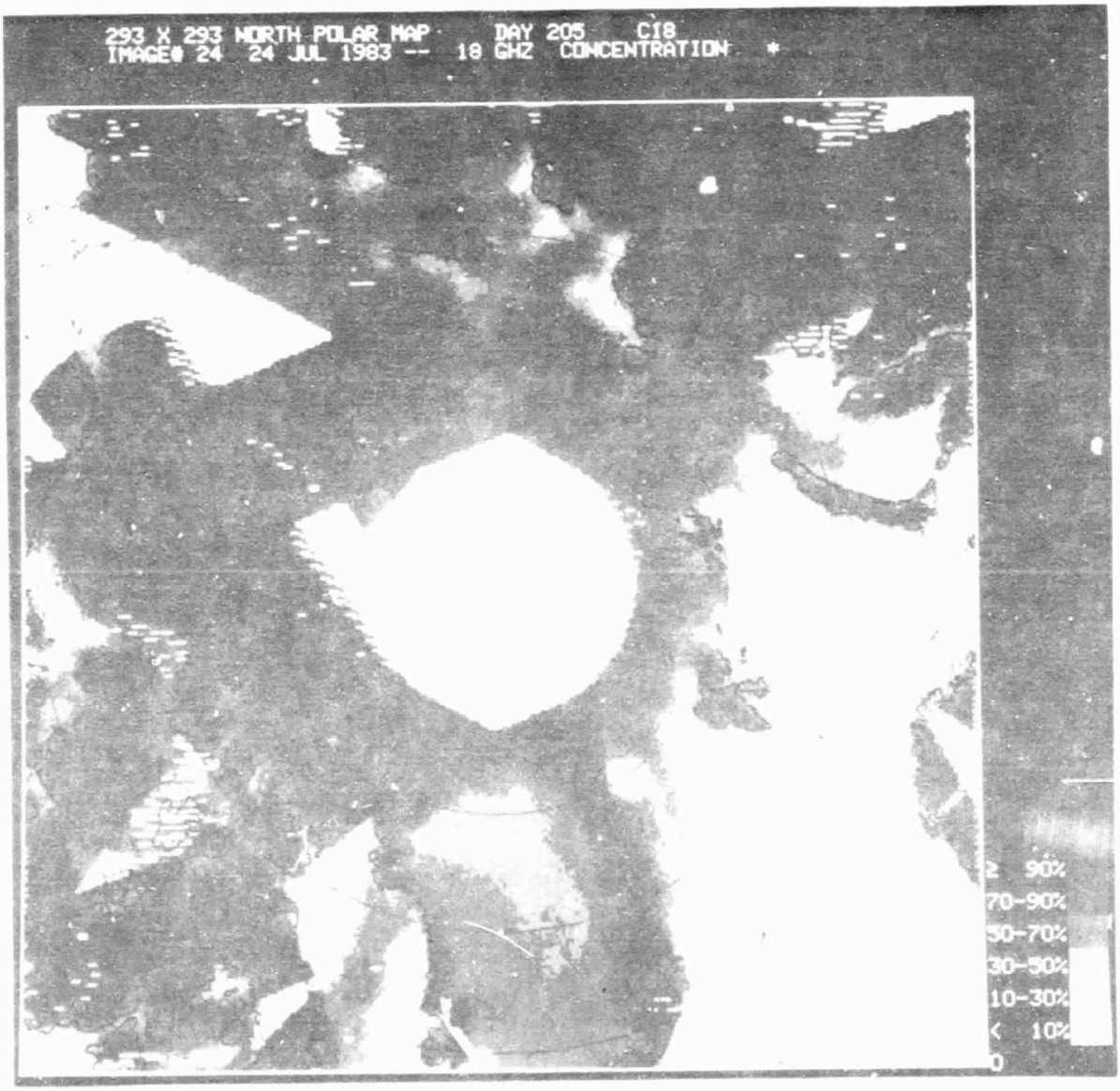
293 X 293 NORTH POLAR MAP DAY 205 C18
IMAGE# 24 24 JUL 1983 -- 18 GHZ CONCENTRATION *
≥ 90%
70-90%
50-70%
30-50%
10-30%
< 10%
0

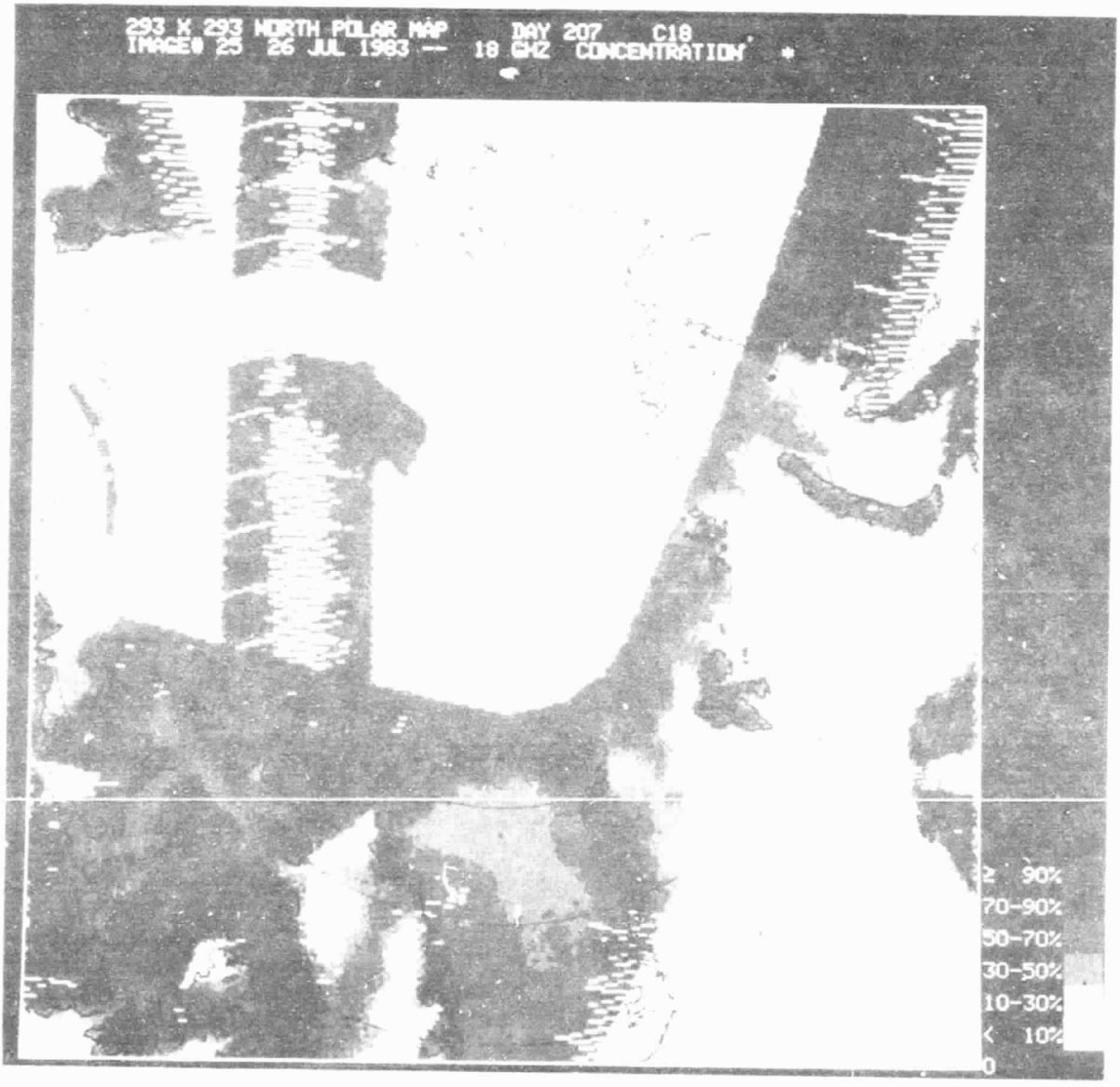
293 X 293 NORTH POLAR MAP DAY 207 C18
IMAGE# 25 26 JUL 1983 -- 18 GHZ CONCENTRATION
≥ 90%
70-90%
50-70%
30-50%
10-30%
< 10%
0


293 X 293 NORTH POLAR MAP DAY 209 C18
IMAGE# 26 28 JUL 1983 -- 18 GHZ CONCENTRATION *
≥ 90%
70-90%
50-70%
30-50%
10-30%
< 10%
0

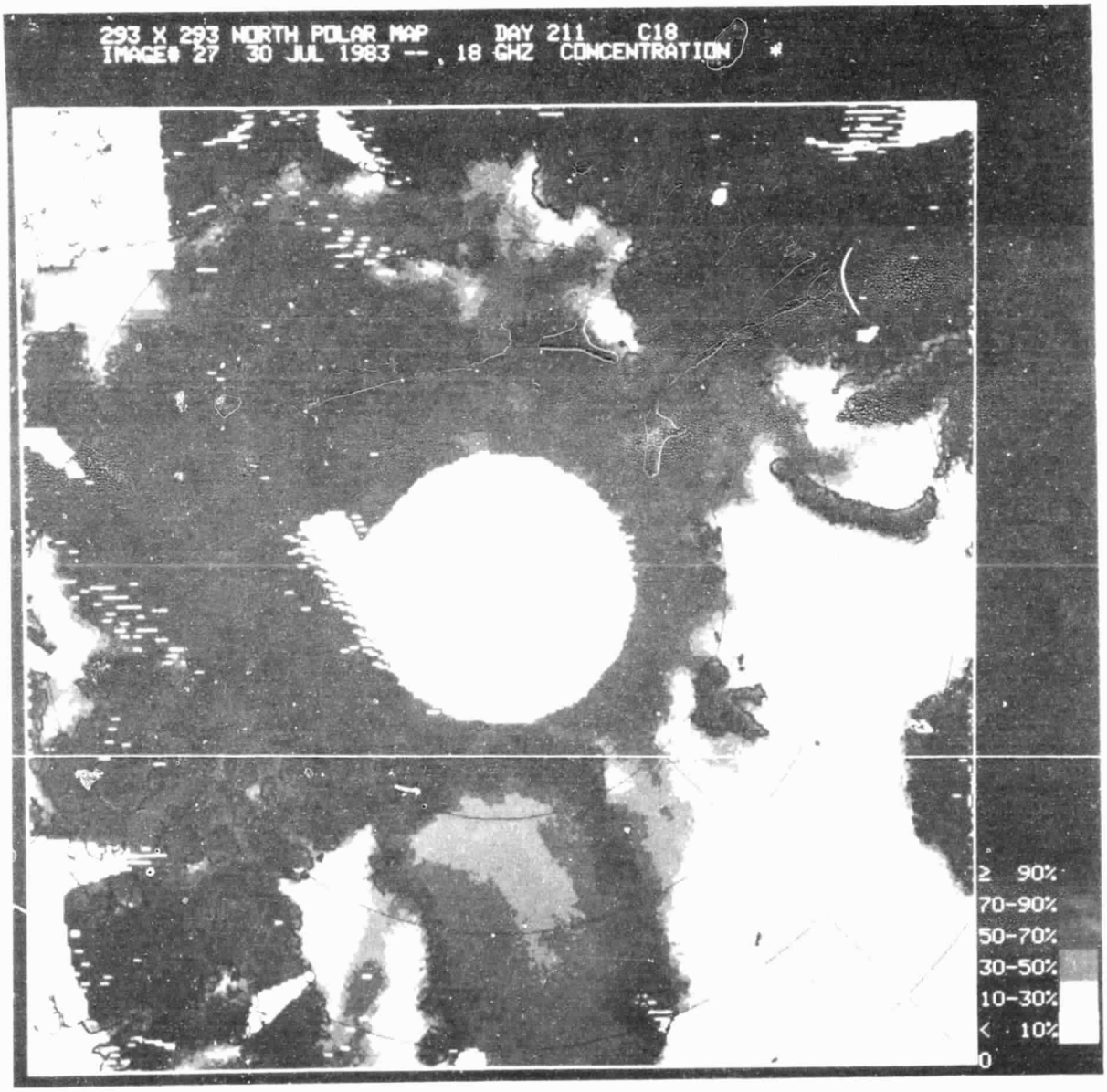
293 X 293 NORTH POLAR MAP DAY 211 C18
IMAGE# 27 30 JUL 1983 -- 18 GHZ CONCENTRATION
≥ 90%
70-90%
50-70%
30-50%
10-30%
< 10%
0

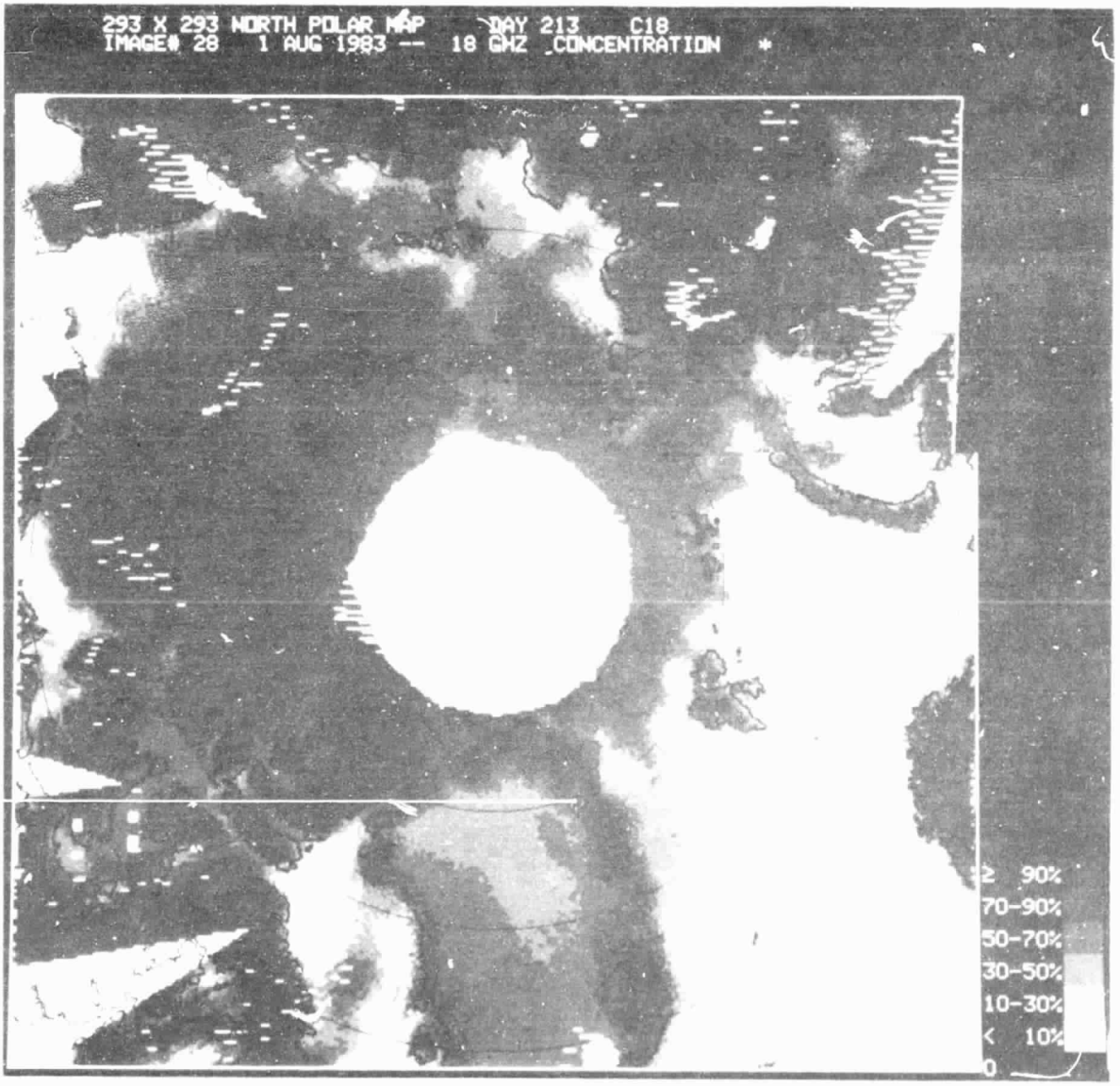
293 X 293 NORTH POLAR MAP DAY 213 C18
IMAGE# 28 1 AUG 1983 -- 18 GHZ CONCENTRATION *
≥ 90%
70-90%
50-70%
30-50%
10-30%
< 10%
0

ORIG
OF POOR

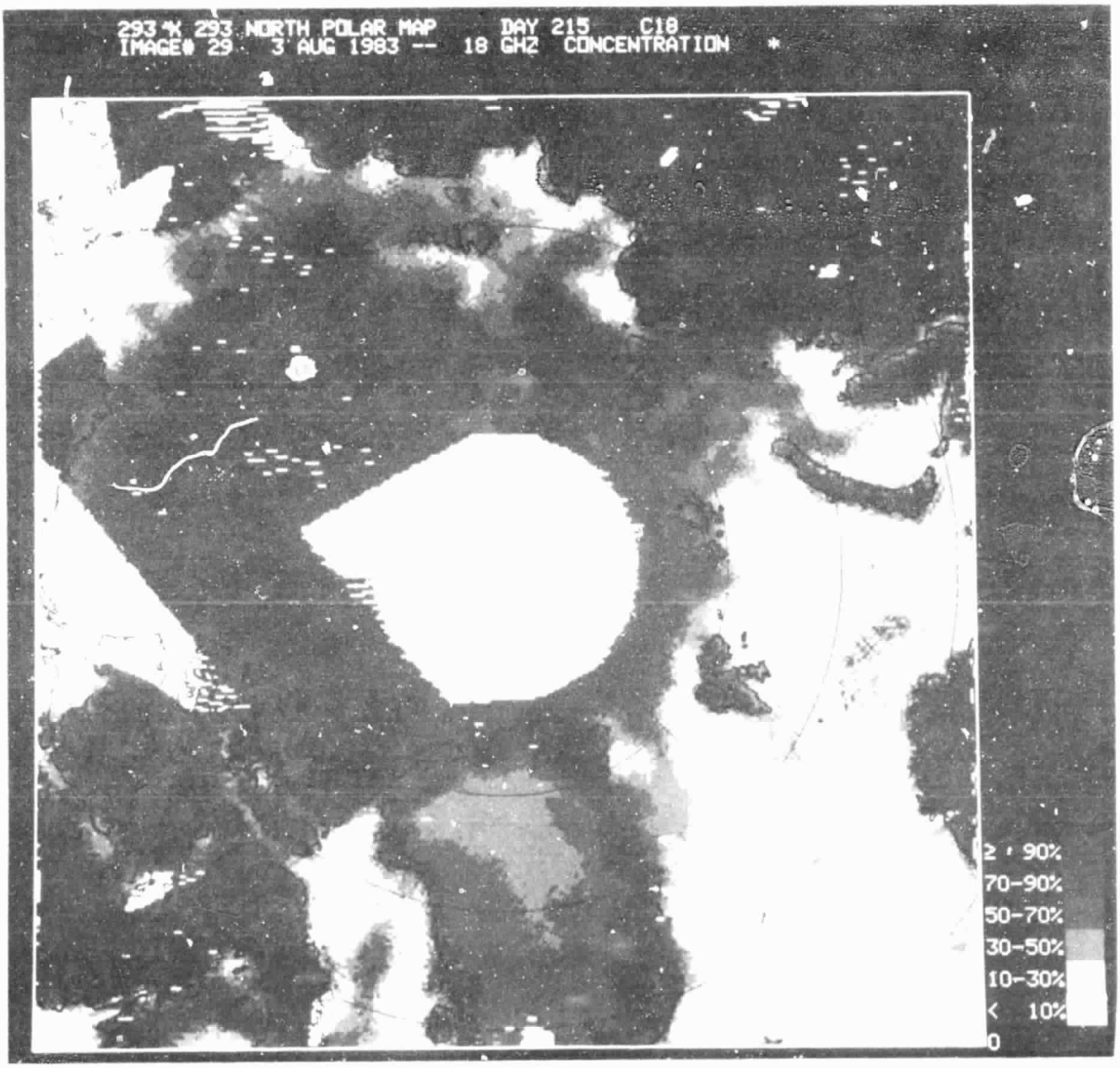
293 X 293 NORTH POLAR MAP DAY 215 C18
IMAGE# 29 3 AUG 1983 -- 18 GHZ CONCENTRATION *
> 90%
70-90%
50-70%
30-50%
10-30%
< 10%
0

ORIGINAL PAGE IS
OF POOR QUALITY

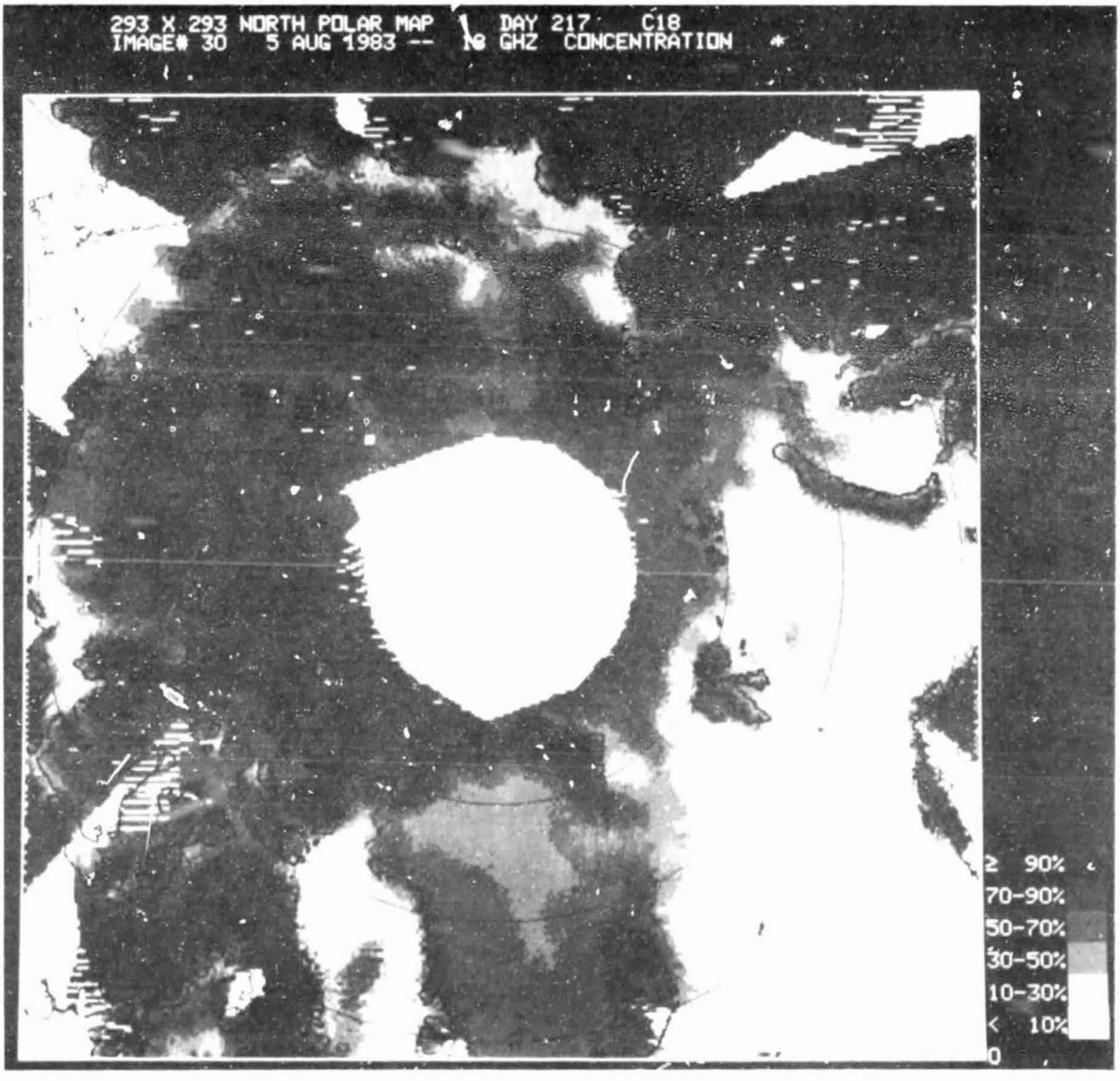


293 X 293 NORTH POLAR MAP DAY 219 C18
IMAGE# 31 7 AUG 1983 -- 18 GHZ CONCENTRATION *
≥ 90%
70-90%
50-70%
30-50%
10-30%
< 10%
0


293 X 293 NORTH POLAR MAP DAY 221 C18
IMAGE# 32 9 AUG 1983 18 GHZ CONCENTRATION
≥ 90%
70-90%
50-70%
30-50%
10-30%
< 10%
0

APPENDIX D

GREY-SCALE IMAGES OF MULTIYEAR SEA ICE FRACTION DURING MIZEX EAST'83

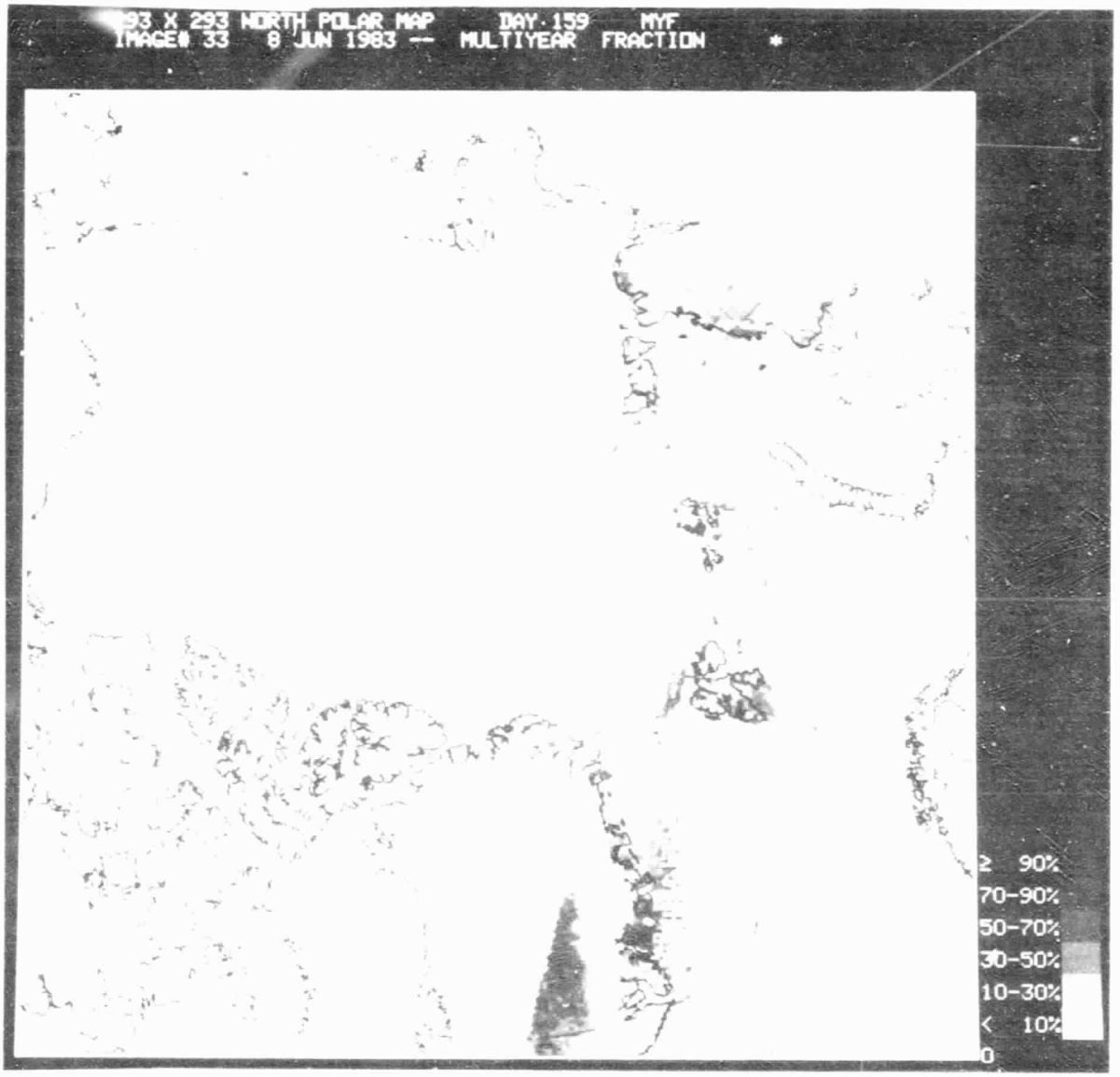

PAGE 114 INTENTIONALLY BLANK

ORIGINAL
OF POOR QUALITY

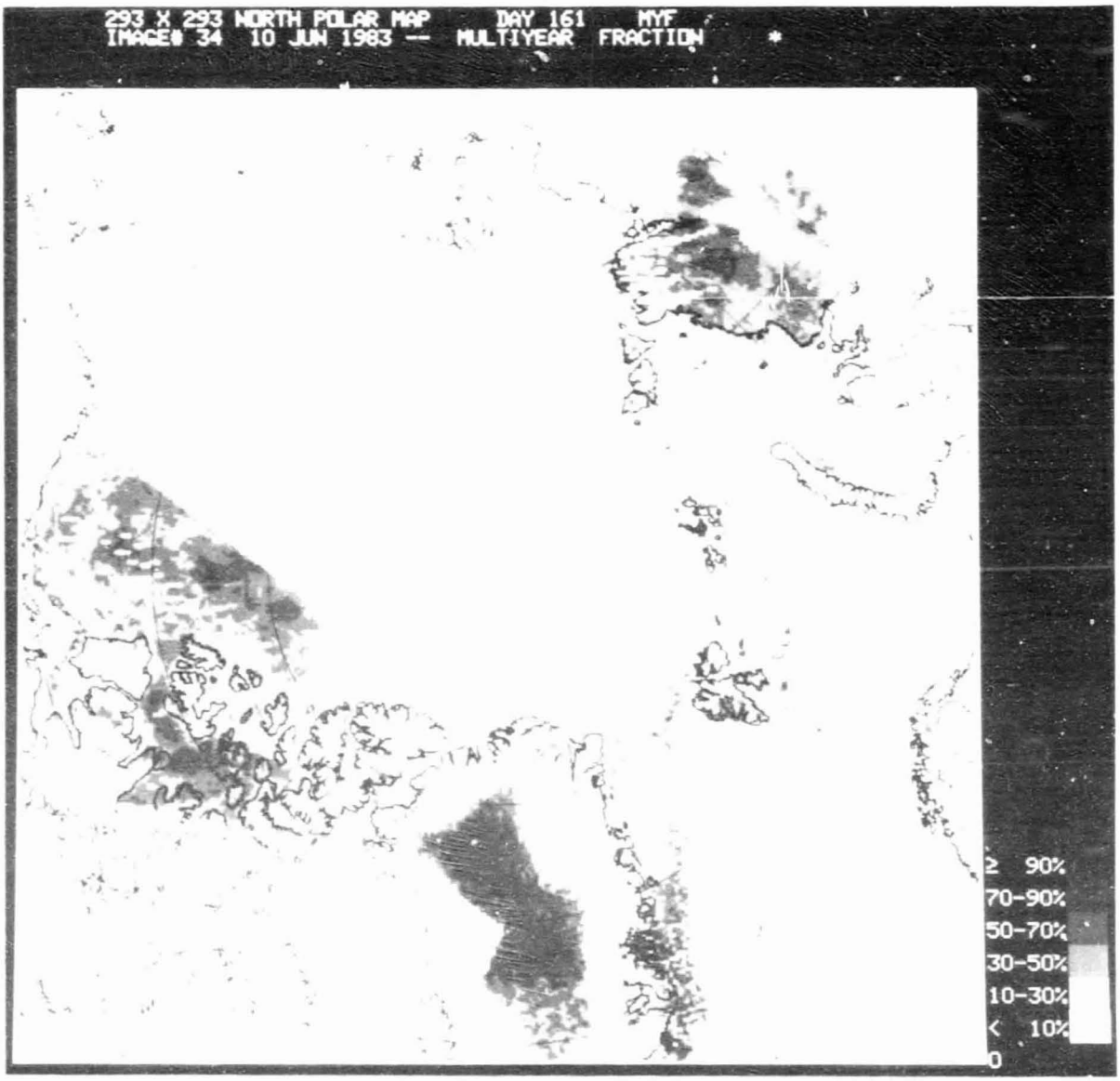

ORIGINAL
OF POOR QUALITY

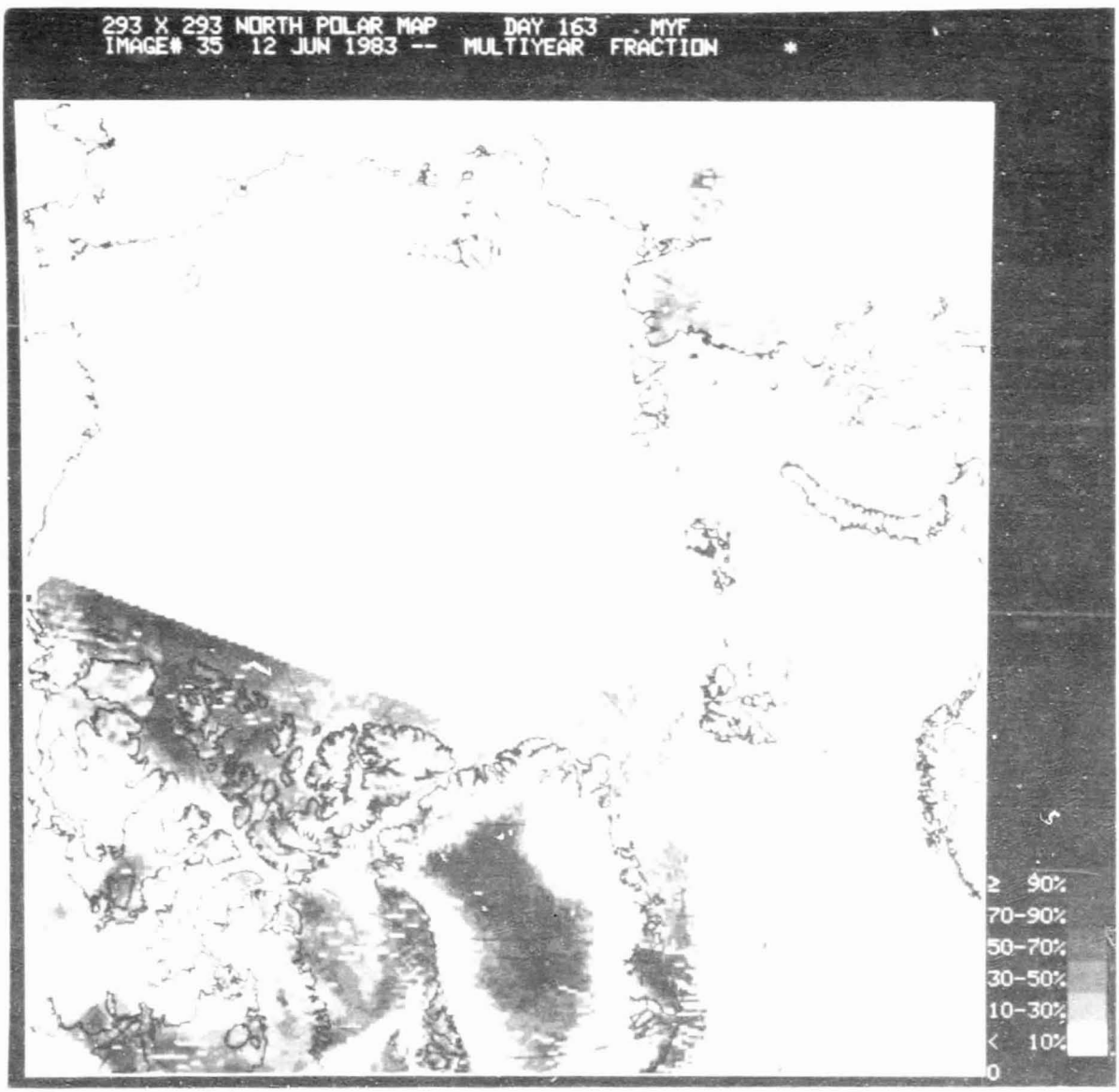

ORIG
OF PO

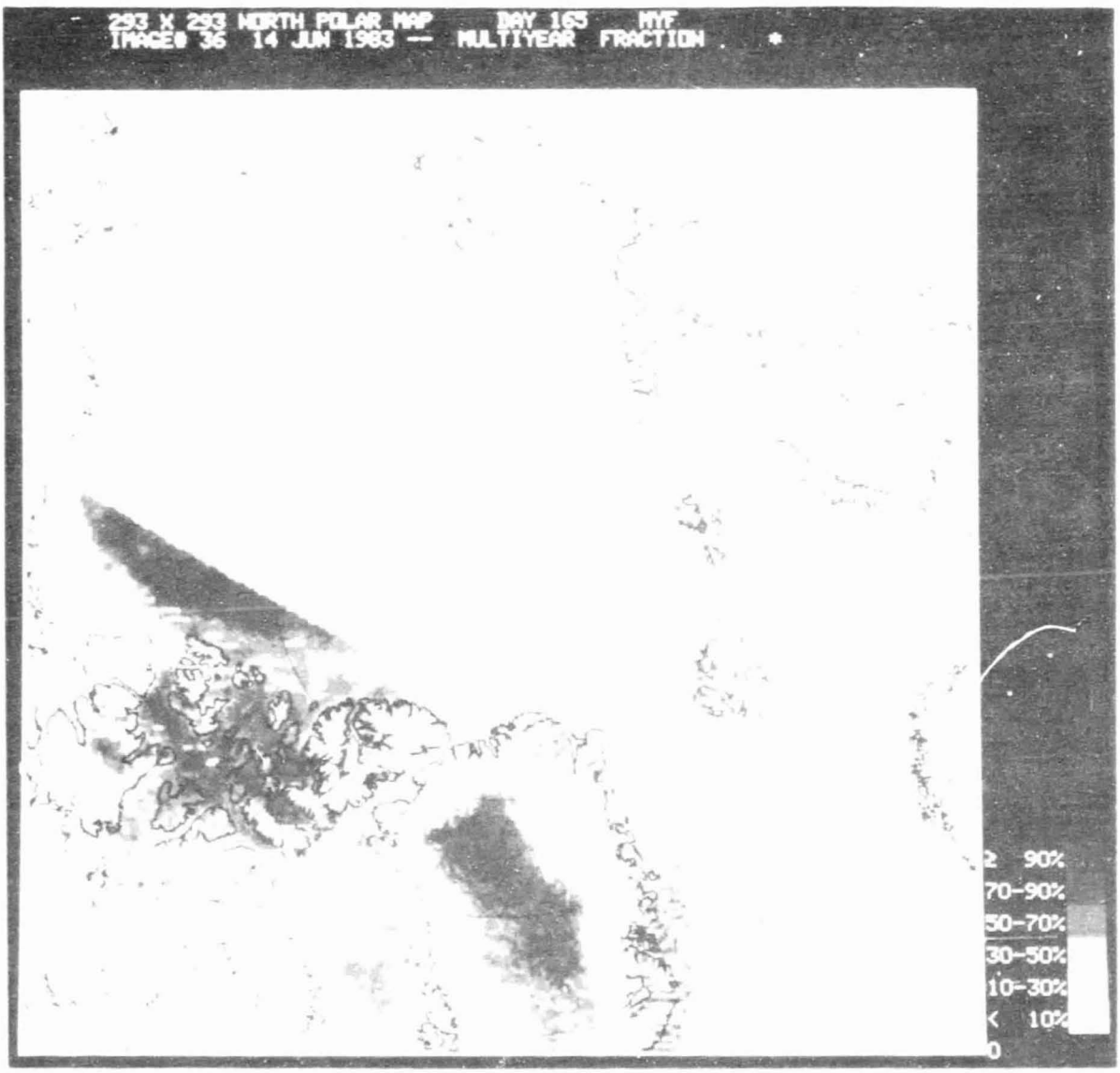
293 X 293 NORTH POLAR MAP DAY 163 MYF
IMAGE# 36 14 JUN 1983 -- MULTIYEAR FRACTION
≥ 90%
70-90%
50-70%
30-50%
10-30%
< 10%
0

OF POOR

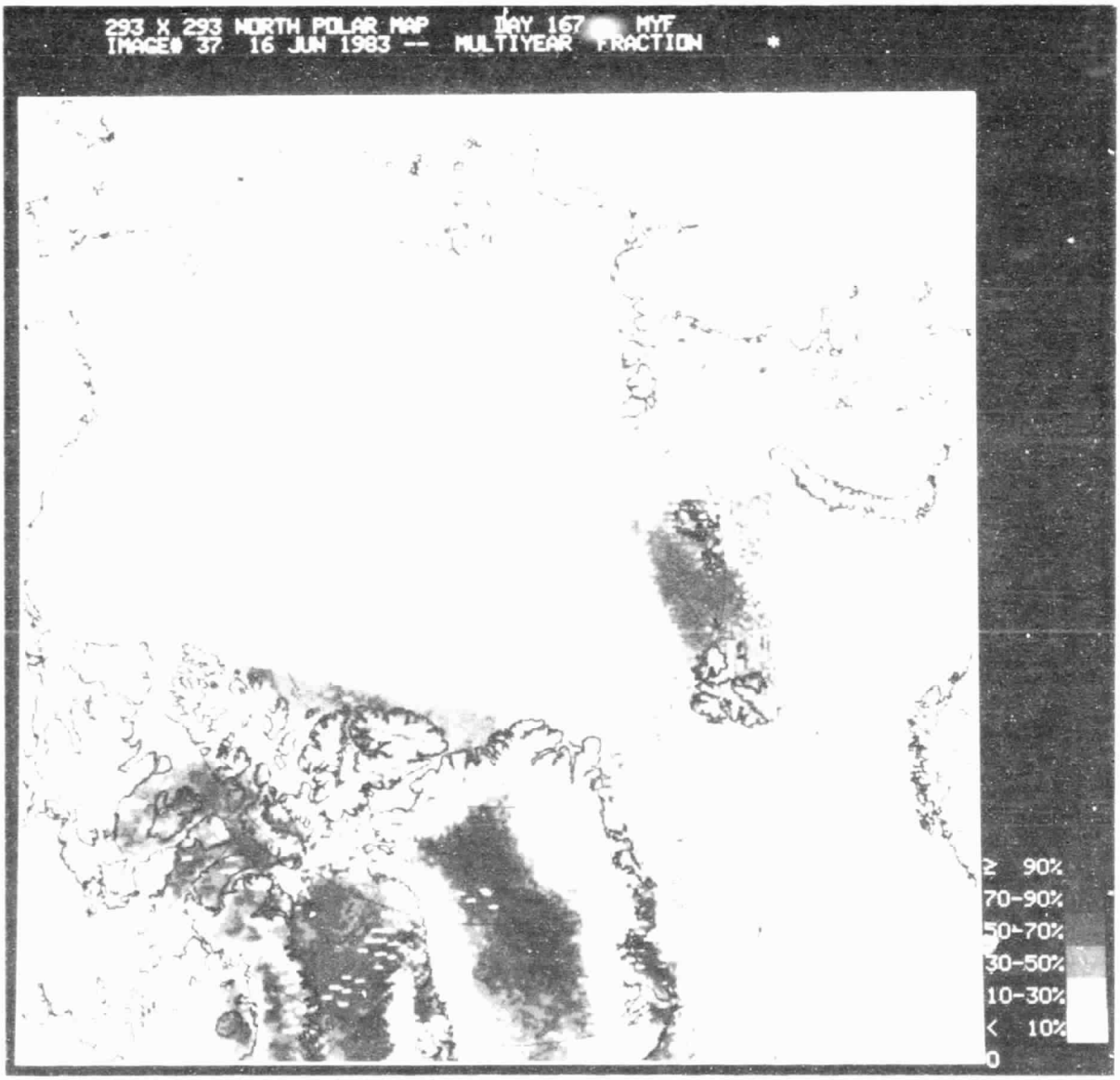
293 X 293 NORTH POLAR MAP
IMAGE# 37 16 JUN 1983 --
DAY 167
MULTIYEAR FRACTION
MYF
*
≥ 90%
70-90%
50-70%
30-50%
10-30%
< 10%
0

ORIGINAL
OF POOR

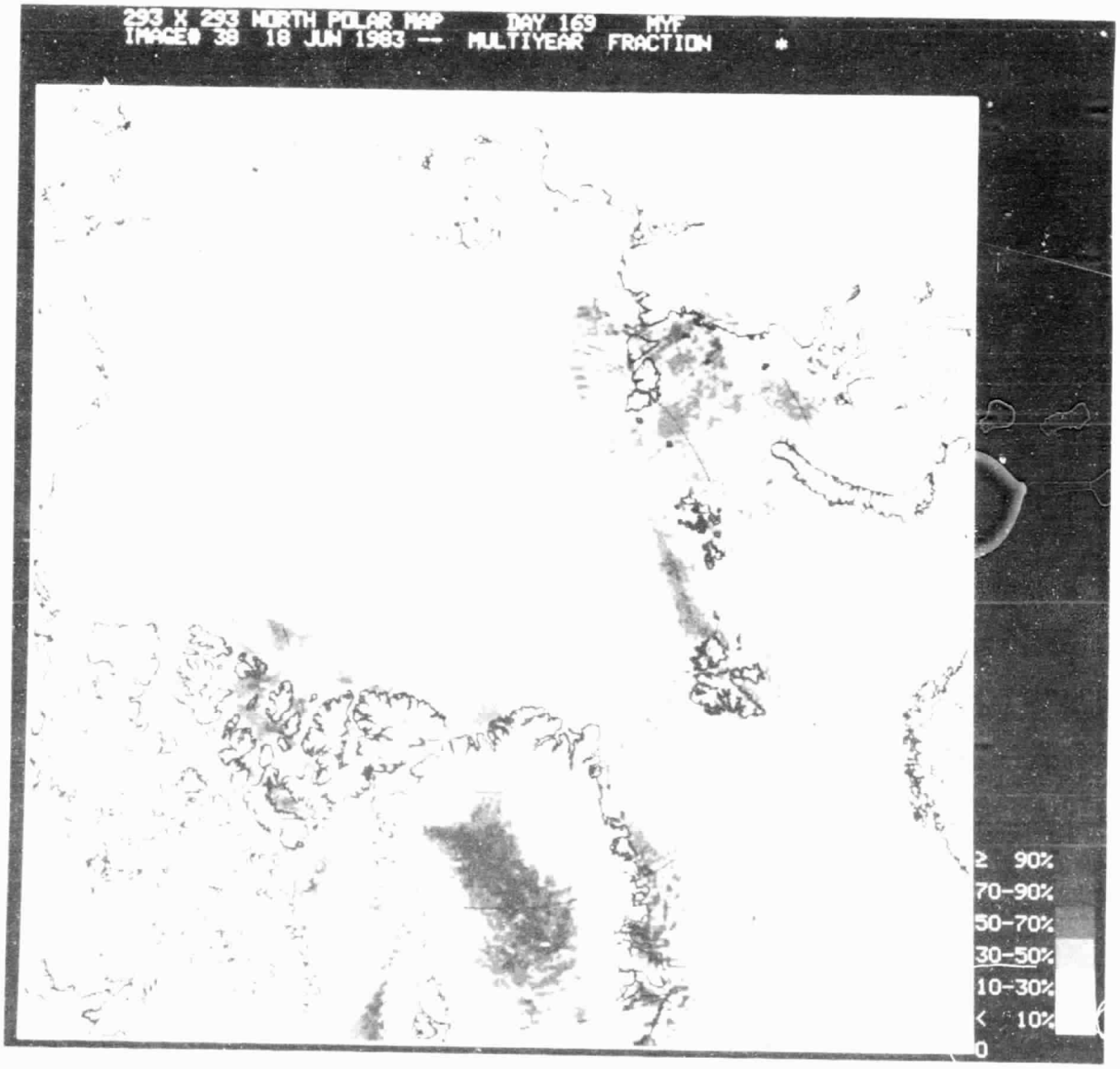

ORIGINAL PAGE IS
OF POOR QUALITY

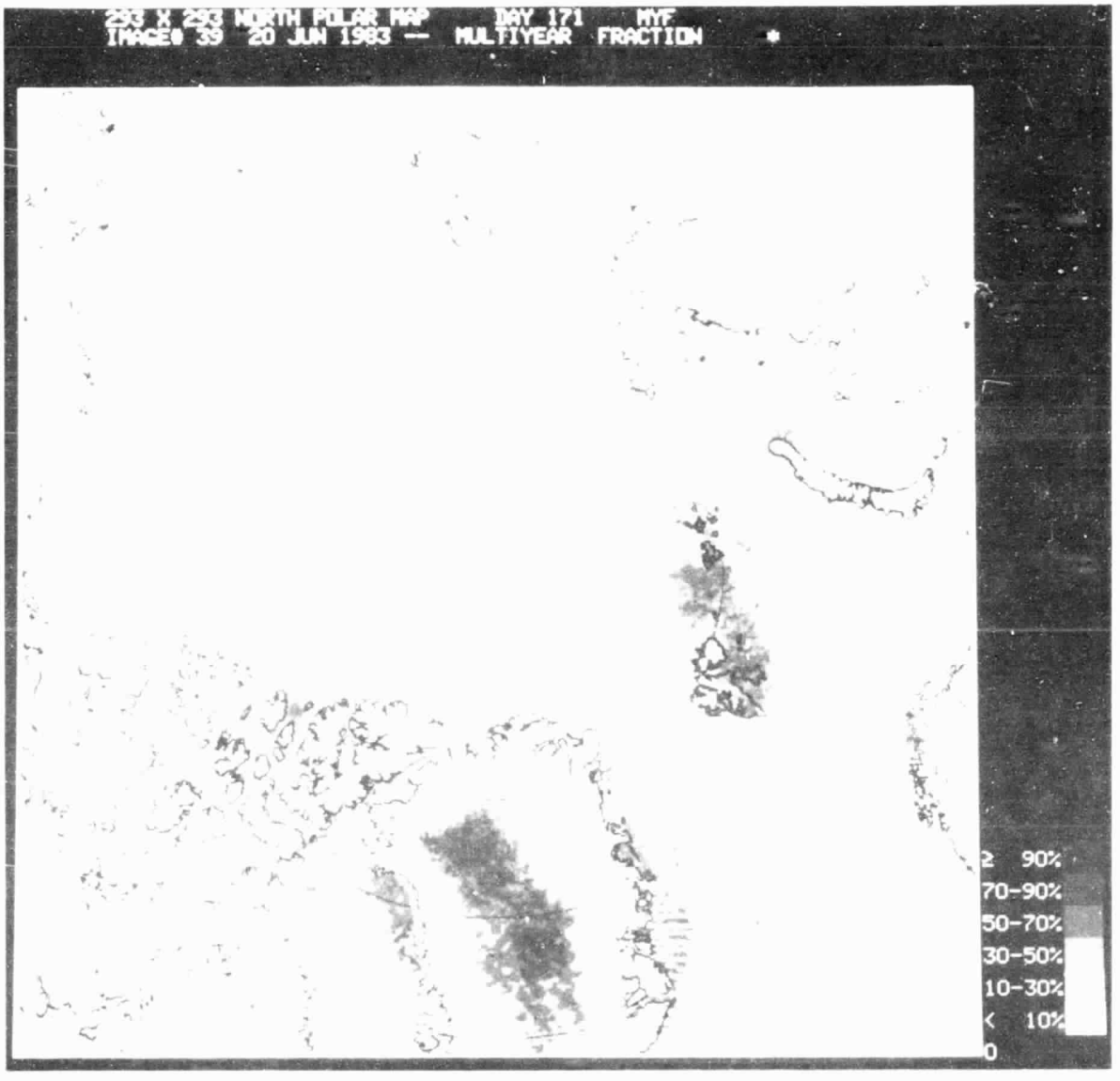

ORIGINAL PAGE IS
OF POOR QUALITY

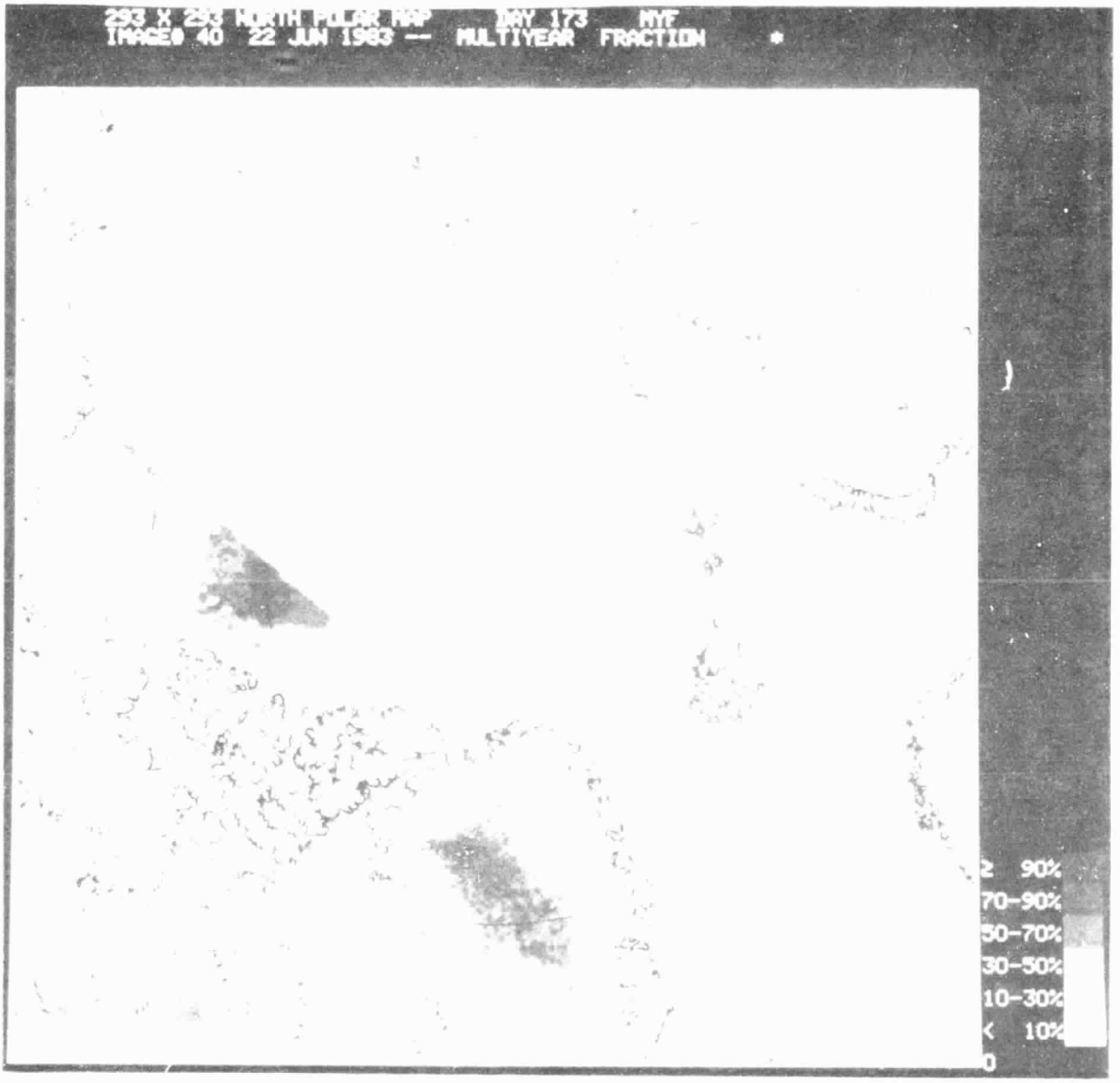

ORIGINAL PAGE IS
OF POOR QUALITY

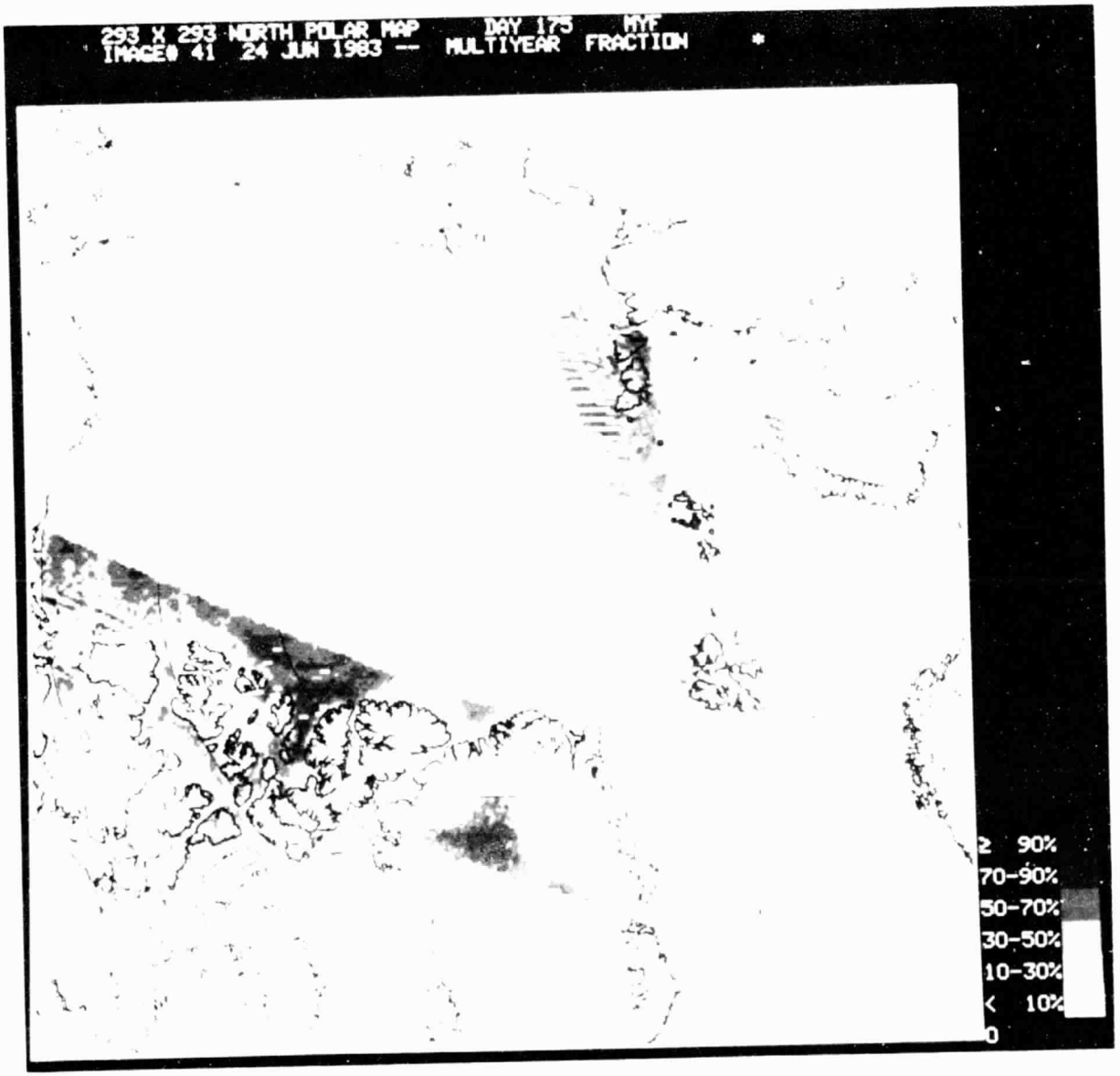

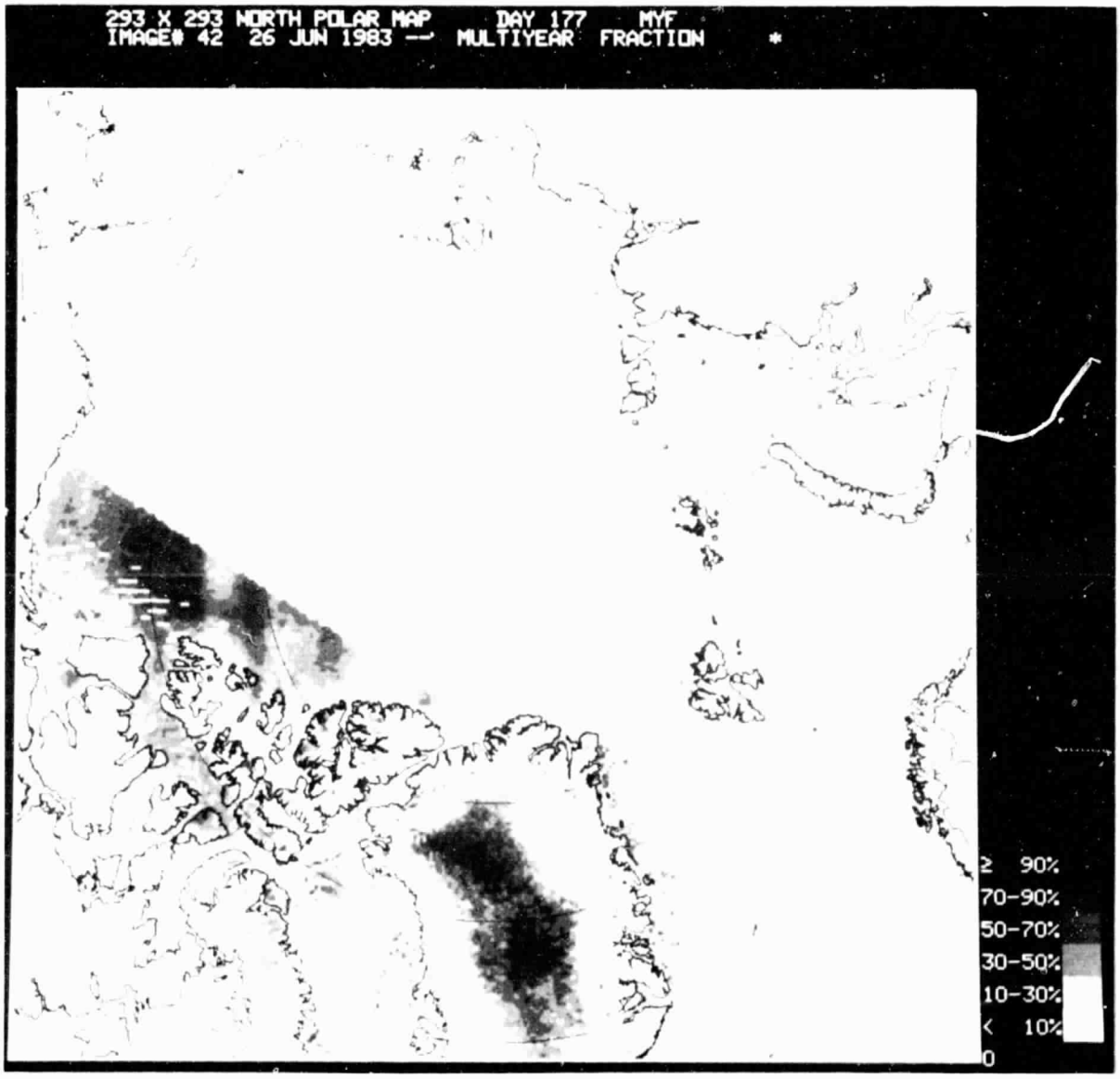
293 X 293 NORTH POLAR MAP DAY 177 MYF
IMAGE# 42 26 JUN 1983 MULTIYEAR FRACTION
≥ 90%
70-90%
50-70%
30-50%
10-30%
< 10%
0

ORIGINAL PAGE IS
OF POOR QUALITY

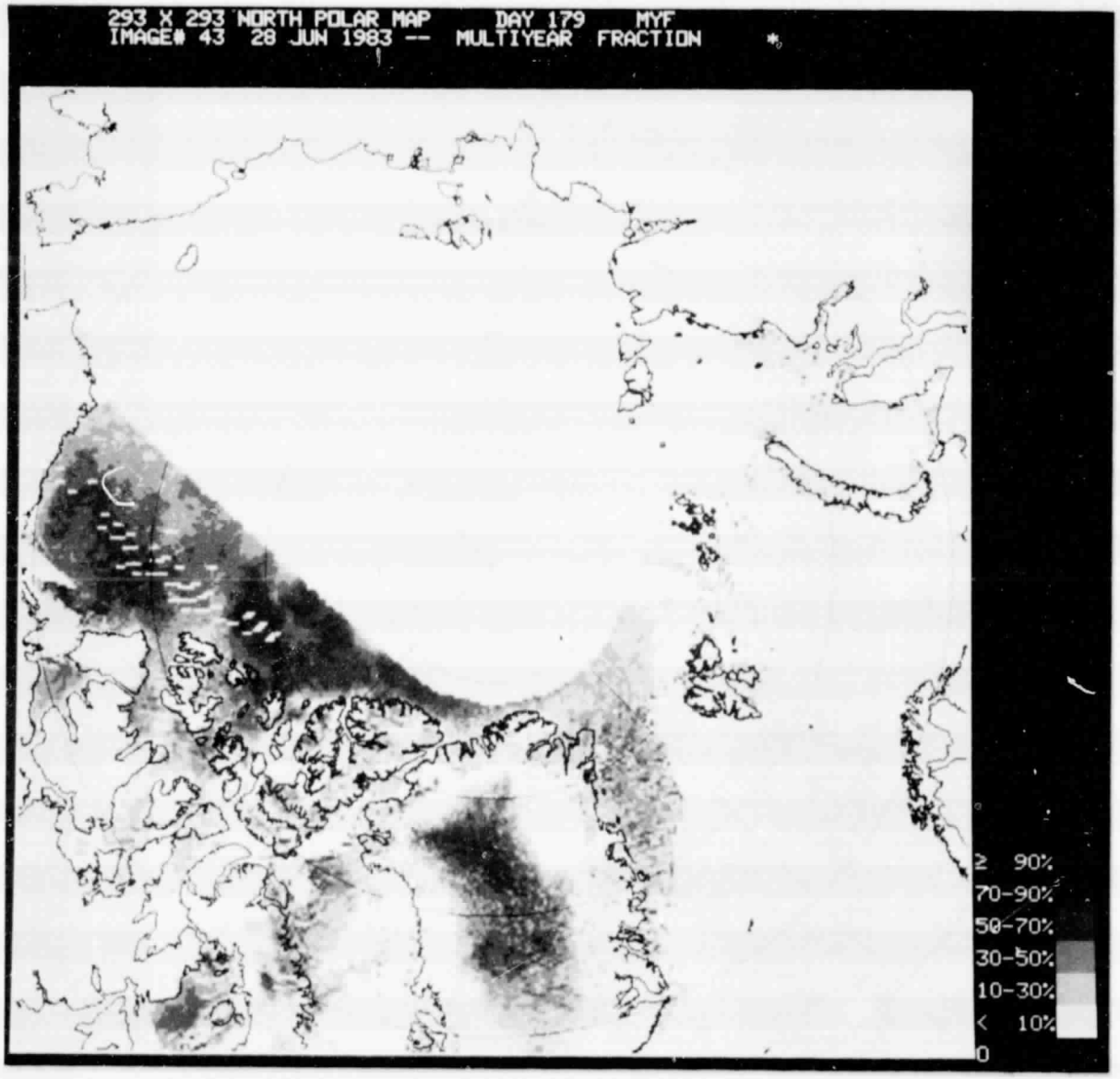

ORIGINAL PAGE IS
OF POOR QUALITY

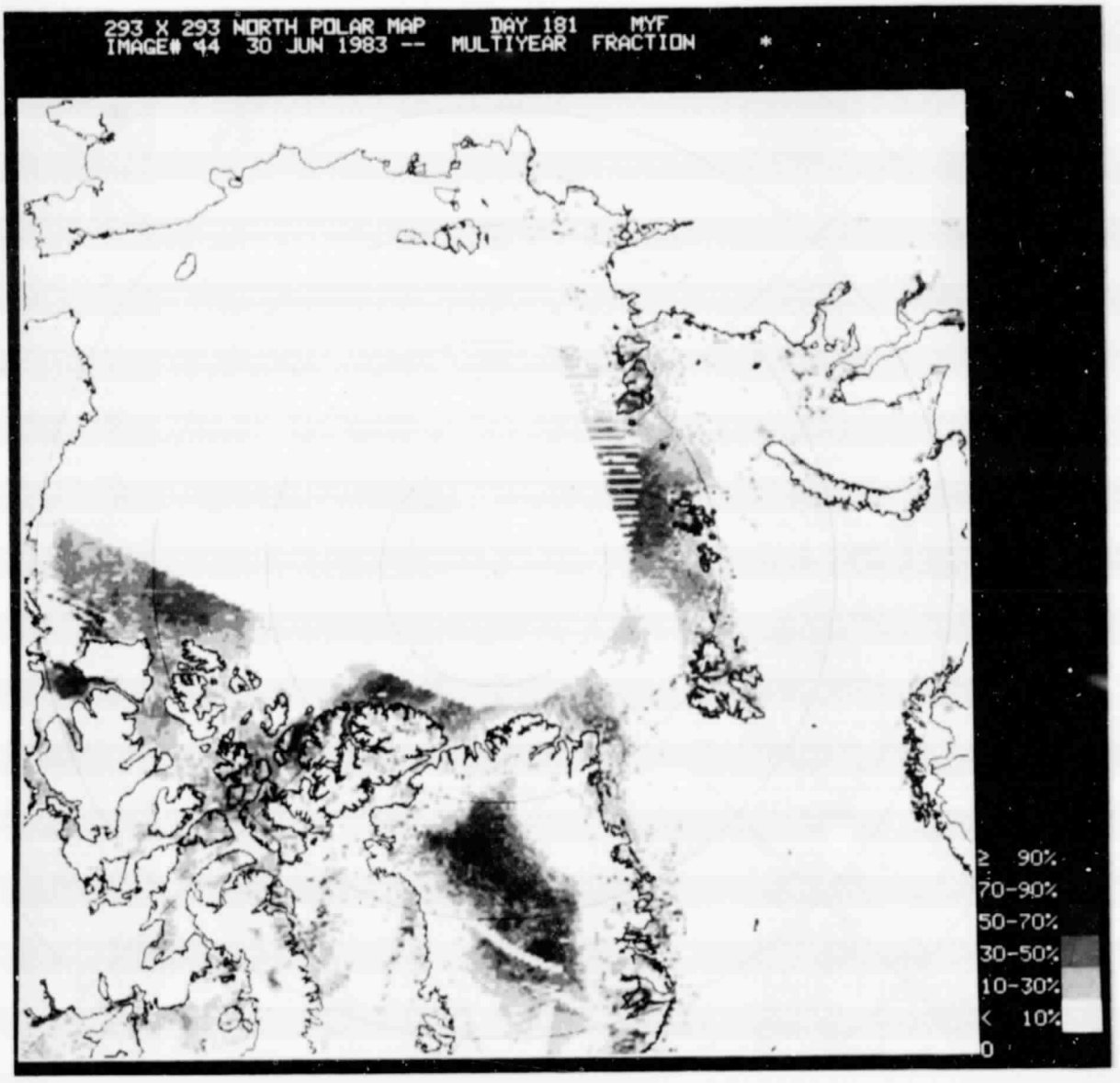

ORIGINAL PAGE IS
OF POOR QUALITY

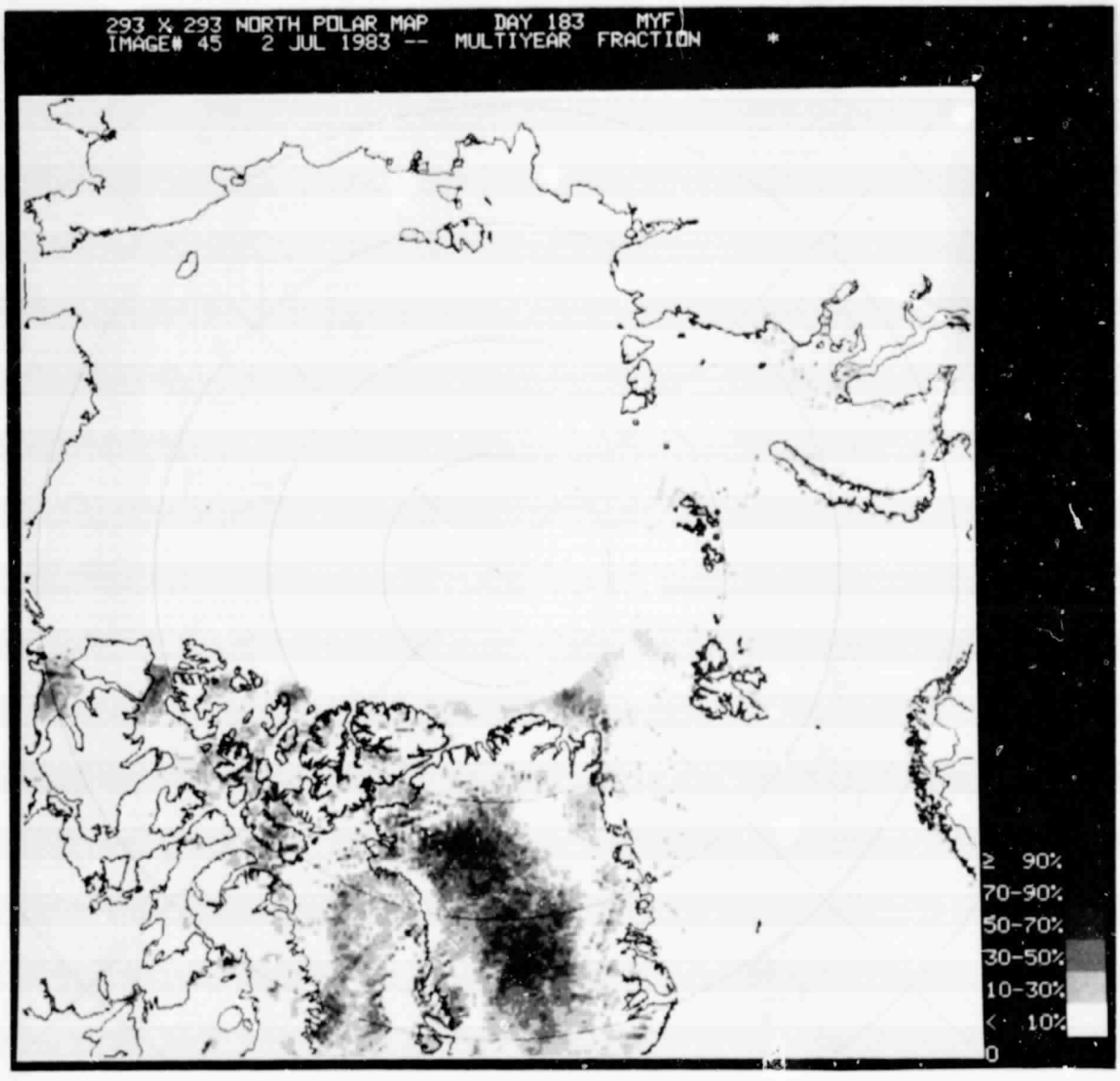

ORIGINAL PAGE IS
OF POOR QUALITY

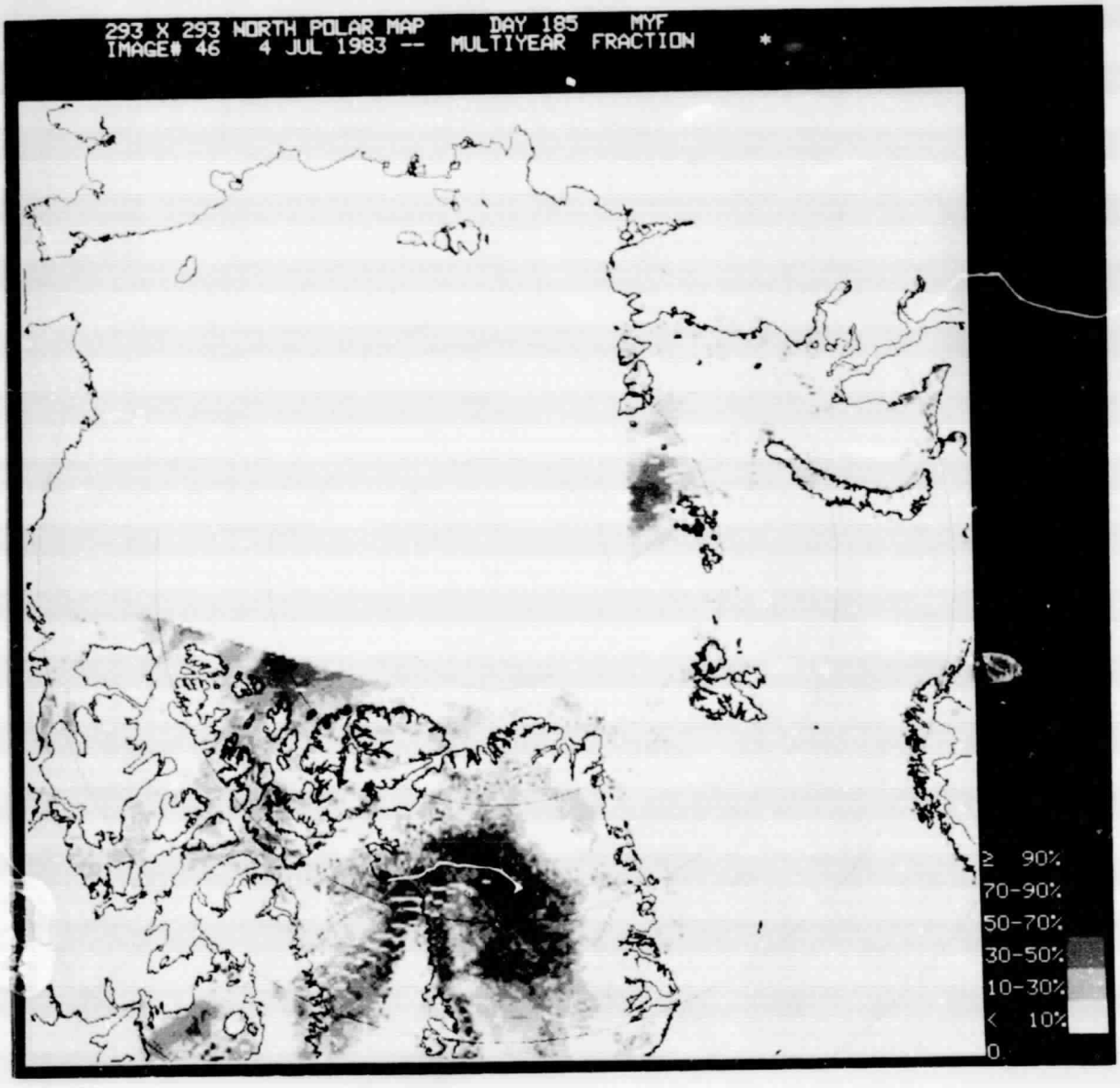

ORIGINAL PAGE IS
OF POOR QUALITY

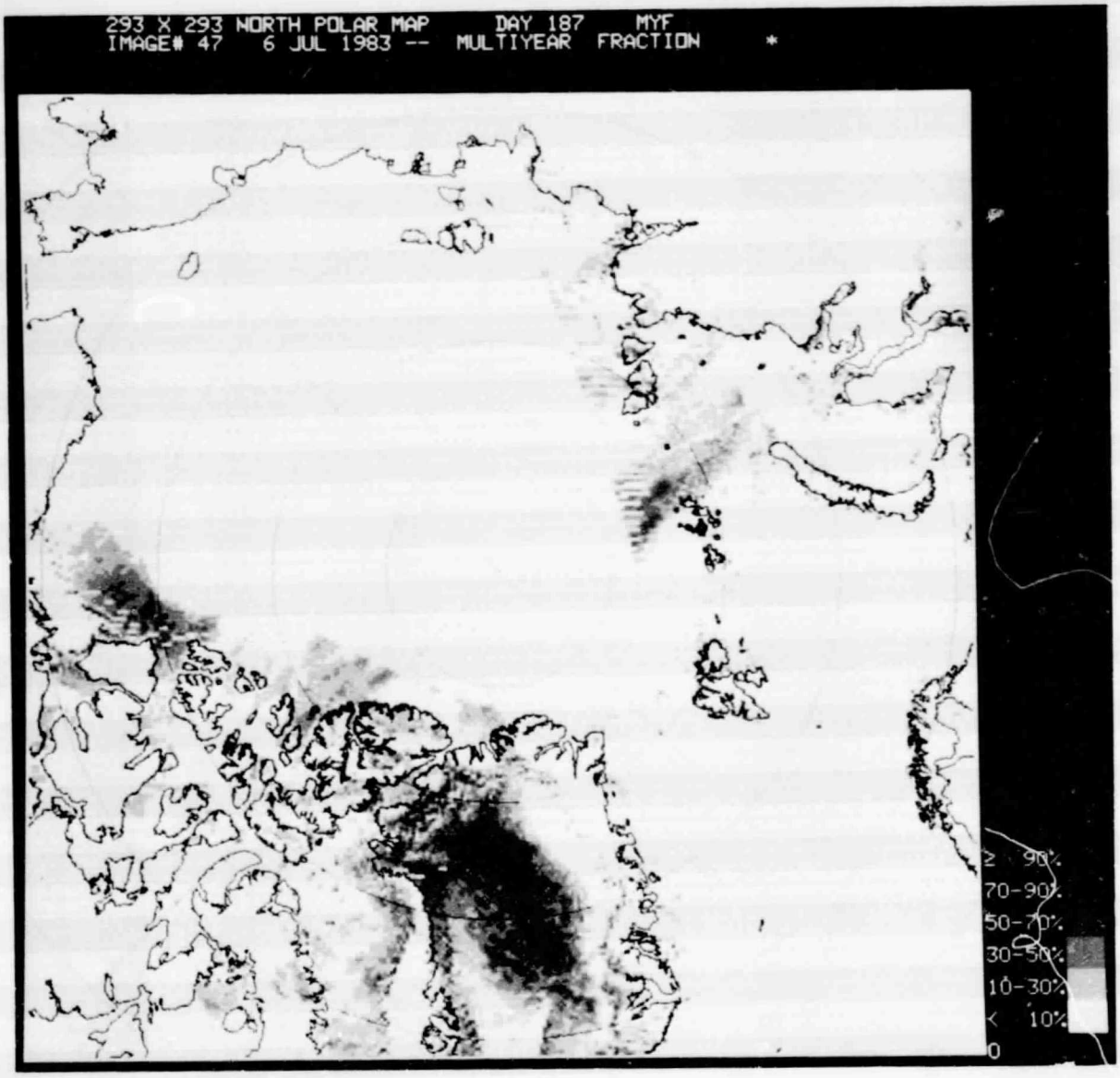

ORIGINAL PAGE IS
OF POOR QUALITY

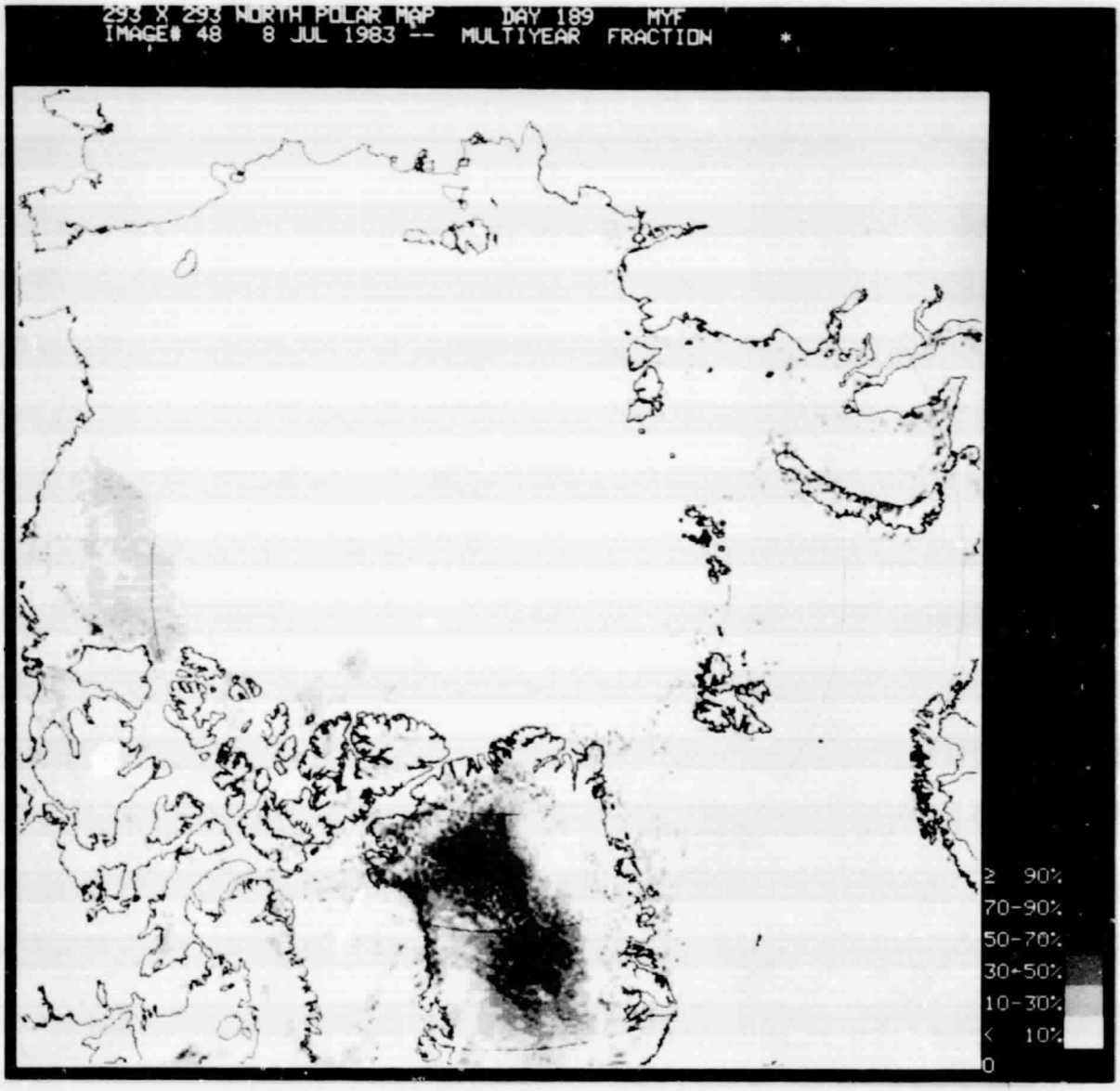

ORIGINAL PAGE IS
OF POOR QUALITY

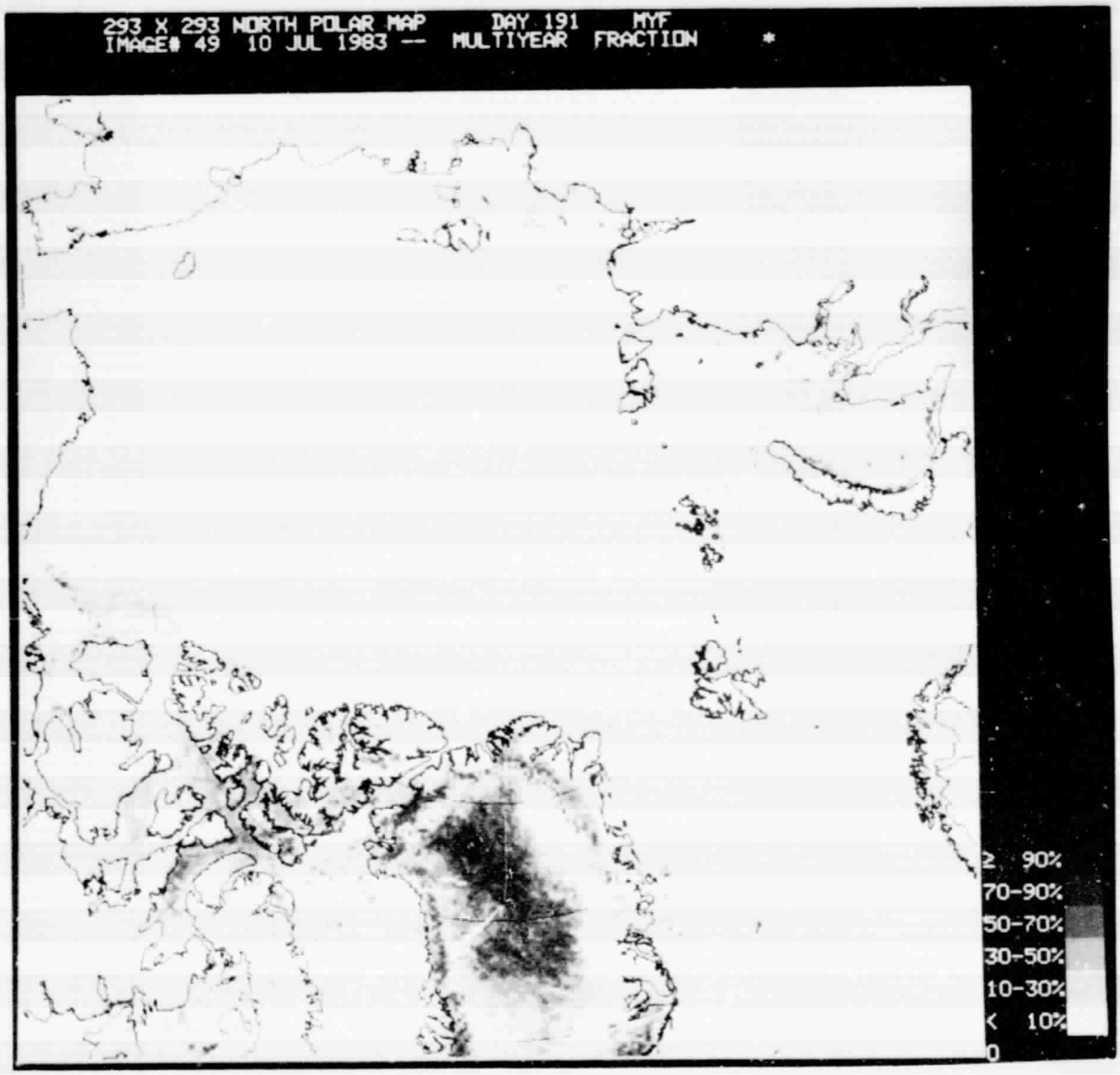

ORIGINAL PAGE IS
OF POOR QUALITY

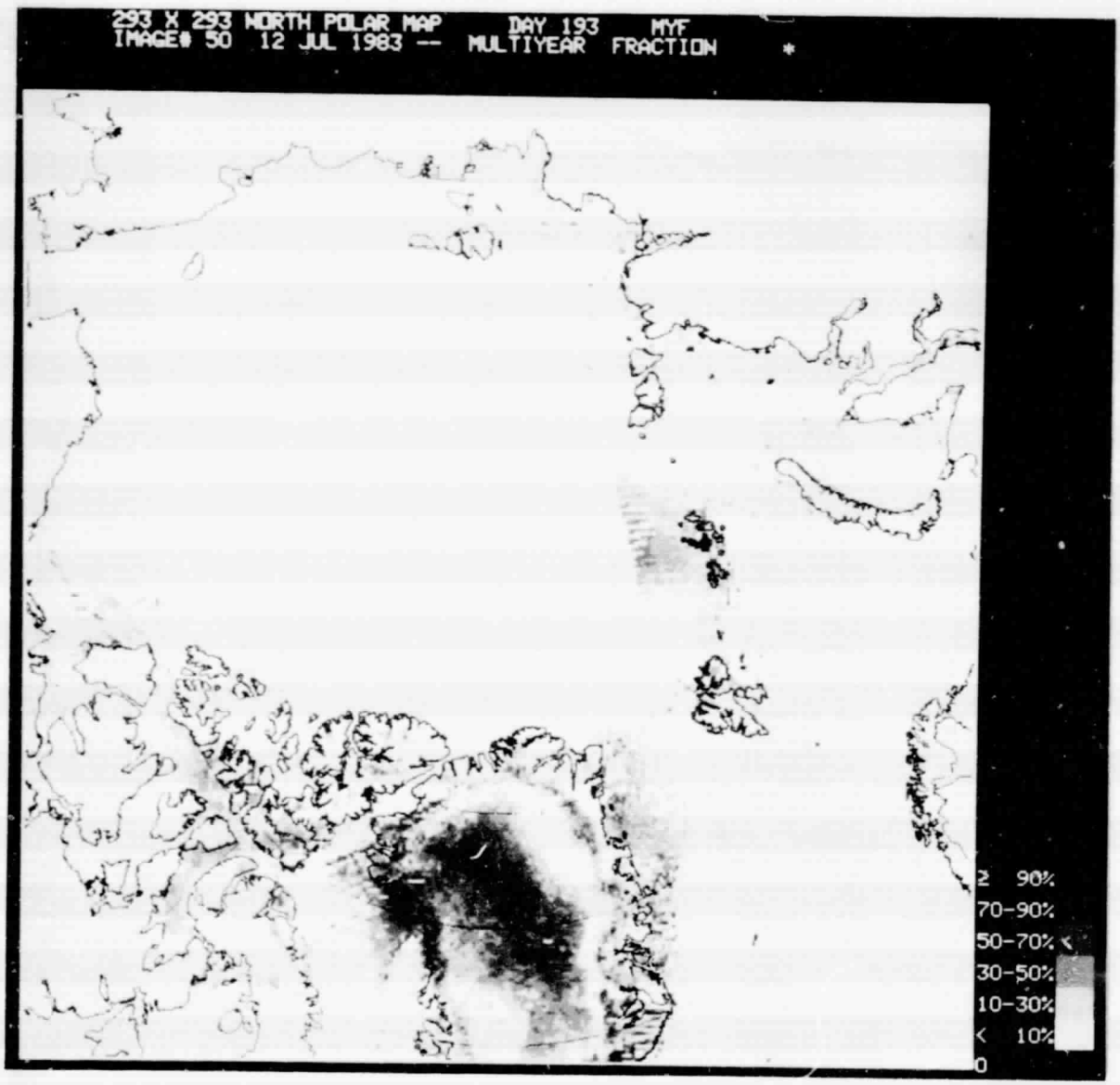

ORIGINAL PAGE IS
OF POOR QUALITY

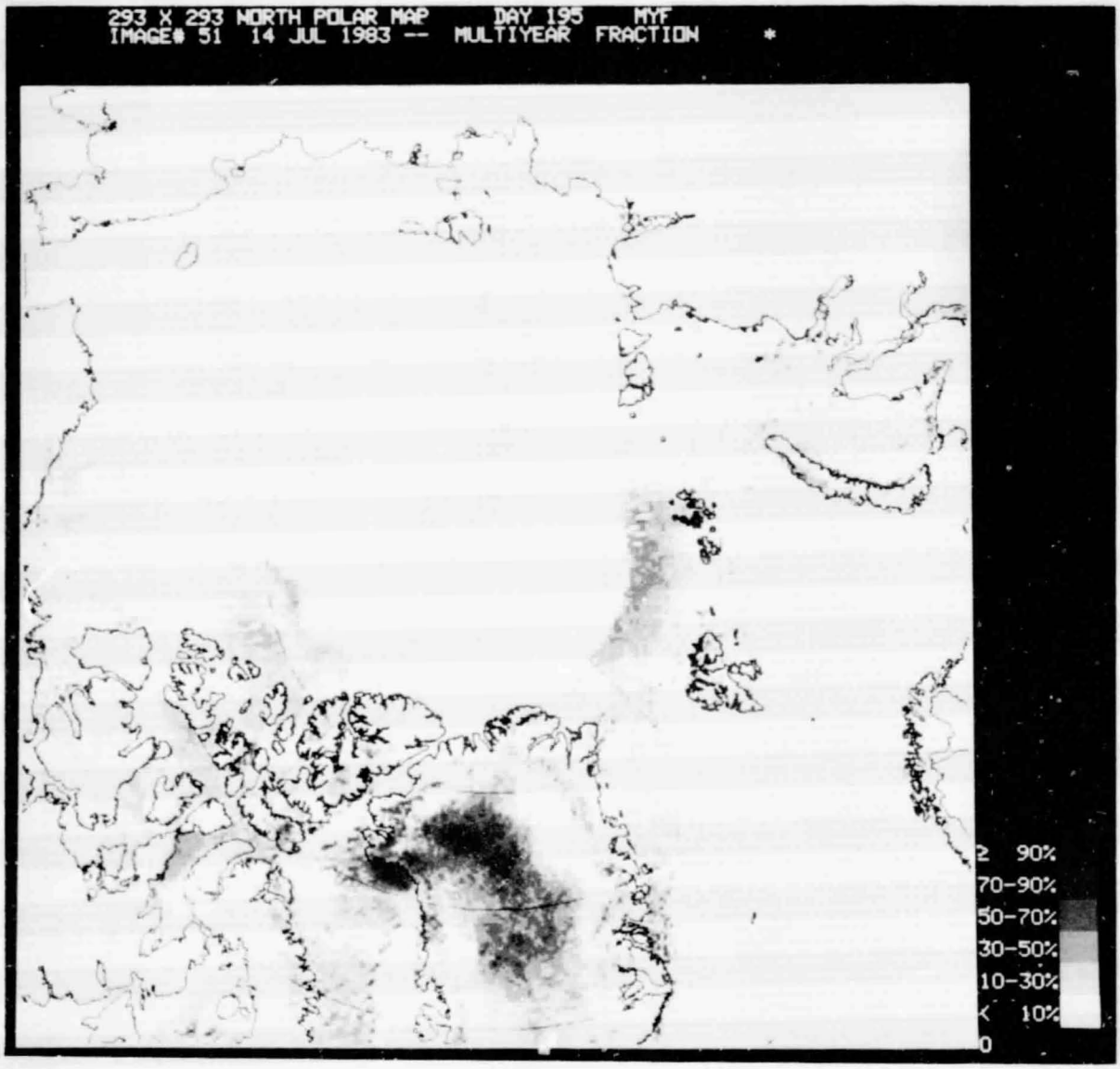

ORIGINAL PAGE IS
OF POOR QUALITY

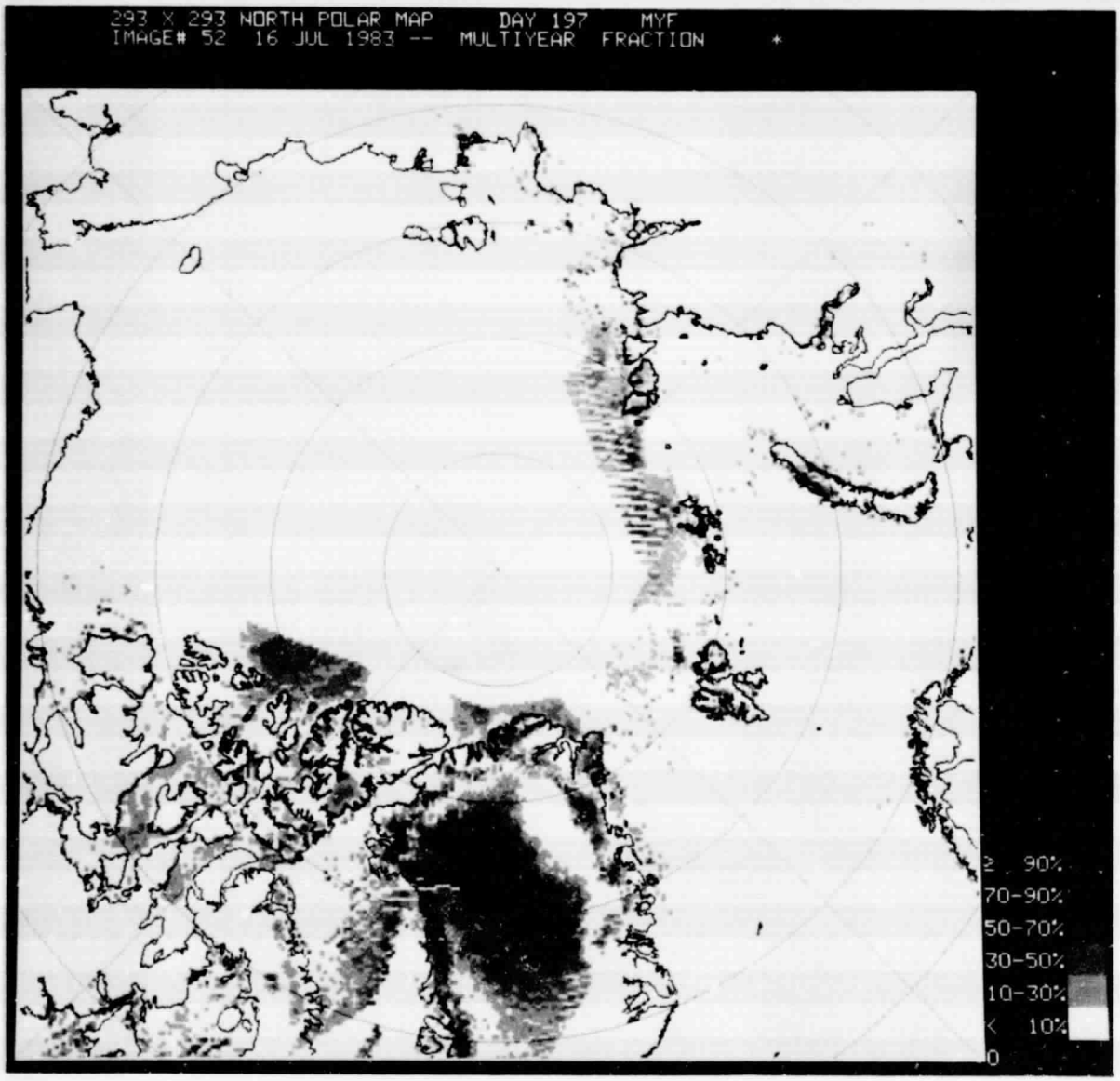

ORIGINAL PAGE IS
OF POOR QUALITY

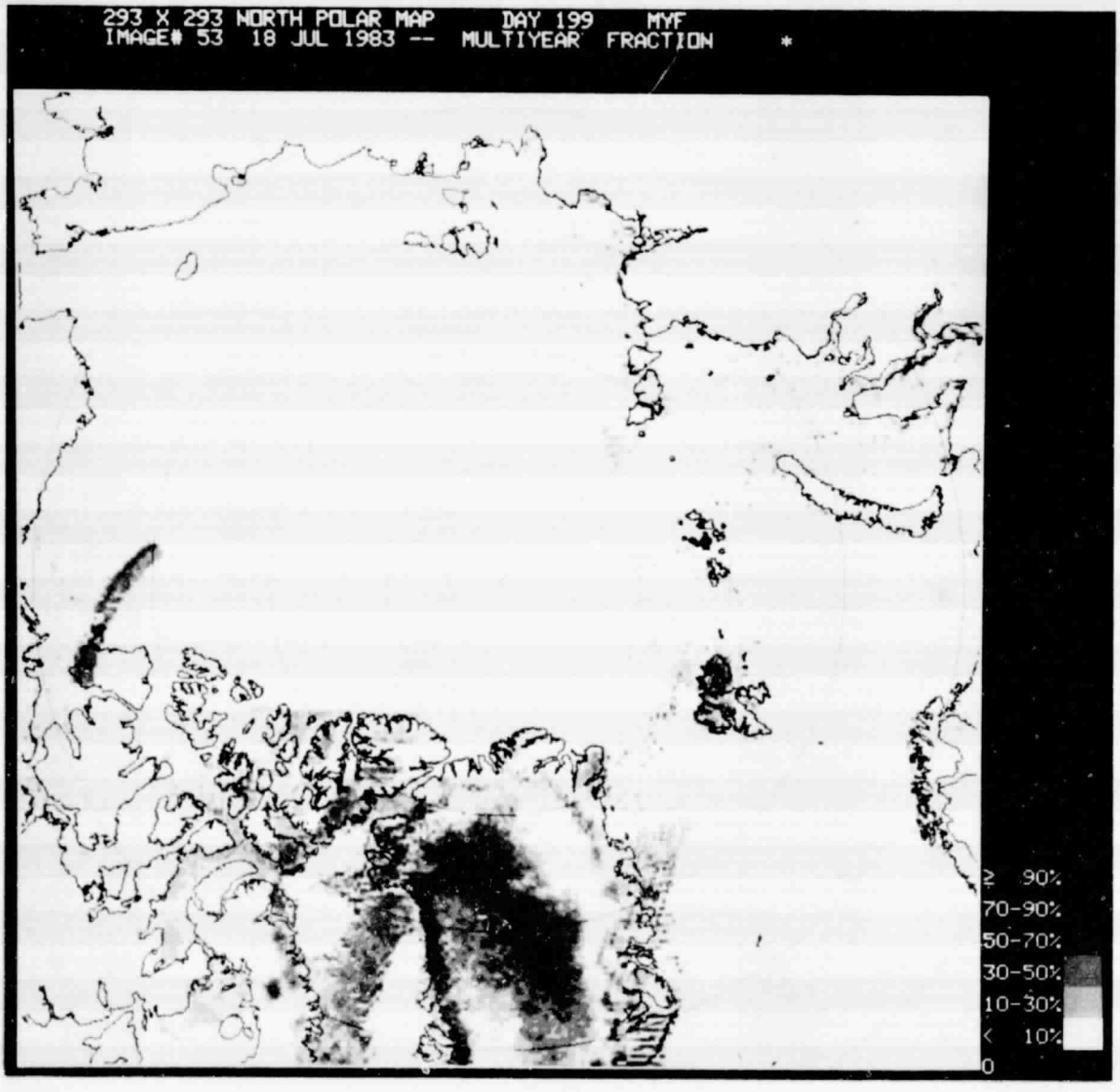

ORIGINAL PAGE IS
OF POOR QUALITY

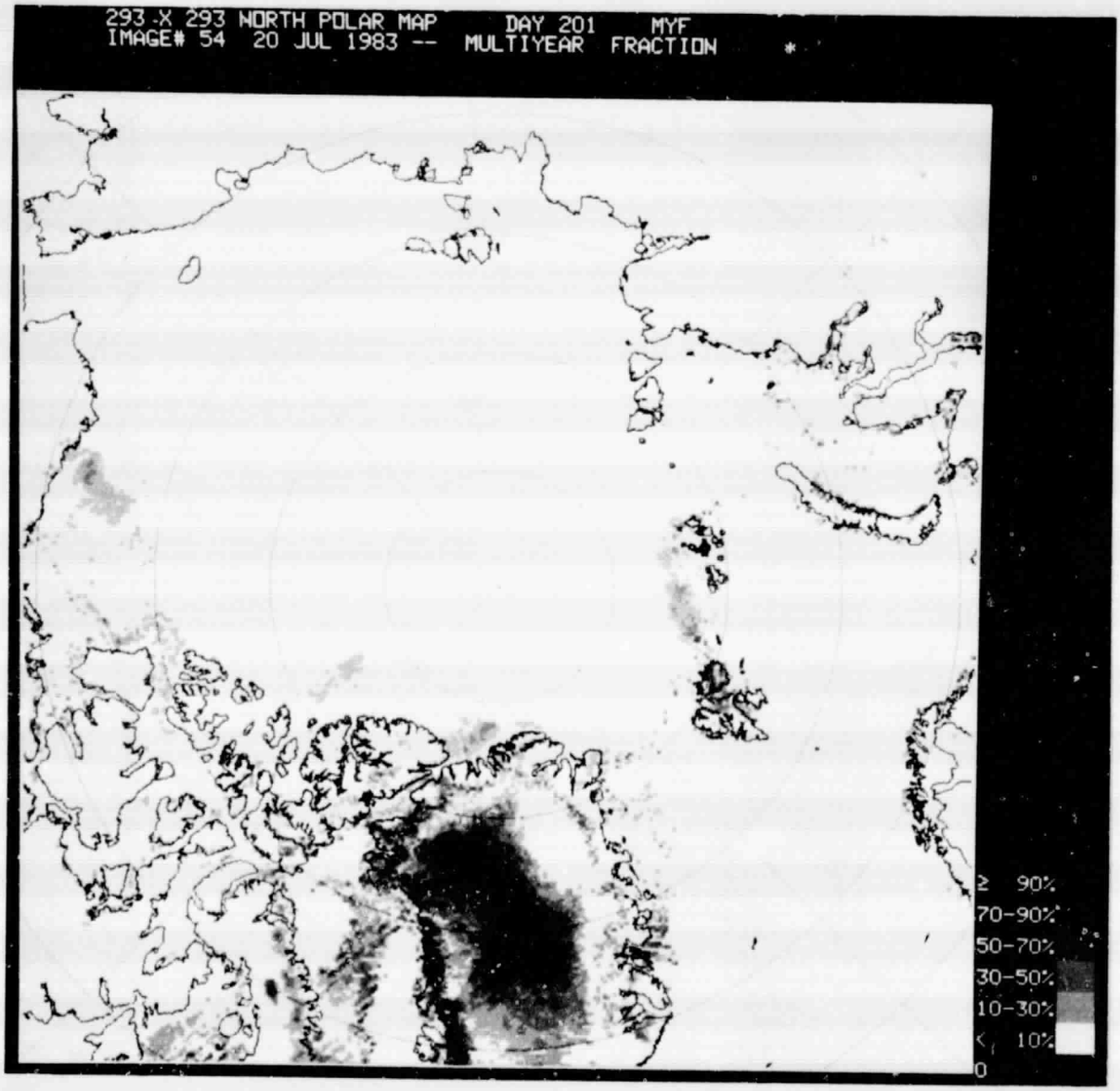

ORIGINAL PAGE IS
OF POOR QUALITY

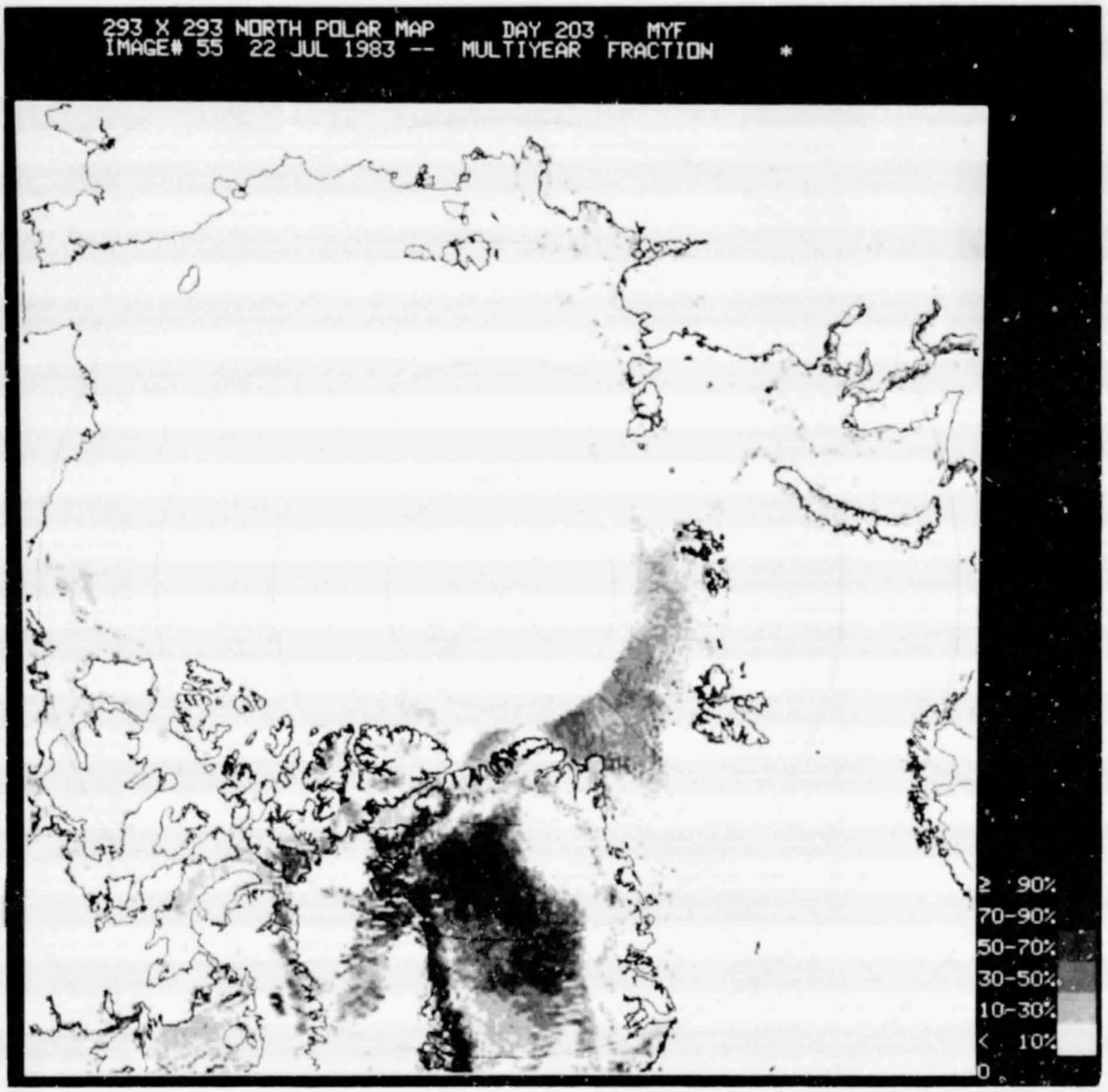

ORIGINAL PAGE IS
OF POOR QUALITY

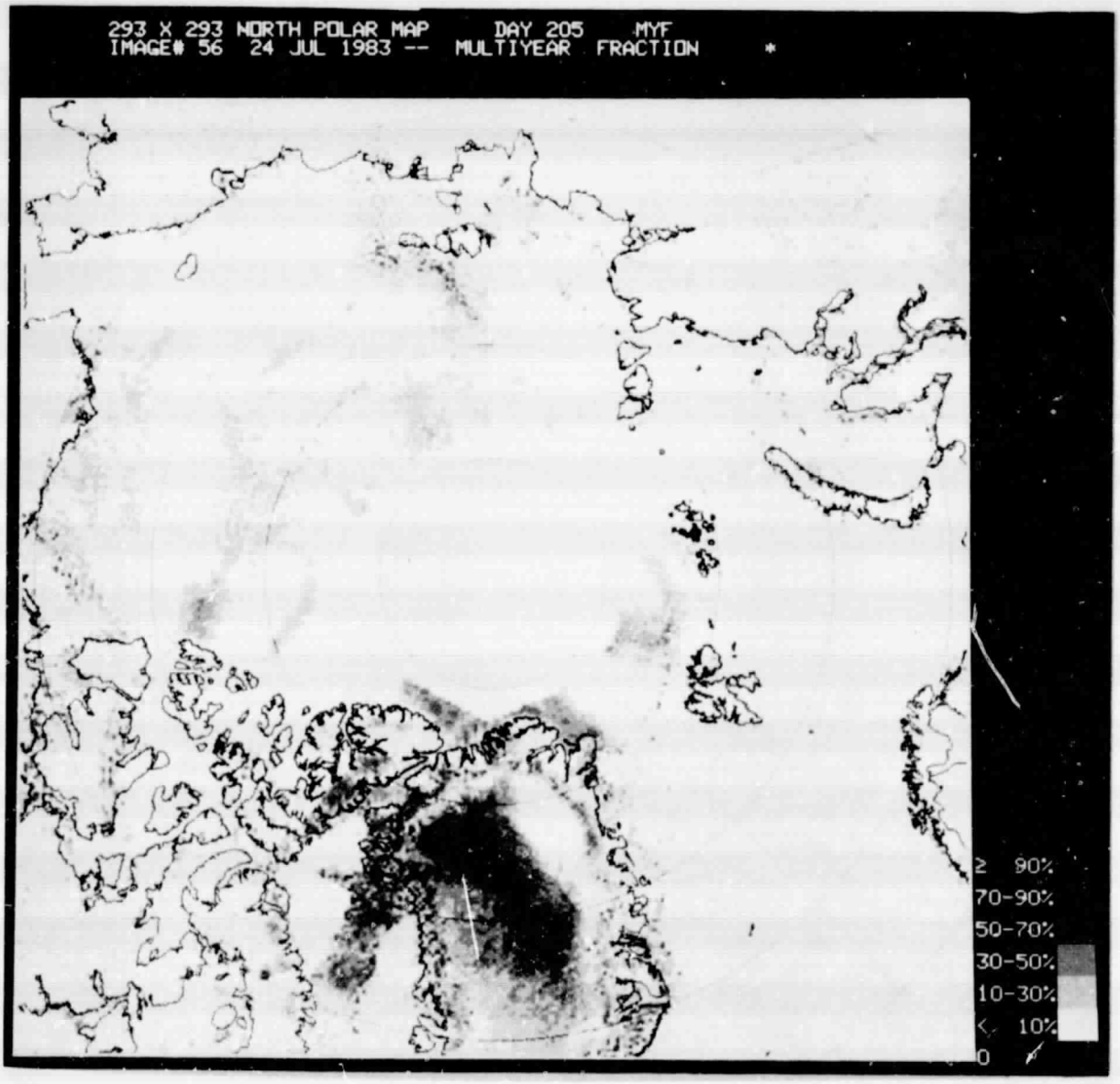

ORIGINAL PAGE IS
OF POOR QUALITY

ORIGINAL PAGE IS
OF POOR QUALITY

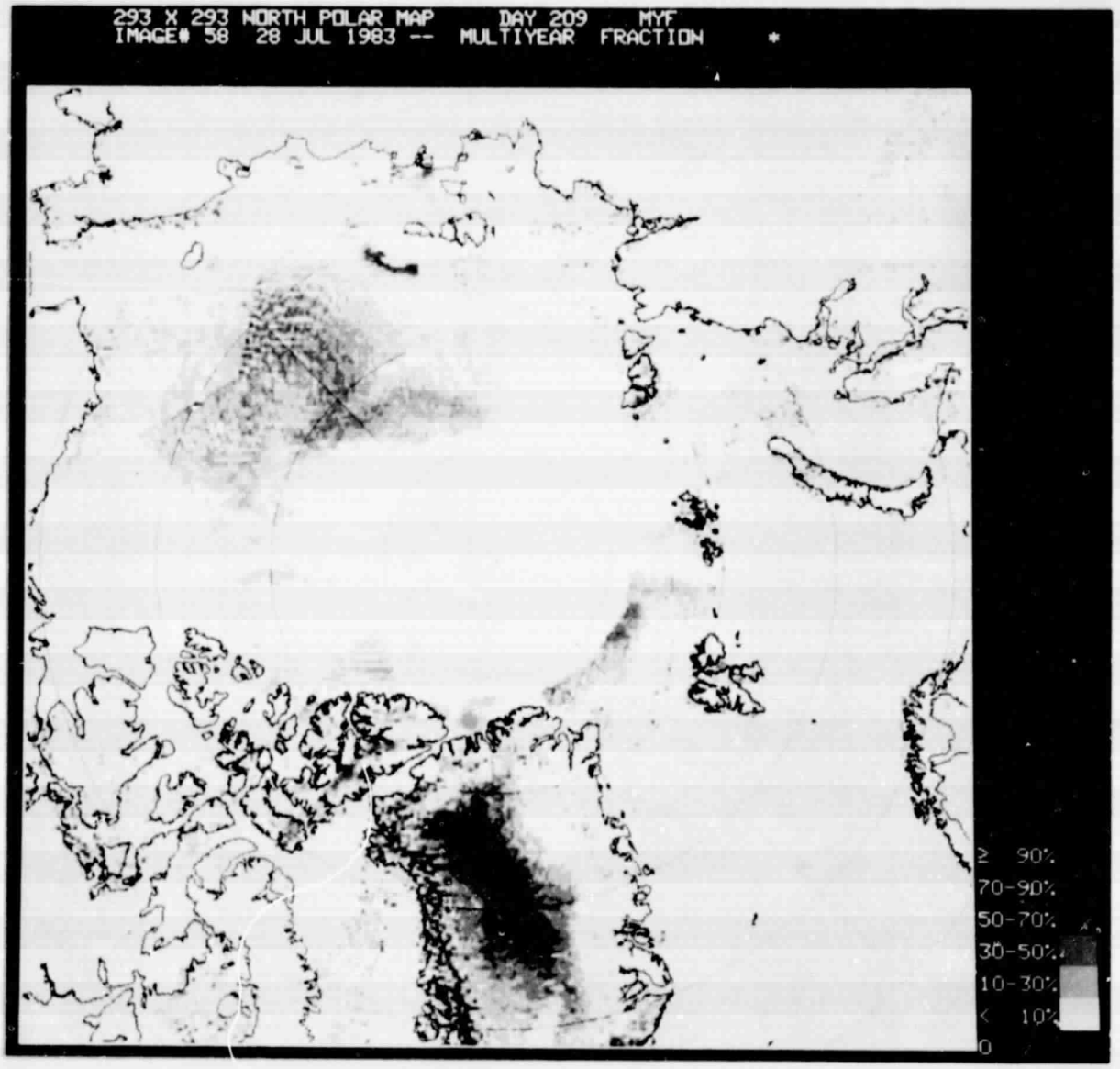

ORIGINAL PAGE IS
OF POOR QUALITY

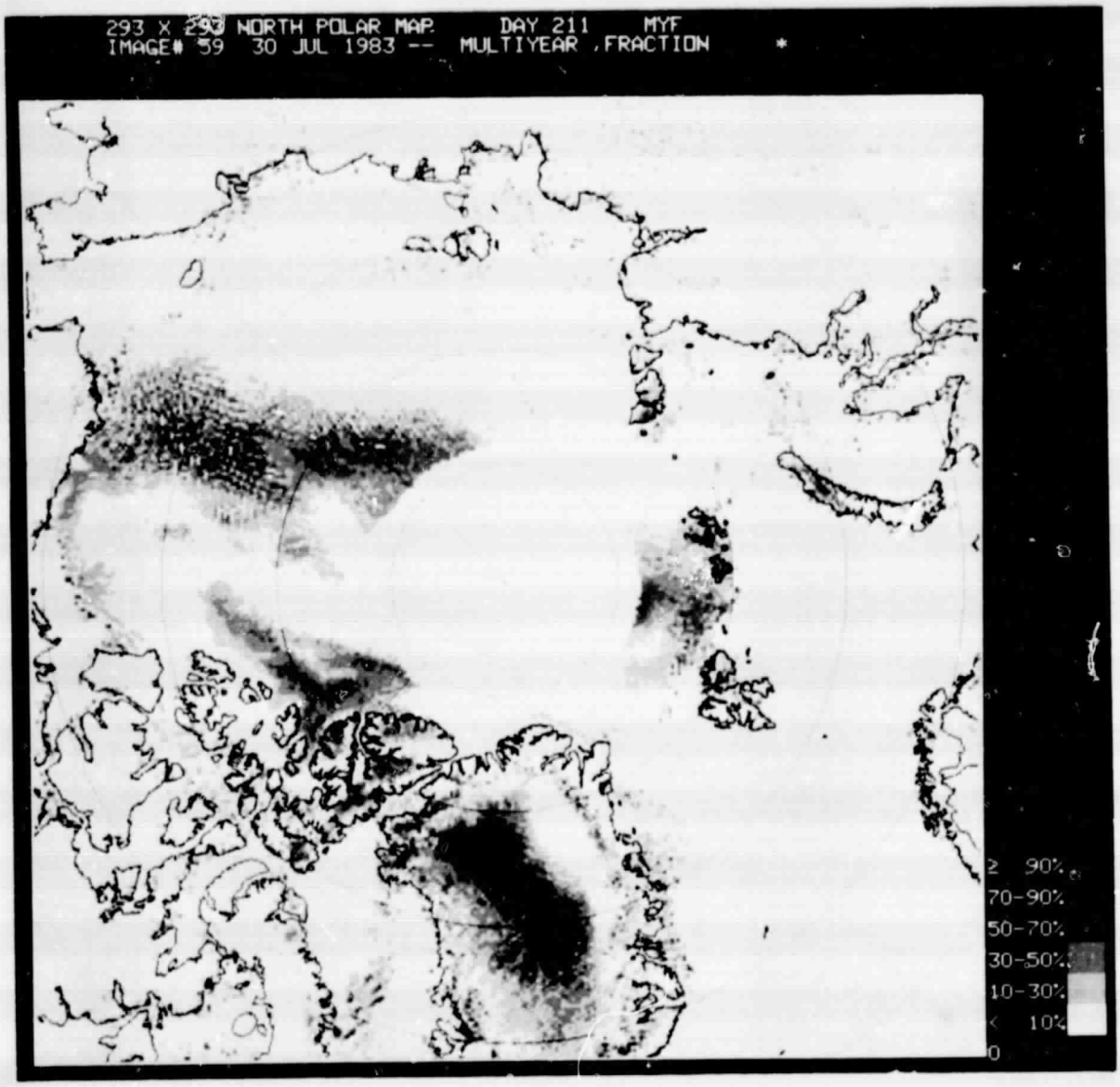

ORIGINAL PAGE IS
OF POOR QUALITY

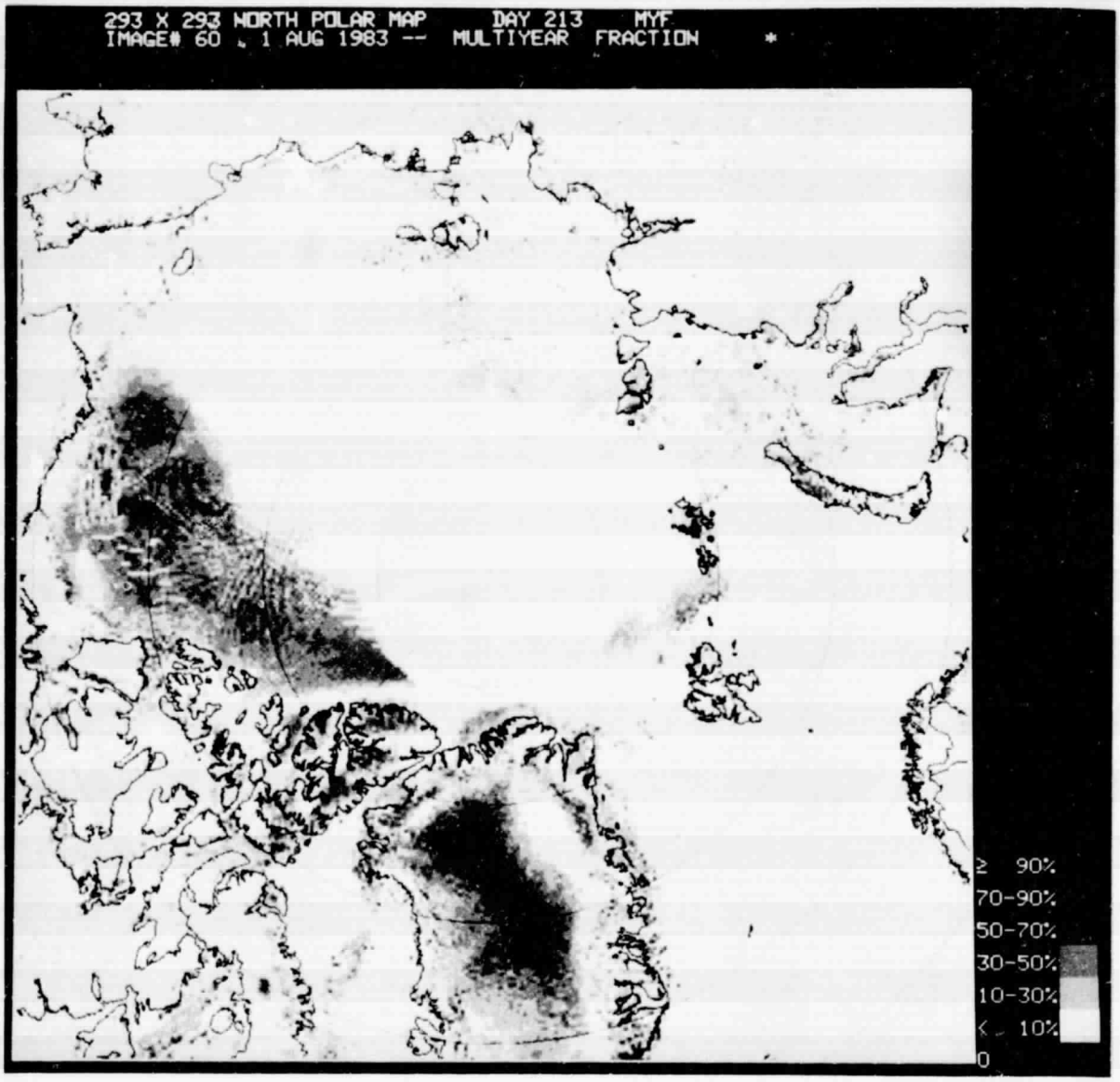

ORIGINAL PAGE IS
OF POOR QUALITY

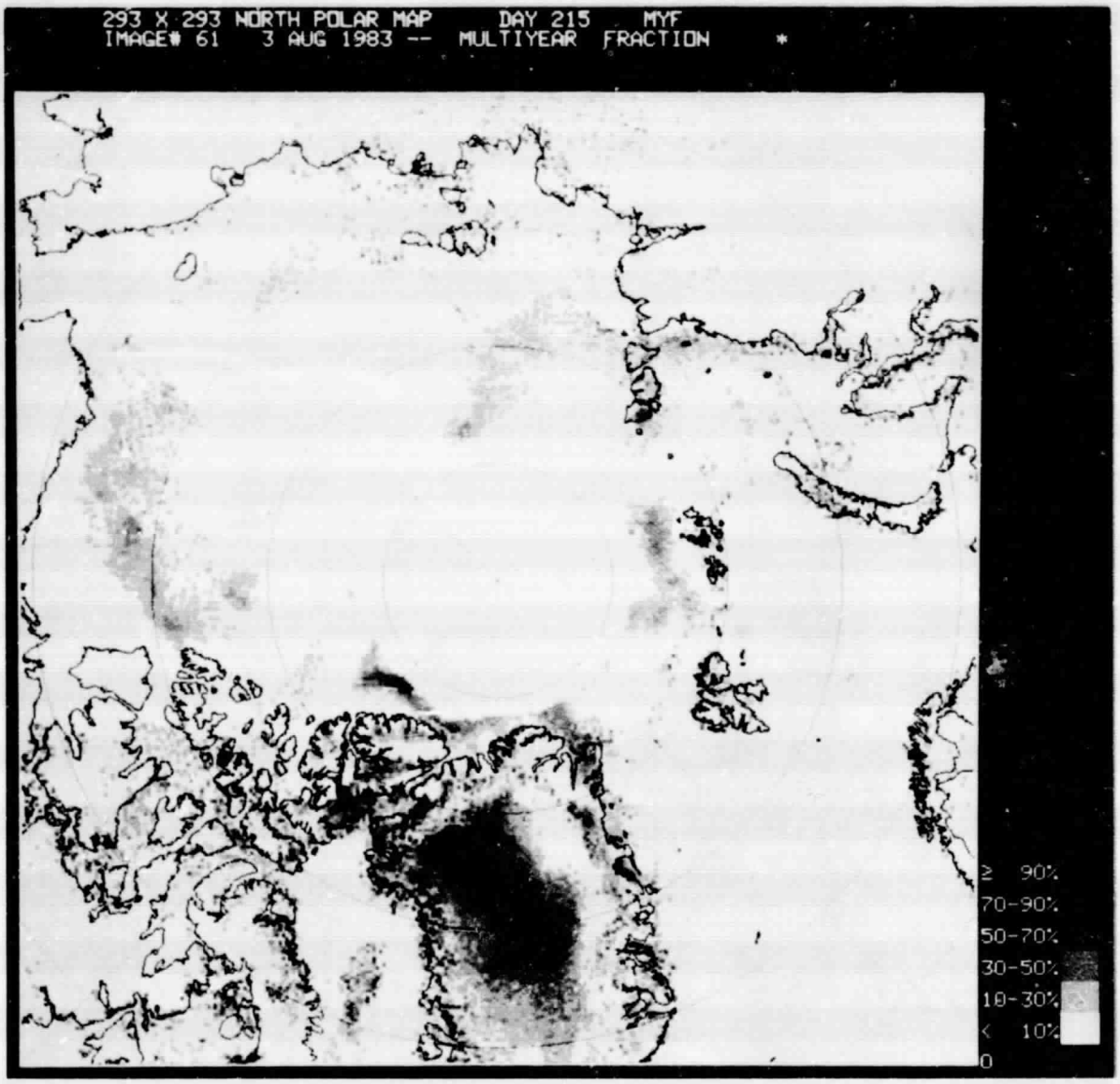

ORIGINAL PAGE IS
OF POOR QUALITY

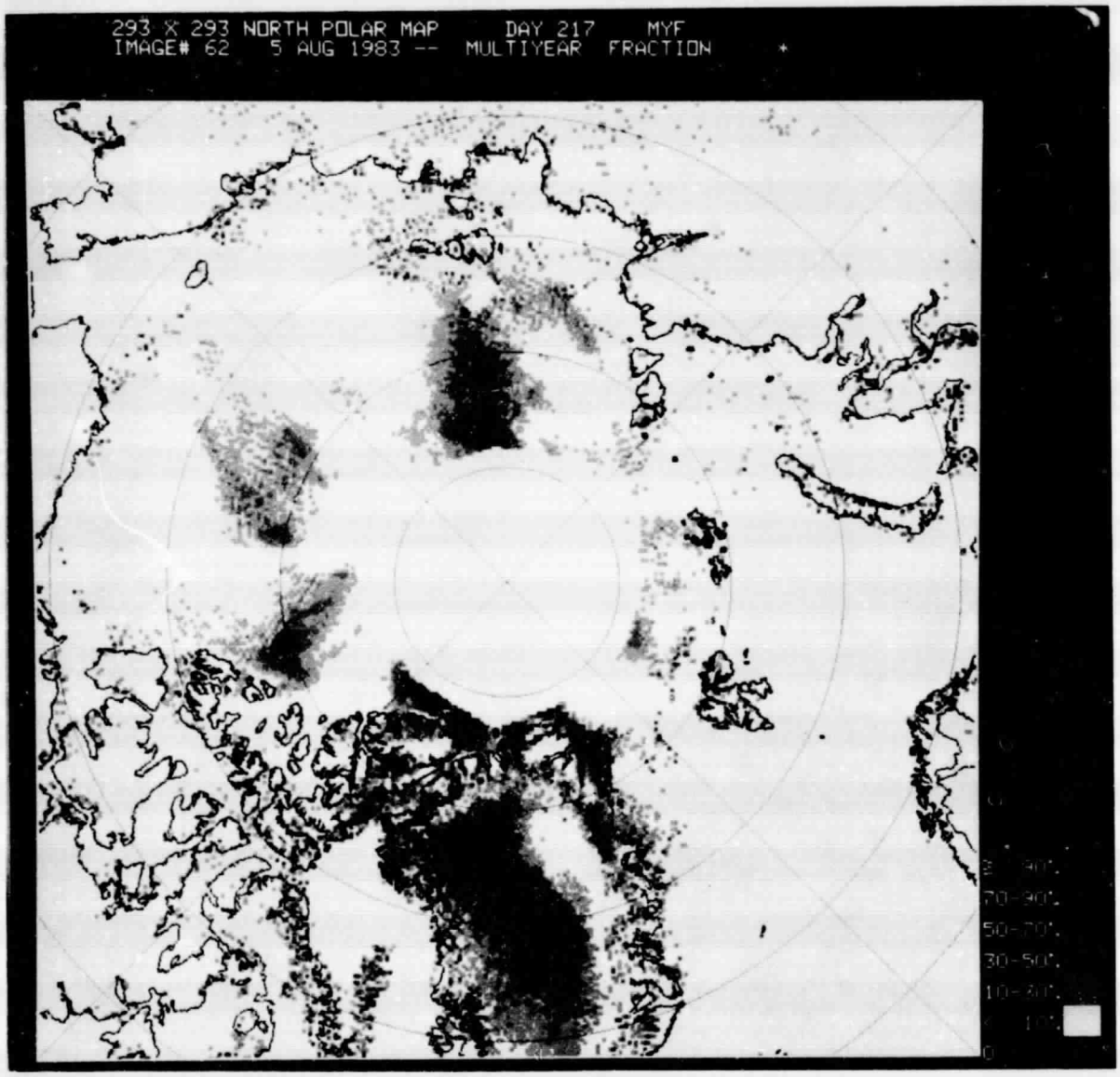

ORIGINAL PAGE IS
OF POOR QUALITY

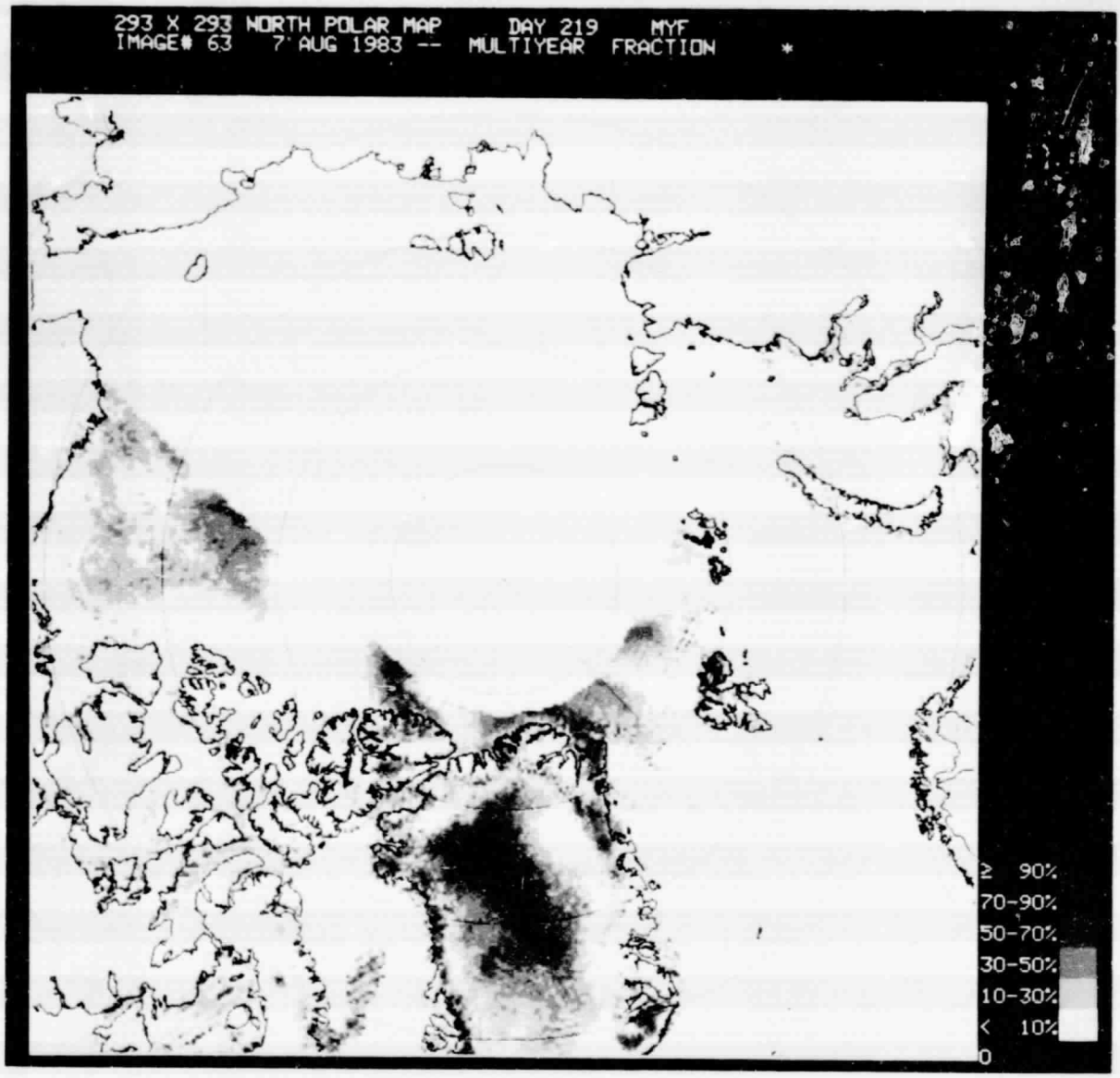

ORIGINAL PAGE IS
OF POOR QUALITY